MOBILIZATION OF TRACE ELEMENTS IN AQUIFERS BY BIODEGRADATION OF HYDROCARBON CONTAMINANTS

THESIS

Scott L. Kearney, 1Lt, USAF

AFIT/GEE/ENV/97D-13

DEPARTMENT OF THE AIR FORCE
AIR UNIVERSITY
AIR FORCE INSTITUTE OF TECHNOLOGY

Wright-Patterson Air Force Base, Ohio

AFIT/GEE/ENV/97D-13

MOBILIZATION OF TRACE ELEMENTS IN AQUIFERS BY BIODEGRADATION OF HYDROCARBON CONTAMINANTS

THESIS

Scott L. Kearney, 1Lt, USAF

AFIT/GEE/ENV/97D-13

Disclaimer

The views expressed in this thesis are those of the author and do not reflect the official policy or position of the Department of Defense or the U. S. Government.

AFIT/GEE/ENV/97D-13

MOBILIZATION OF TRACE ELEMENTS IN AQUIFERS BY BIODEGRADATION OF HYDROCARBON CONTAMINANTS

THESIS

Scott L. Kearney, B. S.

1st Lieutenant, USAF

Presented to the Faculty of the Graduate School of Engineering

of the Air Force Institute of Technology

In Partial Fulfillment of the

Requirements for the Degree of

Master of Science in Engineering and Environmental Management

Wm. Brent Nixon, Maj, USAF
Committee Member

Larry W. Burggraf, Ph. D.
Committee Member

Edward C. Heyse, Maj, USAF, BSC
Committee Chairman

Acknowledgments

I am truly thankful for my thesis advisor, Major Edward C. Heyse, who continually guided and supported this thesis effort with his expert insight and advice. His depth of experience, intuition, and patience were tremendous assets when encountering the many hurdles and obstacles in the thesis process. The extensive comments and recommendations given by Major Heyse were critical in developing the final product. I am also indebted to the expertise of Major Wm. Brent Nixon who took the time to explain the fundamentals of database architecture and query design. His persistent guidance allowed me to find groundwater data in areas where it did not appear to exist. I am additionally grateful for the in-depth chemistry knowledge of Dr. Larry W. Burggraf. His ability to see possible relationships and patterns in the groundwater data proved extremely valuable. I also want to acknowledge the efforts of Corey Peschke who performed several queries for me on the IRPIMS database located at Brooks AFB, TX which greatly assisted in the data collection effort.

I owe my wife, Krystal, a deep sense of love and appreciation for her support throughout this endeavor. She often acted as a single parent for our children, Seth and Leah, when I was not available for many daily household chores and family events. Her understanding and endurance contributed to the success of this effort more than she may ever know.

I can not neglect the role God played in this process. He taught me more than I will ever learn in a text or classroom.

Scott L. Kearney

Table of Contents

Page

List of Figures

List of Tables

Abstract

This study had two objectives: (1) to determine the extent of metal mobility within petroleum-contaminated aquifers, (2) to determine if biodegradation of petroleum hydrocarbons can explain metal mobility. The approach reviewed analytical results from 2305 groundwater sampling events, taken from 958 wells, located at 136 sites found at 53 Air Force installations.

The study showed that high levels of metals are present at petroleum hydrocarbon sites where metals would not generally be expected. Of the metals with drinking water maximum contaminant levels (MCLs), mercury and silver were detected the least frequently. Barium and copper were detected at the sites, but fewer than 2.5 percent of the samples exceeded their MCLs. All other metals exceeded their MCLs in at least 2.5 percent of the samples, with antimony and lead exceeding their MCLs in 19 percent and 10 percent of samples, respectively.

Higher concentrations of barium and manganese were most strongly correlated with petroleum hydrocarbon contamination, and relatively strong correlations also existed for aluminum, arsenic, iron and lead. Major cations such as calcium, magnesium, sodium and potassium were least affected by petroleum hydrocarbon concentrations.

Metals most mobile under reducing conditions had the strongest and most positive correlations with manganese concentrations which is an indicator of redox potential. However, metals with higher mobility in oxidizing conditions also had a positive correlation with manganese suggesting other factors are contributing to metals mobility.

MOBILIZATION OF TRACE ELEMENTS IN AQUIFERS BY BIODEGRADATION OF HYDROCARBON CONTAMINANTS

I. Introduction

Causes of Metal Mobilization

When fuel contamination enters the groundwater, physical and chemical changes occur in the aquifer geochemistry. The primary factor responsible for these changes is the biodegradation of petroleum hydrocarbons which occur by a variety of microbially mediated reaction pathways. Most of the petroleum hydrocarbon constituents such as benzene, toluene, ethylbenzene, and xylenes (BTEX) are susceptible to biodegradation under the conditions normally encountered within the aquifer environment (Malone et al., 1993).

As a result of the microorganisms transforming the fuel compounds into cellular mass and energy, several degradation byproducts such as organic acids are produced that may contribute to metal mobilization. In heavily fuel contaminated aquifer sediments, the production of organic acids may exceed their consumption and dissolved concentrations of Ca^{2+}, Mg^{2+}, and Fe^{2+} have been found to be one to two orders of magnitude higher than in uncontaminated regions of the aquifer (McMahon et al., 1995). The higher concentrations have been attributed to the decreasing pH levels which tends to increase the ability of metals to enter into solution. Organic acids may also lead to complexation with the metals found in the aquifer solids. Laboratory studies have shown that organic

acids like oxalate and citrate are more effective in dissolving minerals by their increased ability to complex cations and silica (Bennett et al., 1988; Bennett, 1991).

The redox potential in the groundwater system will also greatly influence the mobility of the metals. During the biodegradation of the petroleum hydrocarbons, microorganisms facilitate the transfer of electrons from the fuel components to various electron acceptors within the aquifer. Mineral deposits that contain Fe(III) and Mn(IV) are known as primary electron acceptors and increases of their reduced forms, Fe(II) and Mn(II), have been noted in solution (Baedecker and Back, 1979; Champ et al., 1979; Jackson and Patterson, 1982). Microorganisms provide the necessary activation energy for the redox reaction to occur and prefer to use the electron acceptors that will produce the most free energy.

Focus of this Effort in Contrast to Other Studies

Most of the mobility studies performed on petroleum contaminated aquifers have addressed the major cations such as Fe^{2+}, Mn^{2+}, K^{+}, Na^{+}, Ca^{2+}, Mg^{2+}, and Al^{3+}. This research effort expands the scope of elements that may be subject to mobilization by considering other cations and the metals that have established U.S. Environmental Protection Agency (EPA) drinking water standards.

Previous studies have focused strictly on a single fuel-contaminated site. They performed detailed analyses on the site by identifying all the environmental parameters and contaminants involved in the process of mobilization. This research effort will determine how widespread the mobility phenomenon is by including 100+ sites in the

analysis and employing statistical comparisons to determine if there are significant correlations between the fuel contamination and metal concentrations.

Motivation for Research

The U.S. Air Force has hundreds of petroleum hydrocarbon contaminated sites which may be susceptible to metal mobilization. The current methods for monitoring these sites are not able to distinguish the origin of the metal detected in solution. The methods only consider the upgradient metal concentration contrasted with the on-site or downgradient concentrations with no regard to the dynamics of the geochemistry in the aquifer. Typically, historical surveys and record searches are conducted for the contaminated area to determine possible anthropogenic metal sources. Metals present in aquifer minerals are not included in the site survey, but may still contribute to the elevated concentrations of metals in solution.

The remediation design for a fuel-contaminated site will differ depending on the source of the metals in solution. Metals that have been deposited by man, such as from an electroplating process, will require specific treatment and removal from the aquifer when detected in the groundwater. However, metals that are mobilized from naturally occurring aquifer sediments may not require additional remediation efforts. Since these metals are mobilized by the fuel contamination, the primary corrective action ought to focus on treatment of the petroleum hydrocarbons to decrease the mobility of the metals. The difficulty is determining the source of the metals in solution.

Research Objectives

(1) Determine the extent of metal mobility within petroleum-contaminated aquifers.

(2) Determine if biodegradation of hydrocarbons can explain metal mobility.

Thesis Overview

The main body of this thesis is designed with five chapters. Chapter I, "Introduction," provides the brief background for the possible relationship between the petroleum hydrocarbon contaminated aquifers and the mobilization of metals and establishes the Air Force's need for the focus of this research effort. Chapter II, "Literature Review," identifies the works of other authors which explain the current knowledge base for the petroleum hydrocarbon biodegradation processes that may contribute to metal mobilization within the groundwater environment. Chapter III, "Methodology," describes the data gathering process and quality measures used to construct a database that contains groundwater sampling data for petroleum contaminated sites. Chapter IV, "Findings and Analysis," highlights the results from the statistical analyses performed on the groundwater data. Chapter V, "Conclusions," summarizes the significant findings from the research effort and recommendations for future research are provided. The attached appendices provide the necessary support information for understanding the scope and thrust of the this thesis research.

II. Literature Review

Overview

Petroleum hydrocarbon releases to the environment have demanded a significant amount of attention from researchers and regulators alike. Of primary concern has been the impact of petroleum hydrocarbon contamination on groundwater systems that are used for potable water sources. Fortunately, the biodegradation of petroleum hydrocarbons by indigenous aquifer microorganisms into harmless byproducts has been demonstrated in numerous laboratory and field studies (Alvarez and Vogel, 1991; Atlas, 1981; Bartha, 1986; Baedecker et al., 1988; Chiang et al., 1989; Cozzarelli et al., 1990; Leahy and Colewell, 1990; Lee, 1988; Lovley et al., 1995; Evans et al., 1991; Edwards et al., 1992; Grbic-Galic, 1990; Davis et al., 1994; Wilson et al., 1986).

As microorganisms degrade the petroleum hydrocarbons, they change the aquifer environment. In the process of consuming the fuel compounds, several intermediate byproducts such as organic acids and chelators are produced that enhance the mobility of metals. Most of the cations liberated from the aquifer solids form soluble complexes with natural organic chelates which leads to the destruction of the parent minerals and to the increasing mobility of the trace elements.

In most subsurface environments, both aerobic and anaerobic degradation of petroleum hydrocarbons can occur, often simultaneously in different parts of the plume. Large inputs of fuels require large amounts of dissolved oxygen to metabolize the petroleum hydrocarbons. However, groundwater typically has small concentrations of dissolved oxygen which is rapidly consumed when the fuel contaminants are degraded.

When the dissolved oxygen is depleted, biodegradation of many petroleum hydrocarbons will continue under anaerobic conditions, but at a slower rate (Bennett et al., 1993). The microorganisms significantly influence the geochemistry as they are oxidizing the fuels and reducing the aquifer elements. Several metals are very sensitive to these redox changes and will enter the groundwater during this process (Pourbaix, 1974). During anaerobic conditions electron acceptors naturally present in the aquifer such as NO_3^-, SO_4^{2-}, Mn(IV), Fe(III), and CO_2 are reduced as organic compounds are oxidized (Bennett et al., 1993). Reactions that degrade organic compounds can also explain changes in the redox conditions in an aquifer and increases in concentrations of reduced aqueous species, such as NH_4^+, H_2S, Mn^{2+}, Fe^{2+}, and CH_4 (Champ et al., 1979; Jackson and Patterson, 1982).

Acid and Complexation Impacts on Metal Mobility

The transformation of petroleum hydrocarbons to more soluble and potentially more reactive intermediates may have an important effect on the aquifer geochemistry. The organic acid byproducts produced through this process may enhance the dissolution of metals by either the complexation of free cations or through an increase in proton availability (Tan, 1980). These acidic metabolites have been documented as an important soil weathering agent that can attack aquifer sediments, thus increasing metal solubility (Huang and Keller, 1970).

Complex formation facilitated by the organic acids, called chelation, is a common contributor to mobilizing metals and trace elements. The chelators compete for the metal

ions to form stable compounds causing more of the metals to go into solution. However, the chelators do not compete for all the metals with the same affinity which results in certain metals entering solution at a greater rate than others. Table 1 identifies stability constants for two chelators that may be formed from petroleum hydrocarbon biodegradation. The larger the stability constant, the more preferred the complex formation.

Table 1: Stability Constants* for the Formation of Metal Complexes with Acetate and Phthalate (Hering and Morel, 1993)

Cation	Acetate	Phthalate
Hg^{2+}	6.1	--
Zn^{2+}	5.8	2.9
Cr^{3+}	5.4	--
Fe^{3+}	4.0	--
Pb^{2+}	2.7	--
Al^{3+}	2.4	5.0
Cu^{2+}	2.2	4.0
Cd^{2+}	1.9	3.4
Co^{2+}	1.5	2.8
Fe^{2+}	1.4	--
Ni^{2+}	1.4	3.0
Mn^{2+}	1.4	2.7
Mg^{2+}	1.3	--
Ca^{2+}	1.2	2.4
Sr^{2+}	1.1	--
Ba^{2+}	1.1	2.3
Ag^{+}	0.7	--

*Constants are given as logarithms of the overall formation constants for complexes and as logarithms of the overall precipitation constants for solid, at zero ionic strength and 25°C.

The most commonly observed acid components downgradient from the fuel contamination include aromatic, alicyclic, straight-, and branched-chain aliphatic organic

acids. The highest concentrations of the organic acids were found in the most reduced groundwater that is depleted in nitrate and sulfate (Cozzarelli et al., 1990). The nature of the organic acids identified at these sites is probably controlled by the availability of the petroleum hydrocarbons and the electron acceptors available to microorganisms.

The organic acids play an important role in altering mineral dissolution rates. These degradation byproducts have been shown by Bennett and Siegel (1987) to depress the pH in a contaminated aquifer from a background value of 7.7 to 6.7. Studies have shown increased rates of dissolution of minerals such as quartz (Bennett et al., 1988), manganese oxides (Stone, 1987), and iron oxides (Lovley, 1987) have been observed in the presence of organic acids resulting from hydrocarbon biodegration.

It has been suggested by Erlich (1981) that high concentrations of organic acids may build up around bacteria adhering to a mineral surface which would increase the mobility of the minerals within the immediate vicinity. This idea is also confirmed by Gribic-Galic (1990) who indicated the microorganisms prefer to attach to aquifer solids, because the petroleum hydrocarbons are found in higher concentrations at surface interfaces than in the bulk liquid phase. Laboratory studies have also indicated that chemical microenvironments within the aquifer sediments may increase metal mobilization. pH values have been recorded within microbial mats using microelectrodes that are more than one unit below pH values in the overlying solution (Revsbech and Ward, 1984).

The solubility of most elements and the stability of their compounds is extremely sensitive to the pH of the aqueous environment. Only a few elements such as the alkali

metals (Na, K, and Rb) and alkaline earths (Ca, Mg, and Sr) are normally soluble throughout the entire pH range. Most metallic elements are soluble only in acidic solutions, and tend to precipitate as hydroxides with increasing pH (Stumm and Morgan, 1996). Figure 1 illustrates the importance of pH changes on the mobility of various metals that are encountered in the aquifer sediments.

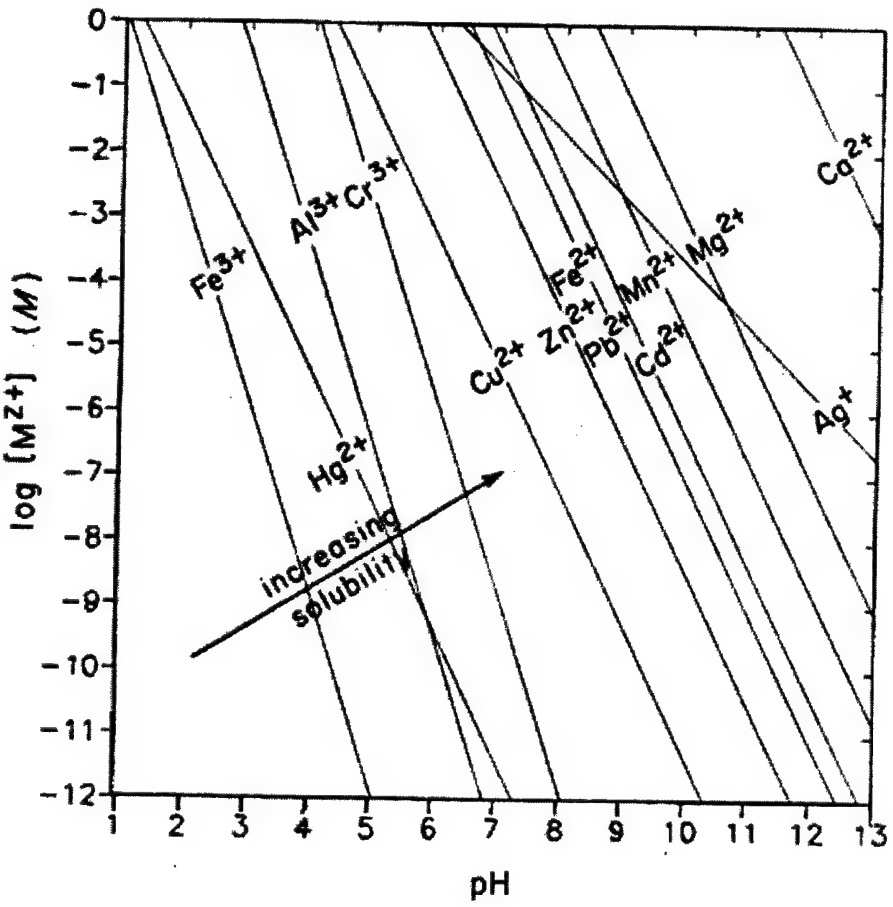

Figure 1: Solubility of Various Metal Ions as a Function of pH at 25°C/1atm (Adapted from Stumm and Morgan, 1996)

The ultimate end products of biodegradation are carbon dioxide and water. Carbon dioxide plays an important role in the carbonate system by forming carbonic acid which will react with carbonate minerals found in the sediments and serve as a pH buffer for the aquifer system. The geochemistry of the aquifer is controlled extensively by the carbonate equilibrium that is established through the carbon dioxide produced.

Redox Potential and Metal Mobility

A redox reaction is a reaction involving the transfer of electrons. The chemical species that receives the electron(s) is reduced and the chemical species that looses the electron(s) is oxidized. The petroleum hydrocarbons are biodegraded by the microbes oxidizing the fuel compounds. As the microbes are degrading the fuel compounds, electrons are transferred to oxidized chemical species present in the aquifer such as Fe(III) and Mn(IV). The rate of biodegradation is generally limited by a lack of electron acceptors rather than by a lack of nutrients such as ammonia, nitrate, or phosphate (Hinchee et al., 1991).

The energy produced by these redox reactions is quantified by the Gibb's free energy of the reaction (ΔG_r) which estimates how much free energy is consumed or can be yielded to the systems during the reaction (CRC Handbook of Chemistry and Physics, 1995). In general, the microbes will prefer those redox reactions that produce the most energy for respiration, cell growth, and reproduction (Bouwer, 1992). The processes illustrated in Figure 2 are the primary means for oxidizing petroleum hydrocarbons in the preferred order of decreasing energy produced. Also included in Figure 2 is the expected

range of the electron activity (pe) which measures the tendency of a solution to accept or transfer electrons. Thus, a high pe indicates a relatively high tendency for oxidation, and a low pe indicates a tendency for reduction.

Almost all types of petroleum hydrocarbons are degraded under aerobic groundwater conditions (Cerniglia, 1984). The background dissolved oxygen concentrations are usually higher than in the contaminant plume as the microbes consume the dissolved oxygen to mineralize the fuel compounds. The use of molecular dissolved oxygen is one of the highest energy producing redox reactions used by microbes. Although denitrification yields slightly more energy than aerobic respiration, dissolved oxygen

Degradation Process	ΔG_r° (kJ/mole)*	Expected pe Range**
Aerobic Respiration	**-3202**	**2.5 to 14**
⇓		
Denitrification	**-3245**	**1 to 13**
⇓		
Manganese (IV) Reduction	**-3202**	**0.5 to 10**
⇓		
Iron (III) Reduction	**-2343**	**-9 to 0.5**
⇓		
Sulfate Reduction	**-514**	**-12 to -2.5**
⇓		
Methanogensis	**-136**	**-12.5 to -3**

Figure 2: The Sequence of Microbially Preferred Reactions for Benzene
*(CRC Handbook of Chemistry and Physics, 1995)
**(Stumm and Morgan, 1996)

concentrations greater than 0.5 mg/L are toxic to anaerobic microbes (Wiedemeier et al., 1995). Therefore, dissolved oxygen must be depleted from the groundwater before anaerobic electron acceptors are used for oxidizing the petroleum hydrocarbons (Grbic-Galic and Vogel, 1987; Lovely et al., 1989; Hutchins et al., 1991; Beller et al., 1992a and 1992b; Edwards and Grbic-Galic, 1992).

The geochemical changes in the aquifer will be impacted by the type and abundance of the electron acceptors and redox potential. Several field studies have established that zones will develop within the contaminated plume downgradient from the site as demonstrated in Figure 3 (Baedecker et al., 1993; Barcelona and Holm, 1991; Bennett et al., 1993; Bjerg et al., 1995; Champ et al., 1979; Chapelle et al., 1995; Christensen et al., 1994a; Eganhouse et al., 1993; Heron and Christensen, 1995; Lovley and Phillips, 1987; Lovley and Goodwin, 1988; Robertson and Blowes, 1995). These redox zones develop as the electron acceptors that produce more energy are depleted and the microbial community adapts to the next available electron acceptor. Environmental conditions and microbial competition will ultimately determine which of these processes will dominate. It has also been demonstrated that the dominant terminal electron accepting process can vary both spatially and temporally (Vroblesky and Chapelle, 1994). These varying conditions within the aquifer will cause the boundaries of the zones to loose their distinction. These conditions will differ for several reasons, such as seasonal recharge events that may change the primary biodegradation process by the influx of dissolved oxygen. The redox zones are compressed on the upgradient portion of the contamination plume, because the groundwater flow is delivering new supplies of

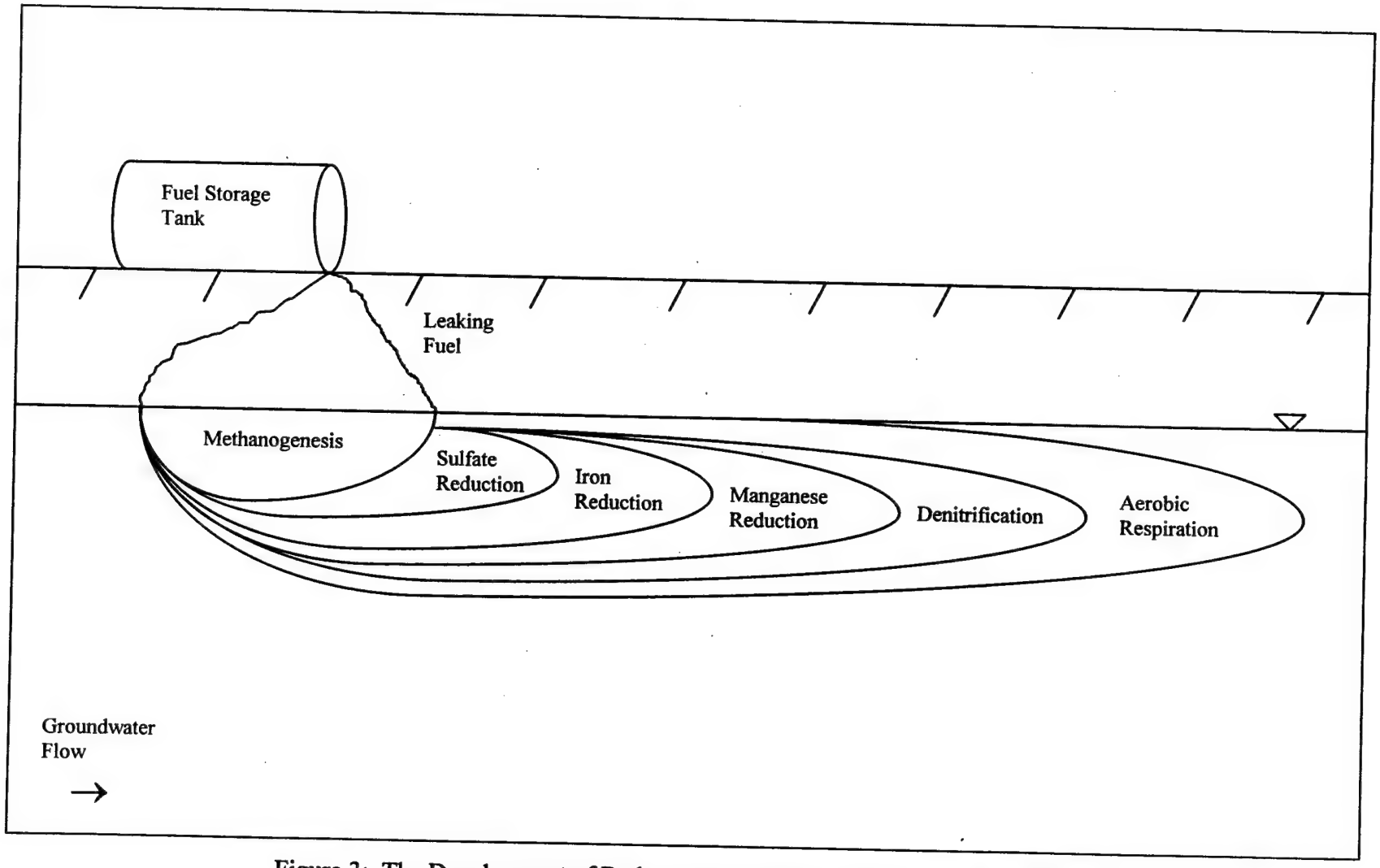

Figure 3: The Development of Redox Zones Within a Fuel Contaminated Plume

reducible species such as O_2, NO_3^-, SO_4^{2-}, and CO_2. The large size of the redox zones on the downgradient portion of the contamination plume results from the depletion of the reducible aquifer species. When the oxygen demand from metabolizing the fuels no longer exceeds the natural supply of dissolved oxygen, the plume will once again become aerobic.

Combined Effects of Redox and pH

The mobility of the metals in the aquifer is determined by the stability of the host minerals and by the electrochemical properties of the elements. Specifically, both the redox system (pe) and the buffer capacity (pH) control the physical and chemical properties of the groundwater system. Each metal can be readily precipitated or adsorbed even under a small change of the equilibrated conditions within the aquifer. In groundwater systems, solubility equilibria may change significantly within a few centimeters or even millimeters both horizontally and vertically (Kabata-Pendias and Pandias, 1992).

The pe-pH diagram of iron in Figure 4 illustrates different phases and compounds that form as the pe and pH levels vary within the system. The behavior of iron is also typical of the behavior of other metals (Mn, V, U, Cu) which occur in two or more valence states (Levinson, 1974). Some general observations from Figure 3 are as follows: (1) oxidizing conditions promote the precipitation of iron, as compared to reducing conditions which promote the dissolution of iron; and (2) acid solutions tend to promote the dissolution of iron and alkaline solution promote precipitation of iron. As iron moves

from a reducing environment to an oxidizing environment, it will precipitate as it forms insoluble oxide and hydroxide compounds. In uncontaminated aquifer conditions, pH is most commonly observed between 5 and 7, and the pe ranges between 8.45 and -1.78 (Levinson, 1974). Where organic matter is abundant as with fuel contamination, conditions of low pH and pe may result in higher solubility of iron and manganese until the groundwater moves to regions within the aquifer that are more oxidizing where they will then precipitate.

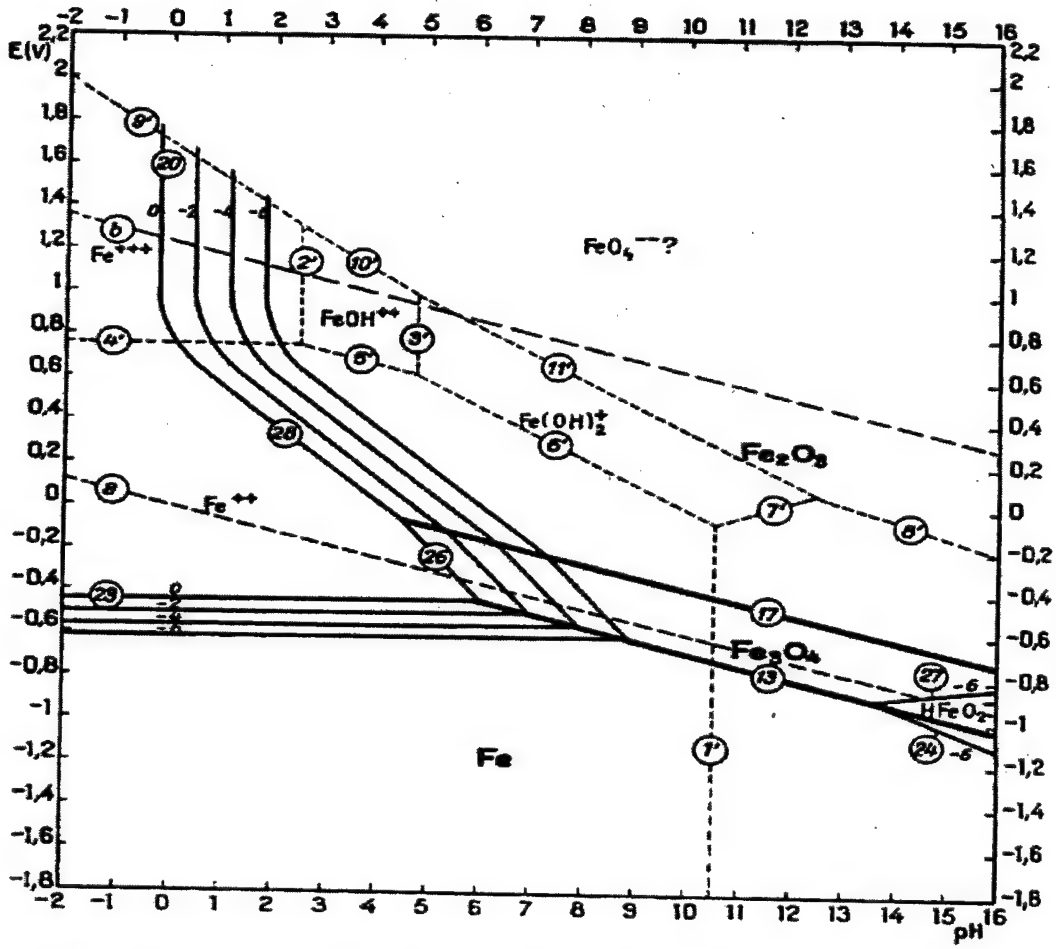

Figure 4: pe-pH Equilibrium Diagram for the System Iron-Water, at 25°C (where pe = Eh / .05916) (Pourbaix, 1974)

The pe-pH diagrams have the essential purpose of demonstrating a thermodynamic framework for electrochemical reactions involving an aqueous solution. Groundwater is often in a highly dynamic state with regard to redox reactions rather than in equilibrium (Lindberg and Runnells, 1984). Most redox reactions have a tendency to proceed at a much slower rate than acid-base reactions, especially in the absence of a suitable biochemical catalysis which is provided by microbes. But in the biodegradation of petroleum hydrocarbons, microbes are present and the redox reactions occur at a more rapid rate. Equilibrium redox predictions for a real system should not be overinterpreted, and should only be viewed as a general guide for: (1) where any given system is headed; and (2) what types of concentrations are feasible in the system (Stumm and Morgan, 1996).

Table 2 identifies the metals which have solubility dependent on redox and pH conditions that are encountered in an aquifer (Pourbaix, 1974). Table 2 is simplified by only considering the metal solid phases that include oxides and hydroxides even though other solids forms such as carbonates, sulfates, and sulfides can exist in the aquifer environment. A metal is considered mobile if the most stable form of the metal is in the soluble phase with a molar concentration greater than 10^{-6}. Alkali and alkali earth metals (including Na, K, Ba, Ca, Mg, and Be) are not included in Table 2 because these elements have only one oxidation state.

Table 2: Metals with Increased Mobility Under Changing pe and pH Conditions

pH Level	Oxidizing Conditions	Reducing Conditions
pH < 7	Sb, As, Cr, Cu, Mo, Se, Ag, V	Co, Fe, Mn, Ni, V
pH ≥ 7	Sb, As, Cr, Se, V	Tl

Redox Zone Identification Studies

The identification of the ongoing processes involved in forming the redox zones within the fuel contaminated plume is difficult to measure, because of the non-equilibrium conditions in the aquifer. Investigations seldom address the existence of a redox zone sequence within the contaminant plume downgradient of the site, but most of the reported investigations provide some information on redox-sensitive parameters allowing for an indirect assessment of the redox zones that are present. A set of criteria presented in Table 3 for characterize the dominant redox conditions based on concentrations of redox-sensitive compounds of groundwater samples taken at the Vejen landfill, Denmark.

Table 3: Criteria for Redox Parameters Used for Assigning Redox Status to Groundwater Samples (all values for concentration in mg/L) (Lyngkild and Christensen, 1992)

Parameter	Aerobic	Nitrate Reduction	Manganese Reduction	Iron Reduction	Sulfate Reduction	Methongenesis
Oxygen	>1.0	<1.0	<1.0	<1.0	<1.0	<1.0
Nitrate-N	--	--	<0.2	<0.2	<0.2	<0.2
Nitrite-N	<0.1	--	<0.1	<0.1	<0.1	<0.1
Ammonium-N	<0.1	--	--	--	--	--
Mn(II)	<0.2	<0.2	>0.2	--	--	--
Fe(II)	<1.5	<1.5	<1.5	>1.5	--	--
Sulfate	--	--	--	--	--	<40
Sulfide	<0.1	<0.1	<0.1	<0.1	>0.2	--
Methane	<0.1	<0.1	<0.1	<0.1	<0.1	>0.1

The redox zones identified by the groundwater samples were later supported by extraction of sediment-bound oxidized iron species. The amount of extractable iron was significantly lowered in the reduced samples, supposedly due to sediment redox processes dissolving Fe(III) minerals (Christensen et al., 1994b).

Patterns of electron acceptor consumption and final product accumulation do not always unequivocally define the distribution of redox processes. It is in this context that hydrogen can be used as an effective indicator of terminal electron-accepting processes (TEAPs). A wide variety of anaerobic microorganisms produce H_2 during the metabolism of hydrocarbon compounds. As rapidly as H_2 is produced, it is consumed by respiratory microorganisms that use oxidized compounds (nitrate, Fe(III), sulfate, CO_2) as terminal electron acceptors (Chapelle et al., 1995). Significantly, different anaerobic terminal electron-accepting processes exhibit different efficiencies in using H_2. Because each TEAP has a characteristic steady state H_2 concentration and it is theoretically independent of biomass or overall rates of microbial metabolism (Lovley and Goodwin, 1988), H_2 concentrations can be an indicator of the TEAP that predominates in a given zone within the contaminated plume.

An important feature of H_2 concentrations is that changes along the flow path are not required in order to identify specific TEAPs. Because H_2 is a continuously cycled intermediate product, with a half-life on the order of seconds, H_2 concentrations reflect nearly instantaneous conditions at a particular well. A single analysis can, in principle, be diagnostic of the predominant TEAP. The H_2 concentrations that are associated with specific redox zones are identified in Table 4.

Table 4: Hydrogen Concentrations Associated with Specific Redox Zones in Contaminated Groundwater Plumes (Chapelle et al., 1995)

Redox Zone	H_2 Concentration (nmol)
Denitrification	<0.1
Iron Reduction	0.1 - 0.8
Sulfate Reduction	1.0 - 4.0
Methanogenesis	5 - 25

Since H_2 may quickly move from the aqueous phase to the gaseous phase, attempts to preserve H_2 samples in the field for transport to the laboratory are typically not successful. All H_2 measurements should be made in the field within 30 minutes of the groundwater sample collection.

In cases where electron acceptor consumption and final product accumulation are known, the redox zone can be more clearly defined. However, the confidence of the diagnosis increases if a combination of electron acceptor consumption, final product accumulation and H_2 concentration are used to identify TEAPs. When all three potential indicators identify the same TEAP, a high degree of confidence in the diagnosis is warranted.

Metal Mobilization Field and Laboratory Research

Some of the more significant studies performed on metal and trace element mobility have employed various means of assessing the metal mobility phenomenon. Baedecker et al. (1993) and Bennett et al. (1993) focused extensively on a fuel-contaminated aquifer located near Bemidji, MN, where a high-pressure pipeline carrying

crude oil burst. The environmental parameters such as the types and concentrations of petroleum hydrocarbons present, the dissolved oxygen levels, the aquifer mineral compositions were well established for the site. They performed on-site surveys and studies as well as incubating aquifer sediments in the laboratory to determine the extent of metals entering solution in such an environment. In the anoxic zone beneath the oil body concentrations of dissolved SiO_2, Sr, K, Fe, and Mn increased significantly as compared to the background concentrations.

Bennett and Seigel (1987), Hiebert and Bennett (1992), and McMahon et al. (1995) observed that quartz and feldspar grains were more etched and pitted in portions of an aquifer containing organic acid rich groundwater than in other regions of the aquifer, and concentrations of dissolved organic carbon were positively correlated with dissolved silica concentrations. They postulated that the ability of organic acids to promote mineral dissolution under field conditions resulted from a concentrated build up of organic acids in the vicinity of microbial cells. The resulting reaction zones may cause mineral dissolution even though the bulk pore water might be oversaturated with respect to the dissolving mineral phase. At the cellular level, this buildup of organic acids would manifest itself by abrupt concentration gradients away from attached cells.

A review by Lovley (1987) indicates the crystalline form of Fe(III) may influence its solubility. Because of the low solubility of Fe(III), the microbes may have to directly contact the Fe(III) to reduce it to Fe(II). The less crystalline the Fe(III) form the more readily it is microbially reduced. The greater ease of reducing the less crystalline forms

of Fe(III) may reflect the fact that the less crystalline Fe(III) has a greater surface area than highly crystalline Fe(III) (Schwertmann and Taylor, 1977).

Summary of Metal and Trace Element Mobilization Factors

The metal and trace element mobility phenomenon is influenced by many geochemical factors that occur within a fuel contaminated plume. Of these influences, pH, redox potential, and complexation are the dominant factors that contribute to metals entering solution. These factors are summarized qualitatively in Table 5.

Table 5: Metal Mobility Influenced by pH, Redox Potential, and Complexation

Metal/Trace Element	pH[a]	Redox Potential[b]	Complexation[c]
Aluminum	X		X
Antimony	X		?
Arsenic	X		?
Barium	X		
Beryllium	X		?
Cadmium	X		X
Calcium	X		
Chromium	X		X
Cobalt	X	X	X
Copper	X		X
Iron	X	X	
Lead	X		X
Magnesium	X		
Manganese	X	X	
Mercury			X
Molybdenum	X		?
Nickel	X	X	
Potassium	X		
Selenium			?
Silver	X		
Sodium	X		
Thallium	X	X	?
Vanadium	X		?
Zinc	X		X

[a] metal is soluble at lower pH values, [b] metal is soluble in reduced form or under reducing conditions,
[c] metals that form complexes more readily than complexes associated with Fe^{2+}, ? not known

Focus of this Research

Many studies have been performed on the biodegradation of petroleum hydrocarbons and on the environmental impacts that result from the fuel contamination in groundwater systems. The research has conclusively shown the aquifer geochemistry is significantly altered during the biodegradation process which tends to promote metal mobility by lowering the pH, lowering the redox potential, and increasing complexation.

This study expands the scope of metal mobility caused by petroleum hydrocarbon biodegradation by considering those metals that have EPA drinking water standards established. It will also include 100+ sites where the groundwater has been monitored for fuel contamination and metals. By including many sites in the study, metal mobility from fuel contamination might be established as a widespread phenomenon that could potentially impact remediation design and regulatory requirements. A statistical analysis of the groundwater samples will attempt to correlate known environmental factors that contribute to metal mobility with the concentrations of the metals under investigation. This study will provide information on the extent of metals mobilization resulting from fuel biodegradation.

III. Methodology

Overview

This research effort analyzes the mobility of 24 trace elements and metals by studying 2305 sampling events from 958 sample locations at 136 fuel-contaminated sites located at 53 Air Force installations identified in Appendix A. The metals and trace elements are included in Appendix B. The groundwater data used for the research meets various quality checks to ensure the contamination at the site is primarily petroleum hydrocarbons and not cross-contaminated from other anthropogenic sources. The data is then explored by statistical methods to determine the extent and cause of metal mobility.

Data Collection

The bulk of the groundwater data analyzed for this research is consolidated in Oracle-driven databases maintained by the Air Force Center for Environmental Excellence (AFCEE), Brooks AFB, TX and by the Omaha District for the Corps of Engineers (CoE). Both the AFCEE database, the Installation Restoration Program Information Management System (IRPIMS), and the CoE database, PETRO (Project Execution Technical Resources On-line), contain extensive monitoring data for Air Force hazardous waste sites. The data collection focused on sites that were classified as leaking underground storage tanks, underground storage tanks, and fuel spills. This requirement for the data attempts to limit the contamination at any site to petroleum hydrocarbons and

to exclude sites contaminated with other anthropogenic compounds. The queries performed for gathering the data are located in Appendix C.

Data Collection Difficulties

Some problems were encountered within the databases when trying to extract groundwater data. The tables and fields that contained the monitoring were often incomplete or nonexistent for various reasons. Often, a specific fuel-contaminated site could be identified for an Air Force installation, but the monitoring wells were not linked or cross-referenced to the site in question. As a result, the groundwater analytical data could not be used without independently identifying the exact well names used for the site.

To overcome this deficiency, the Air Force installations that had no cross-referencing information were contacted to determine which wells were monitoring the fuel contaminated sites. This personal communication identified the wells and allowed access to the groundwater analytical results in IRPIMS. When the well identifications did not match any wells entered in IRPIMS, the personnel from the Air Force installation would send the "hard copy" reports that contained the groundwater data for the fuel contaminated sites which were then manually entered into the thesis research database.

Database Development

The data collected were entered into an MS ACCESS 7.0™ database. This incorporated the data one concise database that could be queried for the remainder of the

research. The database consisted of one table containing nine fields which are described in Table 6.

Table 6: Database Fields and Descriptions

Field Name (Acronym)	Field Description
Site Type Classification Code (STCCODE)	Identifies the type of site that is monitored for contamination
Air Force Installation (AFIID)	Identifies the Air Force installation where the site is located
Site Identification (SITEID)	Identifies the site number associated with a specific site at an Air Force installation
Geohydrologic Flow Classification (GFCCODE)	Identifies the position of the monitoring well in relation to hydraulic flow of the contaminant plume
Location Identification (LOCID)	Identifies the well name associated with a monitoring well
Sampling Date (LOGDATE)	Identifies the date the sampling event occurred
Parameter Label (PARLABEL)	Identifies the groundwater parameter analyzed
Parameter Value (PARVAL)	Identifies the numerical result for the parameter analyzed
Units of Measurement (UNITS)	Identifies the units of measurement associated with the numerical result

Groundwater Data Parameters

The groundwater data collected included every parameter analyzed for the site including trace elements and metals, petroleum compounds, anthropogenic contaminants, and other chemicals. The analyte classifications and types used for this research are identified in Appendix D. Often the parameters analyzed were not present in the groundwater sample at concentrations high enough to be detected by the laboratory

testing equipment or procedures. When a parameter concentration is below the detection limit it is commonly referred to as a non-detect (ND).

Often the fuel components are analyzed individually such as the BTEX compounds and are reported as separate concentrations. To simplify the analyses, the petroleum hydrocarbons are combined to produce one total fuel concentration for each sampling event. Total petroleum hydrocarbon contamination includes the highest concentration for one of the following categories identified in IRPIMS and PETRO:

1. Sum of benzene, toluene, ethylbenzene, total xylenes, methylnaphthalene, acenaphthene, phenanthrene, pyrene, and naphthalene;
2. Diesel components;
3. Oilgrease;
4. Petroleum hydrocarbons;
5. Gasoline components;
6. BTEX (as its own category);
7. JP4;
8. JP5;
9. JP7;
10. JP8.

Besides those listed, most of the petroleum hydrocarbons identified in Appendix D were not detected in groundwater analyses which is attributed to low solubility of large fuel compounds and the natural immiscibility of oil and water.

The nonfuel anthropogenic compounds are addressed in a slightly different manner. To simplify the analyses, only the highest individual concentration is used to represent the anthropogenic contamination for each sampling event. For instance, a sampling event detects 50 ug/L of trichloroethylene and 25 ug/L of acetone, 50 ug/L would represent the contamination caused by anthropogenic compounds.

Some of the analytes such as lead and sec-butyl alcohol may be used as fuel additives. Lead as an additive was phased out in the 1980s, but may still be detected at sites where the contamination occurred before this time. Sec-butyl alcohol may be used to enhance the octane of the fuel mixture and was detected in high concentrations in 34 sampling events from two sites. Although these analytes are not petroleum hydrocarbons, they may be used as fuel additives and were not used to determine the highest anthropogenic concentration for a sampling event.

Groundwater Data Qualification

The wells in the database were not uniformly sampled and tested. Some wells were sampled only for metals and petroleum hydrocarbon contamination. Other wells were sampled for a broad suite of chemicals. To limit confounding factors that may influence the mobility phenomenon, Wilk-Shapiro/Rankit Plots are constructed for each metal. The Wilk-Shapiro Rankit Plot procedure examines whether a variable conforms to a normal distribution. If the assumptions of normality are met, the standarized residuals should be approximately normally distributed with mean 0 and variance 1. The i-th rankit is defined as the expected value of the i-th order statistic for the sample, assuming the sample was from a normal distribution. The order statistics of a sample are the sample values reordered by their rank. If the sample conforms to a normal distribution, a plot of the rankits against the order statistics should result in a straight line, except for random variation. Systematic departure of the rankit plot from a linear trend indicates non-normality.

The first data series includes only the sample data from the wells that had been tested for contaminants other than petroleum hydrocarbons and metals, and did not detect any chemical other than petroleum products. Indicators of nonpetroleum contaminants are listed in Appendix D. This plot demonstrates the presence of metals when only petroleum hydrocarbon contamination is present (metals unlikely to come from waste disposal). The second data series includes all the sample data from all wells at all sites. The purpose of this plot demonstrates the prevalence and concentration of metals at fuel contaminated sites.

The two data series represented by the plots are then statistically compared by testing their sample means to see if a significant difference exists between the sample populations. If a significant difference does not exist then for the entire data set (all wells and all samples) will be used for subsequent analysis.

The data were further qualified by examining the sample outliers that occurred on the plots. The sample site and well locations were identified for the outliers to determine whether a specific site was contributing to the higher concentrations being detected. If one site constitutes all of the outliers in the data set, the metals may be more likely to result from anthropogenic sources.

Metal Mobility Determination

To determine the extent of metal mobility at the fuel contaminated sites, Wilk-Shapiro/Rankit Plots were established for all the metals and trace elements. These plots show whether the sample concentrations are taken from a log-normal distribution. The

primary purpose of the plots is to establish the extent and magnitude for the mobilization of metals across the sites under consideration.

Metal Source Determination

The source of the metals should be distinguished from man-made wastes and naturally occurring deposits within the aquifer. After the wells are qualified by the Wilk-Shapiro/Rankit Plots and the sample mean testing, the metals and trace elements are correlated by hydraulic location and with natural parameters that were analyzed in the groundwater. Scatter plots and regression analyses, where appropriate, are performed for each metal and trace element by comparing the metal concentrations with fuel contaminated aquifer conditions such as pH, dissolved oxygen (DO), alkalinity, fuel concentrations, and known redox indicators like Mn^{2+}.

IV. Findings and Analysis

Data Quality

Even though the data search focused on fuel contaminated sites, some of the groundwater samples were analyzed for other chemicals including volatile organics, pesticides, polychlorinated biphenyls, cyanide, radionuclides and other anthropogenic compounds. Sites or wells were not equally sampled for all analytes limiting the comparisons between the groundwater samples. Unequal sampling could alter the analysis performed on the data by not fully knowing the contamination that is present at the site. Table 7 provides a summary of the extent of analysis for representative analytes of interest. Of the wells sampled for other chemicals, 72 percent were analyzed for volatile organics (such as TCE), 61 percent were analyzed for semivolatile organic, and smaller fractions were analyzed for other chemicals. The detection for "other anthropogenic compounds" (anything that is not a petroleum hydrocarbon, a metal, or indicator of pH or redox condition, see Appendix D) is illustrated in Figure 5. Only the highest anthropogenic contaminant concentration for each well (not individual sample) is used to construct the distribution to illustrate the significance of other anthropogenic contamination without regard to multiple sample events. Figure 5 shows many wells had had a large amount of cross-contamination from other chemicals besides petroleum hydrocarbons indicating other activities may have been occurring in the area. Appendix E details the type of anthropogenic contaminant typically found and the highest concentration observed in all the groundwater samples.

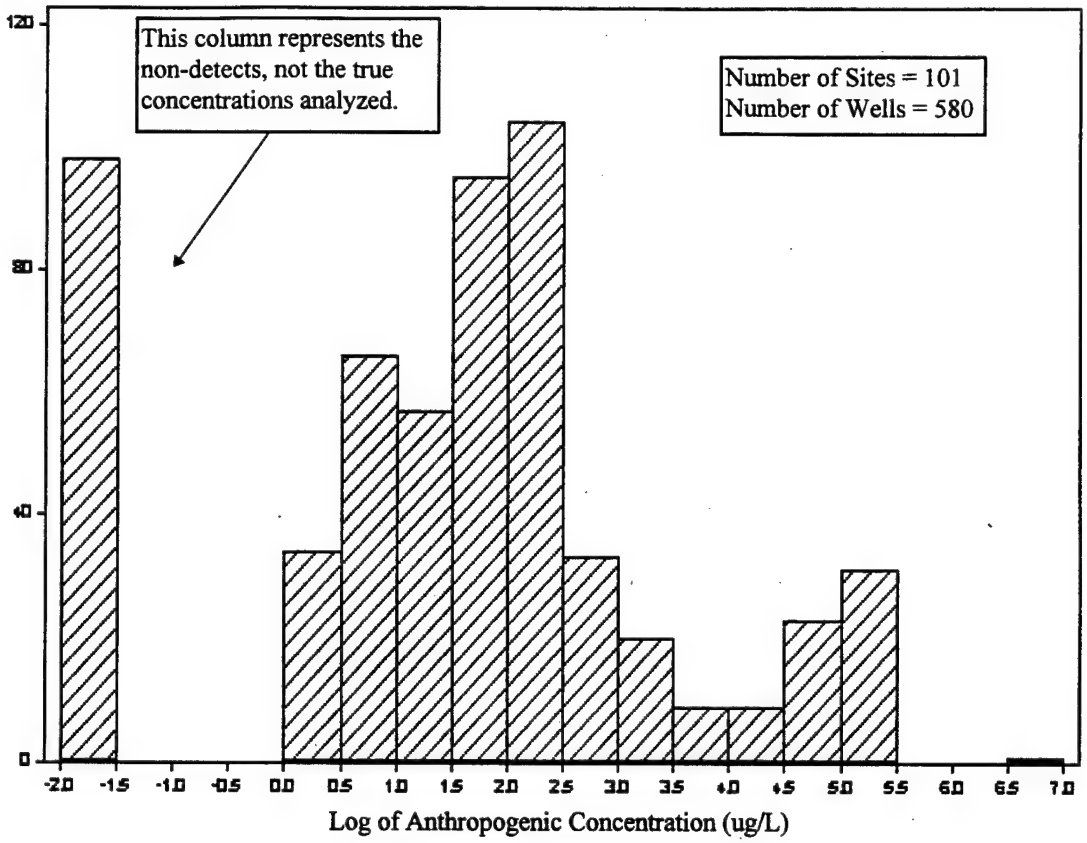

Figure 5: Distribution of Anthropogenic Contamination

Of the 958 wells included in the database, 580 wells were sampled for chemicals defined as "other anthropogenic compounds"; samples from the remaining 378 wells were analyzed only for metals and petroleum hydrocarbons. Of 580 wells that were sampled for anthropogenic compounds, 98 wells did not detect any of these compounds and were used as the anthropogenic non-detect (ND) data series for the rankit plots. Metals present in samples from these 98 wells were assumed most likely to be from dissolution of natural minerals.

Table 7: Summary of Analyte Investigation

Analyte	Sampling Events*	Sampling Locations*	Sites*
Total Number	2305	958	136
Metals			
Aluminum	0.336	0.401	0.566
Antimony	0.361	0.450	0.596
Arsenic	0.402	0.443	0.529
Barium	0.399	0.491	0.684
Beryllium	0.390	0.478	0.632
Cadmium	0.458	0.537	0.699
Calcium	0.352	0.378	0.500
Chromium	0.447	0.534	0.721
Cobalt	0.302	0.343	0.456
Copper	0.462	0.523	0.684
Iron	0.437	0.544	0.654
Lead	0.697	0.756	0.919
Magnesium	0.354	0.383	0.500
Manganese	0.424	0.524	0.625
Mercury	0.335	0.443	0.566
Molybdenum	0.209	0.242	0.301
Nickel	0.438	0.514	0.691
Potassium	0.339	0.357	0.478
Selenium	0.410	0.498	0.647
Silver	0.413	0.506	0.669
Sodium	0.362	0.401	0.537
Thallium	0.330	0.410	0.551
Vanadium	0.300	0.339	0.456
Zinc	0.466	0.534	0.699
Petroleum Hydrocarbons	1.00	1.00	1.00
Redox Indicators			
Alkalinity	0.087	0.118	0.132
Carbon Dioxide	0.009	0.022	0.007
Dissolved Oxygen	0.010	0.025	0.014
Methane	0.009	0.022	0.007
Nitrate	0.107	0.159	0.235
Nitrite	0.030	0.047	0.096
pH	0.216	0.313	0.412
Specific Conductance	0.190	0.281	0.382
Sulfate	0.140	0.228	0.346

*fraction of total number given for individual analytes
(example: fraction of total sampling events analyzed for aluminum = 775 / 2305 = 0.336)

Table 7: Summary of Analyte Investigation (cont)

Analyte	Sampling Events*	Sampling Locations*	Sites*
Other Anthropogenic Compounds			
Acetone	0.155	0.201	0.331
Trichloroethylene (TCE)	0.407	0.437	0.559
Chlordane	0.072	0.100	0.154
PCB	0.042	0.063	0.044
Gross Beta	0.006	0.010	0.022
Cyanide	0.070	0.091	0.103
bis (2-Ethylhexyl) Phthalate	0.287	0.365	0.449
Pentachlorophenol	0.243	0.132	0.426

*fraction of total number given for individual analytes
(example: fraction of total sampling events analyzed for acetone = 358 / 2305 = 0.155)

Once the wells were segregated between anthropogenic detection and non-detection, Wilk-Shapiro Rankit Plots are constructed for each of the 24 trace elements and metals (Appendix F). The first data series (denoted by the diamonds) represents the samples taken from only the 98 wells that analyzed for and did not detect "other" anthropogenic compounds (anthropogenic ND). The second data series (denoted by the circles) in each rankit plot represents the all the samples taken from all the wells included in the database for that particular trace element or metal.

To determine whether the two data series were significantly different, a two sample *t* test with unequal variances was performed to test the sample means of the two data series. The sample means and standard deviations were determined directly from the rankit plots. A straight line was drawn by using an eyeball estimate of the best fit through the distributions of each data series and the distributions were then intersected at the 0

rankit for determining the mean and the 1 rankit for determining the standard deviation. The results of this statistical analysis for each trace element and metal are found in Table 8. P-values less than 0.025 were assumed to indicate a significant difference when performing the statistical analysis.

There are several trace elements and metals that lack sufficient data to perform a statistical analysis. Even though there may be a large number of samples analyzed for a particular metal, if too many samples contain nondetectable levels a mean and standard deviation could not be determined from the rankit plots. This was especially true when the anthropogenic ND data series has only a few samples with detectable concentrations.

The metals detected in the anthropogenic ND wells are attributed to metals mobilizing from naturally occurring minerals in the aquifer. If the anthropogenic ND data series has a higher sample mean than the total data series, the possibility of the metals in the total data series coming from anthropogenic sources is not as likely. When a significant difference occurs statistically in the *t* test and the total data series has a higher sample mean than the anthropogenic ND data series, only the anthropogenic ND data series will be used in the correlation analyses with the natural parameters in the aquifer; otherwise, the entire sample population will be used. Table 9 defines which metals will use the total data series or the anthropogenic ND data series.

Fuel concentrations detected in the anthropogenic ND and total data series were significantly different. The total data series is more contaminated by petroleum hydrocarbons than the anthropogenic ND data series as shown in Figure 6. Higher petroleum hydrocarbon contamination in the total data series could lead to greater metal

mobility due to more biodegradation effects. Higher metals in the total data series could also indicate possible anthropogenic sources contributing to the metals in solution. Little difference was observed between the two data series indicating a low probability of anthropogenic source of metals, but also shows a poor indication of metal mobilization due to petroleum hydrocarbon biodegradation.

Table 8: Statistical Comparison of the Means for the Total & Anthropogenic ND Sample Populations

Metal or Trace Element	Sample Mean*	Sample Standard Deviation	Number of Samples	*t* Statistic	Degrees of Freedom	P-Value
Aluminum	2.0	1.48	775	-8.174	74	<0.0001
Aluminum (ND)**	3.0	0.78	50			
Antimony	0.3	0.70	833	0.0	60	0.5
Antimony (ND)	0.3	1.18	58			
Arsenic	-0.5	1.12	926	-3.731	88	0.0002
Arsenic (ND)	0.0	1.18	77			
Barium	1.7	0.78	919	1.241	103	0.109
Barium (ND)	1.6	0.70	84			
Beryllium	Lack of Data					
Cadmium	Lack of Data					
Calcium	5.0	0.30	811	1.43	70	0.079
Calcium (ND)	4.9	0.57	68			
Chromium	-0.7	1.39	1032	-4.744	106	<0.0001
Chromium (ND)	-0.10	1.09	84			
Cobalt	0.0	0.70	695	0.0	50	0.5
Cobalt (ND)	0.0	1.00	48			
Copper	-0.30	1.15	1065	-1.836	98	0.035
Copper (ND)	-0.05	1.22	86			
Iron	3.0	1.02	1008	-2.183	61	0.016
Iron (ND)	3.3	1.00	56			
Lead	-0.3	1.30	1606	-2.428	176	0.008
Lead (ND)	0.0	1.48	154			
Magnesium	4.3	0.40	816	0.0	78	0.5
Magnesium (ND)	4.3	0.40	68			
Manganese	2.0	1.00	978	-3.465	60	0.0005
Manganese (ND)	2.5	1.00	55			
Mercury	Lack of Data					
Molybdenum	Lack of Data					
Nickel	0.0	1.00	1010	1.343	101	0.091
Nickel (ND)	-0.2	1.00	87			

*the sample means are represented in log units, **ND represents the sample populations that have been analyzed for anthropogenic contamination and did not detect any contamination.

Table 8: Statistical Comparison of the Means for the Total & Anthropogenic ND Sample Populations (cont)

Metal or Trace Element	Sample Mean*	Sample Standard Deviation	Number of Samples	*t* Statistic	Degrees of Freedom	P-Value
Potassium	3.5	0.37	782	0.0	76	0.5
Potassium (ND)	3.5	0.37	66			
Selenium	Lack of Data					
Silver	Lack of Data					
Sodium	4.6	0.70	834	-3.183	85	0.001
Sodium (ND)	4.8	0.63	71			
Thallium	Lack of Data					
Vanadium	-0.3	0.78	692	-2.160	53	0.018
Vanadium (ND)	0.0	0.95	49			
Zinc	0.5	1.12	1073	0.0	105	0.5
Zinc (ND)	0.5	1.12	90			
Fuels	1.5	1.52	2305	4.877	186	<0.0001
Fuels (ND)	0.8	1.82	169			

*the sample means are represented in log units, **ND represents the sample populations that have been analyzed for anthropogenic contamination and did not detect any contamination.

Table 9: Determination of Metal Data Series to be Used for Correlation Analyses

Total & Anthropogenic ND Data Series Not Significantly Different (Use Total Data Series)	Total & Anthropogenic ND Data Series Significantly Different, Anthropogenic ND > Total (Use Total Data Series)	Lack of Sufficient Data to Perform Statistical Analysis (Use Total Data Series)
Sb, Ba, Ca, Co, Mg, Ni, K, Zn	Al, As, Cr, Cu, Fe, Pb, Mn, Na, V	Be, Cd, Hg, Mo, Se, Ag, Tl

Since the correlation analyses will use the total data series for each metal, the impact of petroleum hydrocarbons on the metal mobility phenomenon may be more clearly illustrated by larger data sets and by more extensive fuel contamination.

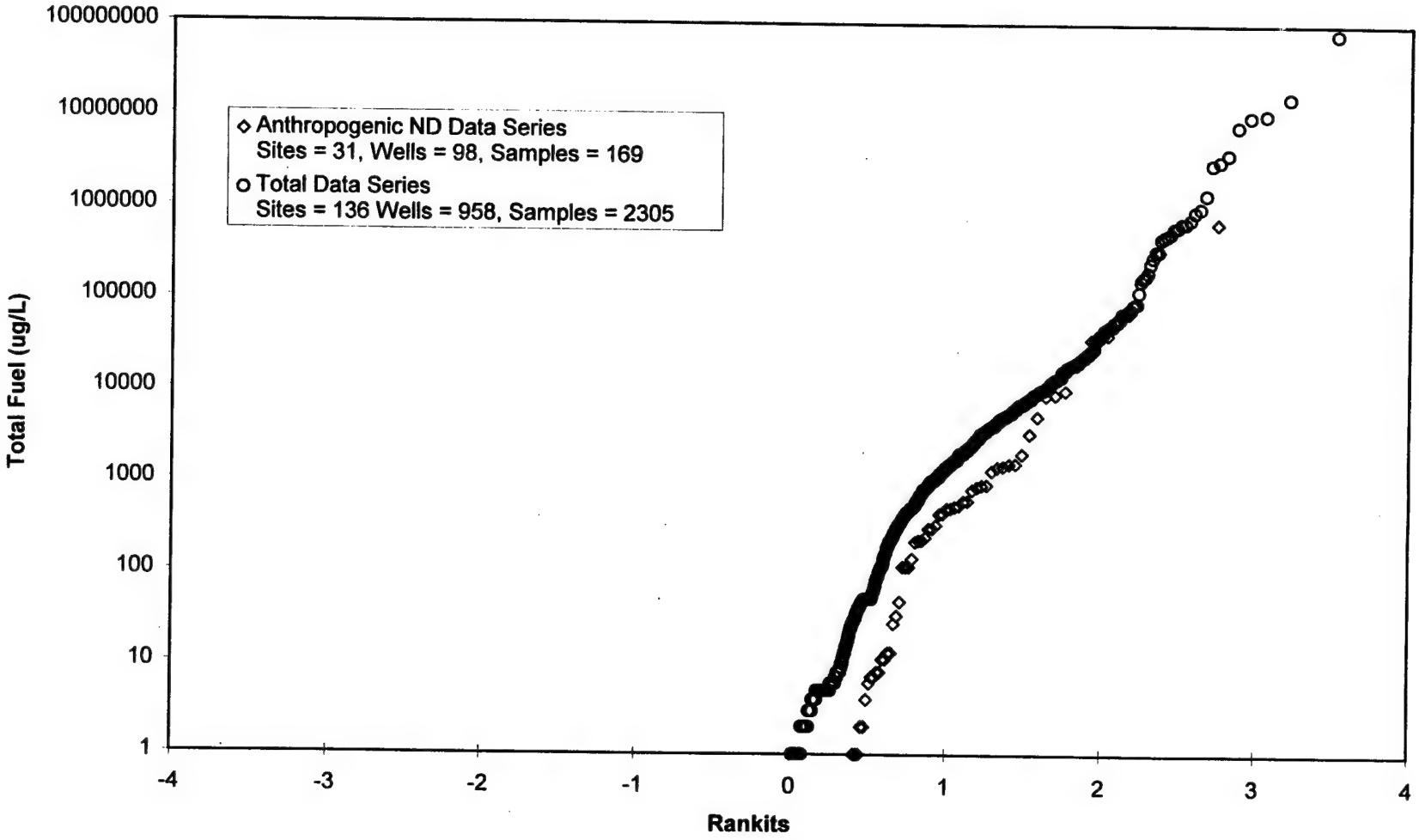

Figure 6: Total Fuel Rankit Plot for Anthropogenic ND & Total Data

Significance of Metal Concentrations

The rankit plots demonstrate that metals are present in the groundwater at fuel contaminated sites. Every metal that has a drinking water standard exceeded the established maximum contaminant level (MCL) for one or more samples. The copper distribution contained only one outlying concentration level that surpassed the MCL and it may not be representative of the true distribution. Metals exceeding the MCL is unexpected, because the primary contamination at the sites investigated is petroleum hydrocarbons and historical site surveys did not reveal any other activities that would contribute to the higher levels detected in the groundwater.

By analyzing the total data series for the metals with drinking water standards, one can determine if they pose a widespread problem. If the MCL intersects the distribution before rankit 2, at least 2.5 percent of the total samples in the distribution exceed the MCL. Antimony and lead exceeded their MCLs in 19 percent and 10 percent of samples, respectively. The metals with MCLs are identified in Table 10 by the degree to which they may pose a problem at fuel-contaminated sites.

Table 10: Potential Mobility Problems by Metals with MCLs

Potential Problem	**Probably not a Problem**	**Insufficient Data to Make Determination**
Sb, As, Be, Cd, Cr, Pb, Ni, Se, Tl	Ag, Ba, Cu	Hg

Causes of Metal Mobilization

Location. The data clearly show that high concentrations of metals are present in groundwater at these fuel-contaminated sites, and that it is possible that the metals are of natural origin. In this section the high metal concentrations are linked to geochemical changes in the aquifer caused by the biodegradation of petroleum hydrocarbons.

Some sites contained several wells. When possible, the wells were classified by their position hydraulically in relation to the site, such as upgradient, background, on-site, or downgradient to the contaminant plume. The upgradient and background wells should have lower fuel contaminant levels as compared to the downgradient and on-site wells. Rankit plots (Figure 7) were constructed to determine the extent of fuel contamination in both the upgradient/background wells and downgradient/on-site wells.

Some of the upgradient/background wells did detect petroleum hydrocarbons with 14 of 147 groundwater samples containing fuel concentrations exceeding 1 ppm. The source of fuels could be originating from an adjacent site that is upgradient from the well where the sample was taken. The petroleum hydrocarbons in the upgradient/background data series could potentially skew the metal concentrations higher and may impact statistical analyses when comparing the means of the data series. Rankit plots were constructed for metals concentrations from both upgradient/background wells and downgradient/on-site wells (Appendix G).

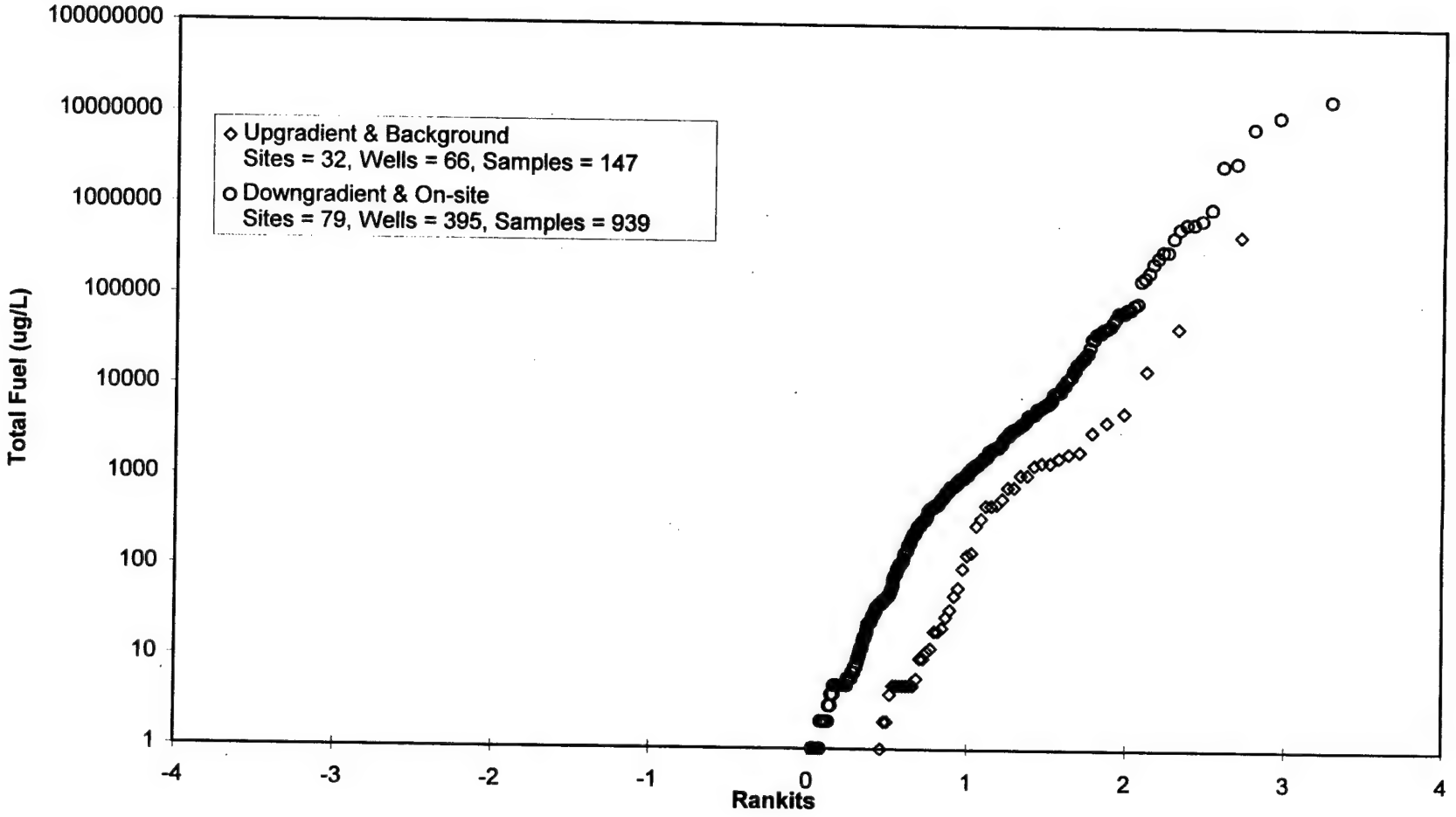

Figure 7: Total Fuel Rankit Plots for Upgradient/Background & Downgradient/On-site Data Series

Visual inspection of the rankit plots leads to classifying the metals in three categories as defined by the upgradient/background data plotting consistently above, about the same, or generally below the background/on-site data. This classification of metals is displayed in Table 11. If less than five data points were above non-detect in a series, the metal was not classified.

The metal concentration means for the two data series are derived from the rankit plots and statistically analyzed by using the two sample *t* test with unequal variances. There is a problem with several of the data series not having enough detectable metal concentrations for determining the mean or standard deviation from the rankit plots and no statistical conclusions could be made. A significant difference in the means was defined by a P-value less than 0.025. The results of these statistical analyses are also summarized in Table 11, and given in detail in Table 12.

Table 11: Summary of Comparison of Upgradient/Background (U/B) and Downgradient/On-site (D/O) Metals Concentrations

Analysis	**U/B < D/O**	**U/B ≈ D/O**	**U/B > D/O**	**Too Little Data**
Visual	Sb, As, Ba, Be, Cd, Cr, Co, Cu, Pb, Mn, Ni, Se, V	Ca, Fe, Mg, K, Na, Zn	Al	Hg, Ag, Tl, Mo
Statistical	Ba, Cu, Mn, Zn	Al, Ca, Cr, Co, Fe, Pb, K, Na	Mg	Sb, As, Be, Cd, Hg, Mo, Ni, Se, Ag, Tl, V

Table 12: Statistical Comparison of the Means for the Upgradient/Background and Downgradient/On-site Sample Populations

Metal or Trace Element	Sample Mean*	Sample Standard Deviation	Number of Samples	*t* Statistic	Degrees of Freedom	P-Value
Aluminum (D/O)**	2.4	1.2	395	-0.499	113	0.309
Aluminum (U/B)***	2.5	1.4	85			
Antimony	Lack of Data					
Arsenic	Lack of Data					
Barium (D/O)	1.7	1.0	479	6.064	123	<0.0001
Barium (U/B)	1.0	1.0	89			
Beryllium	Lack of Data					
Cadmium	Lack of Data					
Calcium (D/O)	5.0	0.4	477	0.0	101	0.5
Calcium (U/B)	5.0	0.5	85			
Chromium (D/O)	-1.15	1.9	500	1.316	157	0.095
Chromium (U/B)	-1.40	1.7	101			
Cobalt (D/O)	-0.3	1.0	376	0.0	126	0.5
Cobalt (U/B)	-0.3	0.9	81			
Copper (D/O)	-1.0	1.9	569	1.959	137	0.024
Copper (U/B)	-1.4	1.9	100			
Iron (D/O)	3.3	1.0	495	0.0	122	0.5
Iron (U/B)	3.3	1.0	89			
Lead (D/O)	0.7	1.1	824	0.0	210	0.5
Lead (U/B)	0.7	1.1	152			
Magnesium (D/O)	4.3	0.5	475	-3.49	125	0.0003
Magnesium (U/B)	4.5	0.4	85			
Manganese (D/O)	2.3	1.0	474	4.56	94	<0.0001
Manganese (U/B)	1.3	2.0	87			
Mercury	Lack of Data					
Molybdenum	Lack of Data					
Nickel (D/O)	Lack of Data					
Potassium (D/O)	3.5	0.4	462	0.0	97	0.5
Potassium (U/B)	3.5	0.5	81			
Selenium	Lack of Data					
Silver	Lack of Data					
Sodium (D/O)	4.7	0.8	501	1.203	124	0.116
Sodium (U/B)	4.6	0.7	86			
Thallium	Lack of Data					
Vanadium	Lack of Data					
Zinc (D/O)	0.5	1.0	571	3.121	115	0.001
Zinc (U/B)	0.0	1.5	100			
Fuels (D/O)	1.0	2.0	939	5.761	197	<0.0001
Fuels (U/B)	0.0	2.0	147			

*the sample means are represented in log units,

** data series represented by downgradient/on-site metal concentrations

*** data series represented by upgradient/background metal concentrations

Concentrations of a few metals (Ba, Cu, Mn, Zn) clearly increase when the well is located downgradient of or on the petroleum hydrocarbon sites. These results may indicate mobilization of these metals due to geochemical changes caused by petroleum hydrocarbon biodegradation. Many of the primary cations show no change in concentration due to location, and many of the metals simply have too few data to make an accurate assessment.

Higher concentrations of manganese in the downgradient/on-site wells is consistent with the studies performed by Champ et al. (1979), Bennett et al. (1993), and Jackson and Patterson (1982). As the fuels are oxidized, Mn(IV) is reduced to Mn(II) which is more soluble. Iron should also solublize more readily under reducing aquifer conditions, but the data does not clearly demonstrate this is occurring. It is possible that the microbes are using higher energy producing electron acceptors during fuel biodegradation and the microbes will not use iron until the other electron acceptors are depleted from the aquifer sediments.

Metals that are less soluble under reducing conditions such as copper, lead, cadmium, and arsenic do not decrease in concentration in the downgradient/on-site data series where reducing conditions are likely to exist. Visual inspection of the rankit plots for these metal indicates they are actually plotting elevated concentrations in the downgradient/on-site data series which is contrary to the theoretical predictions of Pourbaix (1994).

The rankit plots that have the upgradient/background data nearly the same as downgradient/on-site data series are predominately the major cations (Ca^{2+}, K^{+}, Na^{+}, and

Mg^{2+}) and iron. The concentrations of the major cations tend to be greater in the downgradient/on-site series at the tails of the distributions, but greater in the upgradient/background wells near the upper-mid portions of the distribution. Field research (Bennett et al., 1993; Lovley, 1987; McMahon et al., 1995; Tan, 1980) has tended to demonstrate that these metals are mobilized by changing geochemistry during petroleum hydrocarbon biodegradation. The behavior at the tails of these distributions may be evidence of this phenomenon, even though analysis of the entire data set is inconclusive.

pH. Lowering pH increases metals in solution. The pH of a groundwater sample is sensitive to any changes that may occur during the sampling process. Any contact with the atmosphere will allow equilibration of carbon dioxide between the atmosphere and solution, which will affect pH. Further, depending on the length of the well screen, the sample could be mixing many different vertical levels of groundwater resulting in a composite sample which may not accurately represent the aquifer environment. The pH changes associated with petroleum hydrocarbon biodegradation may be occurring on a microscale in the immediate vicinity of the microbes as indicated in the study by Revsbech and Ward (1984). If the pH changes are occurring on a microscale, the sampling techniques used in the field would not be sensitive enough to detect the pH changes on such a small scale.

Unfortunately, the pH data for groundwater analyses does not establish any significant conclusions with the metal concentrations. Figure 8 illustrates the difficulty of performing the correlation analyses with pH by focusing on copper solubility.

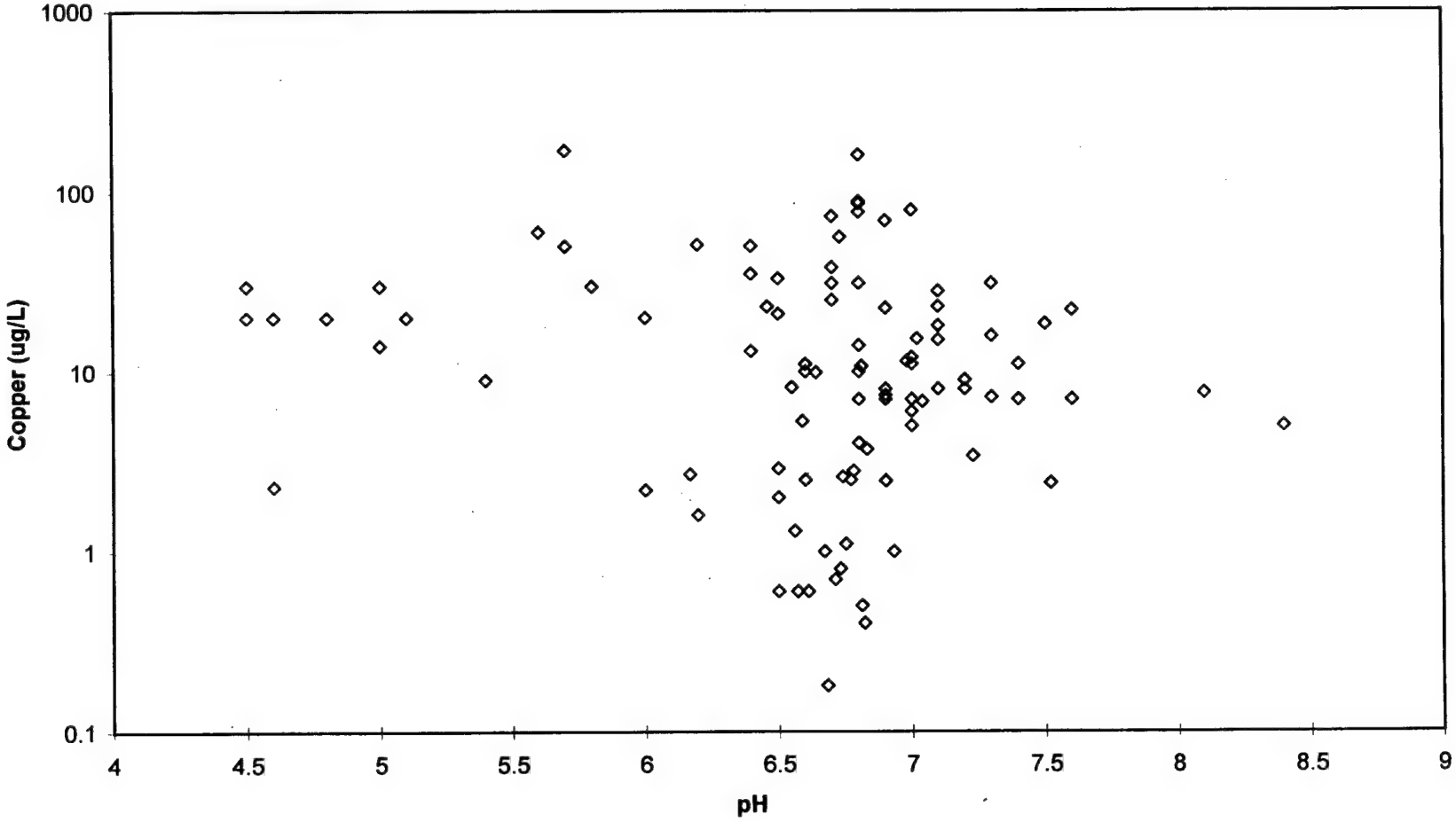

Figure 8: Copper vs pH Scatter

A large range of copper concentrations (from 1 ug/L to 100 ug/L) are detected for a pH level of approximately 7. This wide range of values could be attributed to the varying geological settings that are encountered from site to site. A site that does not have large amounts of copper ore present will not have a high concentration of copper in solution even in low pH conditions. Likewise, if low pH conditions have existed for a long period of time, the copper ore may be depleted and the groundwater flow has removed the soluble copper from the site, leaving only a small copper concentration for detection in the groundwater analysis.

The scatter plot does not show any significant type of correlation between pH and the copper concentrations. This variability in the correlation was typical for the pH analyses on all the metals and not one example could show any type of significant relationship for the pH and metal concentrations. The pH plots for each metal are located in Appendix H. Therefore, pH could not be used as an indicator in this study to validate metal mobilization.

Redox Potential. Changing redox potential in the aquifer will also contribute to metal mobilization. Since direct measurements of the redox conditions in the aquifer were not taken, redox indicators such as low levels of DO and increased concentrations of manganese were used for the analysis.

A strong indicator of microbial activity which facilitates redox reactions can be measured by the concentration of DO in the groundwater. Low levels of DO indicate microbial activity is taking place and reduction reactions may be occurring in the aquifer

environment. Rifai et al. (1988) clearly demonstrated the relationship between fuel component concentrations and DO at an aviation fuel spill.

Groundwater is seldom analyzed for DO; the data set is limited in this study as only 24 samples measured DO concentrations. Figure 9 shows the DO concentrations that were detected in fuel contaminated plumes for the study by Rifai et al. (1988) and those included in this research. The data series for the Rifai study show a more dramatic relationship between fuel concentrations and DO than was indicated by the data series for this study. A similar trend in DO and fuel concentrations does appear between the two data series. The trend would be more apparent for this study, but the plot is skewed by the larger fuel concentrations detected in the Rifai study. Both data series still show that as the fuel concentrations increase, DO is depleted from the groundwater. DO is difficult to accurately measure in the field and great care must be given to prevent the groundwater sample from being exposed to the atmosphere. Once exposed to the atmosphere, oxygen will readily dissolve in the groundwater sample and will no longer represent the DO concentrations within the aquifer which may account for the varying DO concentrations between the two studies.

It has been clearly established that reducing conditions will increase the concentration of Fe^{2+} and Mn^{2+} in solution. Likewise, other metals such as cobalt and nickel could be influenced by the reducing conditions that are encountered during fuel biodegradation.

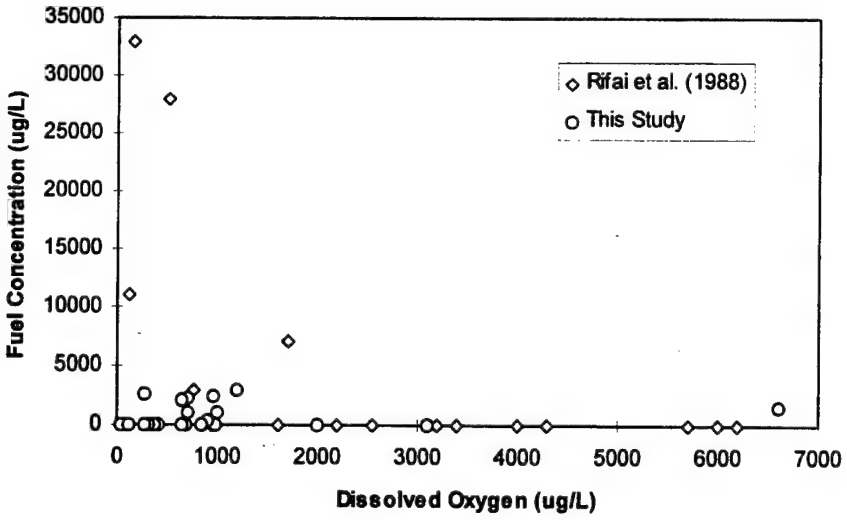

Figure 9: Total Fuel Concentrations vs DO

To explore this possibility, the concentrations of each metal were plotted against the manganese concentrations observed during the same sampling event and a regression analysis was performed to determine whether there a significant correlation exists. Figure 10 is an example of the regression analysis which shows the correlation between nickel and manganese concentrations. The manganese regression plots for each metal are located in Appendix I. The slope for the regression line and the coefficient of determination (R^2) were calculated for each regression plot. The higher the value of R^2, the more successful the linear regression is in explaining the variation of the metal plotted versus the manganese concentrations. Table 13 summarizes the manganese regression results for each metal. Several of the metals (Be, Cd, Hg, Mo, Se, Ag, Tl) are included, but examination of their data plots indicate the data sets are too small to be reliable.

Table 13: Summary of Manganese Regression Analyses

Metal	Slope of Regression Line	R^2
Aluminum	0.4653	0.109
Antimony	0.0089	0.0002
Arsenic	0.2028	0.068
Barium	0.3564	0.284
Beryllium*	0.3518	0.174
Cadmium*	0.067	0.0084
Calcium	0.2131	0.1077
Chromium	0.3458	0.0901
Cobalt	0.2862	0.1904
Copper	0.1823	0.0353
Iron	0.4677	0.1784
Lead	0.0746	0.0067
Magnesium	0.1133	0.0346
Mercury*	0.3897	0.181
Molybdenum*	0.2812	0.0446
Nickel	0.3992	0.1725
Potassium	0.0669	0.0159
Selenium*	0.1818	0.1182
Silver*	-0.0766	0.0173
Sodium	-0.001	<0.0001
Thallium*	-0.3646	0.0669
Vanadium	0.214	0.0795
Zinc	0.0705	0.0055

*sparse data sets

Table 13 indicates that none of the metals show a strong correlation to the manganese concentrations; however, most of the metals (except Ag, Na, Tl) do have positive slopes. Metals such as Co, Fe, Ni, and Tl are more soluble under reducing conditions and should have positive slopes associated with the increasing manganese concentrations. Likewise, other metals such as As, Sb, Cr, and Se are more soluble in oxidizing conditions as they form oxyanions in solution and they should have a negative slope with the increasing manganese concentrations. Major cations such as Na, K, Ca, and Mg have only a single oxidation state, and would not necessarily be expected to have any correlation with Mn.

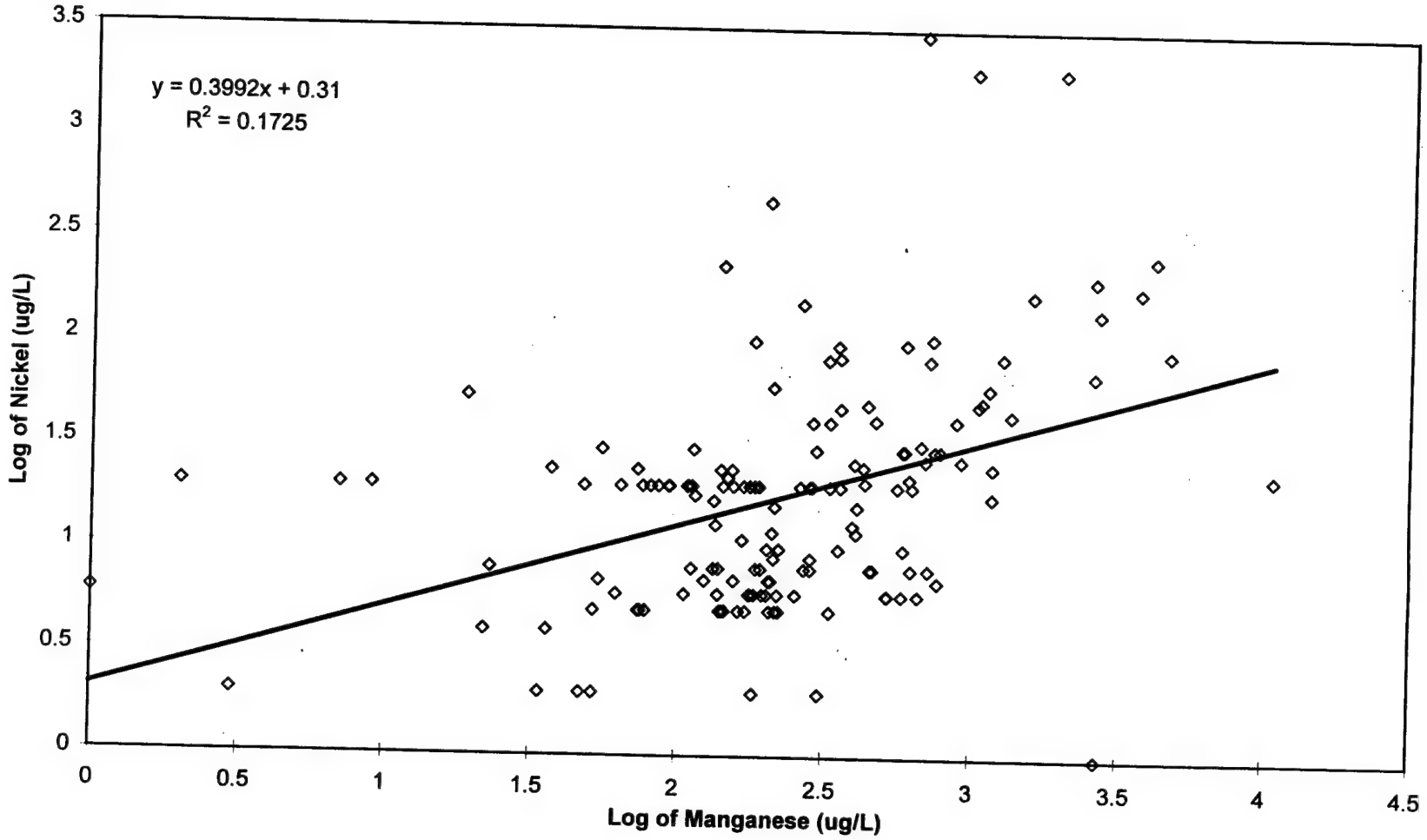

Figure 10: Nickel vs Manganese Scatter Plot

Table 14 summarizes the ranges of the slopes and R^2 values represented by the separate groups. Tl and Se have been omitted because the data sets appear too sparse to be reliable.

Table 14: Manganese Regression Ranges for Metals Soluble Under Reducing or Oxidizing Conditions

Metal Grouping	Range of Slopes	Range of R^2
Soluble Under Reducing Conditions (Co, Fe, Ni)	0.2862 to 0.4677	0.1725 to 0.1904
Soluble Under Oxidizing Conditions (As, Sb, Cr)	0.0089 to 0.3458	0.0002 to 0.1182
Major cations, No Redox Reaction (Na, K, Ca, Mg)	-0.001 to 0.2131	<0.0001 to 0.1077

As predicted, the metals that are most soluble under reducing conditions have greater slopes and R^2 values. The slopes of the metals that are more soluble under oxidizing conditions are unexpectedly also positive. The major cations have the lowest slopes and R^2 values of the three groups.

If manganese is a good indicator of redox potential, the behavior of the metals that are more soluble under reducing conditions, and the major cations that do not undergo redox changes would both appear to conform to theory. The behavior of the metals that become less soluble under reducing conditions would not seem to be explained by redox effects on solubility. One possible explanation for the behavior is that the primary mineral matrix (Ca, Fe, Mn, Al minerals) is dissolved under geochemical conditions caused by petroleum hydrocarbon biodegradation (lower pH, reducing conditions, increased availability of ligands). The dissolution of the parent mineral may be

responsible for the increased concentration of trace metals, regardless of their redox behavior.

Fuel Concentrations. If metals are being mobilized by biodegradation of petroleum hydrocarbons, one would expect some correlation between metals and petroleum hydrocarbon concentrations. Increased levels of petroleum hydrocarbons ought to be associated with lower pH, higher CO_2, greater availability of organic ligands, depletion of oxygen, and more reducing conditions. The correlation would not be universal. Biodegradation could conceivable deplete the petroleum hydrocarbons, but oxidizing conditions may not have been reestablished. Other areas may have high petroleum hydrocarbon concentrations, but no biodegradation due to toxicity. Figure 11 demonstrates a plot of barium versus total fuel concentration observed for the same sampling event. Fuel and metal concentrations are plotted for all metals in Appendix J.

The metal vs fuel scatter plots were statistically analyzed for regression trends. These trends were classified into four categories. Definite trends are comprised of increasing or decreasing with fuel concentration. The other categories include no apparent trend, or there is too little data to tell.

It is difficult to classify some of the metals into these categories. Regression lines with slopes greater than 0.15 will indicate metal concentrations are increasing and slopes less than -0.15 are considered decreasing with fuel concentrations. Metals classified as having no trends have R^2 values less than 0.05 and data series with fewer than 30 data points in the scatter plot had too few points to analyze for a correlation. The results are summarized in Table 15.

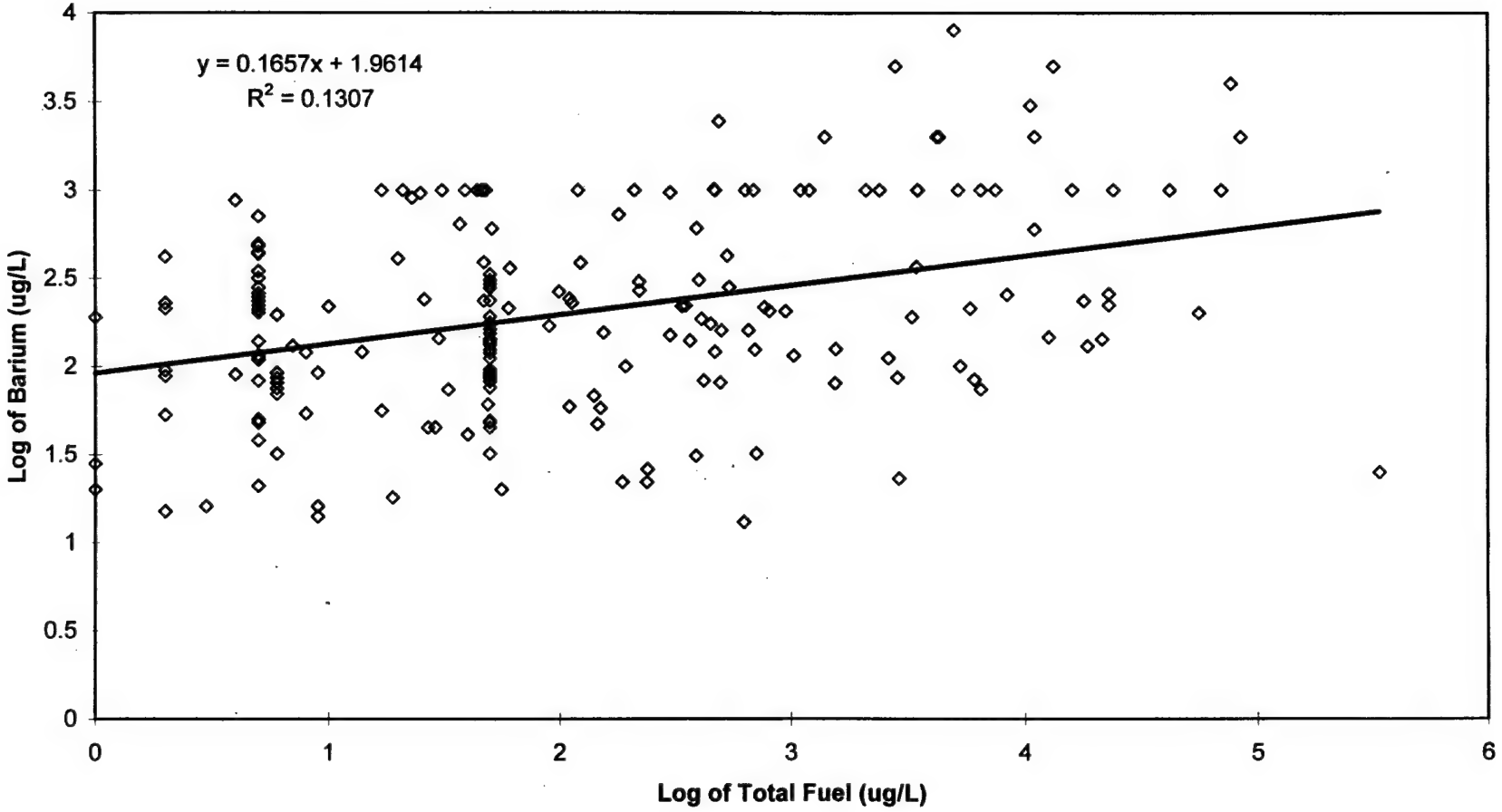

Figure 11: Barium vs Total Fuel Scatter Plot

Table 15: Trends in Plots of Metal vs Fuel Concentrations

Metal Increases With Fuel (Slope > 0.15)	**Metal Decreases With Fuel (Slope < -0.15)**	**No Trend (R^2 < 0.05)**	**Too Little Data (Data pts < 30)**
Al, As, Ba, Fe, Pb, Mn	V	Ag, Sb, Cd, Ca, Cr, Co, Cu, Mg, Ni, K, Na, Zn	Be, Hg, Mo, Se, Tl

The Fe and Mn results are consistent with other researchers (Baedecker et al., 1993; Bennett et al., 1993; Christensen et al., 1994). The Ba and Mn result is consistent with the previous findings of this study where higher concentrations were detected in downgradient and on-site wells. Likewise, the Al and As result is consistent with the increasing Mn concentrations as demonstrated previously in the study. The Pb result may indicate leaded fuels.

The metals that show no correlation were much more evident for the primary cations Ca, Mg, and K which had many more data points. This behavior is consistent with the previous findings of this study where major cation concentrations seemed unaffected by petroleum hydrocarbon biodegradation. The other metals with no apparent trend may be relatively insensitive to fuel concentration as might be expected for Na and Zn, but the trend is not as striking as the ones for the major cations.

Vanadium seemed to decrease with fuel concentration, but the sparse data set adds uncertainty to any conclusions. The other metals are not present in high concentrations so much data is lost to non-detection. Other trends are possible for these metals if lower detection limits could be achieved. Fuel concentration data is in several ways consistent with data concerning well location regressions with Mn to indicate redox state.

Complexation and Carbonate Mineral Solubility. The carbonate system plays an important role in natural water systems. It influences the solubility of carbonate minerals, and bicarbonate and carbonate can form complexes with certain metals. The carbonate system is influenced by biodegradation of petroleum hydrocarbons. The carbon dioxide produced by fuel oxidation increases carbonic acid (lowering pH) and produces more bicarbonate and carbonate ions.

The data set used in this study contained many measurements of alkalinity. If alkalinity is controlled by only carbonates and hydroxide, it is described by equation (1):

$$\text{Alkalinity (as mg/L } CaCO_3) = \{[HCO_3^-] + 2*[CO_3^{2-}] + [OH^-]\} * 50000 \qquad (1)$$

Further, if the pH is below 8 and the total alkalinity is above 50 mg/L as $CaCO_3$ (as is often the case), the total alkalinity can be assumed to be comprised of only bicarbonate.

This section contains plots of barium, copper, lead, and cadmium solubility as influenced by carbonate, oxide, and hydroxide minerals and carbonate and hydroxide complexes (Table 16) as a function of alkalinity and pH. Note that for all four metals, it is the carbonate minerals (not hydroxides or oxides) that control metals solubility. The purpose of the plots is to determine if carbonate mineral solubility and complexes with inorganic ligands can explain the metals concentrations observed at the sites.

Table 16: Minerals and Complexes Used to Determine Metal Solubility

Metal	Minerals	Complexes	Data Source
Ba	$BaCO_3$ (witherite)	$BaCO_3^0$, $BaHCO_3^+$	Nordstrom et al., 1990
Cu	$Cu(OH)_2$, CuO (tenorite); $Cu_2(OH)_2CO_3$ (malachite); $Cu_3(OH)_2(CO_3)_2$ (azurite)	$CuOH^+$, $Cu(OH)_2^0$, $Cu(OH)_4^{2-}$, $Cu_2(OH)_2^{2+}$, $HCuO_2^-$, $CuCO_3^0$, $Cu(CO_3)_2^{2-}$	Morel and Hering, 1993
Pb	$Pb(OH)_2$, $PbCO_3$ (cerussite)	$PbOH^+$, $Pb(OH)_2^0$, $Pb(OH)_3^-$	Morel and Hering, 1993
Cd	$Cd(OH)_2$, $CdCO_3$	$CdOH^+$, $Cd(OH)_2^0$	Morel and Hering, 1993

The barium carbonate (Figure 12) and copper carbonate (Figure 13) solubility limits do not explain the concentrations of the metals detected in solution because the concentrations are far below the solubility limits. The barium and copper concentrations may be limited by some other mineral compounds found within the aquifer (such as sulfates) which were not included in the carbonate solubility calculations. It is also possible the groundwater system had not reached equilibrium with the carbonate minerals which were continuing to dissolve at the time the sample was taken.

Some of the behavior of the lead carbonates (Figure 14) and cadmium carbonates (Figure 15) is consistent with the solubility limits with the carbonate minerals. However, both plots do have metal concentrations that exceed the established carbonate solubility limits. Complexation with ligands which are not considered in the plot may be contributing to the elevated metal concentrations. It also possible that groundwater system has not established equilibrium with the metals in solution and once it reaches equilibrium the metal concentrations may conform to the carbonate solubility limits.

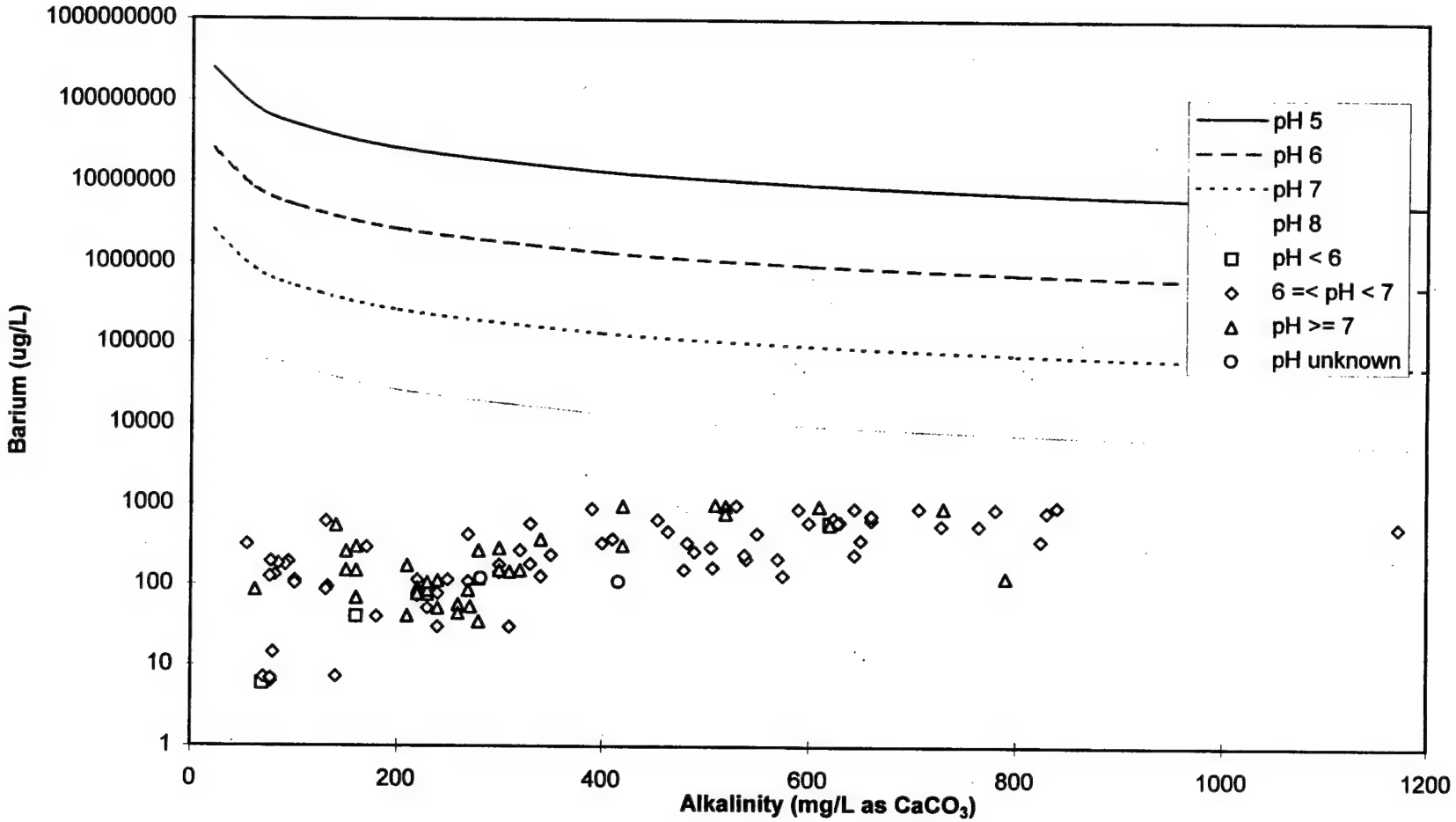

Figure 12: Barium Solubility at 10°C (Nordstrom et al., 1990)

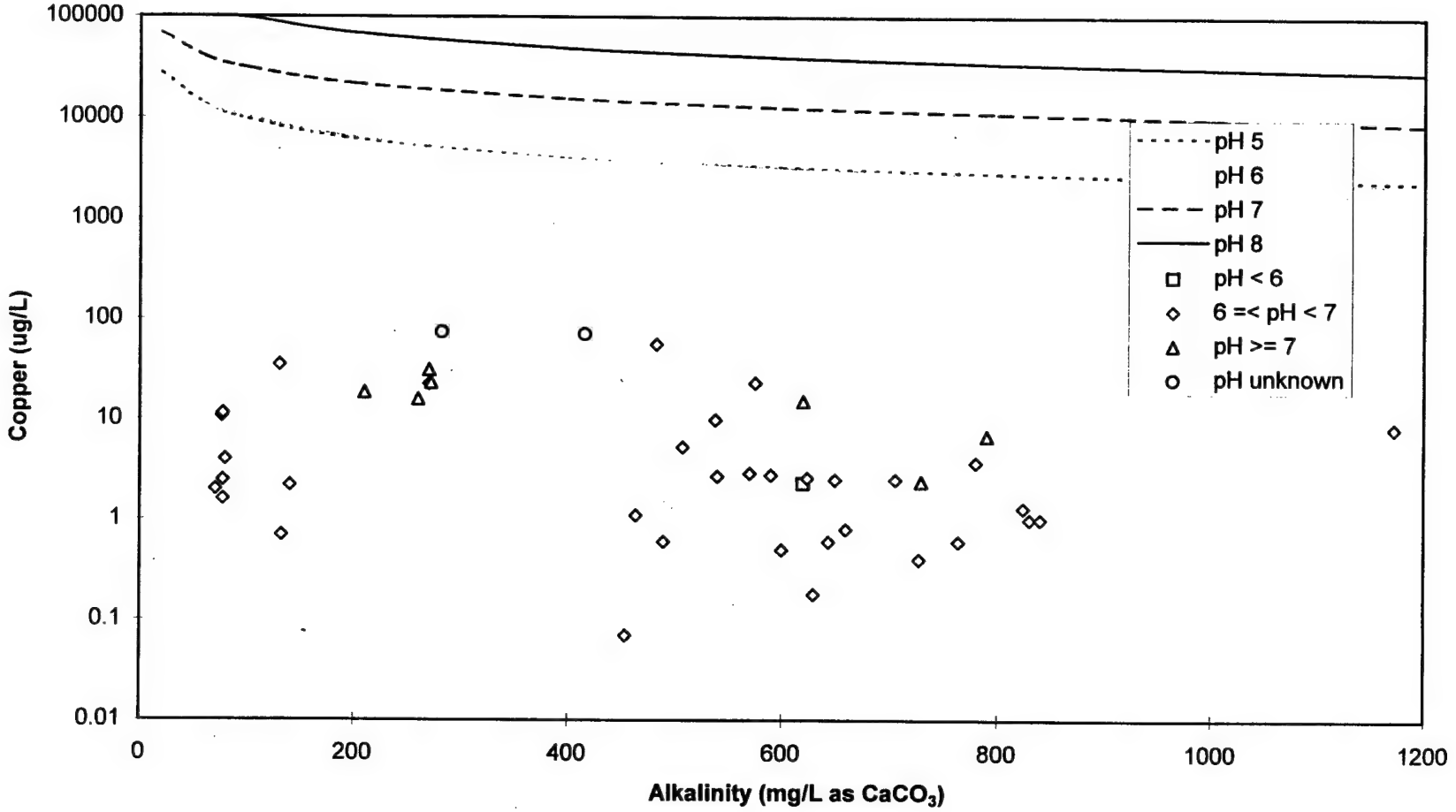

Figure 13: Copper Solubility at 10°C (Morel and Hering, 1993)

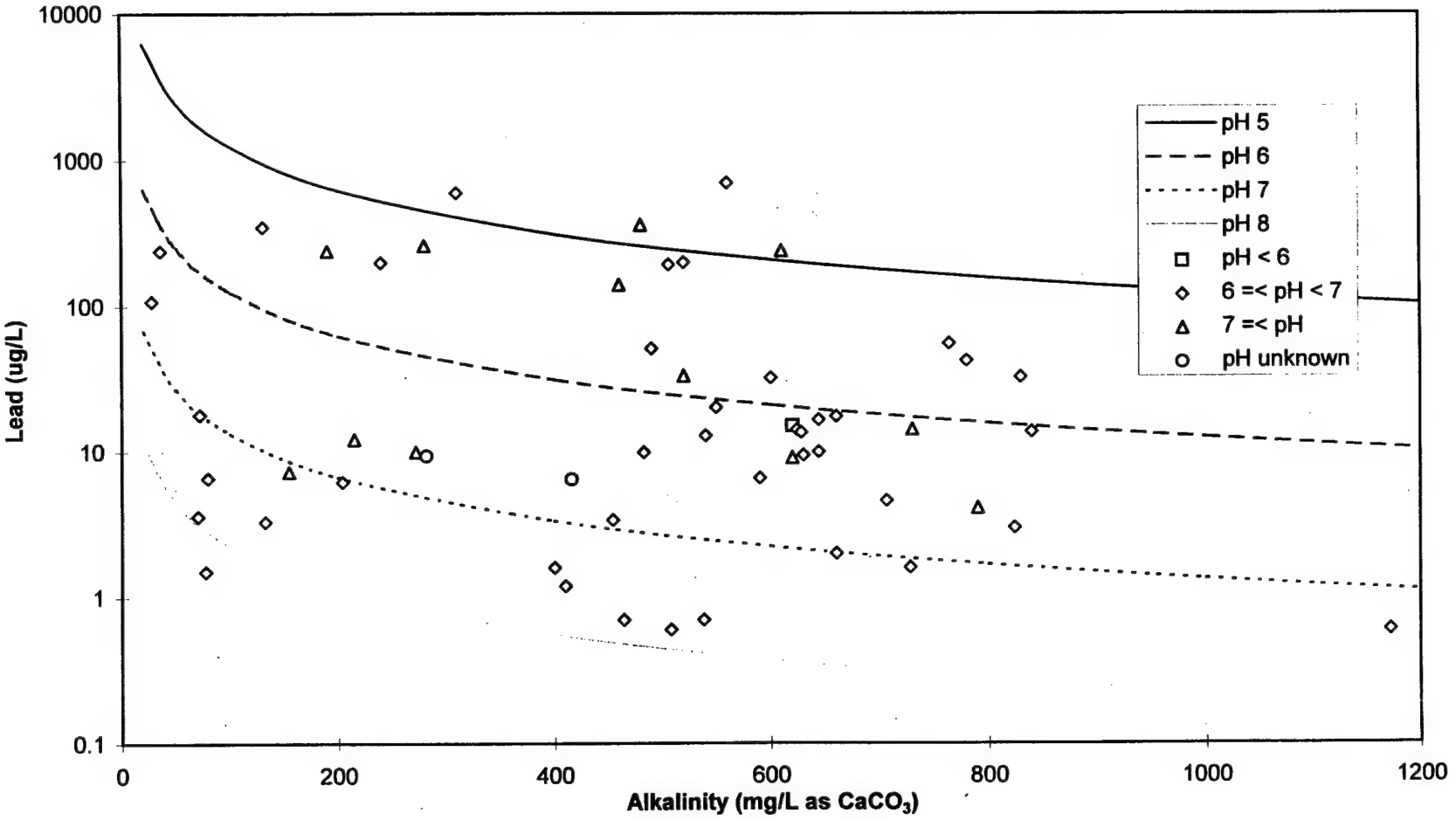

Figure 14: Lead Solubility at 10°C (Morel and Hering, 1993)

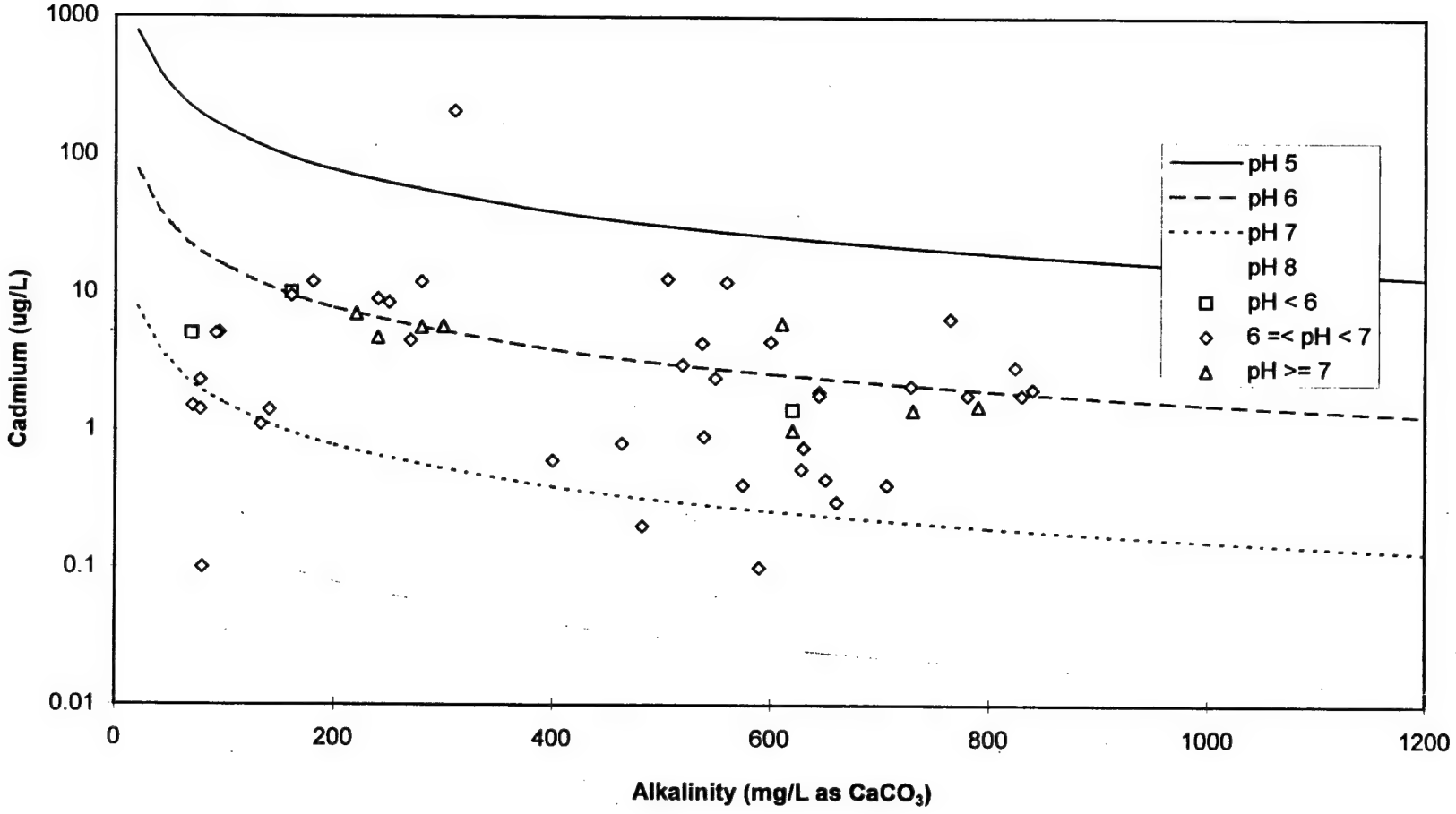

Figure 15: Cadmium Solubility at 10°C (Morel and Hering, 1993)

Alkalinity (assumed to be comprised of bicarbonate ion) does not control the concentration of these four metals in solution. The varying site geological conditions and metal deposits may contribute to the variability between alkalinity and metal concentration. The use of alkalinity may still be used as an indicator of hydrocarbon biodegradation, but the geological parameters must be more clearly defined for each site to fully understand the aquifer environment being investigated.

V. Conclusions

Summary of Significant Findings

This study had two objectives: (1) to determine the extent of metal mobility within petroleum-contaminated aquifers, and (2) to determine if biodegradation petroleum hydrocarbons can explain metal mobility. The approach reviewed the analytical results from 2305 groundwater sampling events, taken from 958 wells, located at 136 fuel contaminated sites found at 53 Air Force installations.

This study showed that high levels of metals are present at petroleum hydrocarbon sites where metals would not generally be expected. Of the metals with MCLs, mercury and silver were detected the least frequently. Barium and copper were detected at the sites, but fewer than 2.5 percent of the samples exceeded their MCLs. All other metals exceeded their MCLs in at least 2.5 percent of the samples, with antimony and lead exceeding their MCLs in 19 percent and 10 percent of samples, respectively.

It was more difficult to attribute the cause of high metals concentrations at these sites. There was no strong evidence that the metals were of anthropogenic origin; it is possible that all of the metals are natural. Higher concentrations of barium and manganese were more strongly correlated with the petroleum hydrocarbon contamination, and there was also some indication of correlation for aluminum, arsenic, iron, and lead. Concentrations of the major cations such as calcium, magnesium, sodium, and potassium were least affected by the petroleum hydrocarbon concentrations. Many of the other

metals were sampled too infrequently or were too often below detection limits to make any strong conclusions.

Correlation of metals with manganese concentrations as an indicator of redox potential had an interesting result. The metals that are most mobile under reducing conditions had the strongest and most positive correlations, and major cations had the weakest and least positive correlation as expected. However, metals that form oxyanions (expected to be mobile under oxidizing conditions) also had a positive correlation with manganese. One possible explanation for this behavior is that these form trace minerals that are caught up in a mineral matrix (such as Al Ca, Fe, or Mn minerals), and are released when this parent mineral structure is dissolved by geochemical changes affected by petroleum hydrocarbon biodegradation.

The specific findings from the study are as follows:

1. All 24 metals investigated in this study were detected in solution at sites that are believed to be contaminated only by petroleum hydrocarbons;

2. Sb, As, Be, Cd, Cr, Pb, Ni, Se, and Tl which have drinking water standards had at least 2.5 percent of their metal concentrations exceeding the established MCL and may pose potential problems due to natural metal mobilization;

3. The downgradient/on-site metal concentrations for Ba, Cu, Mn, and Zn were significantly elevated above the upgradient/background concentrations;

4. Although the downgradient/on-site metal concentrations were not all statistically significantly elevated, As, Ba, Be, Cd, Cr, Co, Cu, Fe, Pb, Mn Ni, Se, and V did have concentrations that were consistently above the upgradient/background concentrations;

5. Reducing groundwater conditions caused by fuel biodegradation are associated with increased manganese solubility. All correlations between metals and Mn concentrations were weak, but the correlations were strongest and most positive for metals that become more soluble under reducing conditions, followed by metals that

become less soluble under reducing conditions, and was least positive and weakest for major cations that are not subject to changes in oxidation state;

6. Carbonate mineral solubility limits as determined by alkalinity and pH did not consistently predict the observed concentrations of barium, copper, lead, or cadmium.

7. Ba, Pb, Fe, and Mn show a positive correlation with fuel concentrations, while major cations like Ca, Mg, and K tend to be relatively constant regardless of fuel concentrations.

Recommendations for Future Research

Further field data collection must include specific aquifer parameters such as DO, methane, nitrate/nitrite, sulfate, and organic acids produced by the microbes during the biodegradation of petroleum hydrocarbons. These parameters would allow a more direct correlation to the factors that may be influencing the metal mobility. Where possible, it would be interesting to compare fuel contaminated sites with the pristine background aquifer conditions to see if a more significant variation is observed in the metal concentrations. The aquifer solids should also be analyzed to determine the quantities of the trace elements available for dissolution in the groundwater. There are several sites with elevated metal concentrations identified in the data that would be excellent candidates for this type of follow-up study.

Appendix A: Summary of Bases, Sites, and Wells

Air Force Installation, State	Number of Sites	Number of Wells
Air Force Plant No. 4, TX	6	29
Air Force Plant No. 6, GA	1	3
Air Force Plant PJKS Waterton, CO	5	15
Andrew AFB, MD	4	24
Barksdale AFB, LA	3	3
Beale AFB, CA	1	7
Campion AFS, AK	1	4
Cape Canaveral AFS, FL	3	7
Charleston AFB, SC	2	13
Carswell AFB, TX	1	9
Dover AFB, DE	7	41
Duluth International Airport AFRES, MN	1	6
Edward AFB, CA	4	67
Eglin AFB, FL	1	3
Elmendorf AFB, AK	6	17
F. E. Warren AFB, WY	2	11
Fairchild AFB, WA	3	22
Galena Airport AFS, AK	3	53
Gunter Annex, AL	1	4
Hickam AFB, HI	1	7
Hill AFB, UT	1	4
Homestead AFB, FL	10	108
Hanscom AFB, MA	1	5
Holloman AFB, NM	5	23
Kelly AFB, TX	1	3
Laughlin AFB, TX	1	12
Langley AFB, VA	2	10
Loring AFB, ME	2	8
MacDill AFB, FL	4	36
March AFB, CA	4	17
Mather AFB, CA	1	1
Maxwell AFB, AL	1	3
McConnell AFB, KS	3	27
McGuire AFB, NJ	2	3
McChord AFB, WA	1	5
McEntire ANGB, SC	1	4
Minneapolis/St. Paul International Airport ARS, MN	1	5
Moody AFB, GA	1	17
Myrtle Beach AFB, SC	3	11
Nellis AFB, NV	2	53
Niagara Falls International Airport ARS, NY	1	3
Norton AFB, CA	3	19

Air Force Installation, State	Number of Sites	Number of Wells
O'Hare International Airport ARS, IL	1	4
Pease AFB, NH	1	5
Plattsburgh AFB, NY	4	13
Robins AFB, GA	1	30
Shaw AFB, SC	2	47
Travis AFB, CA	3	16
Volk Field ANGB, WI	1	1
Vandenberg AFB, CA	2	6
Williams AFB, AZ	1	28
Wright-Patterson AFB, OH	10	74
Wurtsmith AFB, MI	3	12

Appendix B: Metal &Trace Element With Maximum Contaminant Levels (MCL)

Trace Element Name	MCL (mg/L)
Aluminum	NA
Antimony	0.006
Arsenic	0.05
Barium	2.0
Beryllium	0.001
Cadmium	0.005
Calcium	NA
Chromium	0.1
Cobalt	NA
Copper	1.3
Iron	NA
Lead	0.015
Magnesium	NA
Manganese	NA
Mercury	0.002
Molybdenum	NA
Nickel	0.1
Potassium	NA
Selenium	0.05
Silver	0.05
Sodium	NA
Thallium	0.002
Vanadium	NA
Zinc	NA

Appendix C: Oracle Queries for IRPIMS and PETRO

The following queries where performed to gather the groundwater data for the analysis. The queries are the same for both IRPIMS and PETRO. To fully understand the structure of the databases, one should consult AFCEE or the Omaha Corps of Engineers. The IRPIMS Data Loading Valid Value List identifies the field and value codes for the data contained in the database and can be obtained from AFCEE.

Query 1: identifies the Air Force installation, Site ID, and Site Description

```
SELECT AFIID, SITEID, STCCODE, SITEIDESC
FROM GSI
WHERE STCCODE IN ('LU','US','SS')
;
```

Query 2: cross-references the Site ID with the Location ID and Site Description.

```
SELECT GSI.AFIID, GSI.SITEID, SLX.LOCID, GSI.STCCODE, GSI.SITEDESC
FROM GSI, SLX
WHERE GSI.SITEID=SLX.SITEID
AND GSI.STCCODE in ('LU','US','SS')
AND GSI.AFIID=SLX.AFIID
;
```

Query 3: identifies all the groundwater analytical results performed for the Site ID and Location ID in question.

```
SELECT DISTINCT SLX.AFIID, SLX.LOCID, RESULTS.MATRIX,
RESULTS.LOGDATE, RESULTS.ANMCODE, GSI.STCCODE, GSI.SITEID
FROM SLX, GSI, RESULTS
WHERE SLX.LOCID=RESULTS.LOCID
AND SLX.AFIID=RESULTS.AFIID
AND GSI.AFIID=SLX.AFIID AND GSI.SITEID=SLX.SITEID
AND GSI.STCCODE in ('LU','US','SS')
AND RESULTS.SACODE LIKE 'N%'
AND RESULTS.MATRIX='WG'
;
```

When the cross-reference did not exist between the Site ID and Location ID, the bases were personally contacted for the groundwater data and manually entered into the Access database.

Appendix D: Categories & Parameters for Groundwater Analytes

Category	Parameter Label	Parameter Name
Metals & Trace Elements	AG	Silver
	AL	Aluminum
	AS	Arsenic
	B	Boron
	BA	Barium
	BE	Beryllium
	CA	Calcium
	CD	Cadmium
	CO	Cobalt
	CR	Chromium
	CU	Copper
	FE	Iron
	HG	Mercury
	K	Potassium
	MG	Magnesium
	MN	Manganese
	MO	Molybdenum
	NA	Sodium
	NI	Nickel
	PB	Lead
	SB	Antimony
	SE	Selenium
	SI	Silicon
	SIL	Silica
	TL	Thallium
	V	Vanadium
	ZN	Zinc
Trace Element Compound	PBO	Organic Lead
Redox Indicators & Natural Ions	ACID	Total Acidity
	ALK	Total Alkalinity as CaCO3
	BR	Bromide
	CL	Chloride
	CO2	Carbon Dioxide
	DO	Dissolved Oxygen in Water
	DOC	Dissolved Organic Carbon
	F	Fluoride
	FL	Fluorene
	HARD	Hardness as CaCO3
	HCO3	Bicarbonate
	I	Iodide
	KN	Total Nitrogen Kjeldahl
	NH4	Exchangeable Ammonia

Category	Parameter Label	Parameter Name
Redox Indicators & Natural Ions (cont)	NO2N	Nitrogen as Nitrite
	NO3N	Nitrogen as Nitrate
	NO3NO2N	Nitrogen as Nitrate and Nitrite
	P	Total Phosphorus
	PDORTHO	Dissolved Orthophosphate
	PH	pH
	PO4	Total Orthophosphate as PO4
	PORTHO	Total Orthophosphate as P
	SC	Specific Conductance
	SO4	Sulfate
	SS	Suspended Solids (Residue, Non-Filterable)
	TDS	Total Dissolved Solids (Residue, Filterable)
	TEMP	Temperature
	TURB	Turbidity
Petroleum Hydrocarbons	4P3H	4-Propyl-3-Heptene
	ACNP	Acenaphthene
	ANTH	Anthracene
	BTBZN	n-Butylbenzene
	BTBZS	sec-Butylbenzene
	BTBZT	t-Butylbenzene
	BTEX	Benzene, Toluene, Ethylbenze, and Xylene combined as one measurement
	BZ	Benzene
	BZAA	Benzo(a)Anthracene
	BZAP	Benzo(a)Pyrene
	BZBF	Benzo(b)Fluoranthene
	BZGHIP	Benzo(g,h,i)Perylene
	BZKF	Benzo(k)Fluoranthene
	BZME	Toluene
	BZMED8	Toluene-D8
	C24N	n-Tetracosane
	C25N	Pentacosane
	C28N	n-Octacosane
	DBAHA	Dibenz(a,h)Anthracene
	DIESELCOMP	Diesel Components
	DMBZA712	7,12-Dimethylbenz(a)Anthracene
	E2DM4BZ	2-Ethyl-1,4-Dimethyl Benzene
	E4DM2BZ	4-Ethyl-1,2-Dimethyl Benzene
	EBZ	Ethylbenzene
	EDMBZ	Ethyl Dimethyl Benzene
	EM3BZ	1-Ethyl-3-Methyl Benzene
	EMBZ	Ethyl Methyl Benzene

Category	Parameter Label	Parameter Name
Petroleum Hydrocarbons (cont)	ETMCYC6NT	trans-1-Ethyl-2-Methyl-Cyclohexane
	GASCOMP	Gasoline Components
	GASOLINE	Specific Indentification of Gasoline
	HPC10C23	Heavy Petroleum Distillates C10-C23
	JP4	Jet Fuel #4
	JP5	Jet Fuel #5
	JP7	Jet Fuel #7
	JP8	Jet Fuel #8
	MTNPH1	1-Methylnaphthalene
	MTNPH2	2-Methylnaphthalene
	NAPH	Naphthalene
	OILGREASE	Total Recovery of Oil/Grease
	PHAN	Phenanthrene
	PHC	Petroleum Hydrocarbons
	PHCD	PHC as Diesel Fuel
	PHCG	PHC as Gasoline
	PHCJ	PHC as Jet Fuel
	POC	Purgeable Organic Carbons
	PYR	Pyrene
	TMB123	1,2,3-Trimethyl Benzene
	TMB124	1,2,4-Trimethylbenzene
	TMB135	1,3,5-Trimethylbenzene
	TMBZ	Trimethyl Benzene
	TMEBZ	Tetramethyl Benzene
	TMEBZ1234	1,2,3,4-Tetramethylbenzene
	TMEBZ1235	1,2,3,5-Tetramethylbenzene
	TMEBZ1245	1,2,4,5-Tetramethylbenzene
	TOC	Total Organic Carbon
	TPH	Triphenylene
	XYLENE	Total Xylene
	XYLENES	Total Xylene
	XYLENES1213	O & M Xylenes
	XYLENES1214	O & P Xylenes
	XYLM	M-Xylene (1,3-Dimethylbenzene)
	XYLMP	M,P-Xylene(Sum of Isomers)
	XYLO	O-Xylene(1,2-Dimethylbenzene)
	XYLP	P-Xylene(1,4-Dimethylbenzene)
Anthroprogenic Contaminants	245T	2,4,5-T (TrichlorophenoxyaceticAcid)
	24D	2,4-D (Dichlorophenoxyacetic Acid)
	24DB	2,4 Dichlorophenoxybutryic Acid
	24DCPHYAA	2,4-Dichlorophenylacetic Acid

Category	Parameter Label	Parameter Name
Anthroprogenic Contaminants (cont)	ACAMFL2	2-Acetylaminofluorene
	ACE	Acetone
	ACNPY	Acenaphthylene
	ACPHN	Acetophenone
	ACRL	Acrolein
	ACRN	Acrylonitrile
	ALDRIN	Aldrin
	ALPHA	Gross Alpha
	AMINOBPH4	4-Aminobiphenyl (4-Biphenylamine)
	AMINONAPH1	1-Naphthylamine
	AMINONAPH2	2-Aminonaphthalene (Beta Naphthylamine)
	ANILINE	Aniline (Phenylamine, Aminobenzene)
	ANLNAM3	m-Phenylenediamine
	ANLNAM4	p-Phenylenediamine
	ARAMITE	Aramite
	AZIPM	Azinphos, Methyl (Guthion)
	AZOBENZENE	Azobenzene
	BBP	Benzyl Butyl Phthalate
	BDCME	Bromodichloromethane
	BECEM	bis (2-Chloroethoxy) Methane
	BETA	Gross Beta
	BHCALPHA	Alpha Hexachlorocyclohexane
	BHCBETA	Beta Hexachlorocyclohexane
	BHCDELTA	Delta Hexachlorocyclohexane
	BHCGAMMA	Lindane
	BIS2CEE	bis (2-Chloroethyl) Ether (2-Chloroethyl Ether)
	BIS2CIE	bis (2-Chloroisopropyl) Ether
	BIS2CIED12	bis(2-Chloroisopropyl) Ether-D12
	BIS2EHP	bis (2-Ethylhexyl) Phthalate
	BPPE4	4-Bromophenyl Phenyl Ether
	BR4FBZ	1-Bromo-4-Fluorobenzene
	BRBZ	Bromobenzene
	BRCLME	Bromochloromethane
	BRME	Bromomethane
	BU2OH	sec-Butyl Alcohol
	BZACID	Benzoic Acid
	BZD	Benzidine
	BZLAL	Benzyl Alcohol
	BZLCL	Benzyl Chloride
	BZLDCL	Benzal Chloride
	BZOTCL	Benzotrichloride

Category	Parameter Label	Parameter Name
Anthroprogenic Contaminants (cont)	BZTZLN	Benzothiazolone
	C4BZ1234	1,2,3,4-Tetrachlorobenzene
	C4BZ1235	1,2,3,5-Tetrachlorobenzene
	C4BZ1245	1,2,4,5-Tetrachlorobenzene
	C4M2PH	4-Chloro-2-Methylphenol
	C4M3PH	4-Cholor-3-Methylphenol
	CARBAZOLE	Carbazole
	CDS	Carbon Disulfide
	CEVETH	2-Chloroethyl Vinyl Ether
	CHLORDANE	Chlordane
	CHLORDANEA	Alpha-Chlordane
	CHLORDANEG	Gamma-Chlordane
	CHLRL	Chloral
	CHRYSENE	Chrysene
	CL10BZ2	Decachlorobiphenyl
	CL3NATE	Trichloronate
	CLACTH	Chloroacetaldehyde
	CLANIL4	4-Chloroaniline
	CLBZ	Chlorobenzene
	CLBZLATE	Chlorobenzilate
	CLBZME	Chlorotoluene
	CLBZME2	2-Chlorotoluene
	CLBZME4	4-Chlorotoluene
	CLC7N	1-Chloroheptane
	CLEA	Chloroethane
	CLFBZ2	1-Chloro-2-Fluorobenzene
	CLHX1	1-Chlorohexane
	CLME	Chloromethane
	CLMME	Chloromethyl Methyl Ether
	CLNPH1	1-Chloronaphthalene
	CLPH2	2-Chlorophenol
	CLPH2D4	2-Chlorophenol-D4
	CLPYRIFOS	Chlorpyrifos
	CMETHB	bis-Chloromethylether
	CN	Cyanide
	CAN	Cyanide, Amenable to Chlorination
	CNPH2	2-Chloronaphthalene
	COUMAPHOS	Coumaphos
	CPHOSPH	Cyclophosphamide
	CPPE4	4-Chlorophenyl Phenyl Ether
	CTCL	Carbon Tetrachloride
	CYM	Cymene
	CYMM	m-Cymene
	CYMO	o-Cymene (o-Isopropyltoluene)
	CYMP	p-Cymene (p-Isopropyltoluene)

Category	Parameter Label	Parameter Name
Anthroprogenic Contaminants (cont)	DALAPON	Dalapon
	DBAJACR	Dibenz(a,j)Acridine
	DBCME	Dibromochloromethane
	DBCP	1,2-Dibromo-3-Chloropropane
	DBF	Dibenzofuran
	DBMA	Dibromomethane
	DBUTYLC	Dibutylchlorendate
	DBZD33	3,3'-Dichlorobenzidine
	DCA	Dichloroethanes
	DCA11	1,1-Dichloroethane
	DCA12	1,2-Dichloroethane
	DCA12D4	1,2-Dichloroethane-D4
	DCBE14T	trans-1,4-Dichloro-2-Butene
	DCBETOT	Total 1,4-Dichloro-2-Butene
	DCBTA14	1,4-Dichlorobutane
	DCBZ12	1,2-Dichlorobenzene
	DCBZ12D4	1,2-Dichlorobenzene-D4
	DCBZ13	1,3-Dichlorobenzene
	DCBZ14	1,4-Dichlorobenzene
	DCE11	1,1-Dichloroethene
	DCE12C	cis-1,2-Dichloroethylene
	DCE12T	trans-1,2-Dichloroethene
	DCE12TOT	Total 1,2-Dichloroethene
	DCP11	1,1-Dichloropropene
	DCP13	1,3-Dichloropropene Mixture
	DCP13C	cis-1,3-Dichloropropene
	DCP13T	trans-1,3-Dichoropropene
	DCP24	2,4-Dichlorophenol
	DEP26	2,6-Dichlorophenol
	DCPA12	1,2-Dichloropropane
	DCPA13	1,3-Dichloropropane
	DCPA22	2,2-Dichloropropane
	DCPROP	Dichloroprop
	DDD	1,1-bis(Chlorophenyl)-2,2-Dichloroethane
	DDD24	o,p'-DDD
	DDD44	p,p'-DDD
	DDE	1,1-bis(Chlorophenyl)-2,2-Dichloroethene
	DDE24	o,p'-DDE
	DDE44	p,p'-DDE
	DDT	1,1-bis(Chlorophenyl)-2,2,2-Trichloroethane
	DDT24	o,p'-DDT
	DDT44	p,p'-DDT
	DDTS	DDT Total

Category	Parameter Label	Parameter Name
Anthroprogenic Contaminants (cont)	DEMETON	Demeton
	DEPH	Diethylphthalate
	DIALLATE	Diallate
	DIAZ	Diazinon
	DICAMBA	Dicamba
	DICHLORVOS	dichlorvos
	DIELDRIN	Dieldrin
	DIMETHAT	Dimethoate
	DINOSEB	Dinoseb
	DISUL	Disulfoton
	DMBZD33	3,3'-Dimethylbenzidine
	DMP24	2,4-Dimethylphenol
	DMPH	Dimethylphthalate
	DN46M	4,6-Dinitro-2-Methylphenol
	DNBP	Di-n-Butyl Phthalate
	DNBZ14	1,4-Dinitrobenzene
	DNOP	Di-n-Octylphthalate
	DNP24	2,4-Dinitrophenol
	DNT24	2,4-Dinitrotoluene
	DNT26	2,6-Dinitrotoluene
	DPA	Diphenylamine
	DPHY12	1,2-Diphenylhydrazine
	EDB	1,2-Dibromoethane
	EE	Diethyl Ether
	EHXN	2-Ethylhexanoic Acid
	EMETHACRY	Ethyl Methacrylate
	EMSULFN	Ethyl Methanesulfonate
	ENDO	Endosulfan
	ENDOSULFANA	Alpha Endosulfan
	ENDOSULFANB	Beta Endosulfan
	ENDOSULFANS	Endosulfan Sulfate
	ENDRIN	Endrin
	ENDRINALD	Endrin Aldehyde
	ENDRINKET	Endrin Ketone
	ENM2BZ	1-Ethenyl-2-Methyl-Benzene
	ETEGLY	Ethylene Glycol
	ETEGLYMBTE	Ethylene Glycol Mono Butyl Ether
	ETHANOL	Ethanol
	ETHOPROP	Ethoprop
	FBZ	Fluorobenzene
	FC11	Trichlorofluoromethane
	FC113	1,1,2-Trichloro-1,2,2-Trifluoroethane
	FC12	Dichlorodifluoromethane
	FENSTHION	Fensulfothion

Category	Parameter Label	Parameter Name
Anthroprogenic Contaminants (cont)	FENTHION	Fenthion
	FLA	Fluoranthene
	GAMMA	Gross Gamma
	HCBU	Hexachlorobutadiene
	HCCP	Hexachlorocyclopentadiene
	HCLBZ	Hexachlorobenzene
	HCLEA	Hexachloroethane
	HCPR	Hexachloropropene
	HEPT-EPOX	Heptachlor Epoxide
	HEPTACHLOR	Heptachlor Epoxide
	HXO2	2-Hexanone
	HYRAZINE	Hydrazine
	IME	Iodomethane
	INDAN	2,3-Dihydro-1H-Indene
	INP123	Indeno(1,2,3-c,d)Pyrene
	IPBZ	Isopropylbenzene
	ISOP	Isophorone
	ISOSAFR	Isosafrole
	M2HXA	2-Methyl Hexanoic Acid
	MALA	Malathion
	MB2CAN44	4,4'-Methylene-bis(2-Chloroaniline)
	MBAS	Methylene Blue Active Substances
	MECHLAN3	3-Methylcholanthrene
	MEK	Methyl Ethyl Ketone
	MEPH2	2-Methylphenol
	MEPH3	3-Methylphenol
	MEPH4	4-Methylphenol
	MERPHOS	Merphos
	MEVINPHOS	Mevinphos
	MIBK	Methyl Isobutyl Ketone
	MMH	Methyl Hydrazine
	MMSULFN	Methyl Methansulfonate
	MPEA11	Alpha Dimethylphenethylamine
	MTLNCL	Methylene Chloride
	MTPYRLN	Methapyrilene
	MTXYCL	Methoxychlor
	NALED	Naled
	NAPHQ14	1,4-Naphthoquinone
	NND3MBZ	N,N-Diethyl-3-Methyl Benzamide
	NNSBU	N-Nitroso-Di-N-Butylamine
	NNSE	N-Nitrosodiethylamine
	NNSM	N-Ntrosodimethylamine
	NNSME	Nitrosomethylethylamine
	NNSMRPH	N-Nitrosomorpholine

Category	Parameter Label	Parameter Name
Anthroprogenic Contaminants (cont)	NNSPH	N-Nitrosodiphenylamine
	NNSPPRD	N-Nitrosopiperidine
	NNSPR	N-Nitrosodi-n-Propylamine
	NNSPYRL	N-Nitrosopyrrolidine
	NO2ANIL2	2-Nitroaniline
	NO2ANIL3	3-Nitroaniline
	NO2ANIL4	4-Nitroaniline
	NO2BZ	Nitrobenzene
	NO2BZD5	Nitrobenzene-D5
	NTPH2	2-Nitrophenol
	NTPH4	4-Nitrophenol
	OX22CLP	2,2'-Oxybis(1-Chloro)Propane
	PARAE	Ethyl Parathion
	PARALD	Paraldehyde
	PARAM	Methyl Parathion
	PBZN	n-Propylbenzene
	PCA	1,1,2,2-Tetrachloroethane
	PCB	Total PCB
	PCB1016	PCB-1016 (Arochlor 1016)
	PCB1221	PCB-1221 (Arochlor 1221)
	PCB1224	PCB-1221 (Arochlor 1224)
	PCB1232	PCB-1232 (Arochlor 1232)
	PCB1242	PCB-1242 (Arochlor 1242)
	PCB1248	PCB-1248 (Arochlor 1248)
	PCB1254	PCB-1254 (Arochlor 1254)
	PCB1260	PCB-1260 (Arochlor 1260)
	PCE	Tetrachloroethylene
	PCLEA	Pentachloroethane
	PCMC	4-Chlororesorcinol
	PCP	Pentachlorophenol
	PDMAABZ	p-Dimethylaminoazobenzene
	PECLBZ	Pentachlorobenzene
	PECLNO2BZ	Pentachloronitrobenzene
	PH246BR	2,4,6-Tribromophenol
	PH2F	2-Fluorophenol
	PHD5	Phenol-D5
	PHEN2F	2-Fluorobiphenyl
	PHEND14	Terphenyl-D14
	PHENO	o-Terphenyl
	PHENOL	Phenol
	PHENOLD6	Phenol-D6
	PHNACTN	Phenacetin
	PHORATE	Phorate
	PHTA	1,2-Benzenedicarboxylic Acid
	PICOLINE2	2-Picoline
	PR2BRCL	2-Bromo-1-Chloropropane

Category	Parameter Label	Parameter Name
Anthroprogenic Contaminants (cont)	PRONAMD	Pronamide
	PYRDN	Pyridine
	RA-226	Radium-226
	RONNEL	Ronnel
	SAFROLE	Safrole
	SEVIN	Sevin (Carbaryl)
	SILVEX	Silvex (2,4,5-TP)
	STIROFOS	Stirofos (Tetrachlorvinphos)
	STY	Styrene
	SULFROFOS	Bolstar
	TBME	Bromoform
	TBPNO	Tributylphosphine Oxide
	TBUTMEE	tert-Butyl Methyl Ether
	TC1112	1,1,1,2-Tetrachloroethane
	TCA	Trichloroethane
	TCA111	1,1,1-Trichloroethane
	TCA112	1,1,2-Trichloroethane
	TCB123	1,2,3-Trichlorobenzene
	TCB124	1,2,4-Trichlorobenzene
	TCB135	1,3,5-Trichlorobenzene
	TCDD2378	2,3,7,8-Tetrachlorodibenzo-p-Dioxin
	TCE	Trichloroethylene
	TCLME	Chloroform
	TCP2346	2,3,4,6-Tetrachlorophenol
	TCP245	2,4,5-Trichlorophenol
	TCP246	2,4,6-Trichlorophenol
	TCPR	Trichloropropane
	TCPR123	1,2,3-Trichloropropane
	TETRALIN	Tetralin
	TFBZME	1,1,1-Trifluorotoluene
	TLDNOHCL	o-Toluidine Hydrochloride
	TLDNONT5	5-Nitro-o-Toluidine
	TMCYHX	Trimethyl Cyclohexane
	TNB135	1,3,5-Trinitrobenzene
	TOKUTHION	Tokuthion (Prothiofos)
	TOTPHEN	Total Recoverable Phenolics
	TOX	Total Organic Halides
	TOX_BR	Total Organic Halides-Brominated
	TOX_CL	Total Organic Halides-Chlorinated
	TOX_I	Total Organic Halides - Iodinated
	TOXAP	Toxaphene
	TPHENA	Phenol (Acid Fraction)
	TPHP	Triphenyl Phosphate

Category	Parameter Label	Parameter Name
Anthroprogenic Contaminants (cont)	UDMH	1,1-Dimethylhydrazine
	VA	Vinyl Acetate
	VC	Vinyl Chloride
	XYL2456CLM	2,4,5,6-Tetrachloro-Meta-Xylene
	ZINOPHOS	Zinophos

Appendix E: Frequency and Highest Concentration of Anthropogenic Contamination

Contaminant	Number of Wells Where Contaminant is the Maximum Contaminant	Highest Concentration Observed (ug/L)
Trichloroethylene (TCE)	73	5400000
Acetone	54	756
1,1-Dichloroethene	34	104000
Fluorobenzene	32	143000
2,4,6-Tribromophenol	30	425
1-Bromo-4-Fluorobenzene	24	111
bis(2-Ethylhexyl) Phthalate	22	390
Total Organic Halides	18	240
1,2-Dichloroethane-D4	17	118
Methylene Chloride	14	16000
1,1,1-Trichloropropane	11	29100
Total Recoverable Phenolics	10	80
cis-1,2-Dichloroethylene	9	1100
1,2-Dibromoethane	8	1030
Chloroform	7	23
trans-1,2-Dichloroethene	7	47000
Tetrachloroethylene	6	3508
1,2-Dichloroethane	6	2300
Nitrobenzene-D5	5	110
Pentachlorophenol	5	1400
Terphenyl-D14	5	290
Gross Beta	5	21
Chlorobenzene	4	880
1,4-Dichlorobenzene	4	1900
Di-n-Butyl Phthalate	3	54
Chloromethane	3	13
1,2-Dichlorobenzene	3	48
Methyl Ethyl Ketone	3	140
Methyl Isobutyl Ketone	3	1680
Phenol	3	83000
Phenol-D5	2	86
Isopropylbenzene	2	40
Trichlorofluoromethane	2	6
2,4,5,6-Tetrachloro-Meta-Xylene	2	120
Bromochloromethane	2	97

Contaminant	Number of Wells Where Contaminant is the Maximum Contaminant	Highest Concentration Observed (ug/L)
Cyanide	2	275
tert-Butyl Methyl Ether	2	650
Benzoic Acid	2	1150
2-Fluorobiphenyl	2	103
Total 1,2-Dichloroethene	2	92
1,3-Dichlorobenzene	1	3000
Dibenzofuran	1	11
4-Chloroaniline	1	5
Carbon Disulfide	1	61
Dibutylchlorendate	1	122
Vinyl Chloride	1	11
1,1,1-Trichloroethane	1	11
Tributylphosphine Oxide	1	100
1,2-Benzenedicarboxylic Acid	1	10
N, N-Diethyl-3-Methyl Benzamide	1	40
Diethyl Ether	1	29
2-Methyl Hexanoic Acid	1	70
1,2-Dichloropropane	1	4000
Isophorone	1	33000
Di-n-Butyl Phthalate	1	12
Dimethylphthalate	1	11
2,4-Dimethylphenol	1	87
Diethylphthalate	1	36

Appendix F: Rankit Plot for Anthropogenic ND & Total Data Series

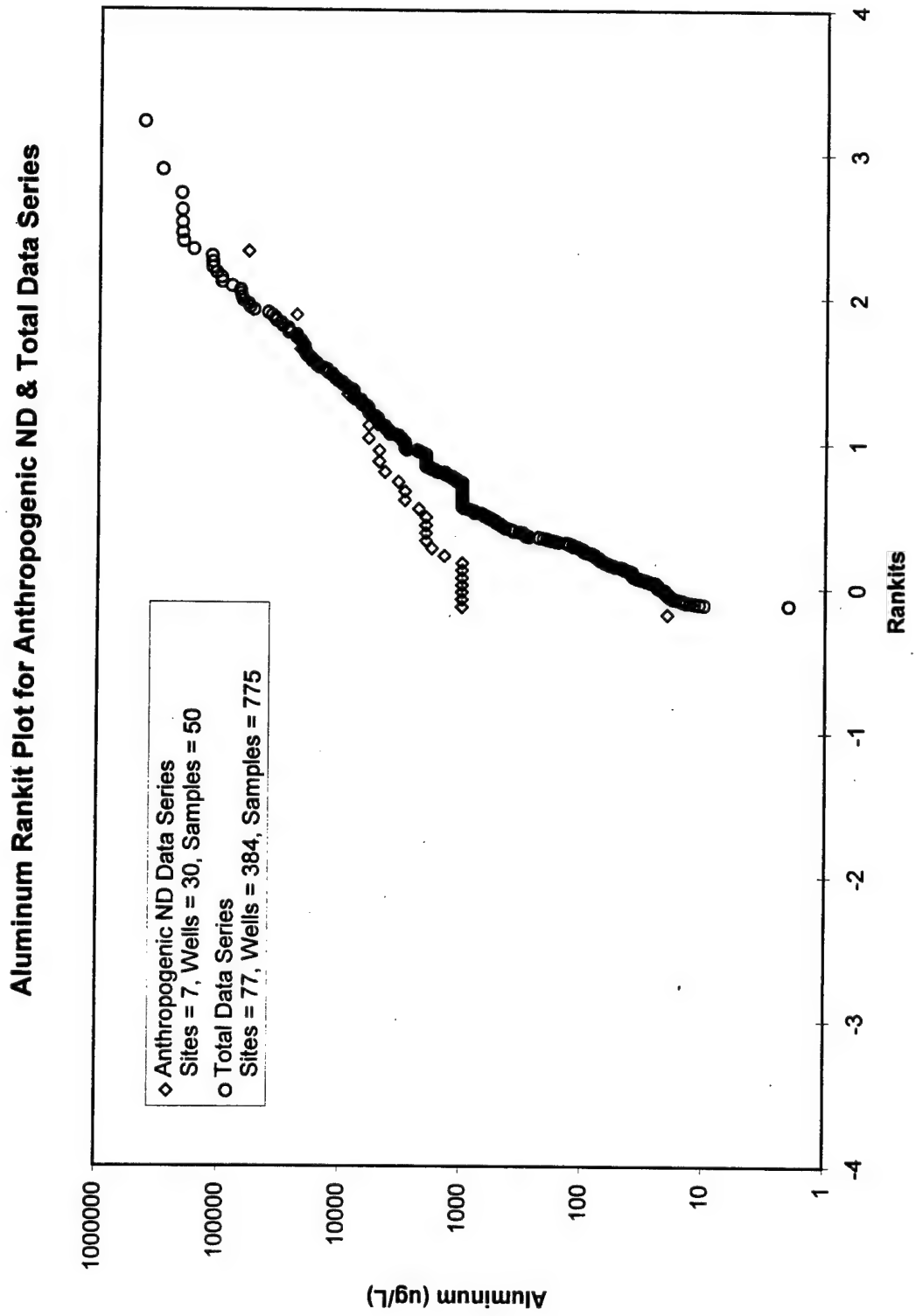

Antimony Rankit Plot for Anthropogenic ND & Total Data Series

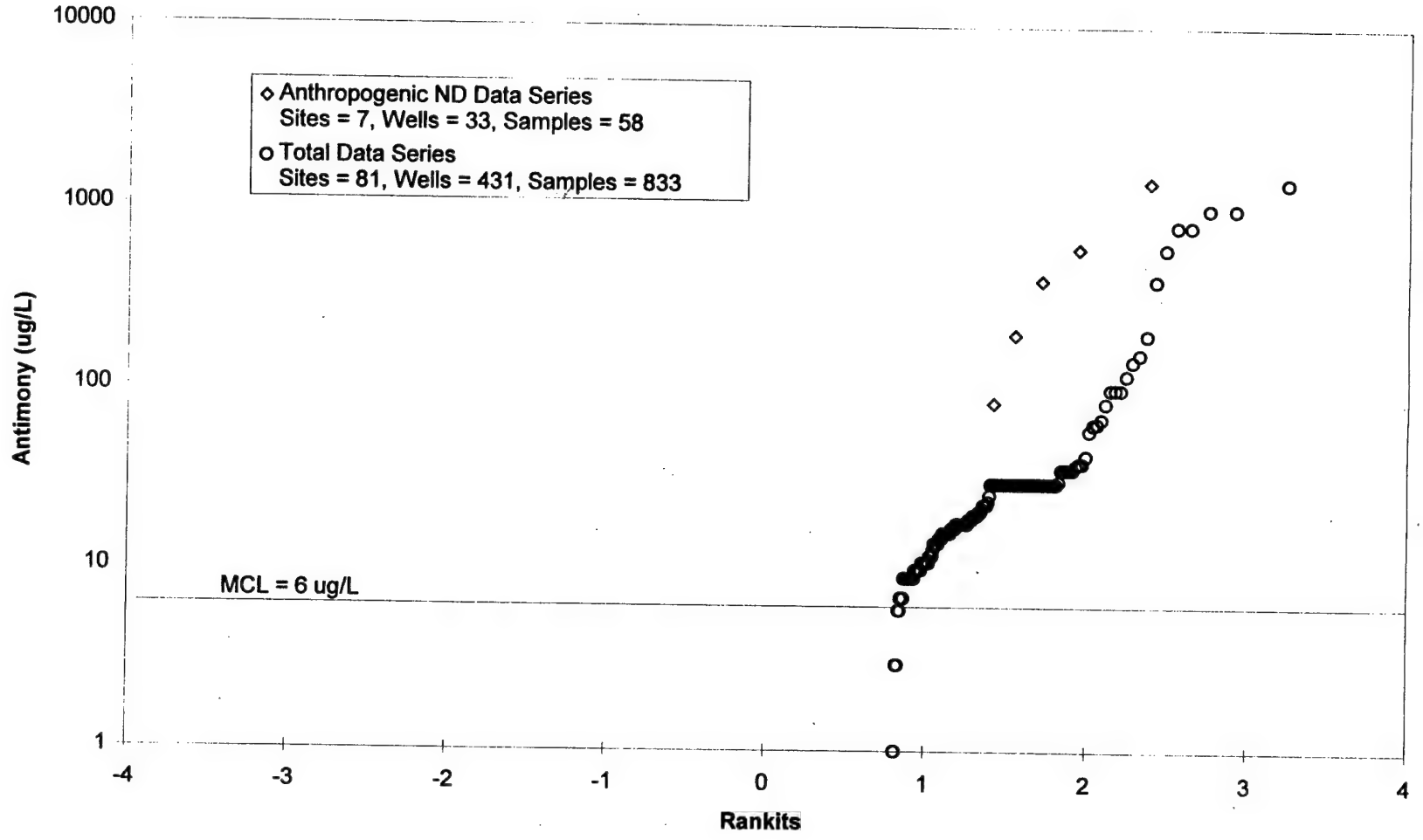

Arsenic Rankit Plot for Anthropogenic ND & Total Data Series

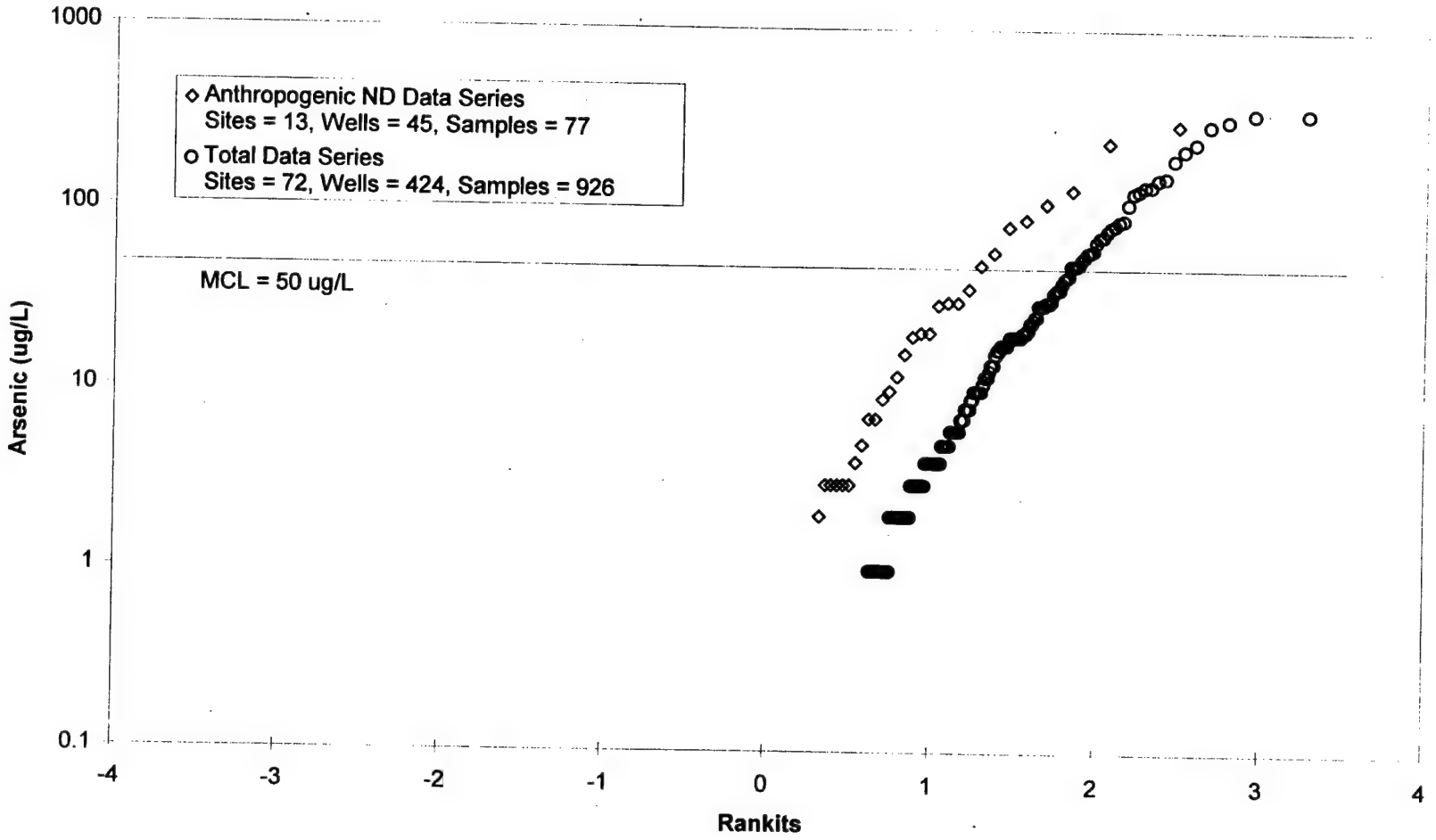

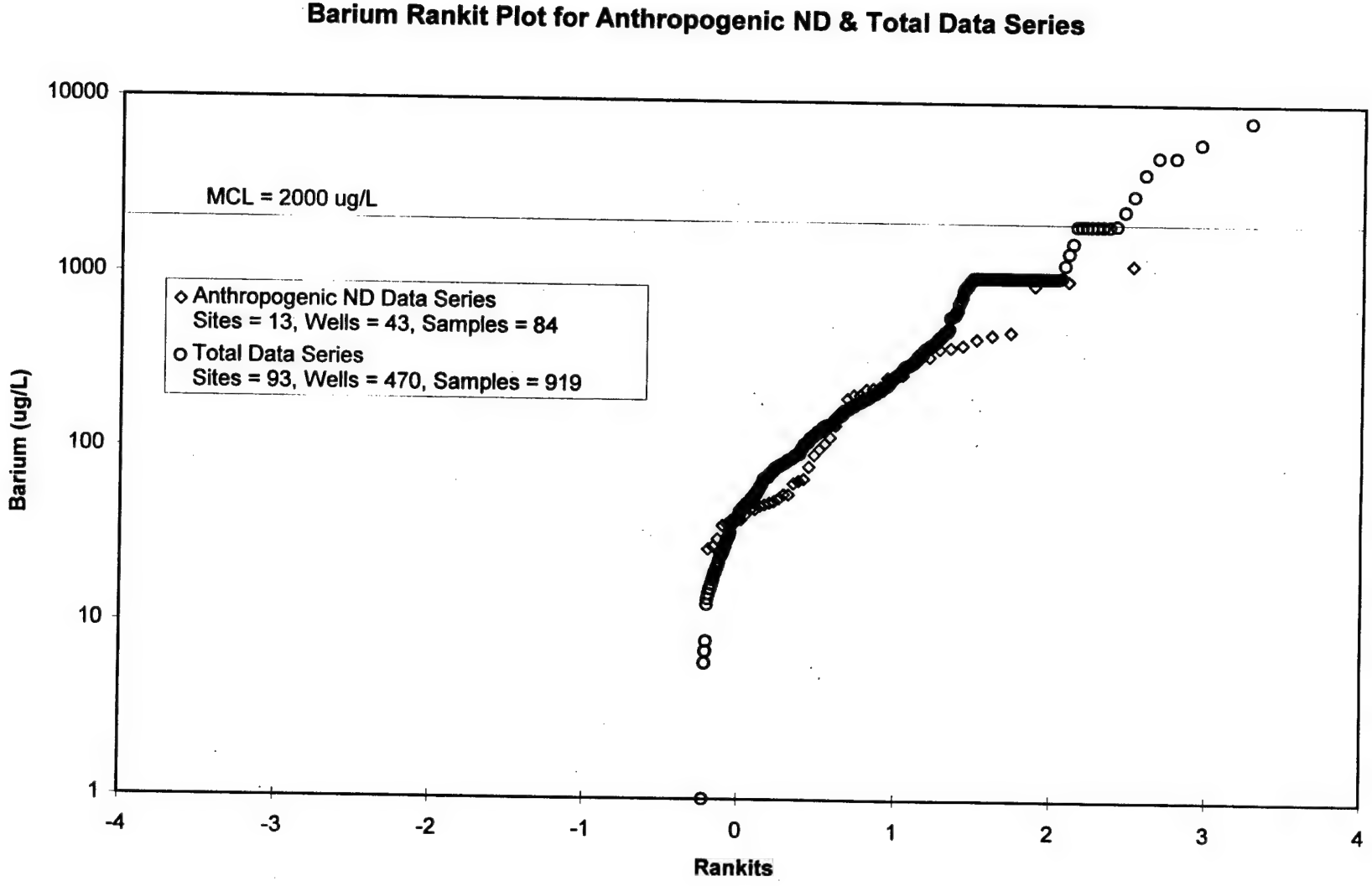
Barium Rankit Plot for Anthropogenic ND & Total Data Series
10000
1000
100
10
1
Barium (ug/L)
MCL = 2000 ug/L
◇ Anthropogenic ND Data Series
Sites = 13, Wells = 43, Samples = 84
o Total Data Series
Sites = 93, Wells = 470, Samples = 919
-4
-3
-2
-1
0
1
2
3
4
Rankits

Beryllium Rankit Plot for Anthropogenic ND & Total Data Series

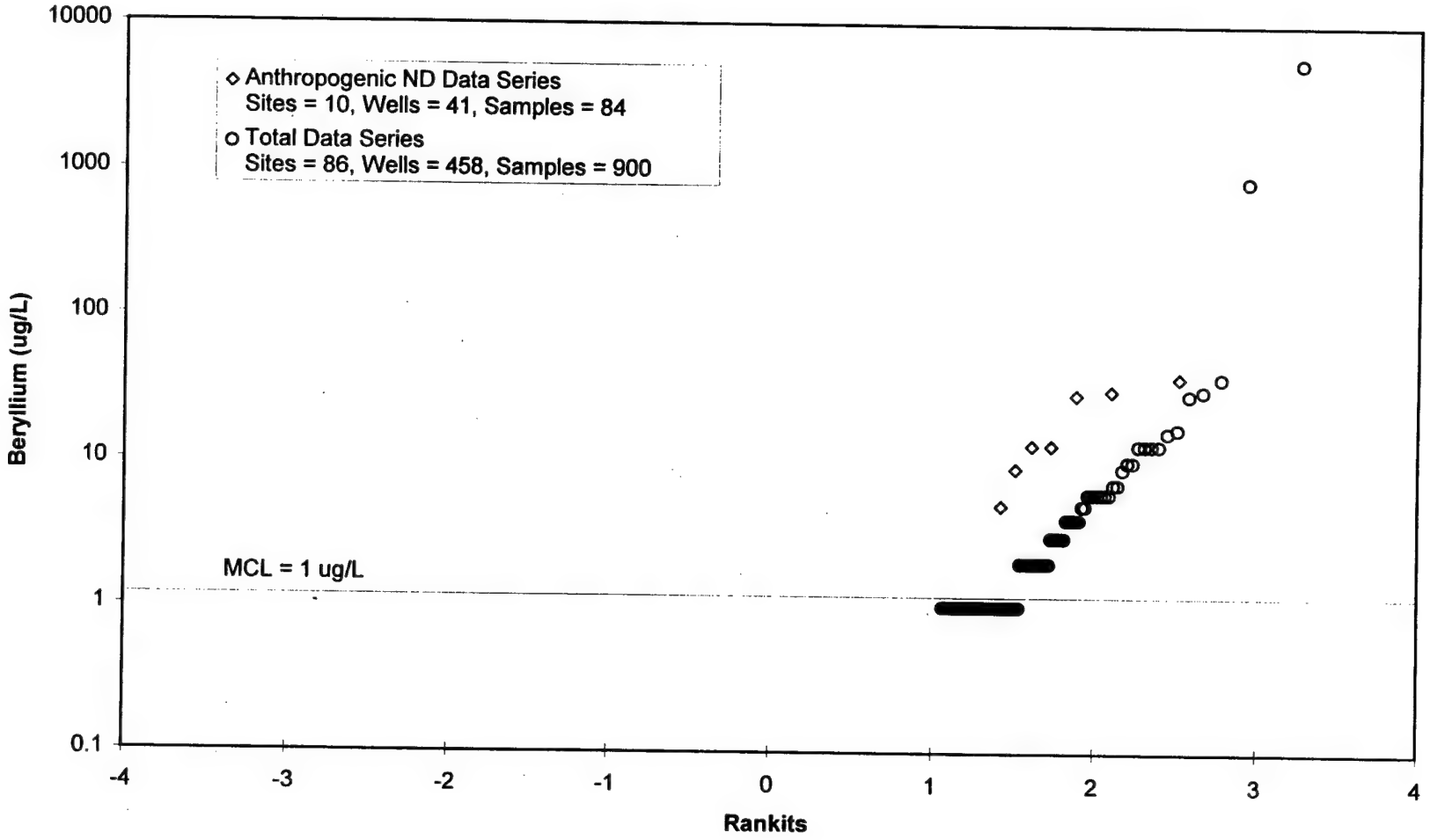

Cadmium Rankit Plot for Anthropogenic ND & Total Data Series

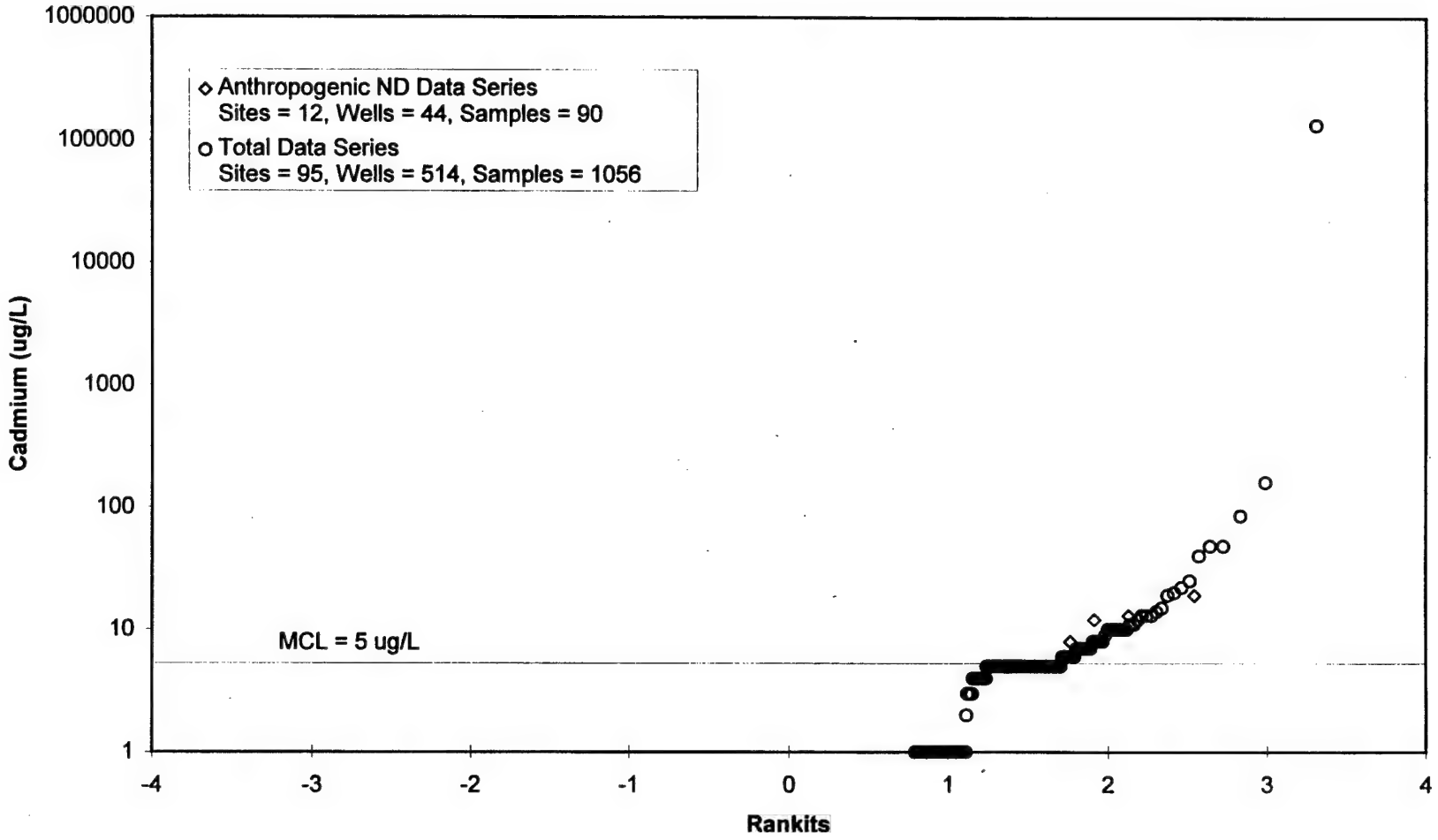

Calcium Rankit Plot for Anthropogenic ND & Total Data Series

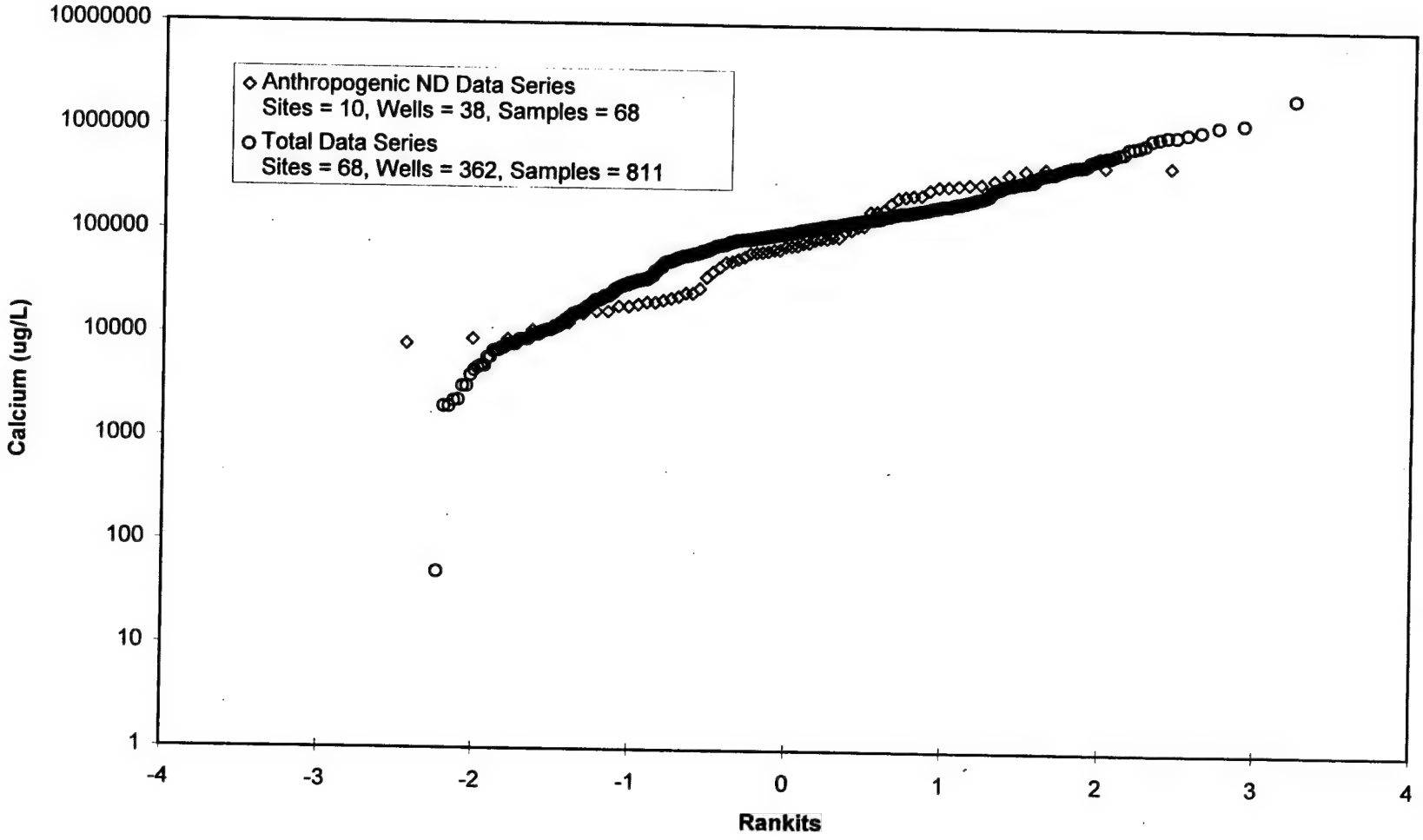

Chromium Rankit Plot for Anthropogenic ND & Total Data Series

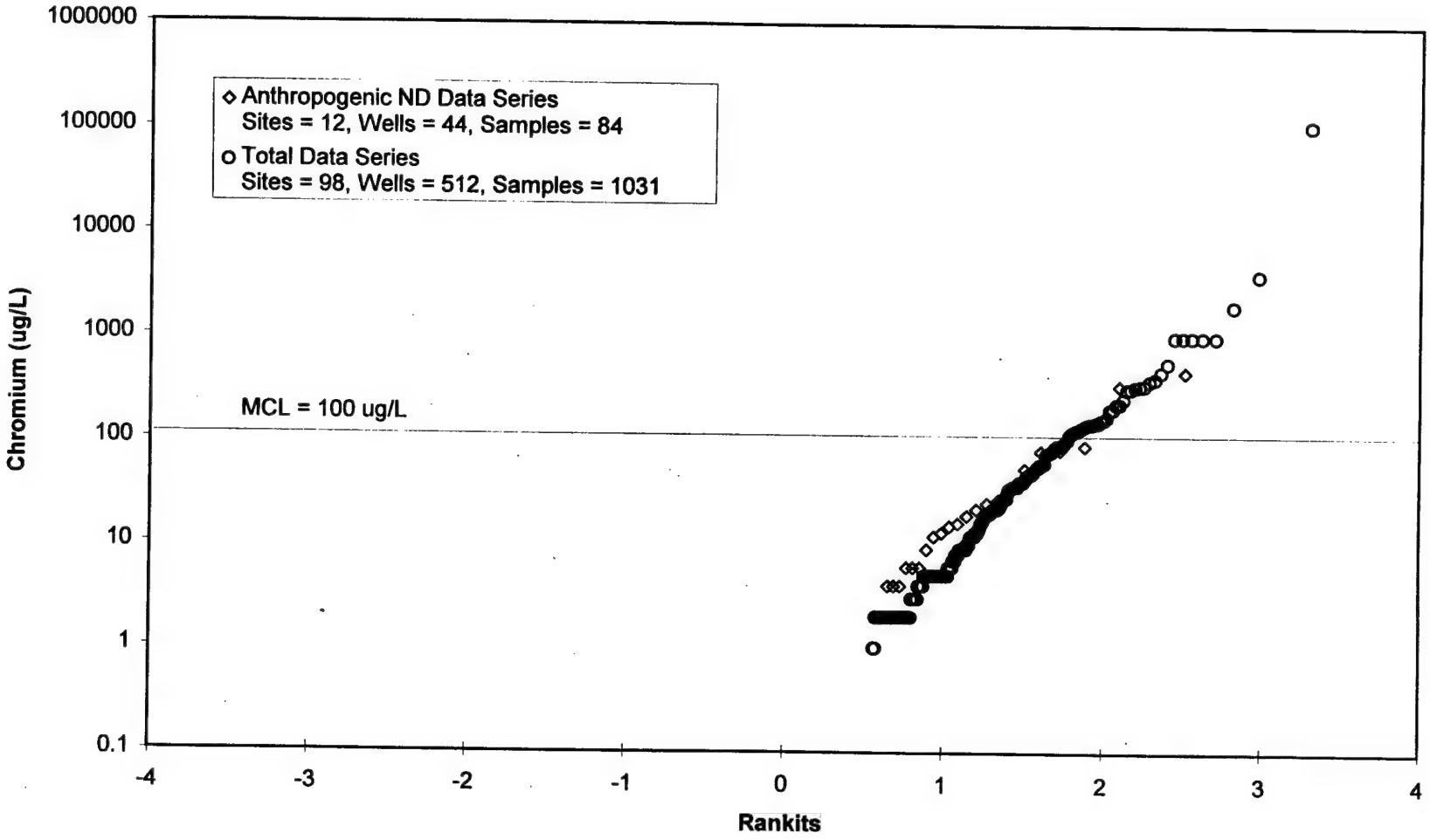

Cobalt Rankit Plot for Anthropogenic ND & Total Data Series

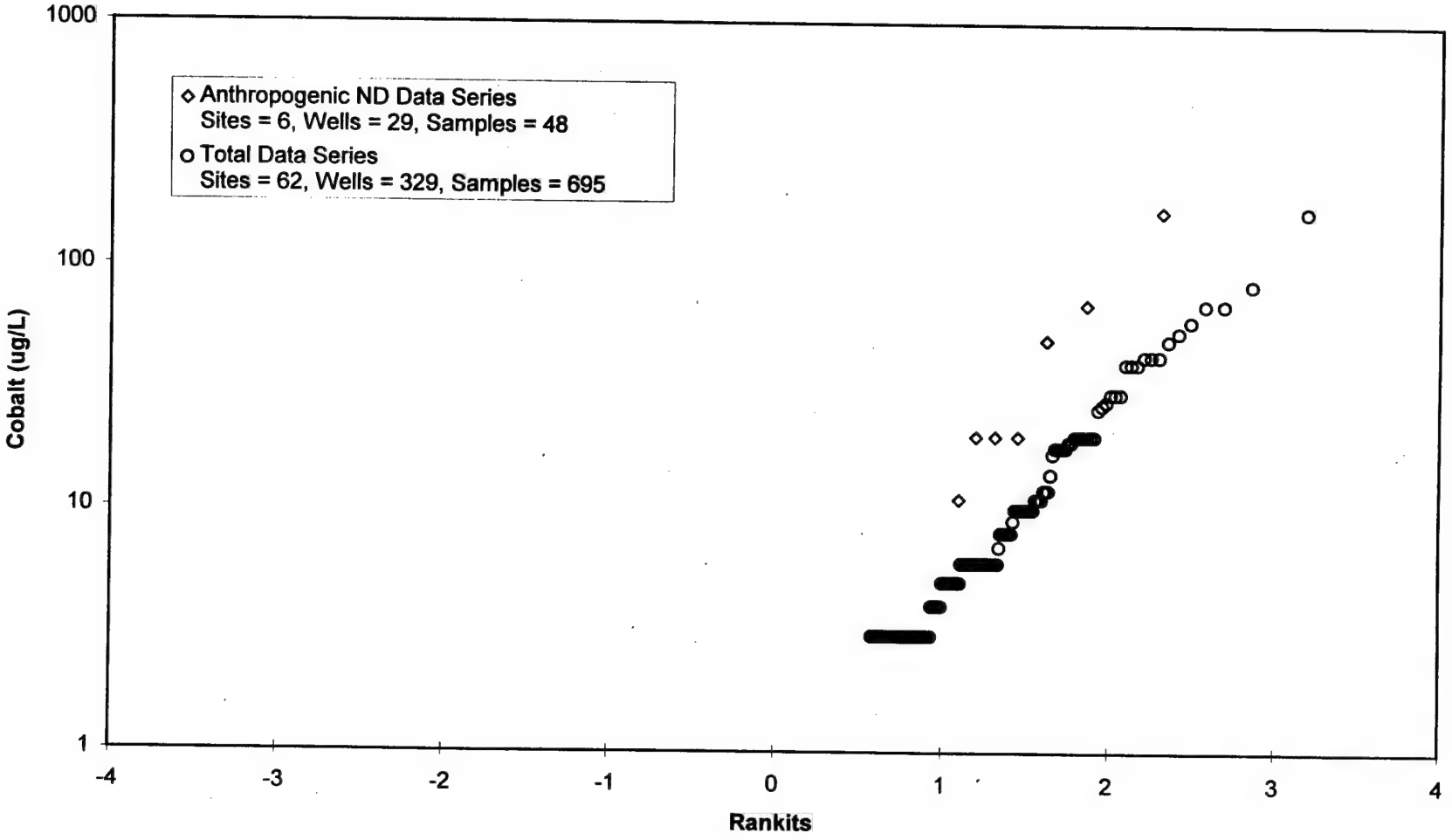

Copper Rankit Plot for Anthropogenic ND & Total Data Series

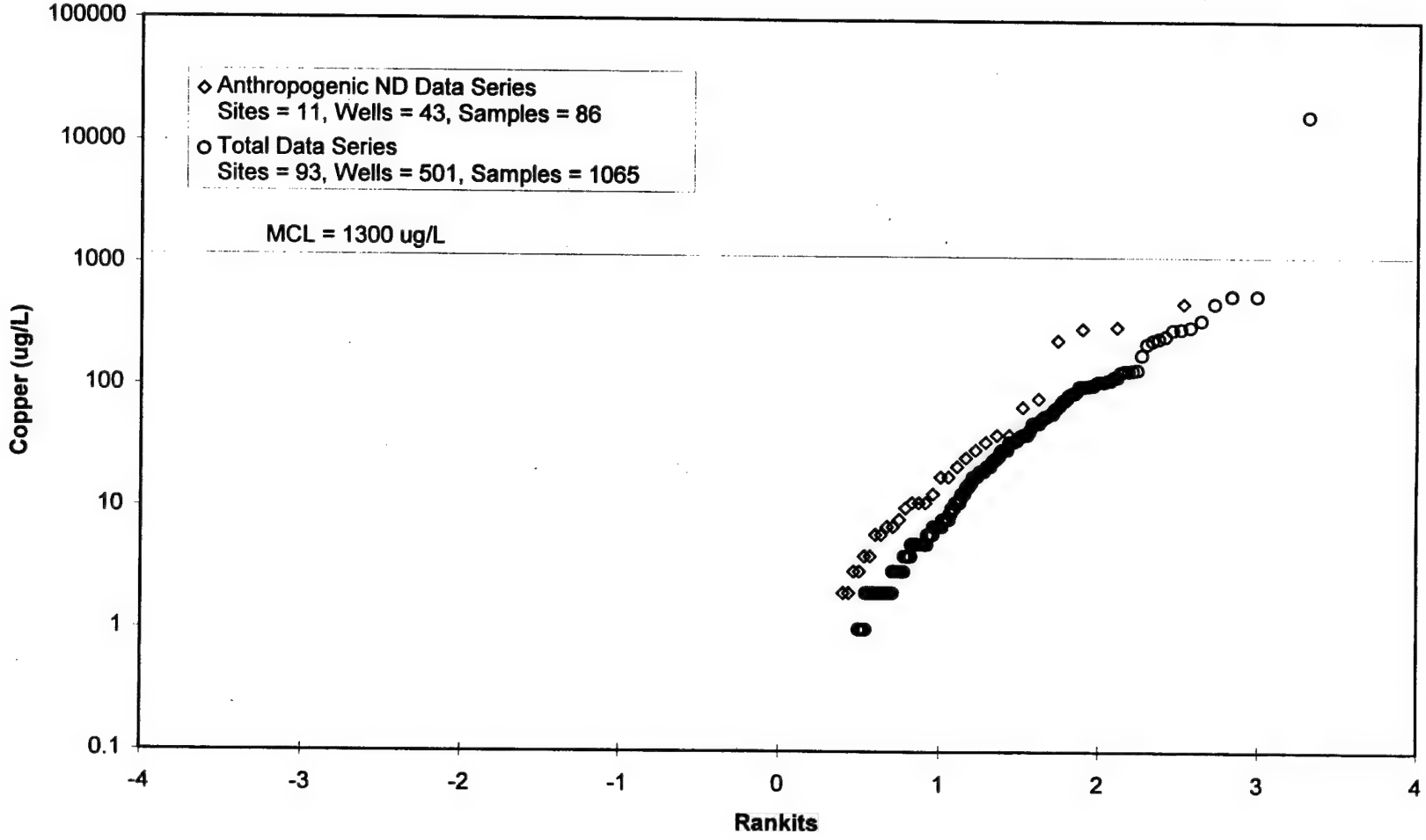

Iron Rankit Plot for Anthropogenic ND & Total Data Series

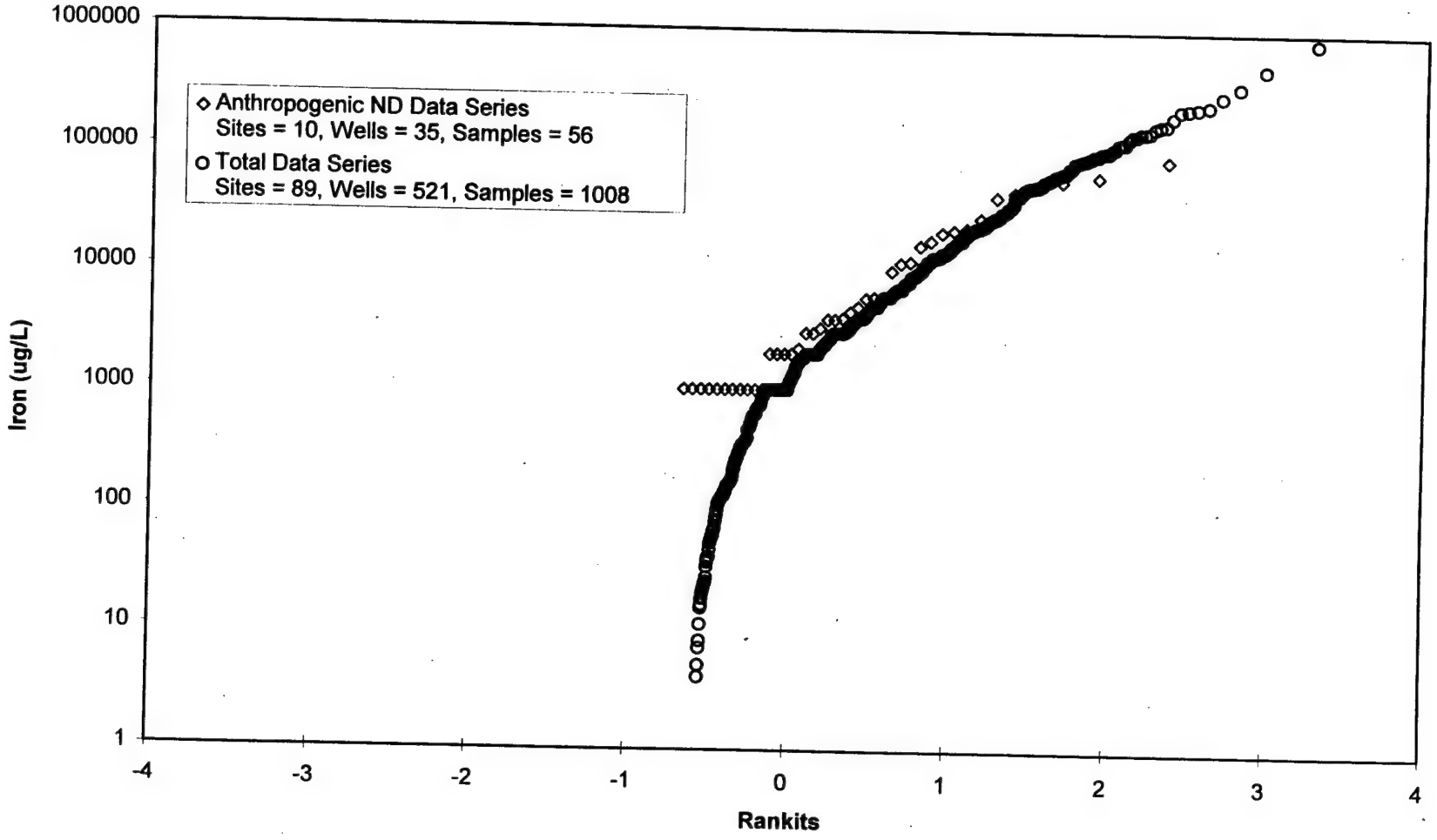

Lead Rankit Plot for Anthropogenic ND & Total Data Series

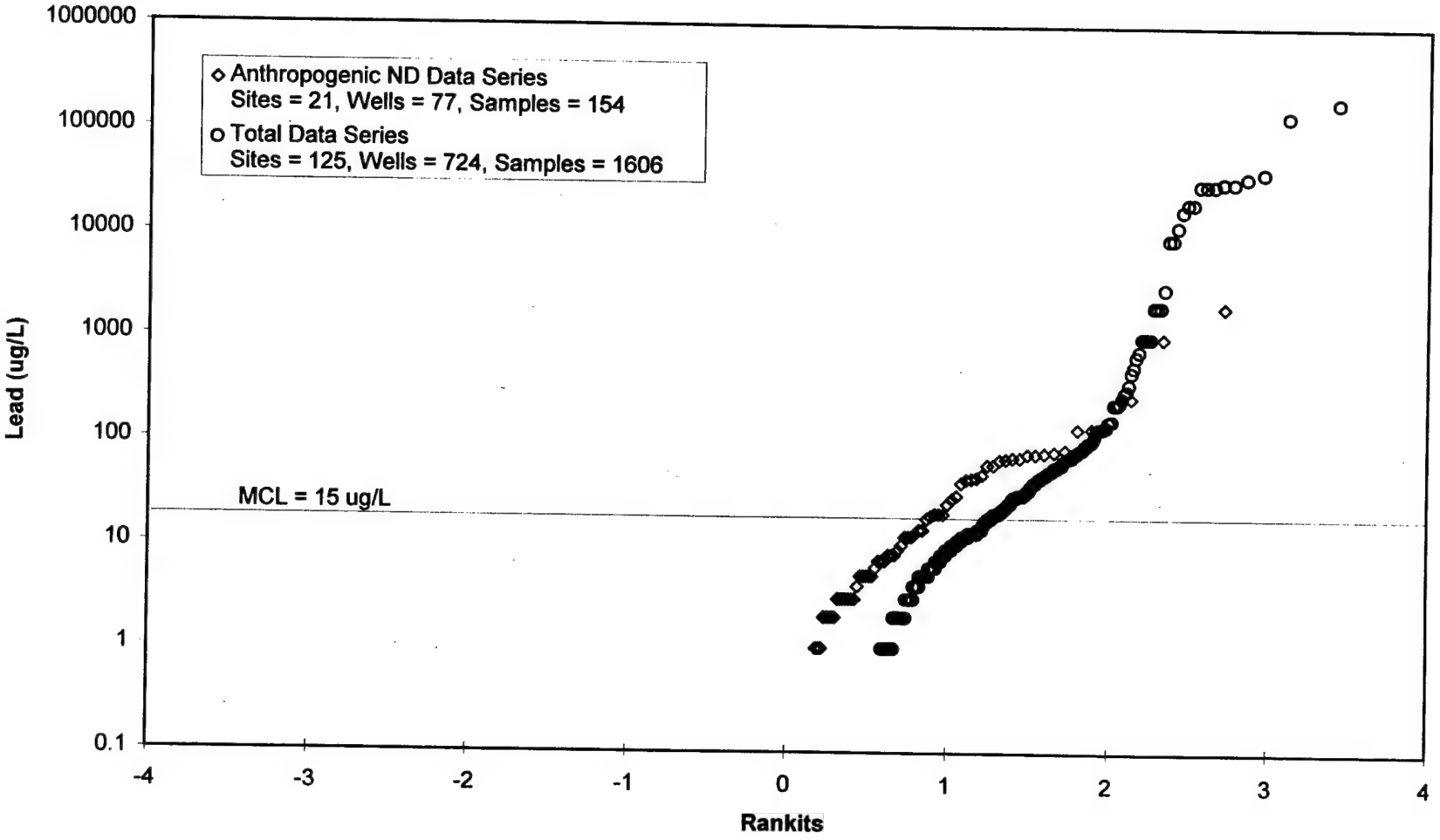

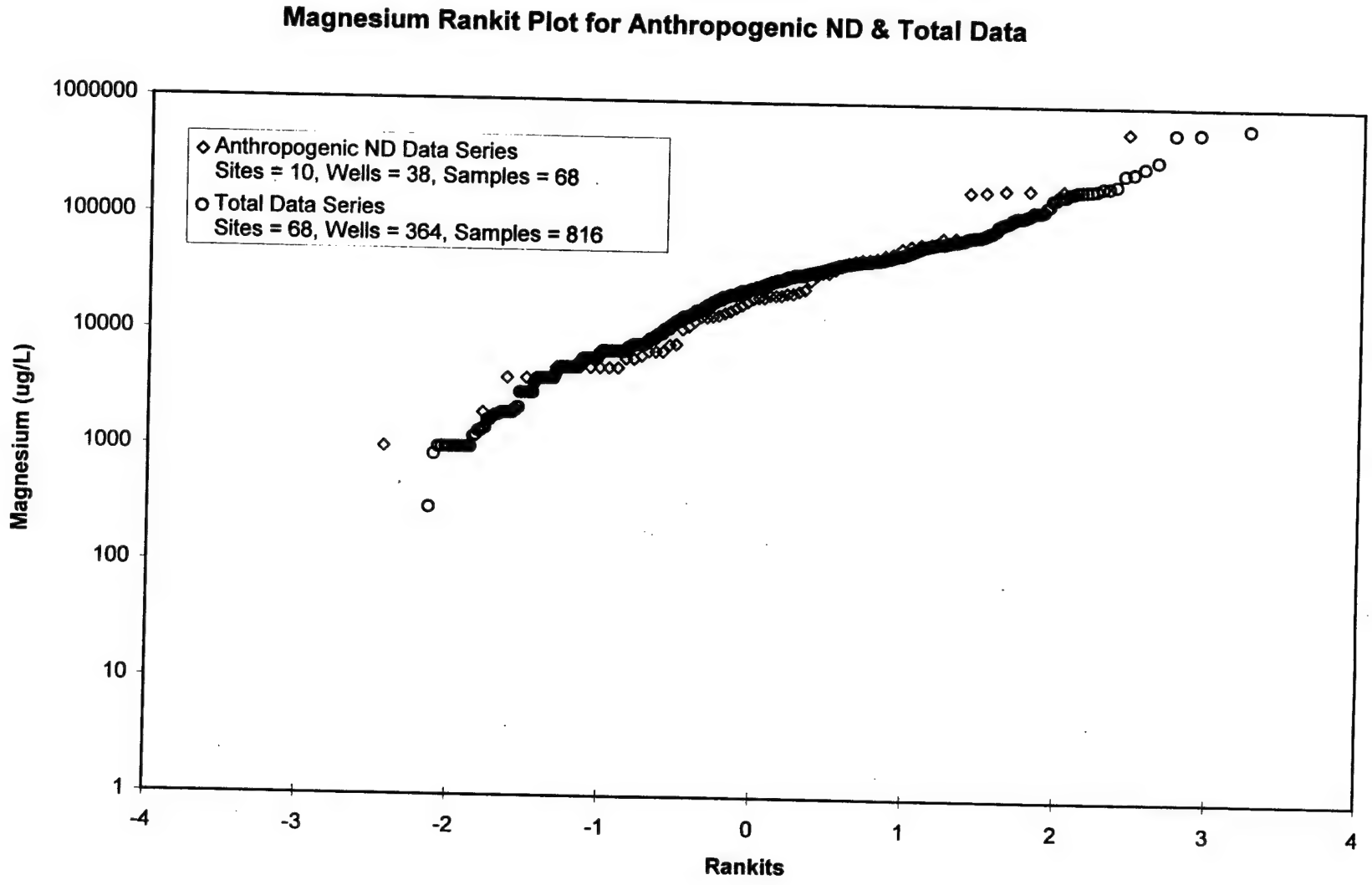
Magnesium Rankit Plot for Anthropogenic ND & Total Data
Anthropogenic ND Data Series
Sites = 10, Wells = 38, Samples = 68
Total Data Series
Sites = 68, Wells = 364, Samples = 816
Magnesium (ug/L)
1000000
100000
10000
1000
100
10
1
-4
-3
-2
-1
0
1
2
3
4
Rankits

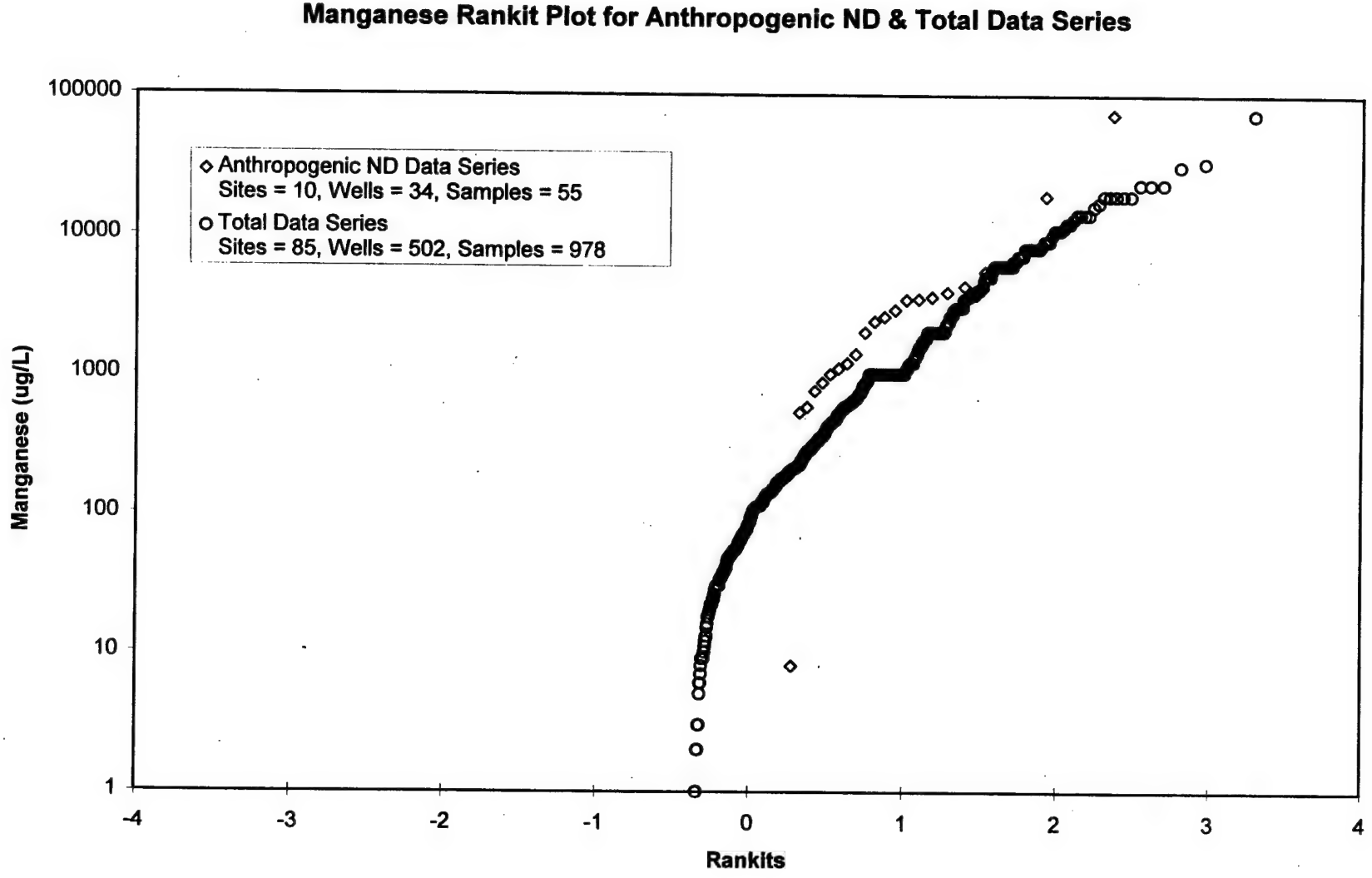
Manganese Rankit Plot for Anthropogenic ND & Total Data Series
Anthropogenic ND Data Series
Sites = 10, Wells = 34, Samples = 55
Total Data Series
Sites = 85, Wells = 502, Samples = 978
Manganese (ug/L)
100000
10000
1000
100
10
1
-4
-3
-2
-1
0
1
2
3
4
Rankits

Mercury Rankit Plot for Anthropogenic ND & Total Data Series

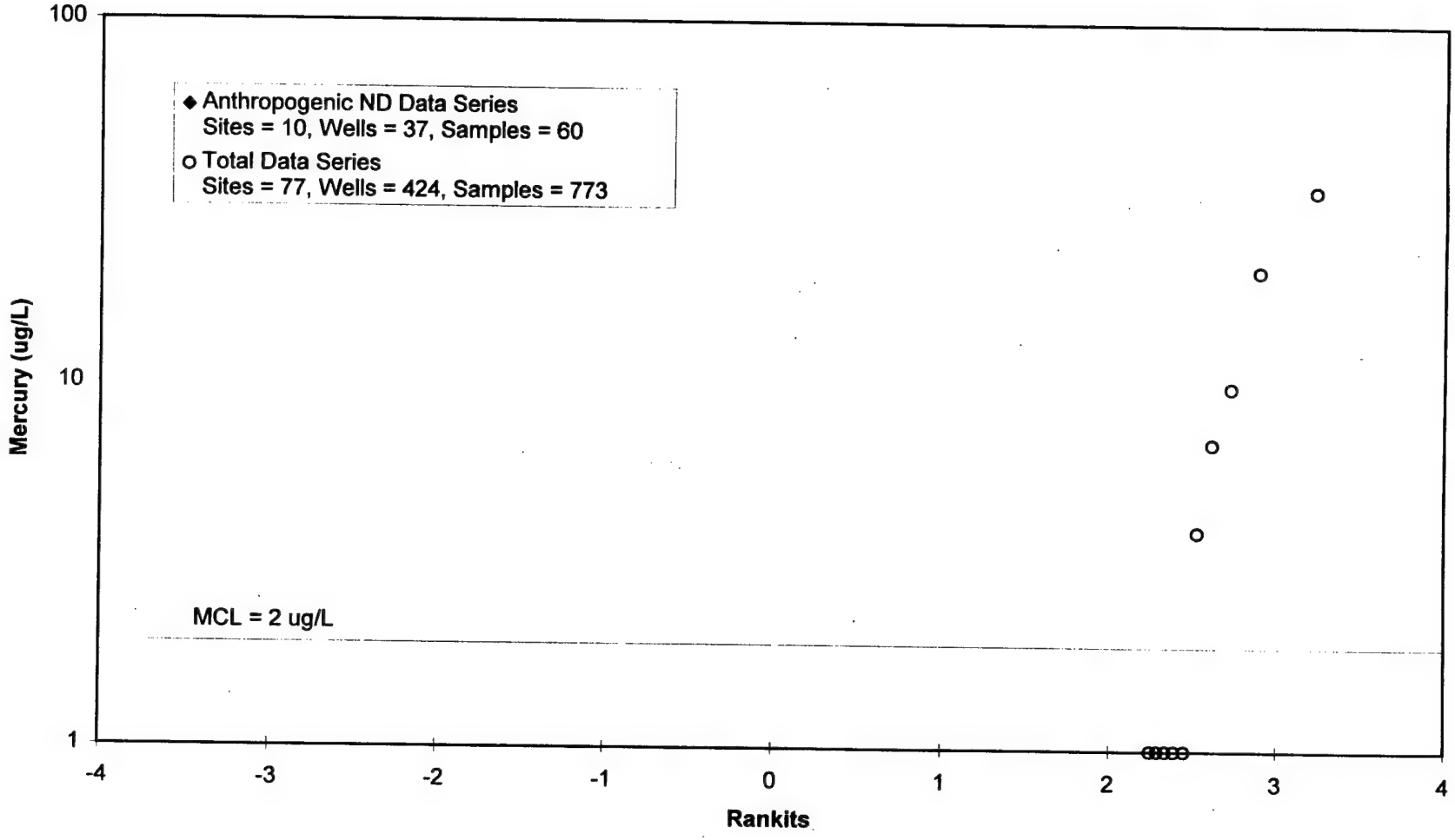

Molybdenum Rankit Plot for Anthropogenic ND & Total Data Series

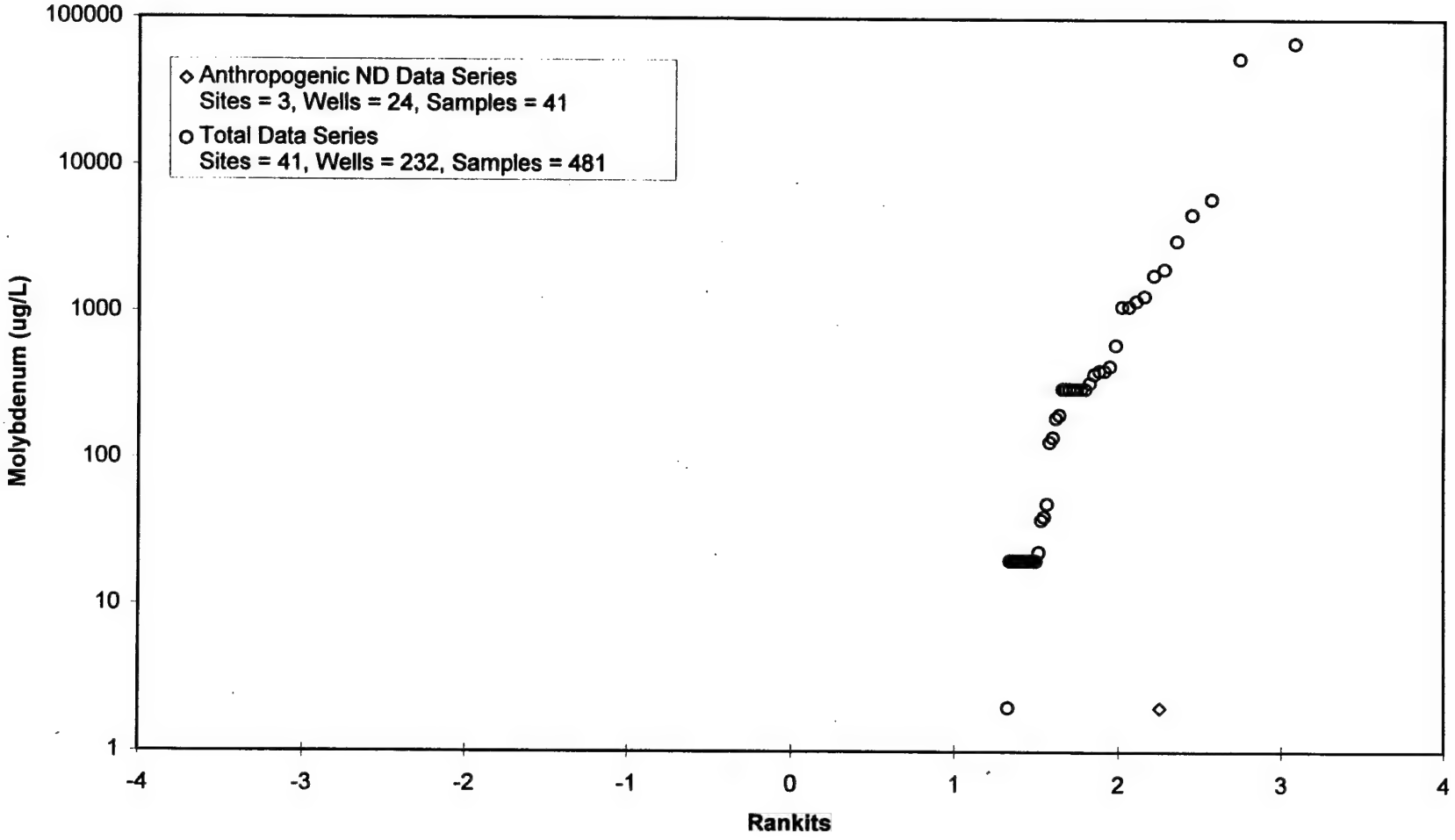

Nickel Rankit Plot for Anthropogenic ND & Total Data Series

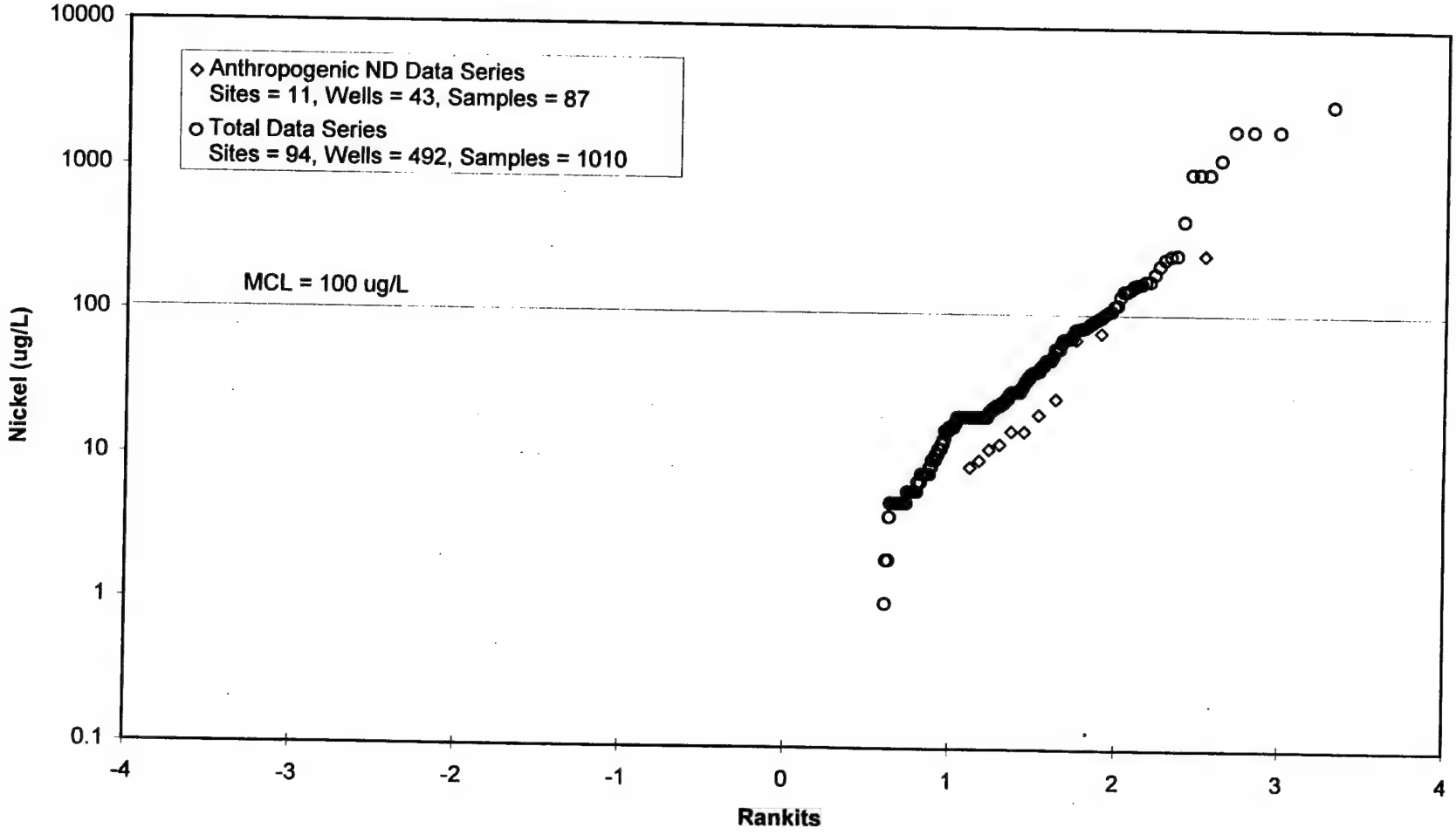

Potassium Rankit Plot for Anthropogenic ND & Total Data Series

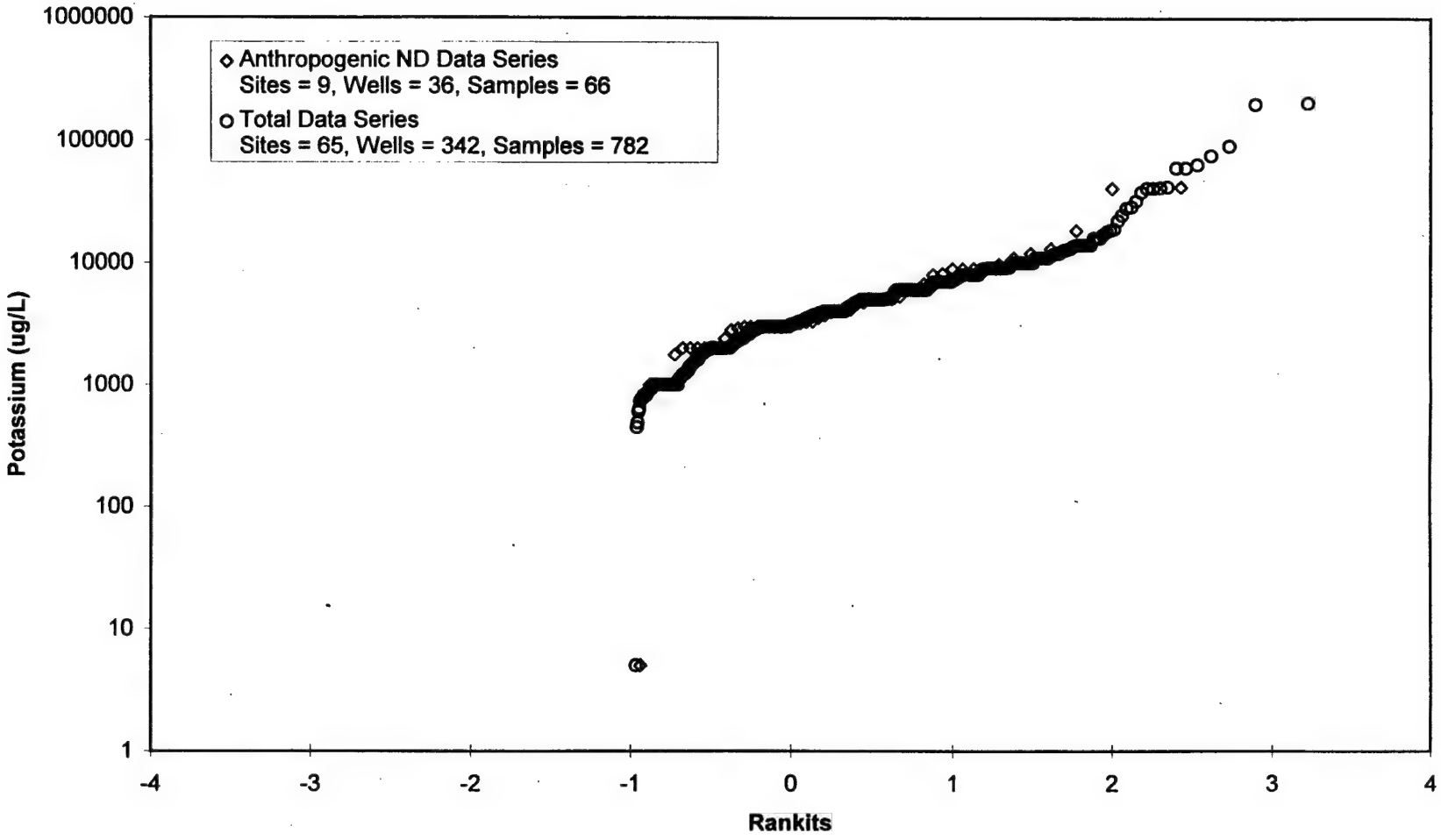

Selenium Rankit Plot for Anthropogenic ND & Total Data Series

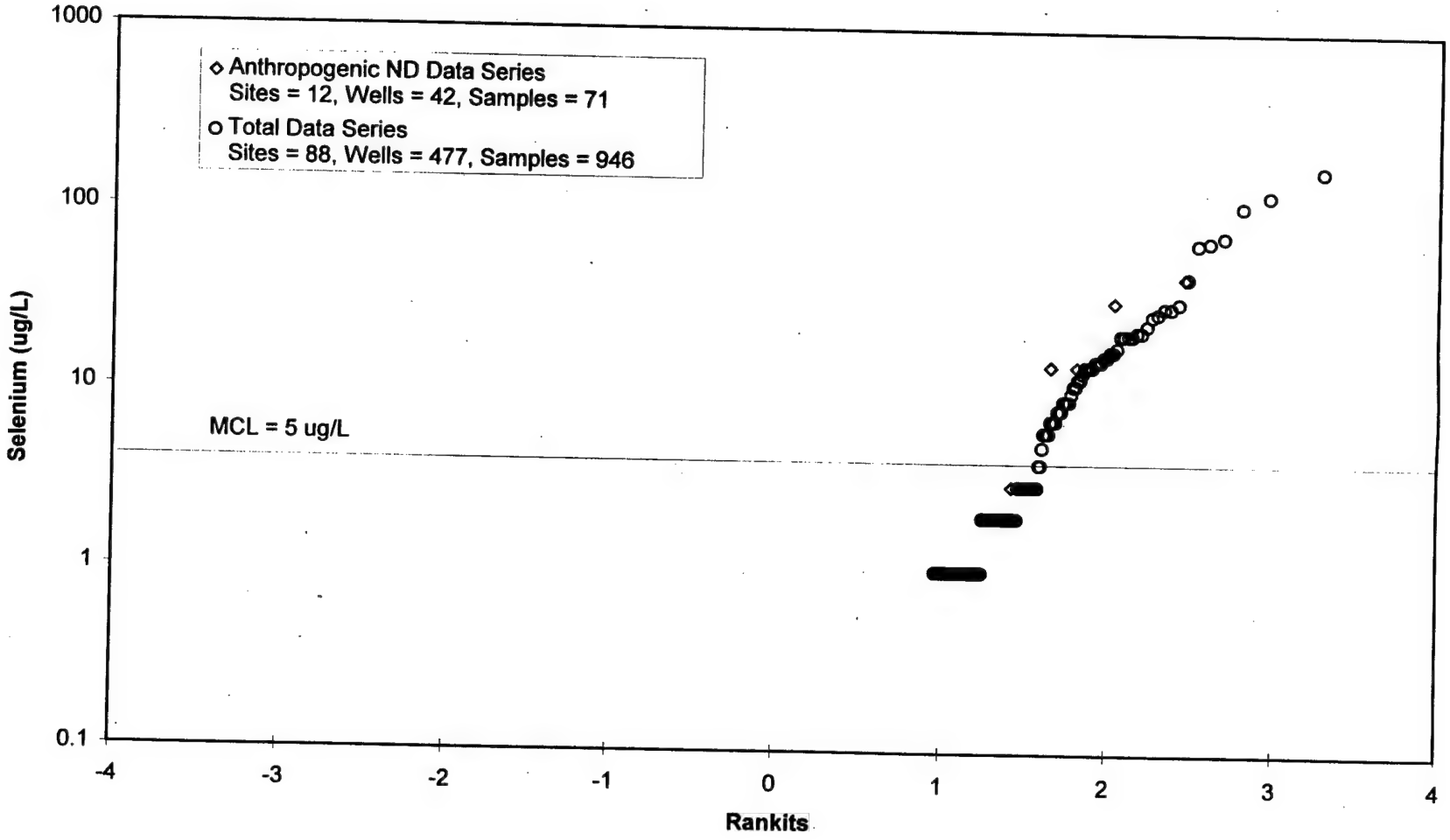

Silver Rankit Plot for Anthropogenic ND & Total Data Series

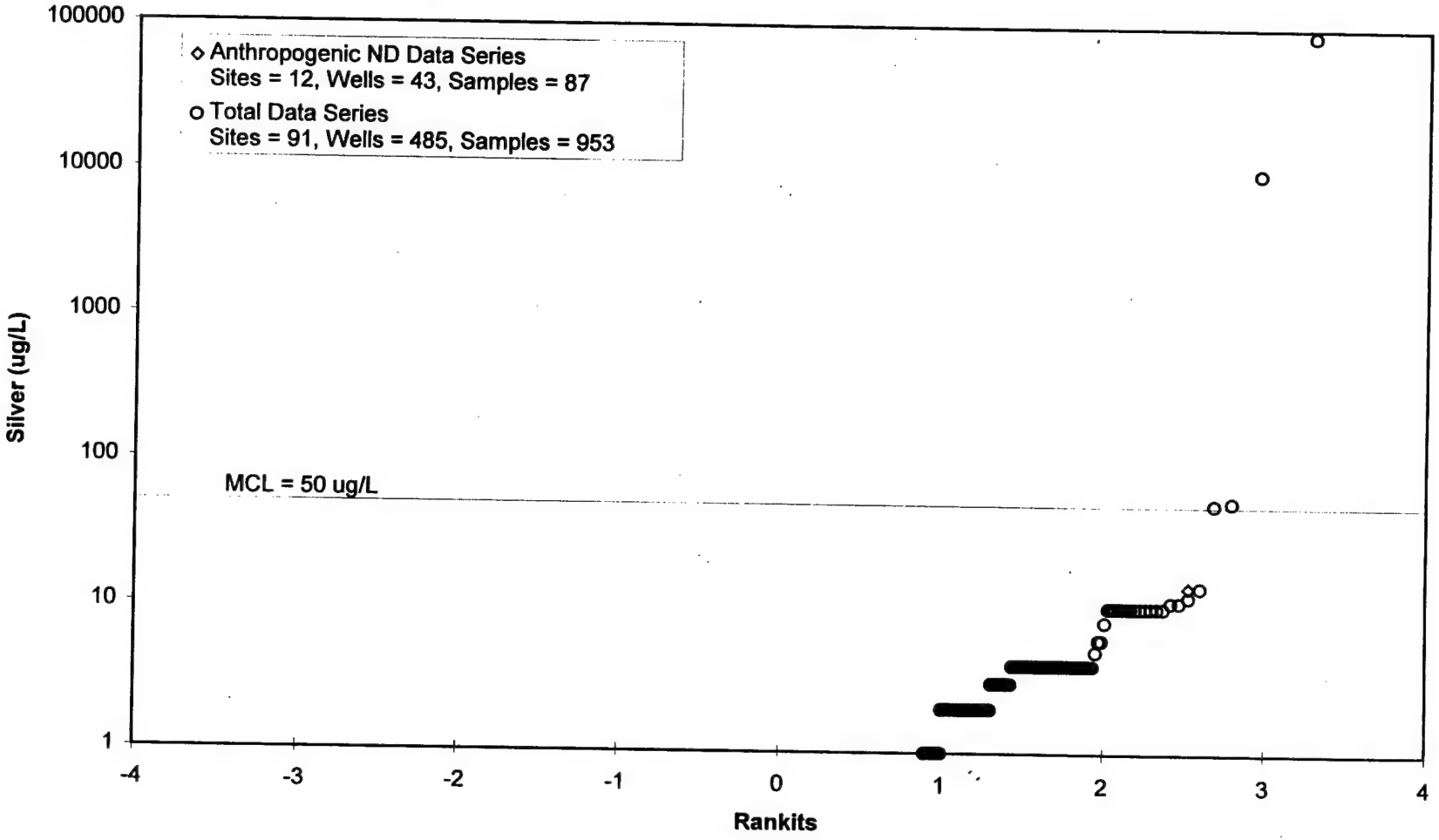

Sodium Rankit Plot for Anthropogenic ND & Total Data Series

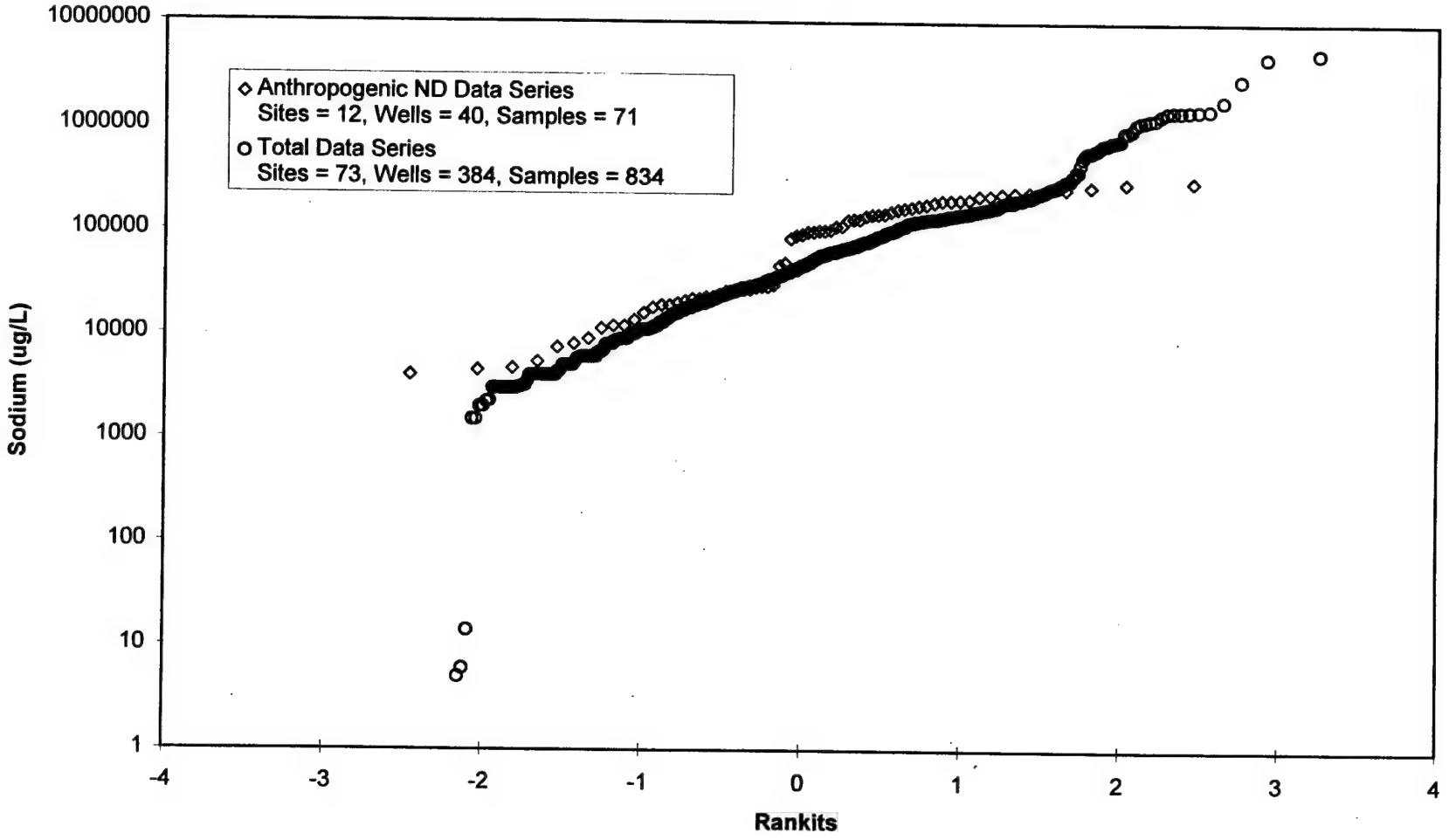

Thallium Rankit Plot for Anthropogenic ND & Total Data Series

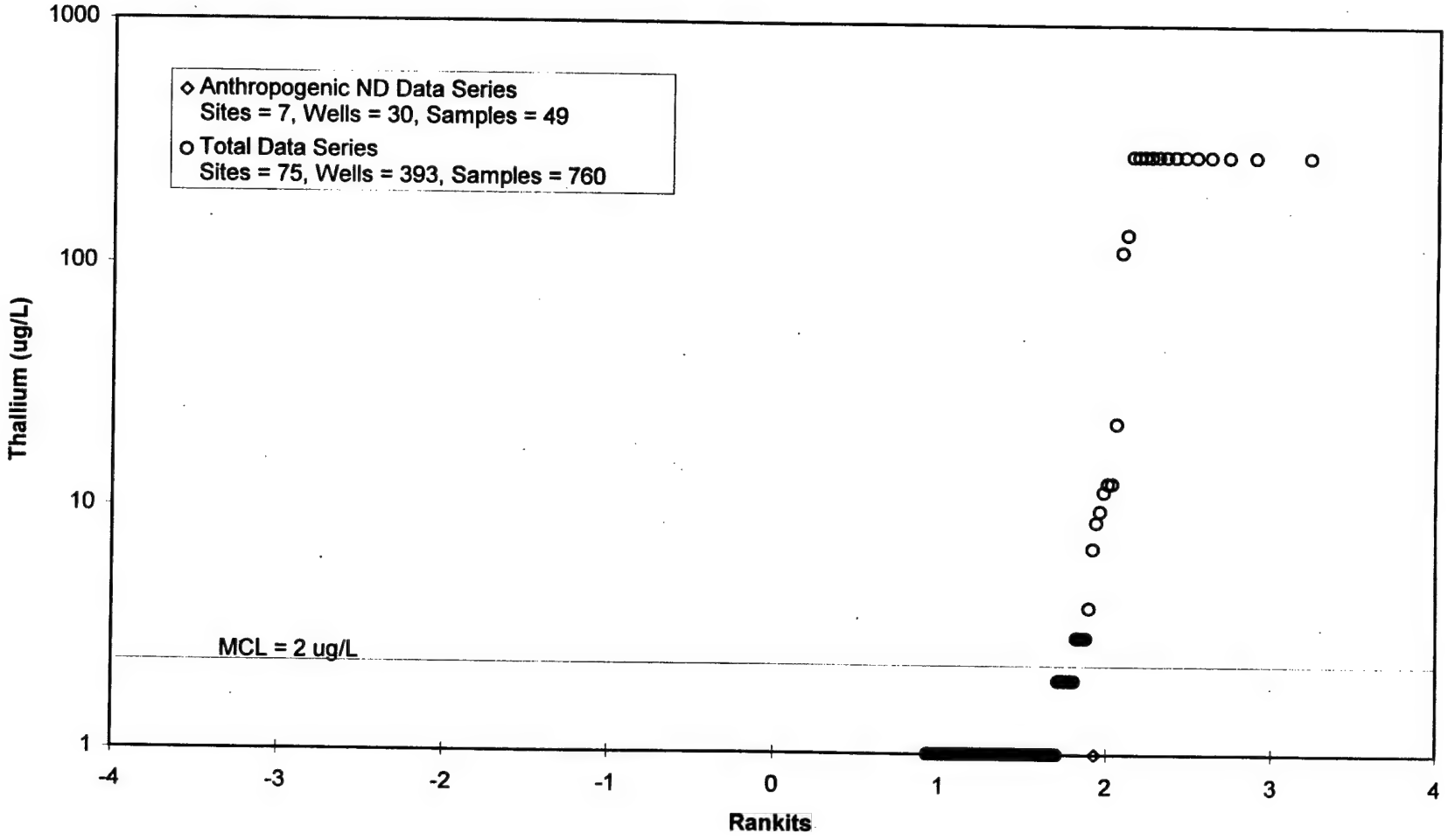

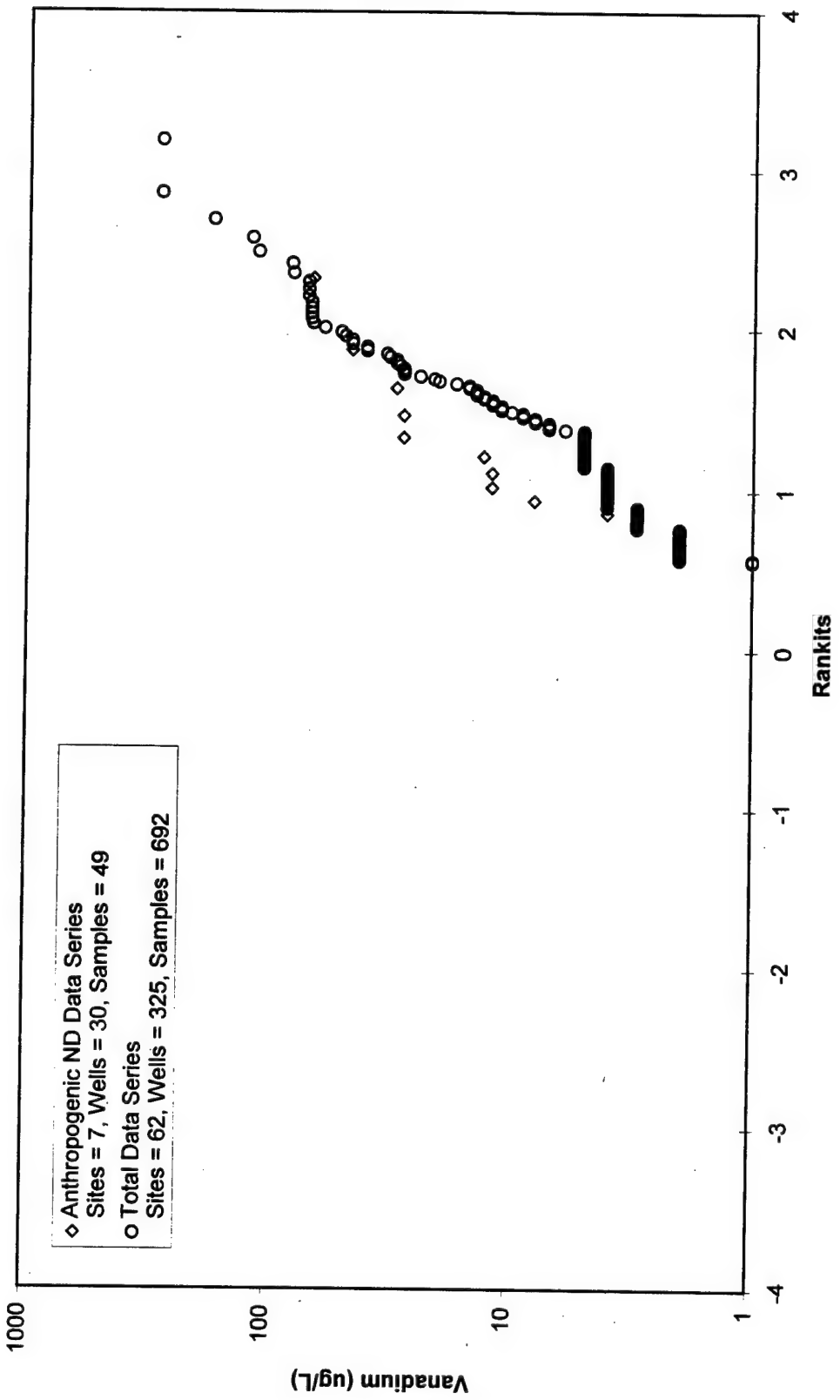
Vanadium Rankit Plot for Anthropogenic ND & Total Data Series
◇ Anthropogenic ND Data Series
Sites = 7, Wells = 30, Samples = 49
o Total Data Series
Sites = 62, Wells = 325, Samples = 692
Vanadium (ug/L)
1000
100
10
1
-4
-3
-2
-1
0
1
2
3
4
Rankits

Zinc Rankit Plot for Anthropogenic ND & Total Data Series

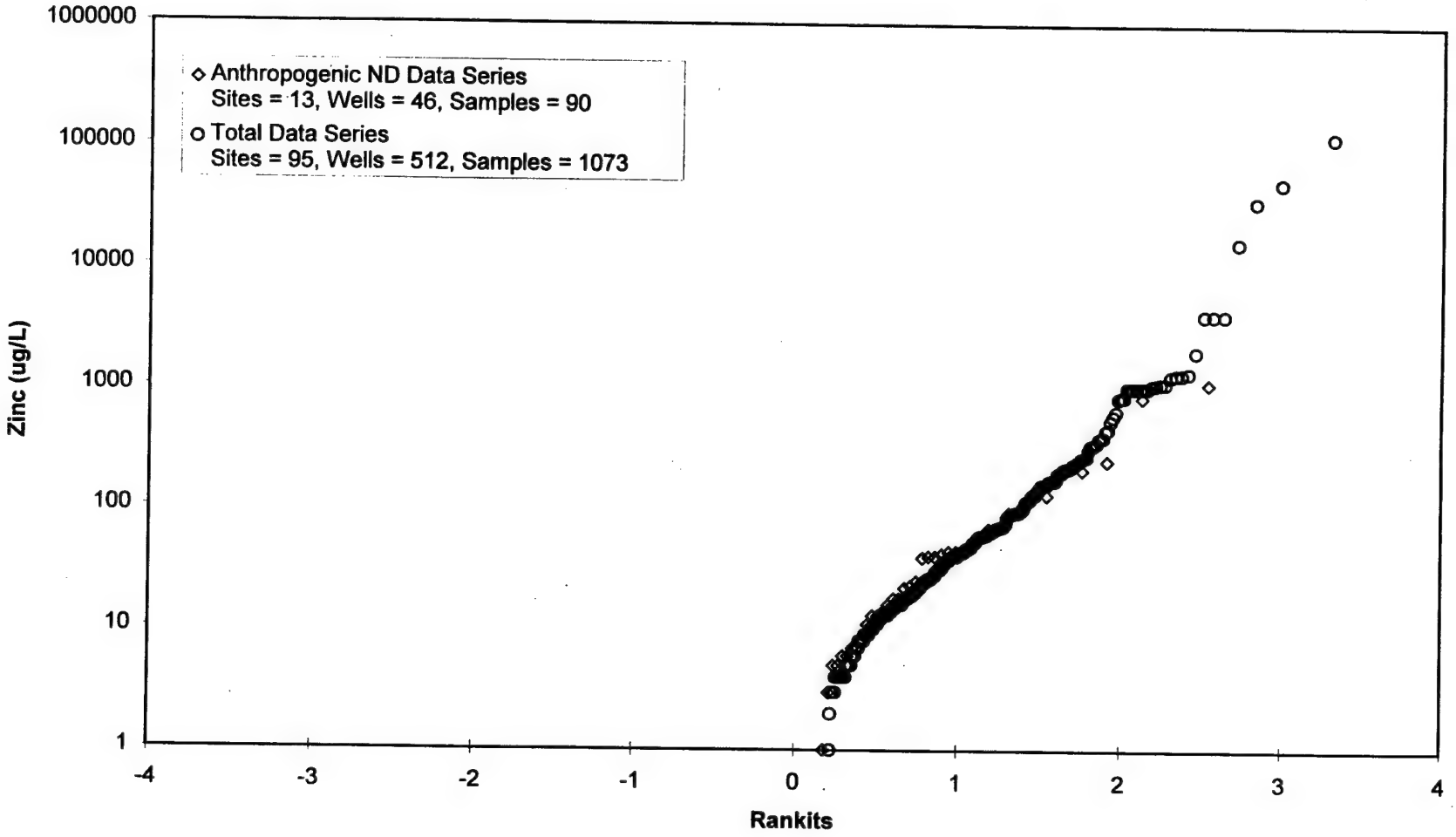

Appendix G: Rankit Plots for Upgradient/Background & Downgradient/On-site Data Series

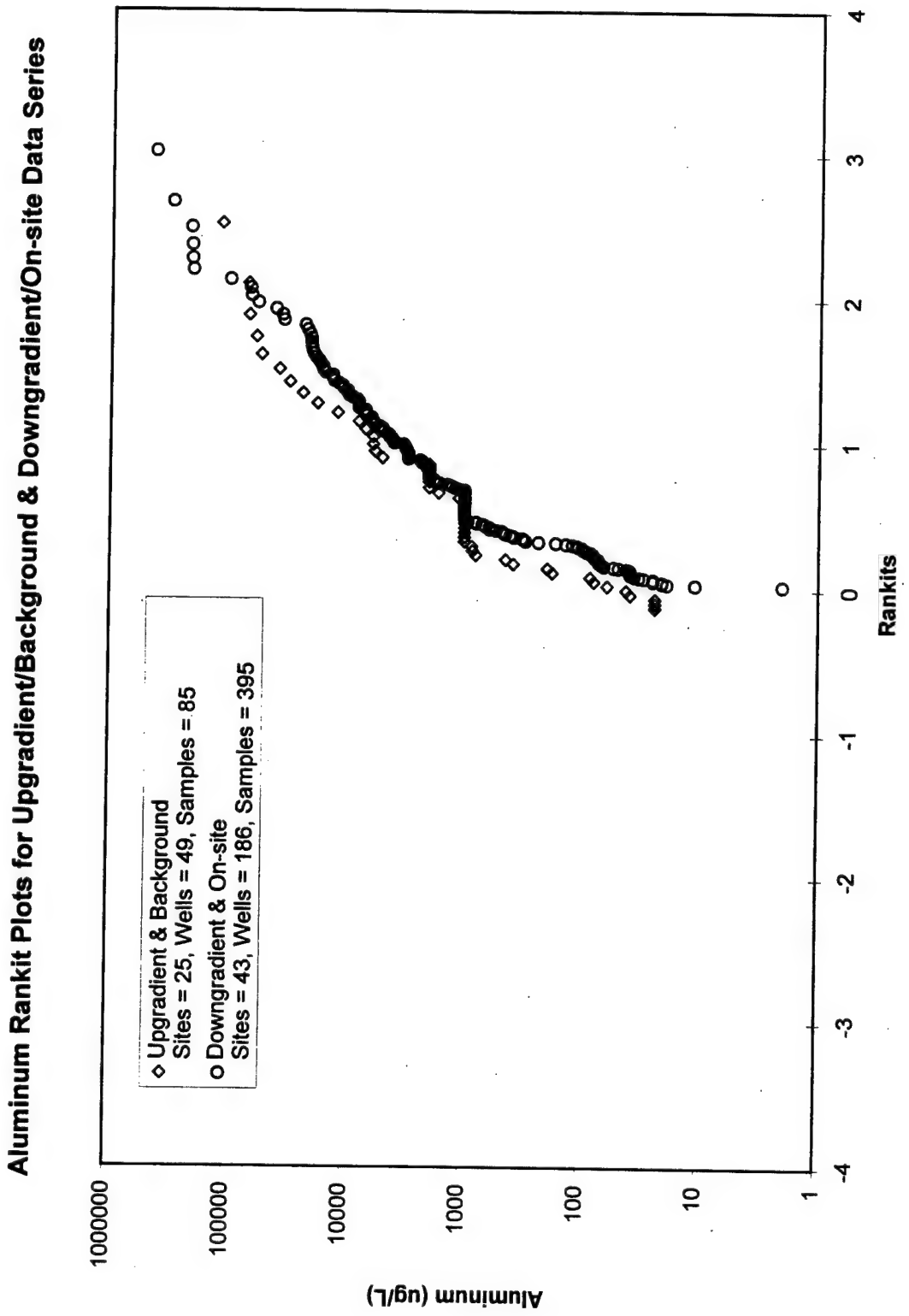

Antimony Rankit Plots of Upgradient/Background & Downgradient/On-site Data Series

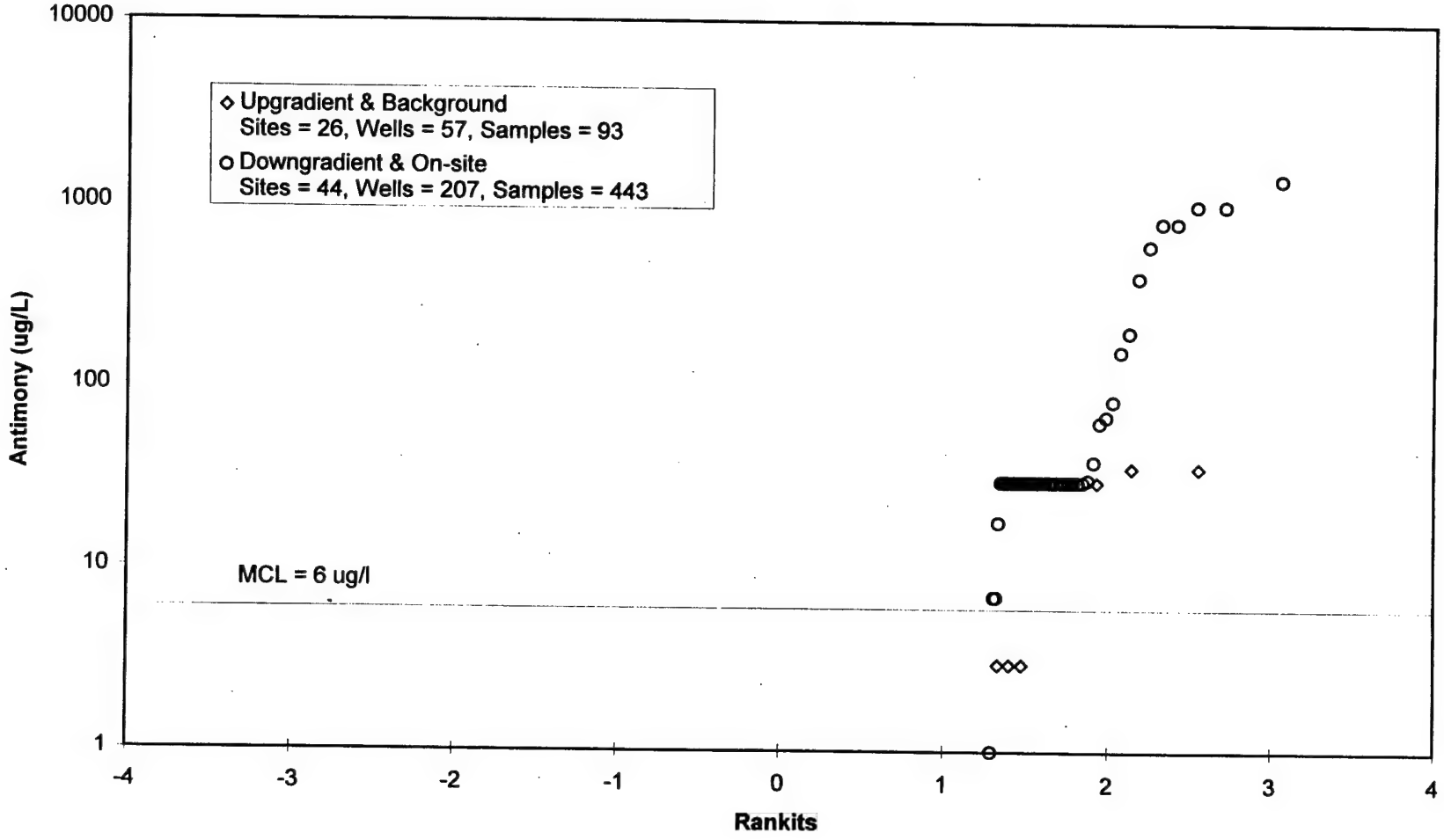

Arsenic Rankit Plots of Upgradient/Background & Downgradient/ On-site Data Series

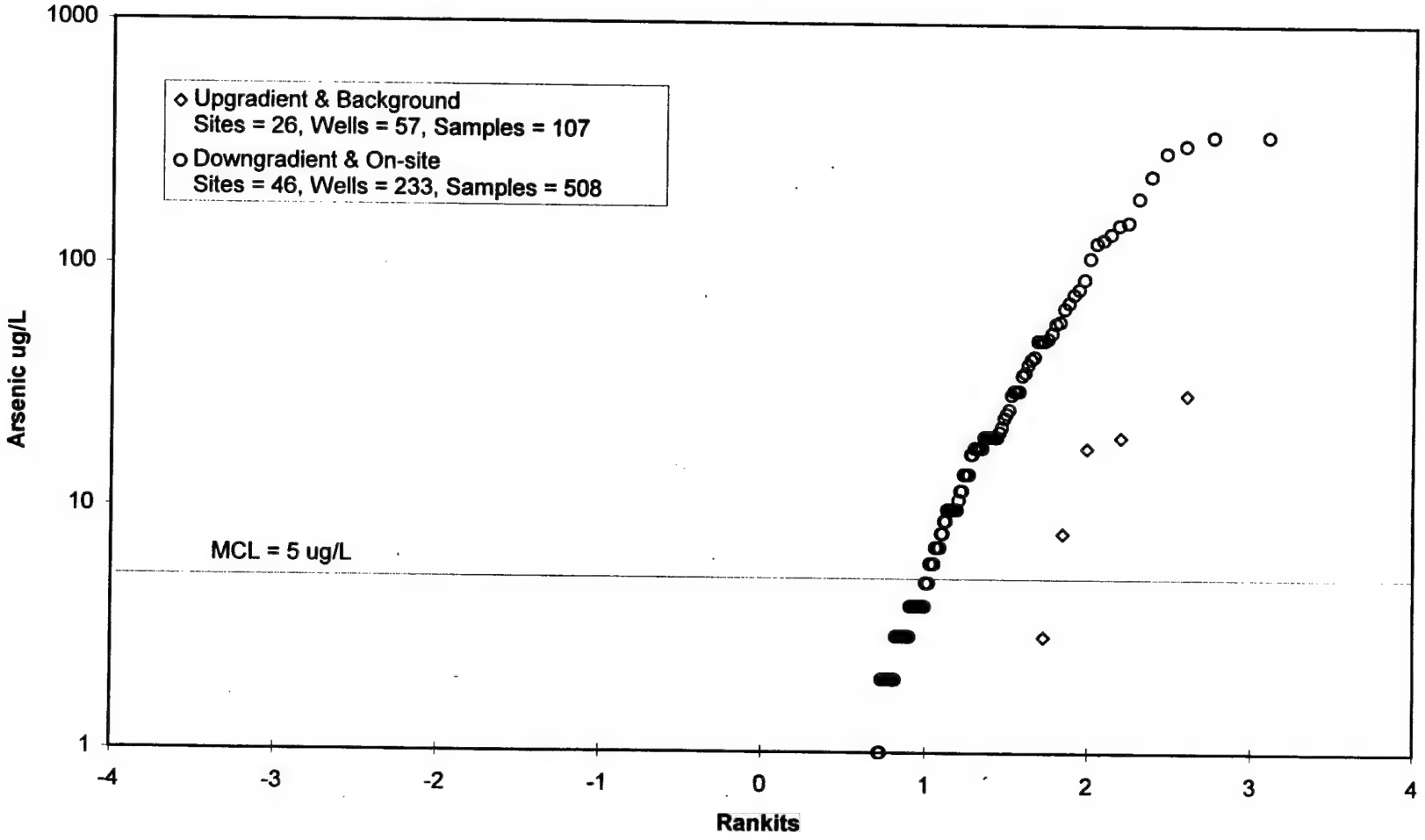

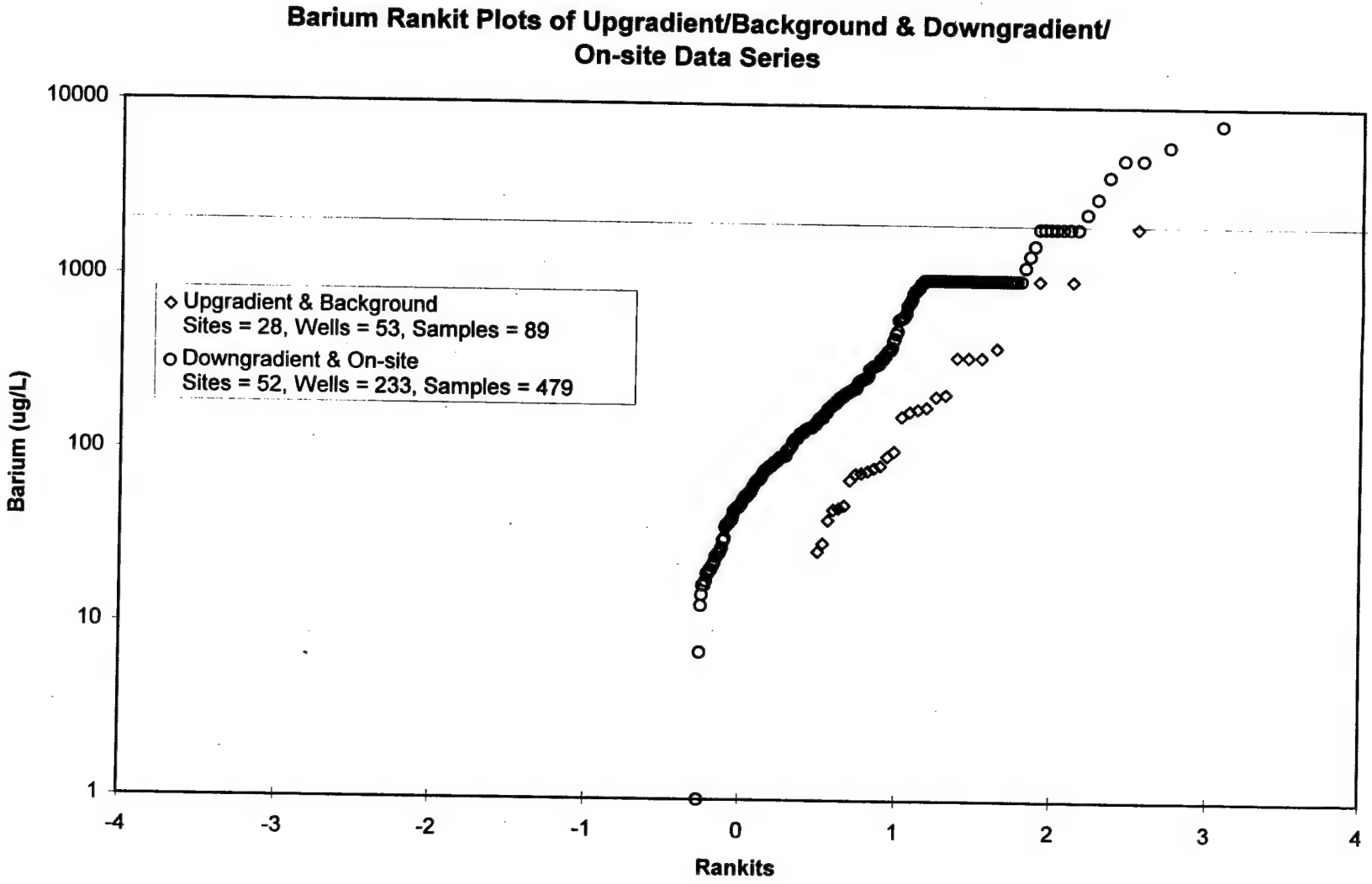
Barium Rankit Plots of Upgradient/Background & Downgradient/
On-site Data Series
10000
1000
100
10
1
Barium (ug/L)
Upgradient & Background
Sites = 28, Wells = 53, Samples = 89
Downgradient & On-site
Sites = 52, Wells = 233, Samples = 479
-4
-3
-2
-1
0
1
2
3
4
Rankits

Beryllium Rankit Plots for Upgradient/Background & Downgradient/On-site Data Series

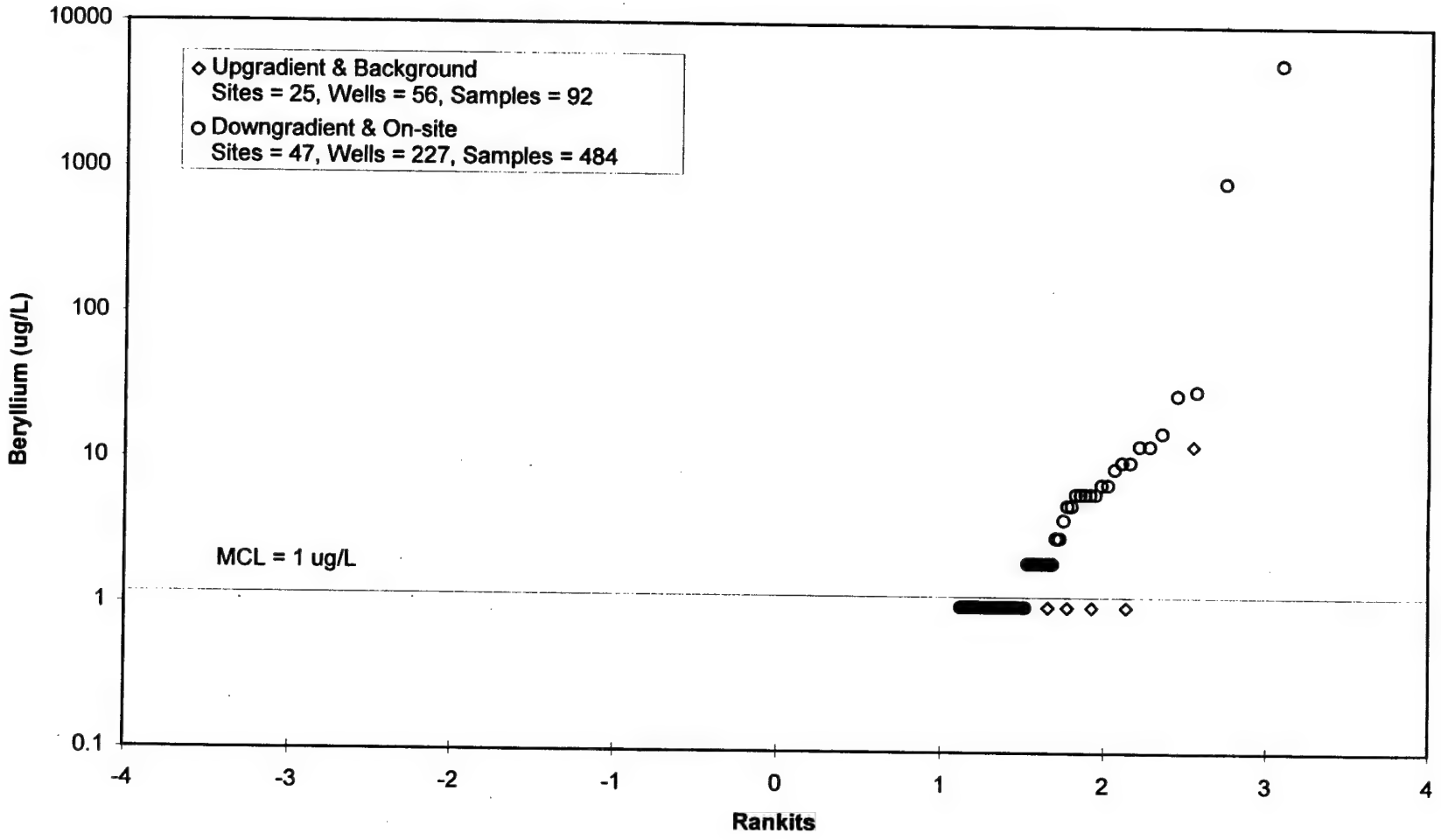

Cadmium Rankit Plots for Upgradient/Background & Downgradient/On-site Data Series

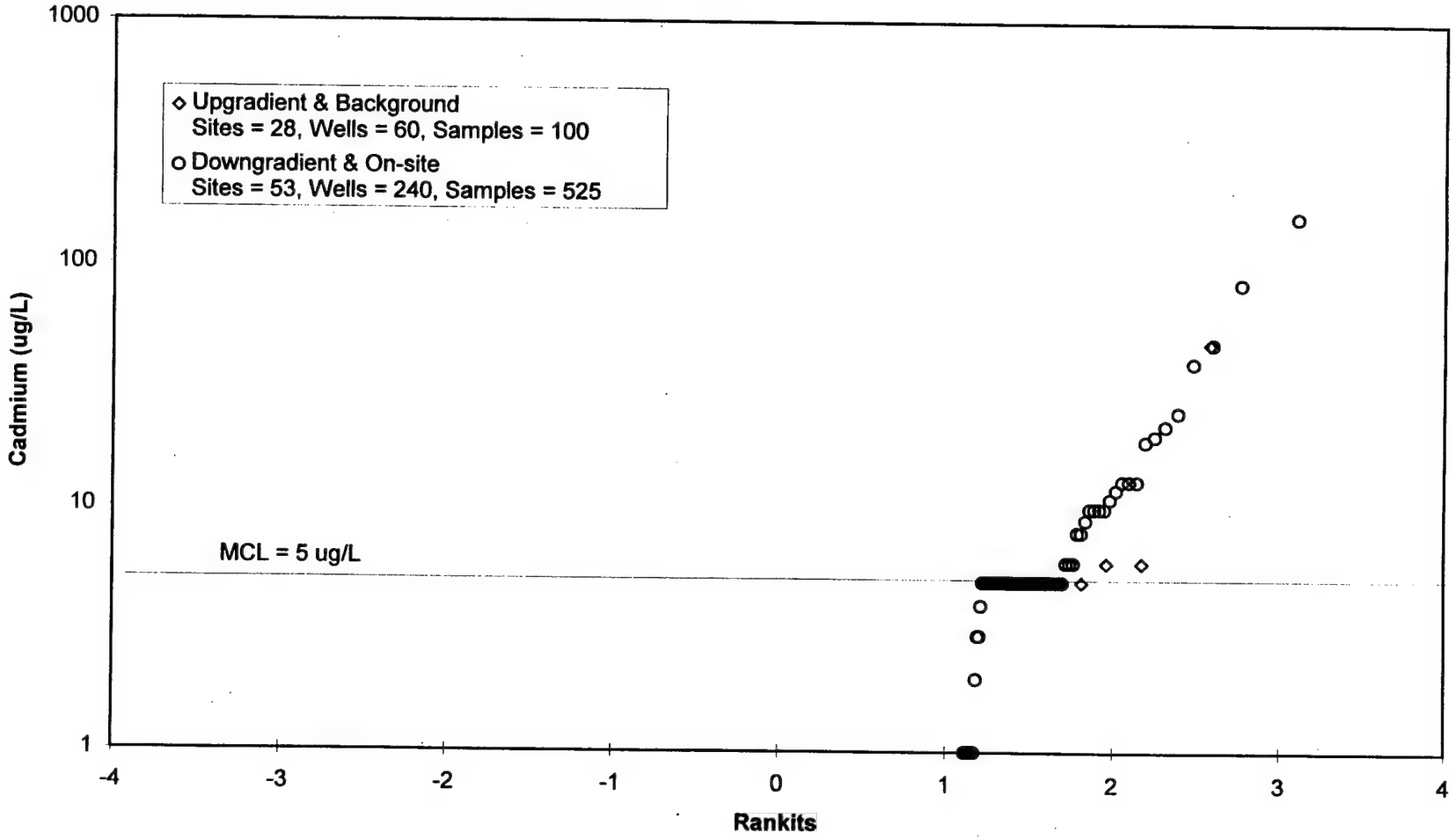

Calcium Rankit Plots for Upgradient/Background & Downgradient/On-site Data Series

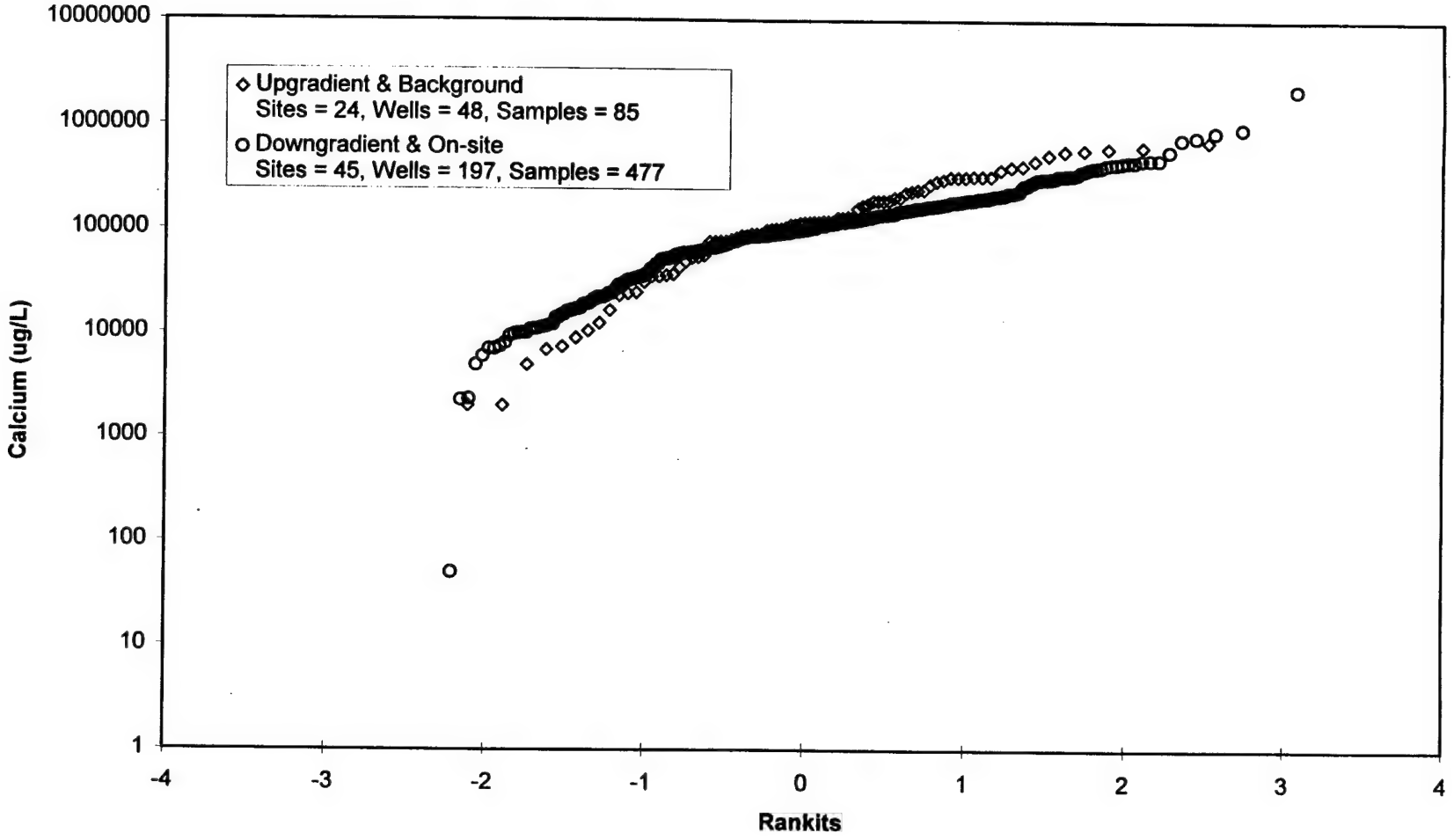

Chromium Rankits Plots for Upgradient/Background & Downgradient/On-site Data Series

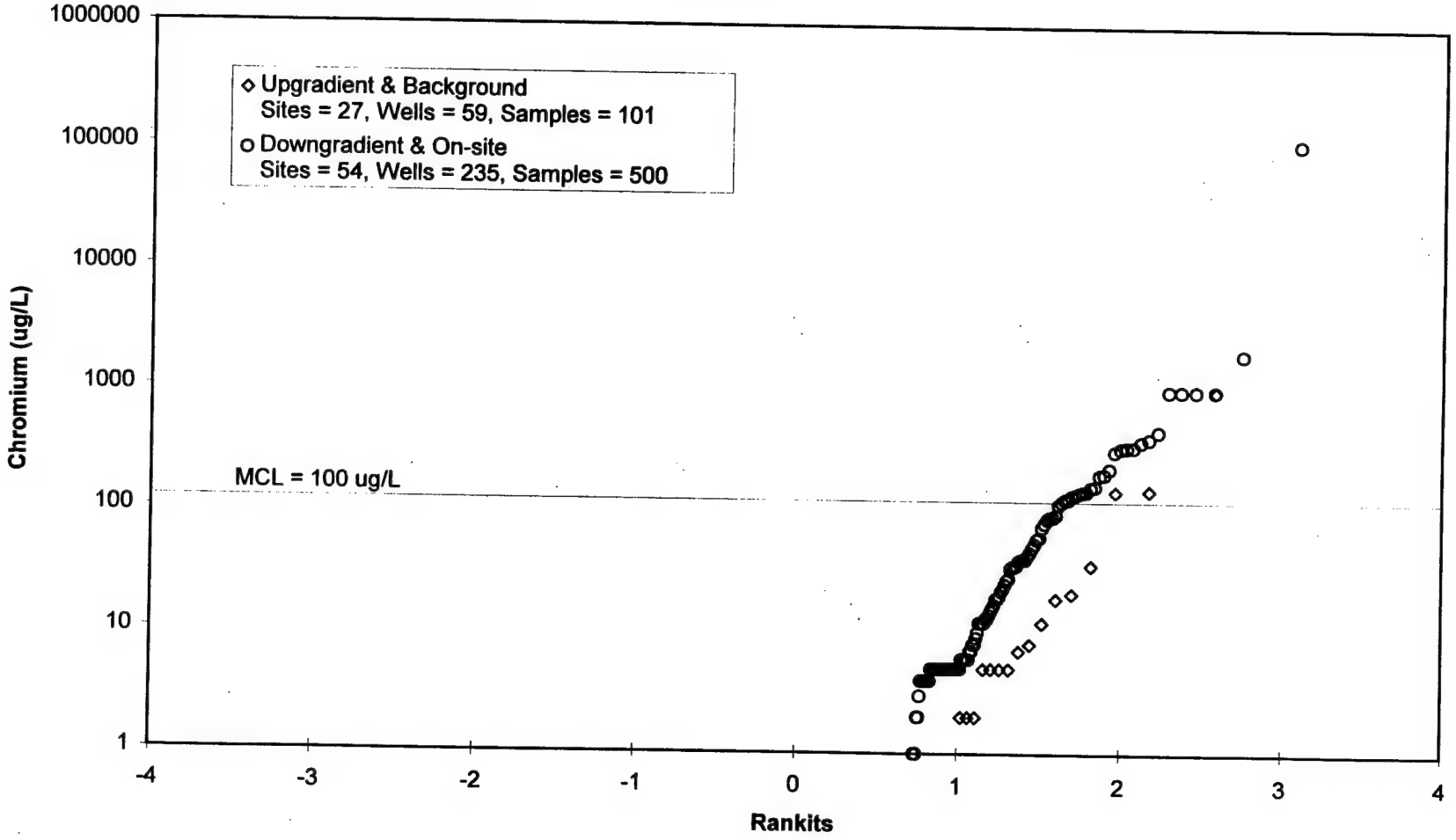

Cobalt Rankit Plots for Upgradient/Background & Downgradient/On-site Data Series

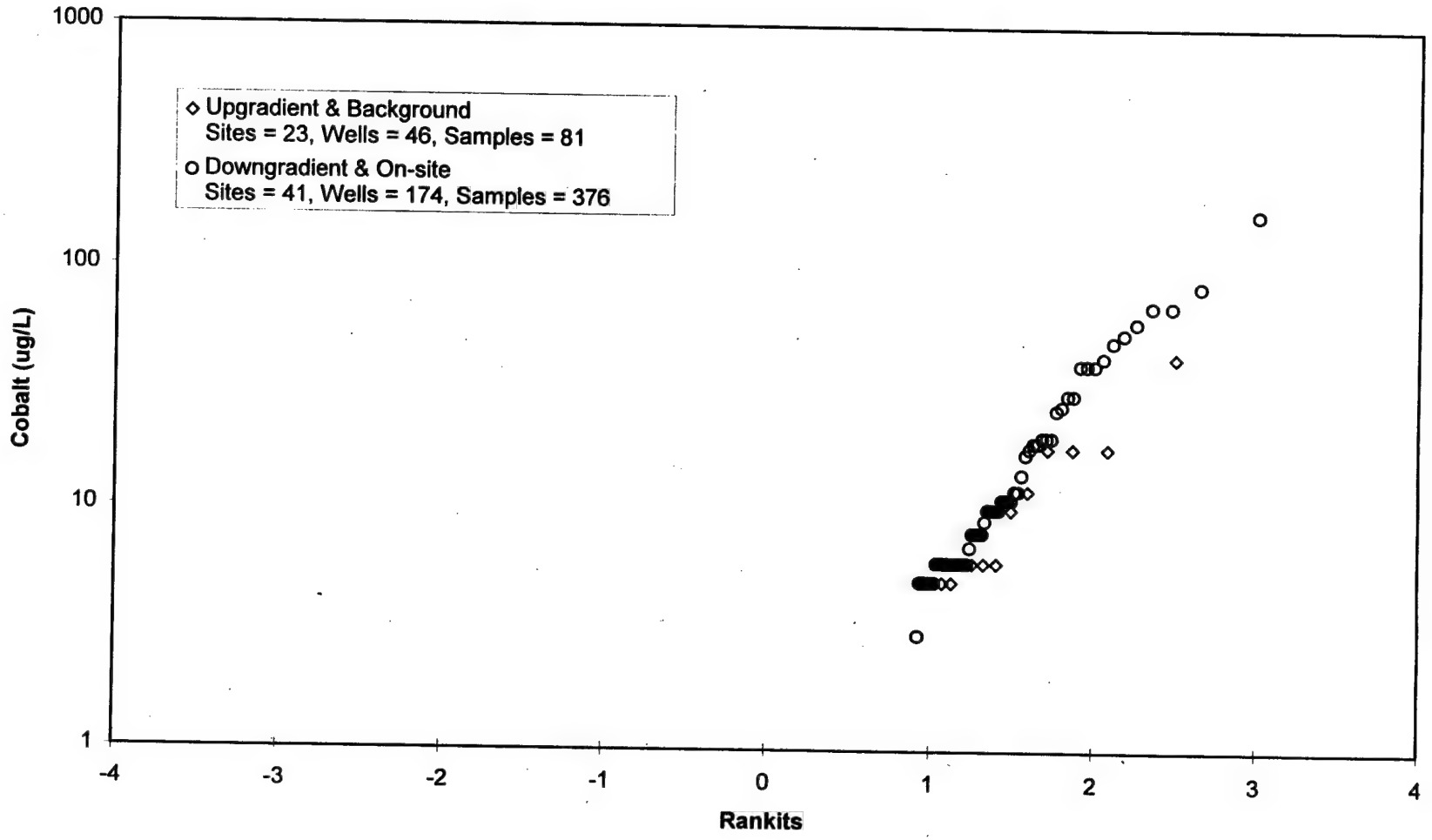

Copper Rankit Plot for Upgradient/Background & Downgradient/On-site Data Series

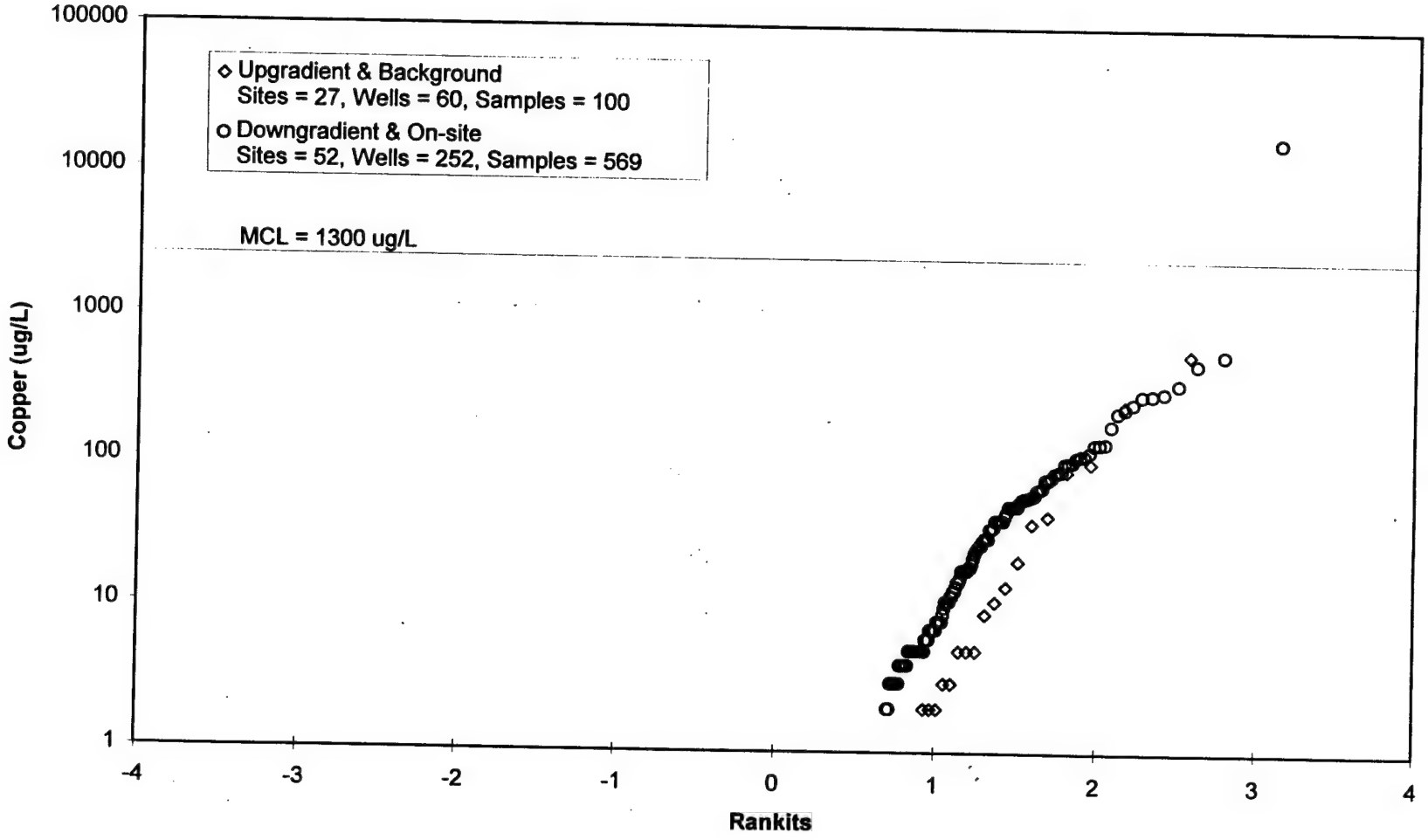

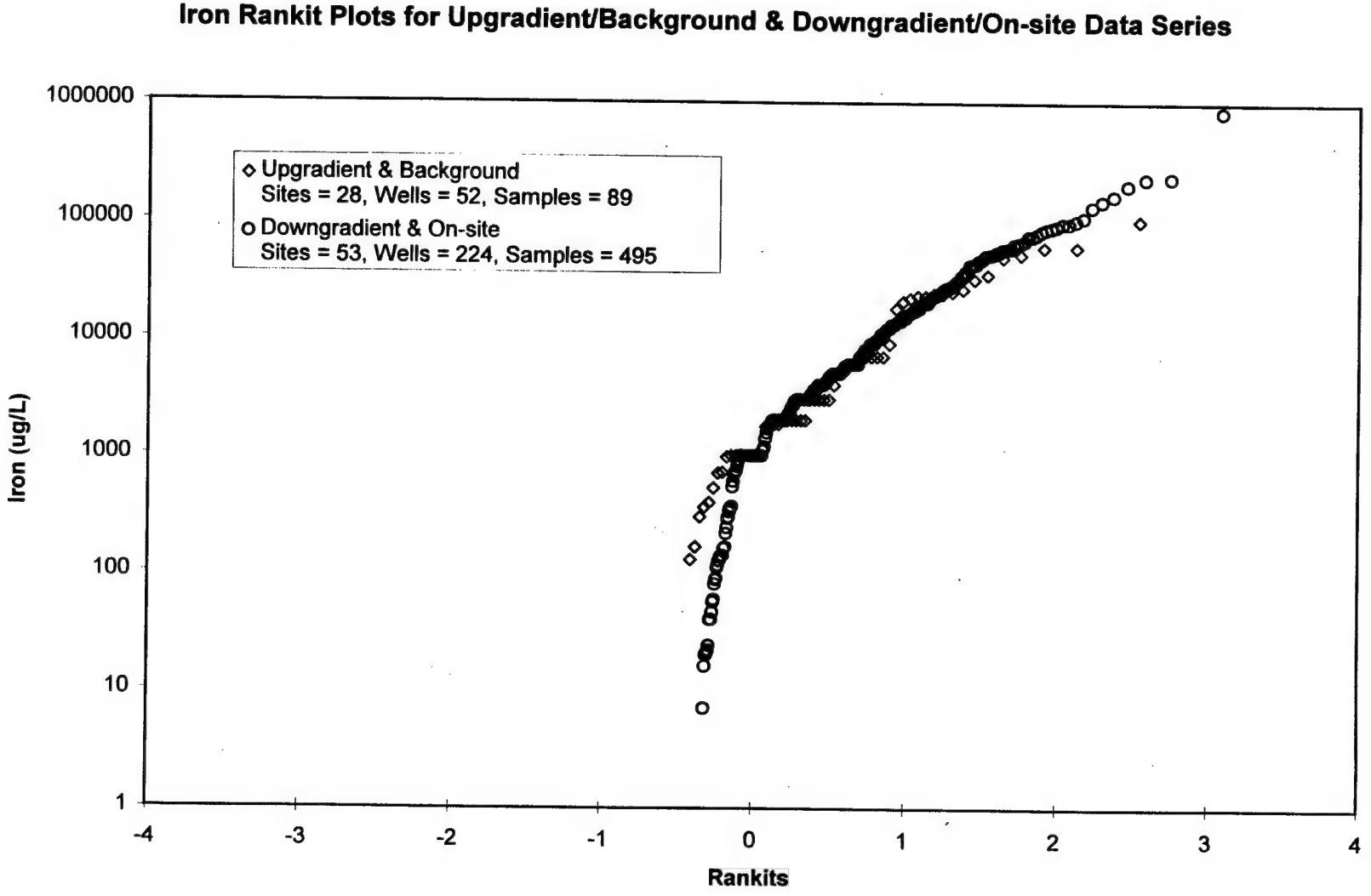
Iron Rankit Plots for Upgradient/Background & Downgradient/On-site Data Series
◇ Upgradient & Background
Sites = 28, Wells = 52, Samples = 89
o Downgradient & On-site
Sites = 53, Wells = 224, Samples = 495
Iron (ug/L)
1000000
100000
10000
1000
100
10
1
-4
-3
-2
-1
0
1
2
3
4
Rankits

Lead Rankit Plots for Upgradient/Background & Downgradient/On-site Data Series

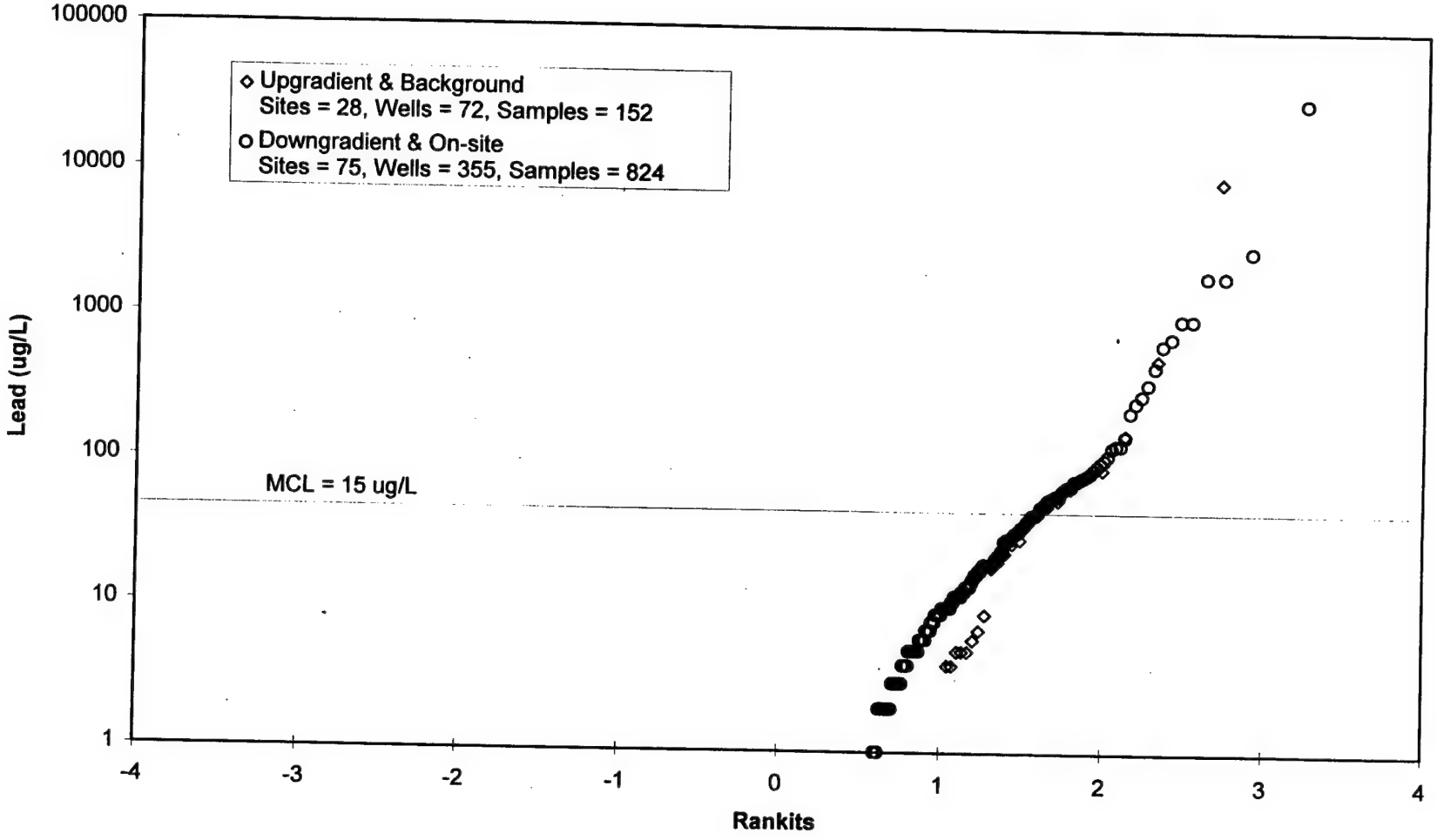

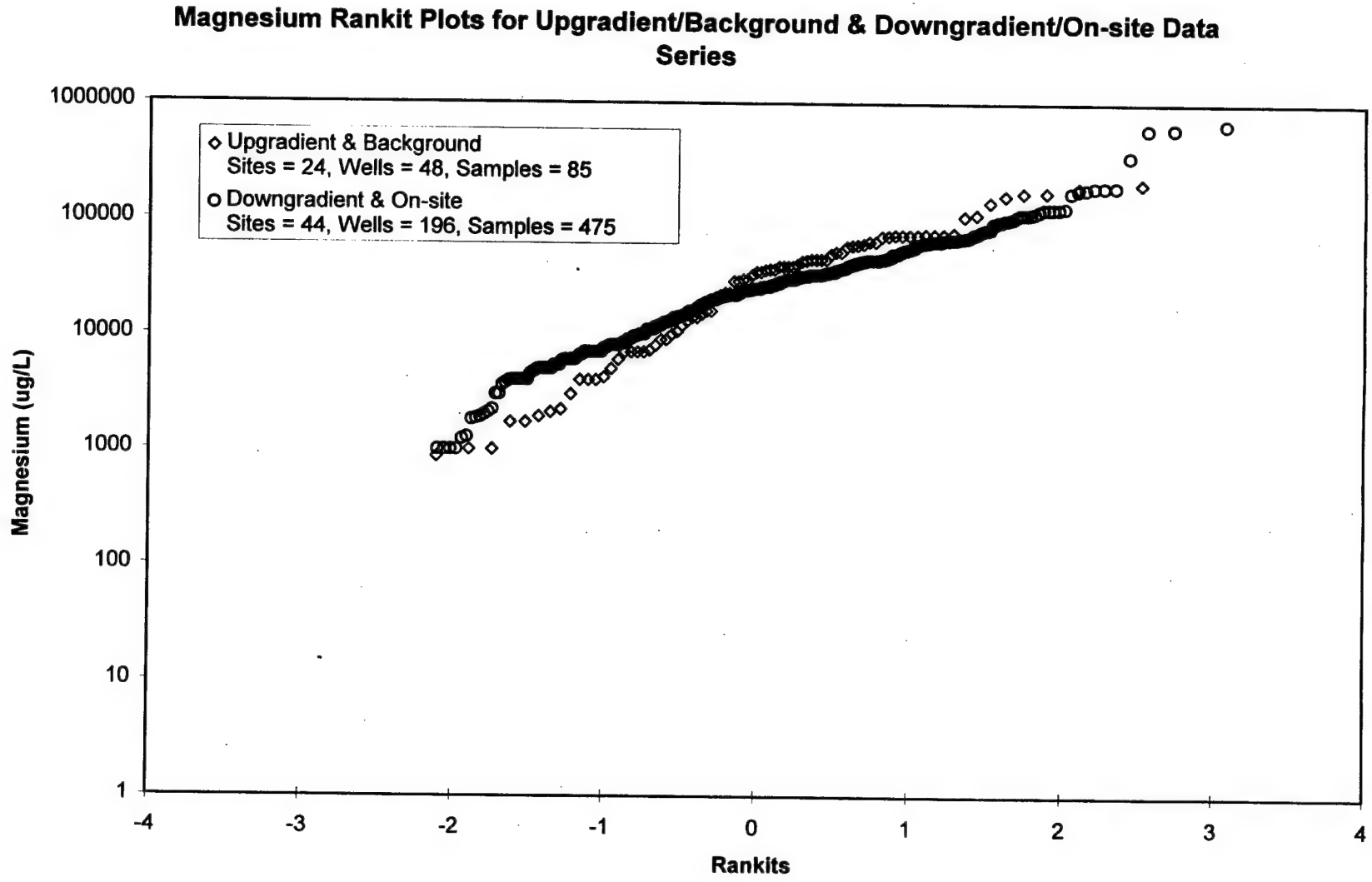
Magnesium Rankit Plots for Upgradient/Background & Downgradient/On-site Data Series
Upgradient & Background
Sites = 24, Wells = 48, Samples = 85
Downgradient & On-site
Sites = 44, Wells = 196, Samples = 475
Magnesium (ug/L)
1000000
100000
10000
1000
100
10
1
-4
-3
-2
-1
0
1
2
3
4
Rankits

Manganese Rankit Plots for Upgradient/Background & Downgradient/On-site Data Series

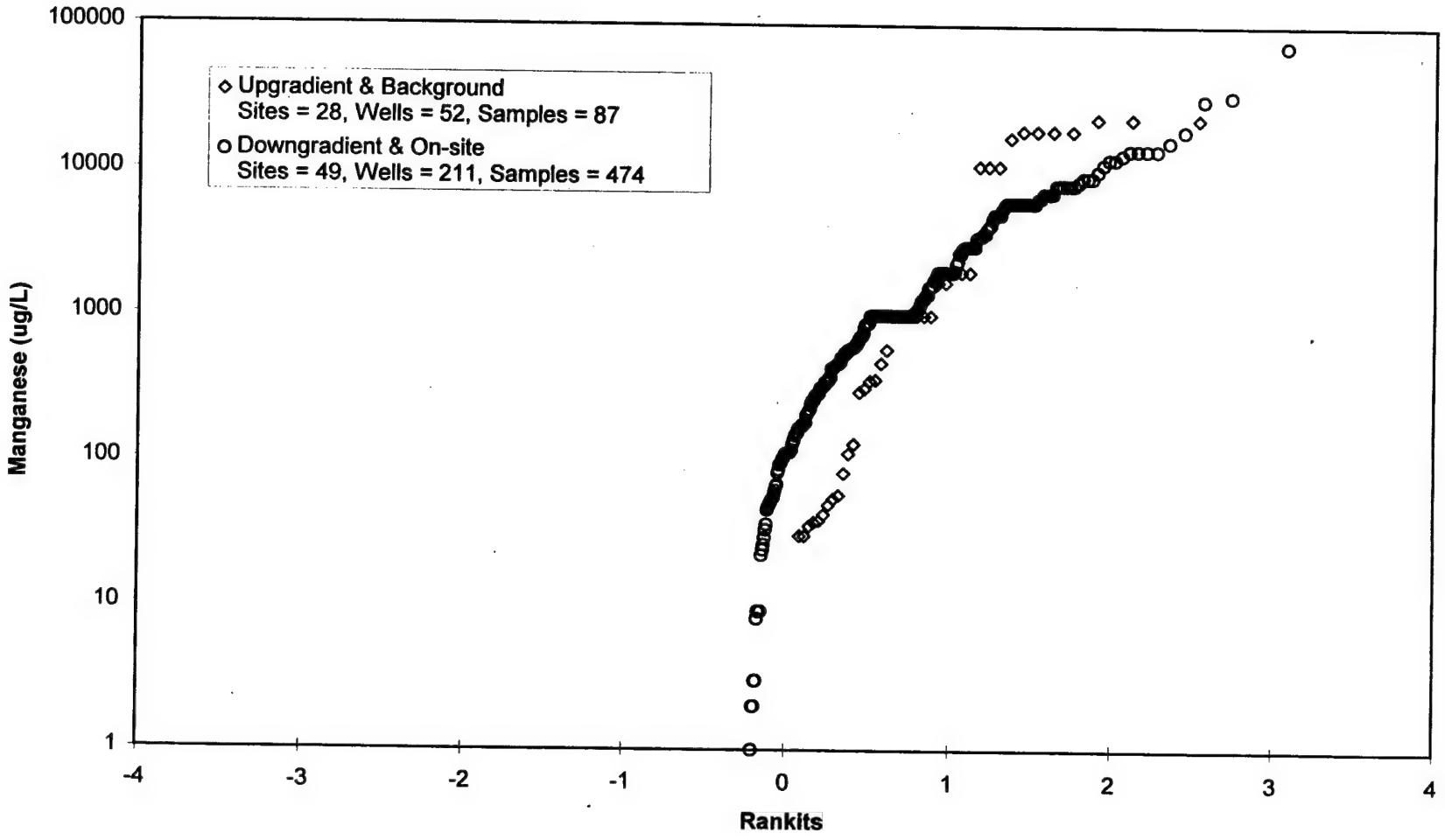

Mercury Rankit Plots for Upgradient/Background & Downgradient/On-site Data Series

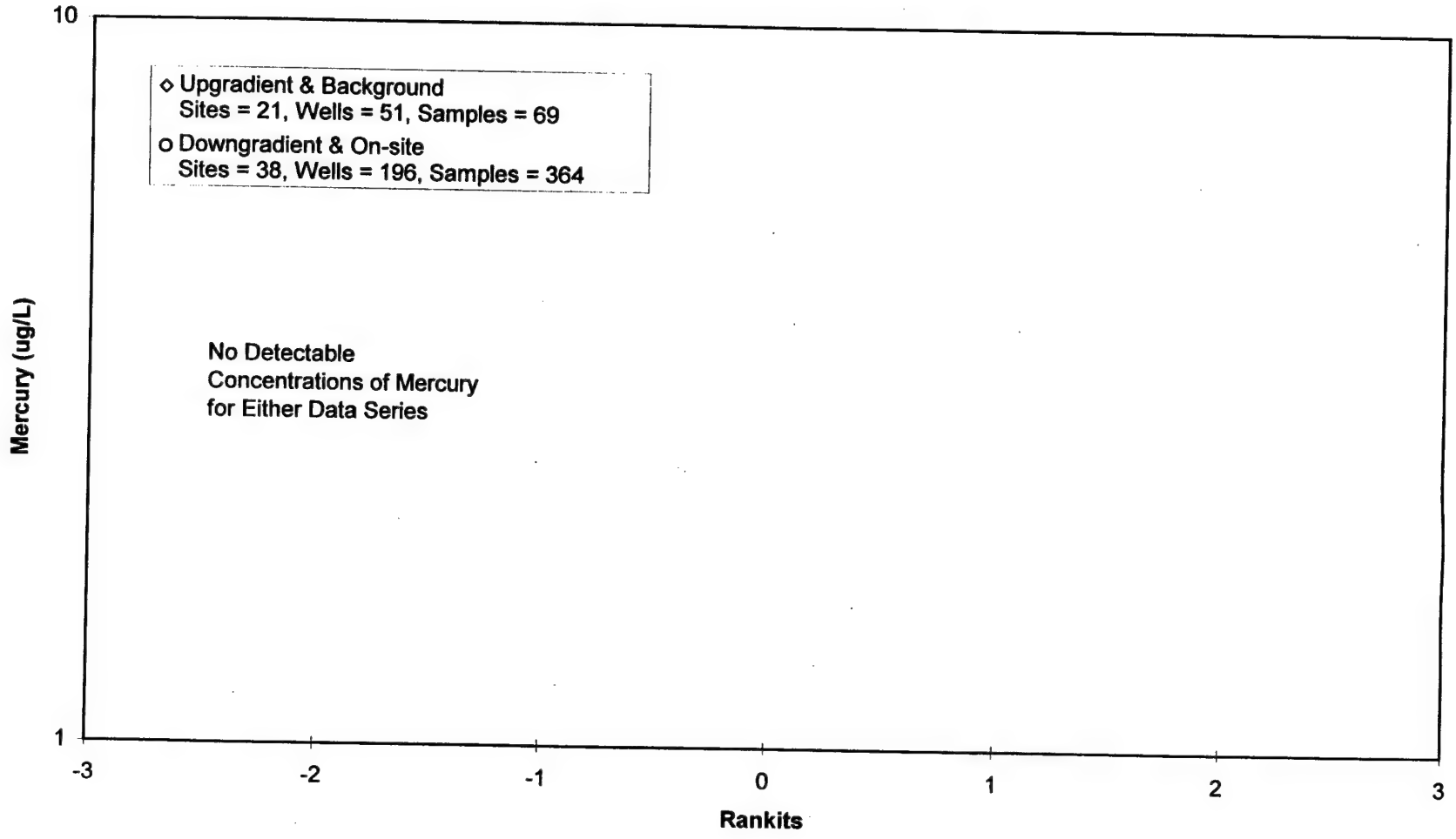

Molybdenum Rankit Plots for Upgradient/Background & Downgradient/On-site Data Series

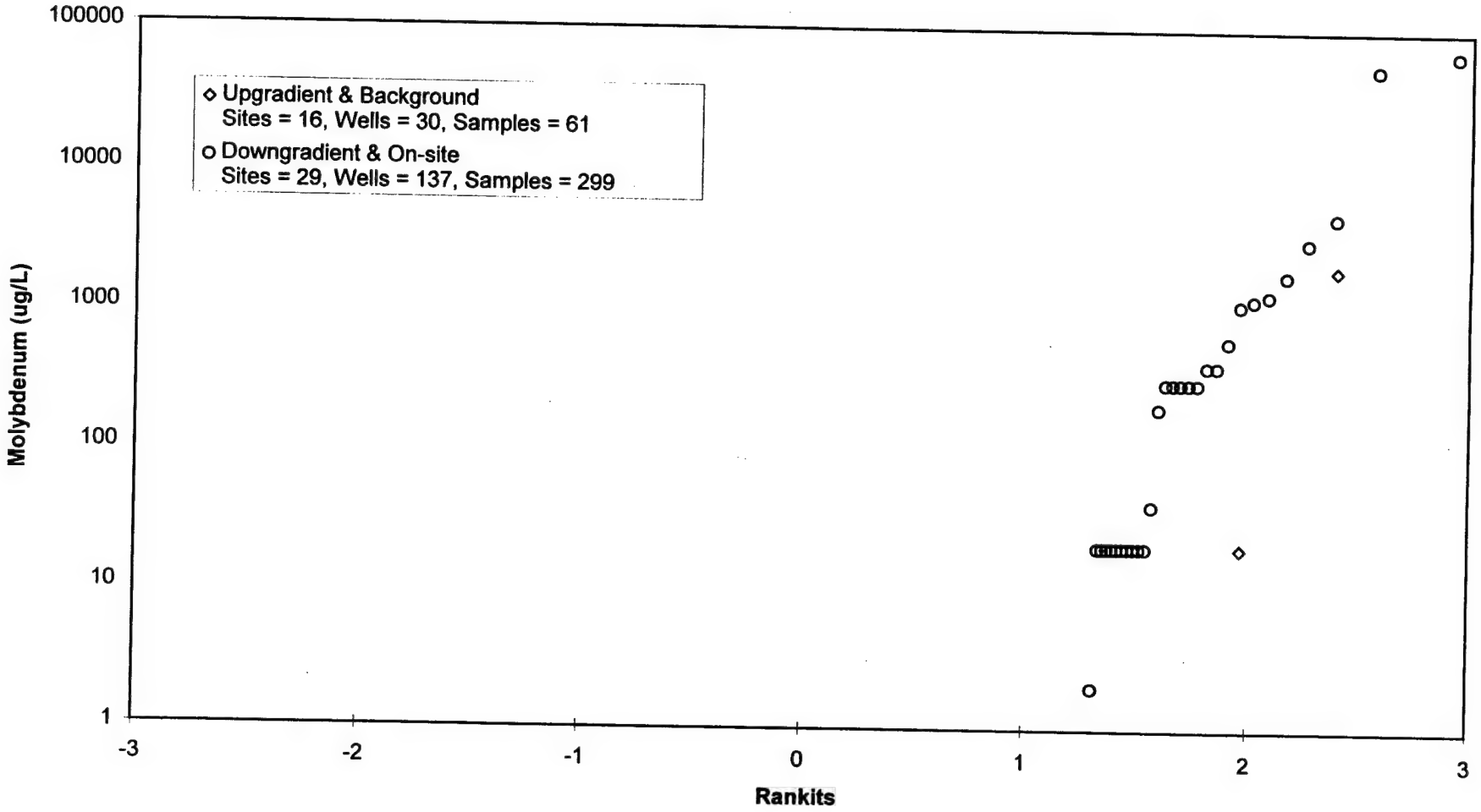

Nickel Rankit Plots for Upgradient/Background & Downgradient/On-site Data Series

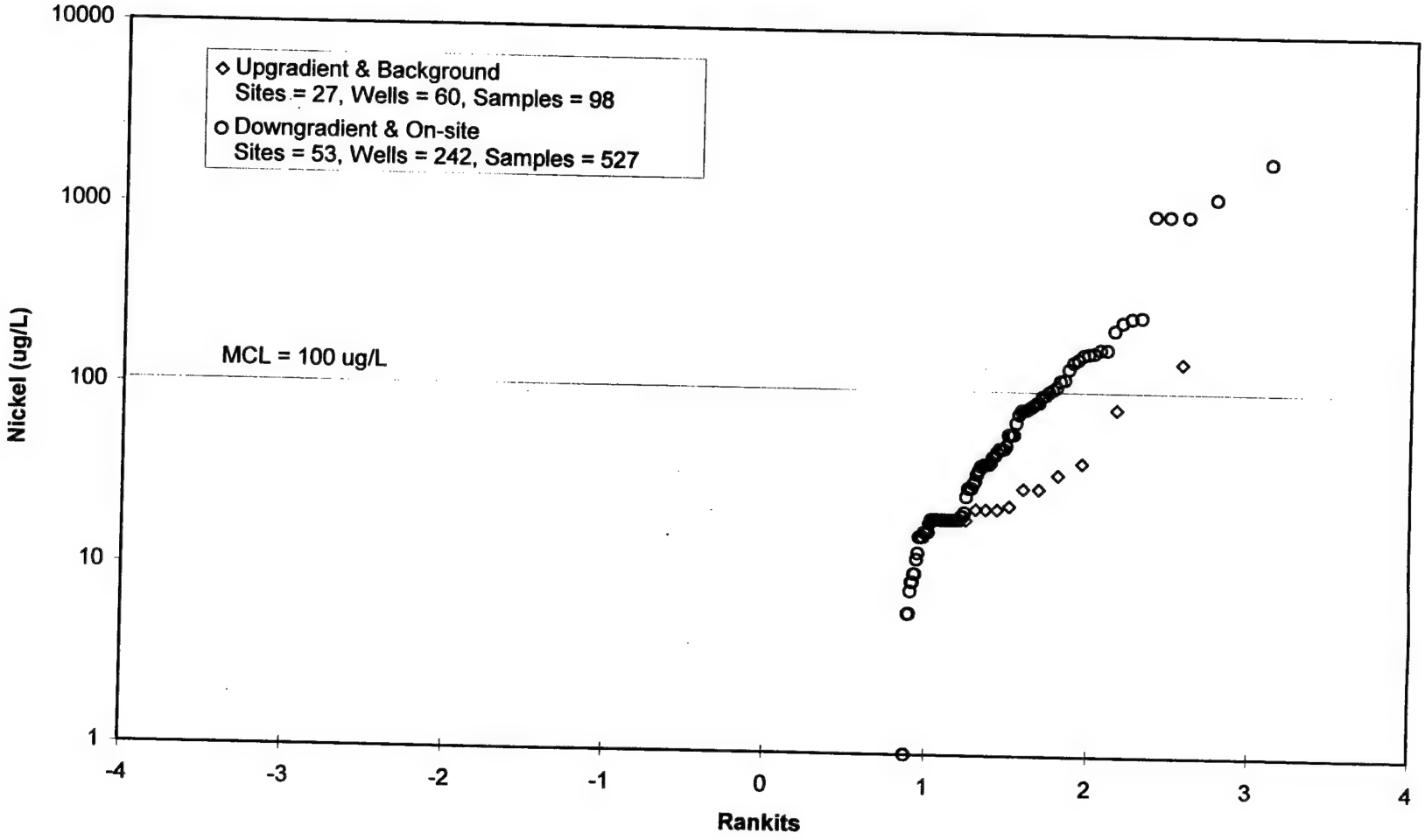

Potassium Rankit Plots for Upgradient/Background & Downgradient/On-site Data Series

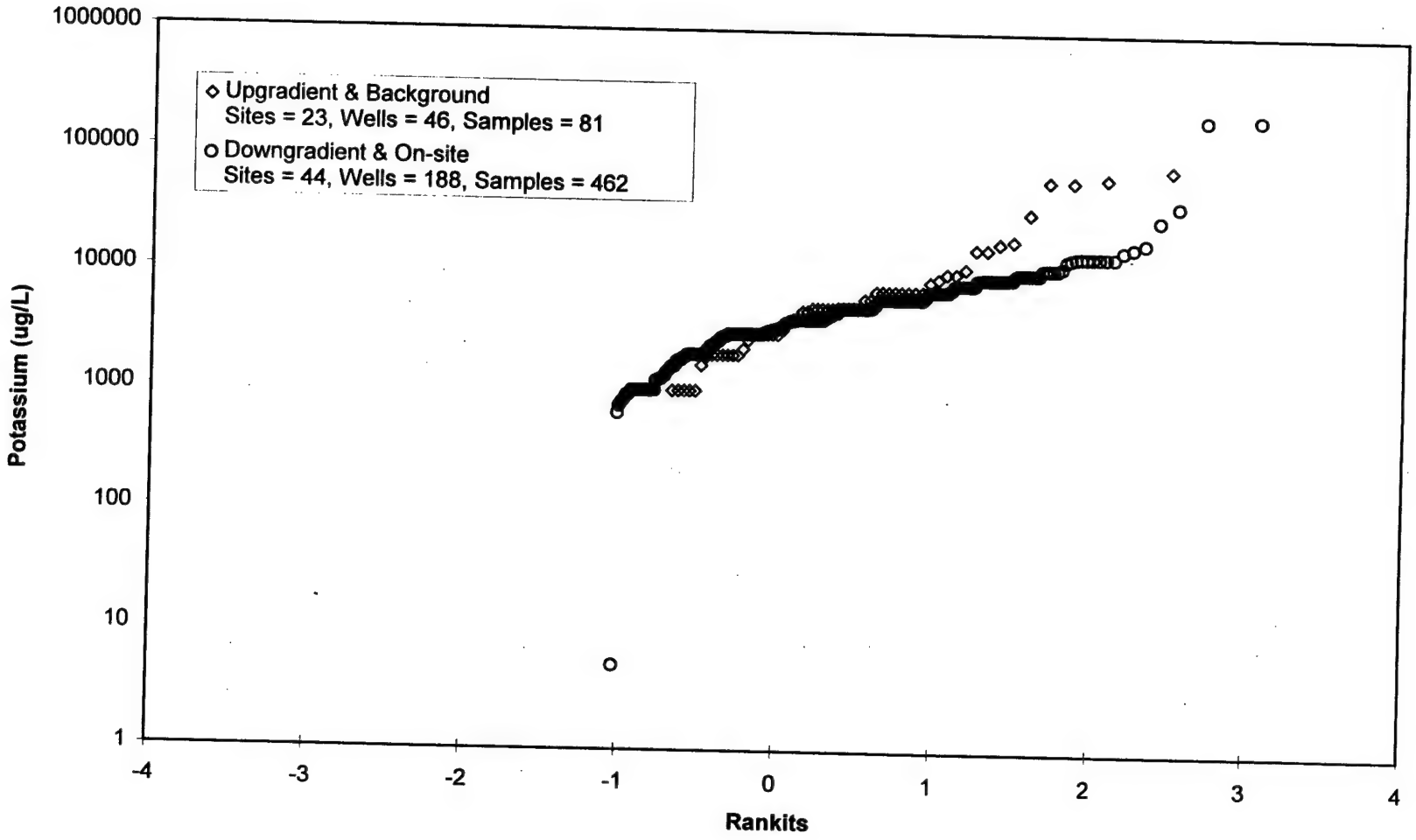

Selenium Rankit Plots for Upgradient/Background & Downgradient/On-site Data Series

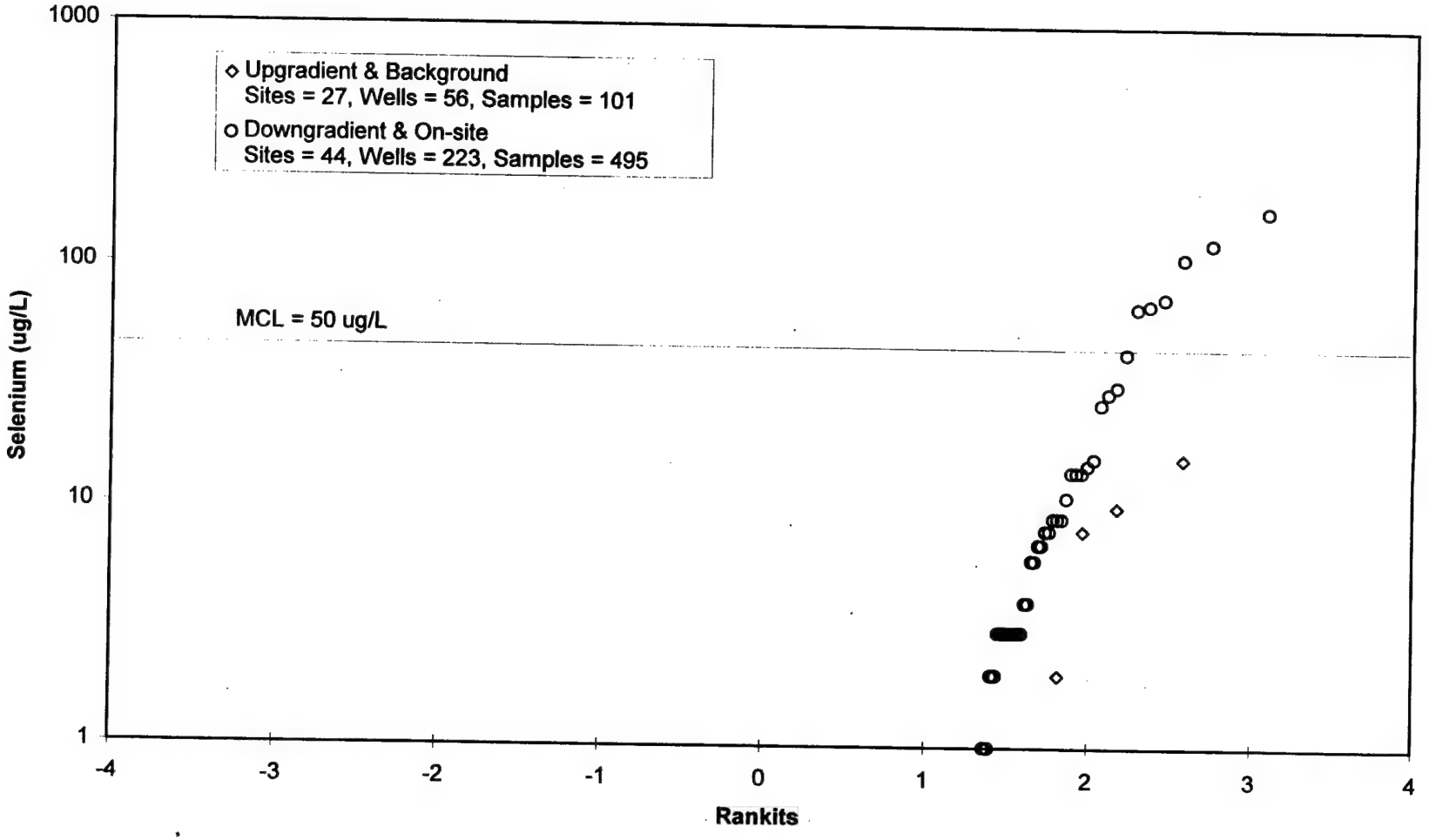

Silver Rankit Plots for Upgradient/Background & Downgradient/On-site Data Series

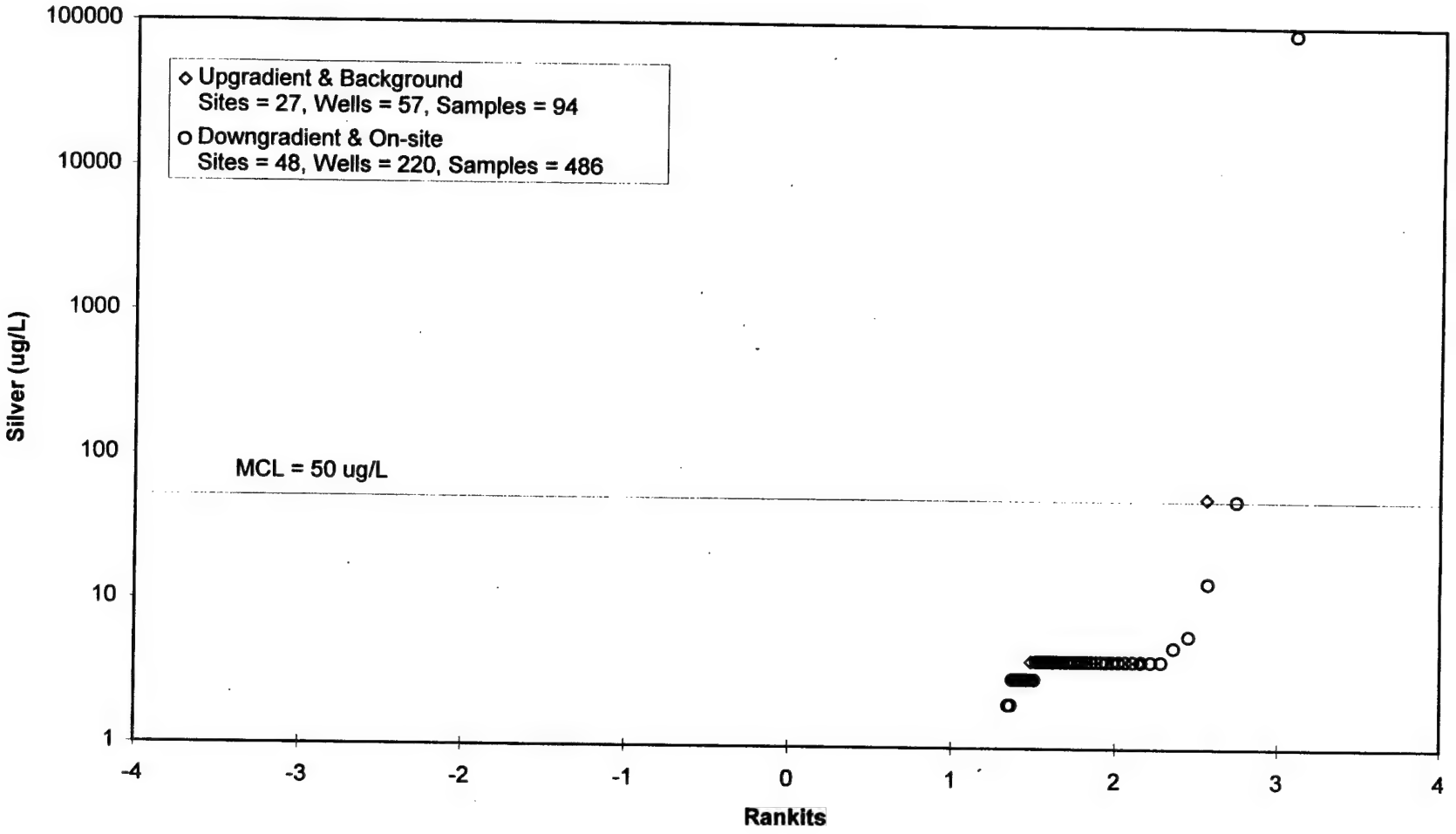

Sodium Rankit Plots for Upgradient/Background & Downgradient/On-site Data Series

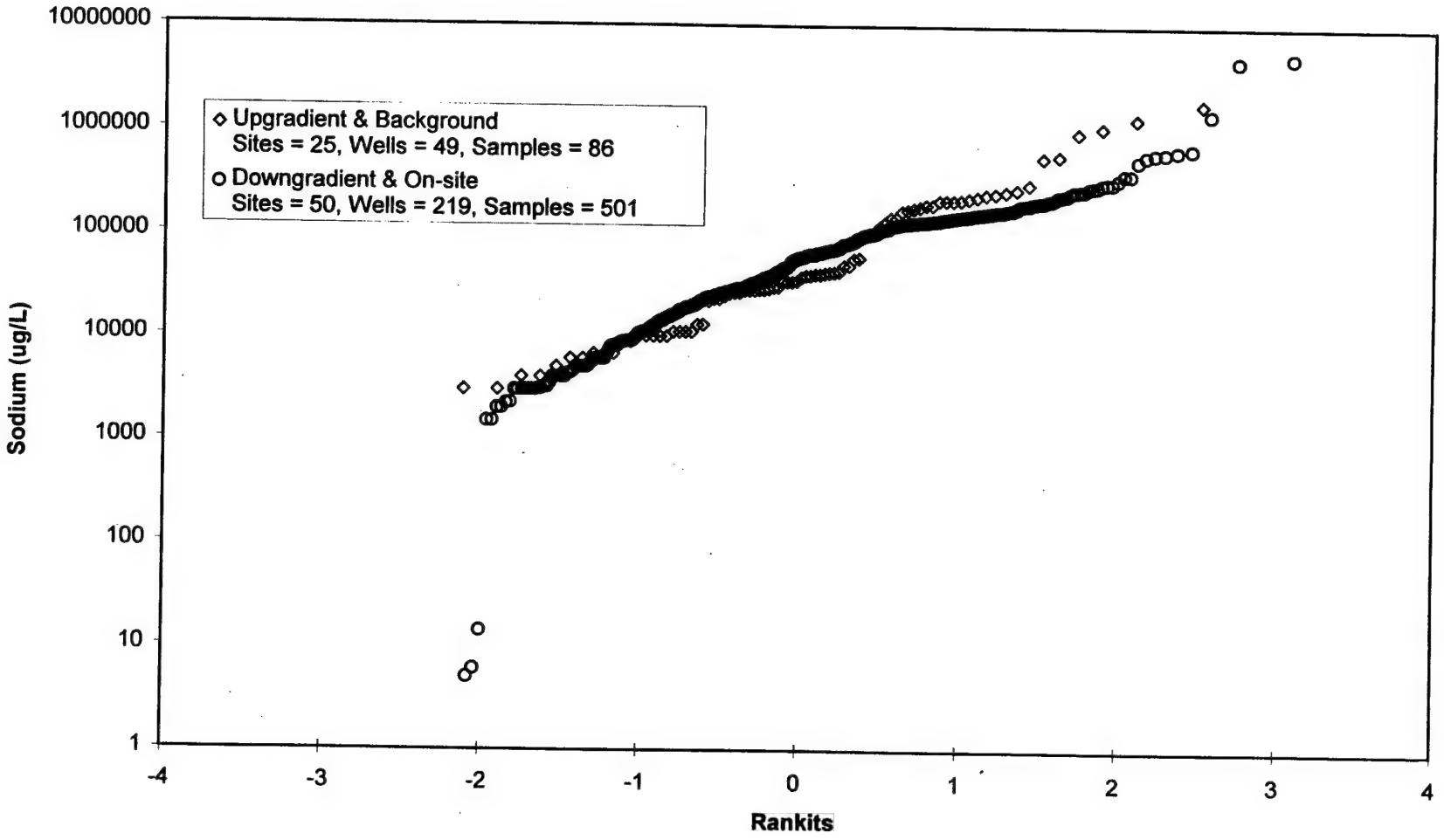

Thallium Rankit Plots for Upgradient/Background & Downgradient/On-site Data Series

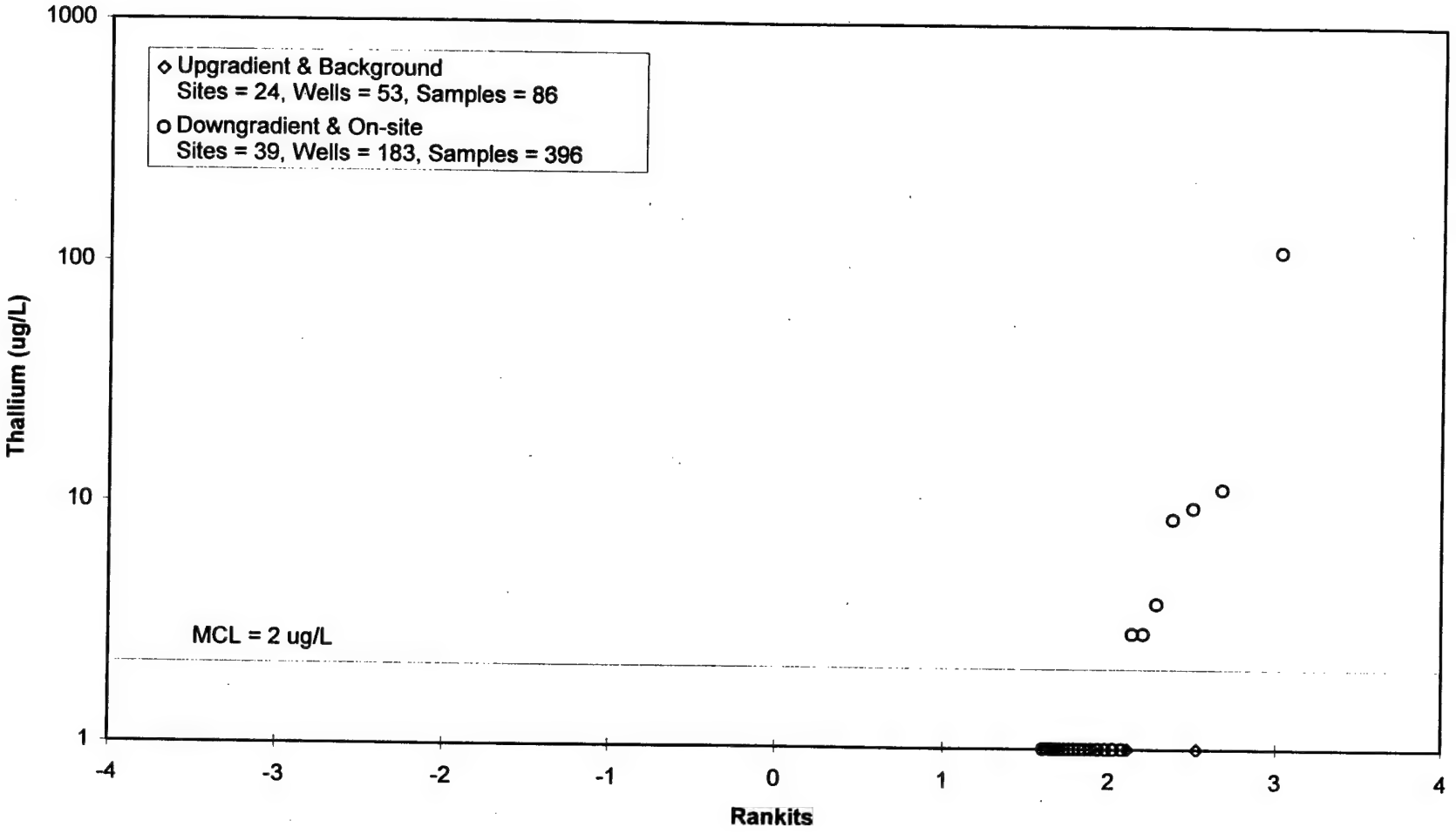

Vanadium Rankit Plots for Upgradient/Background & Downgradient/On-site Data Series

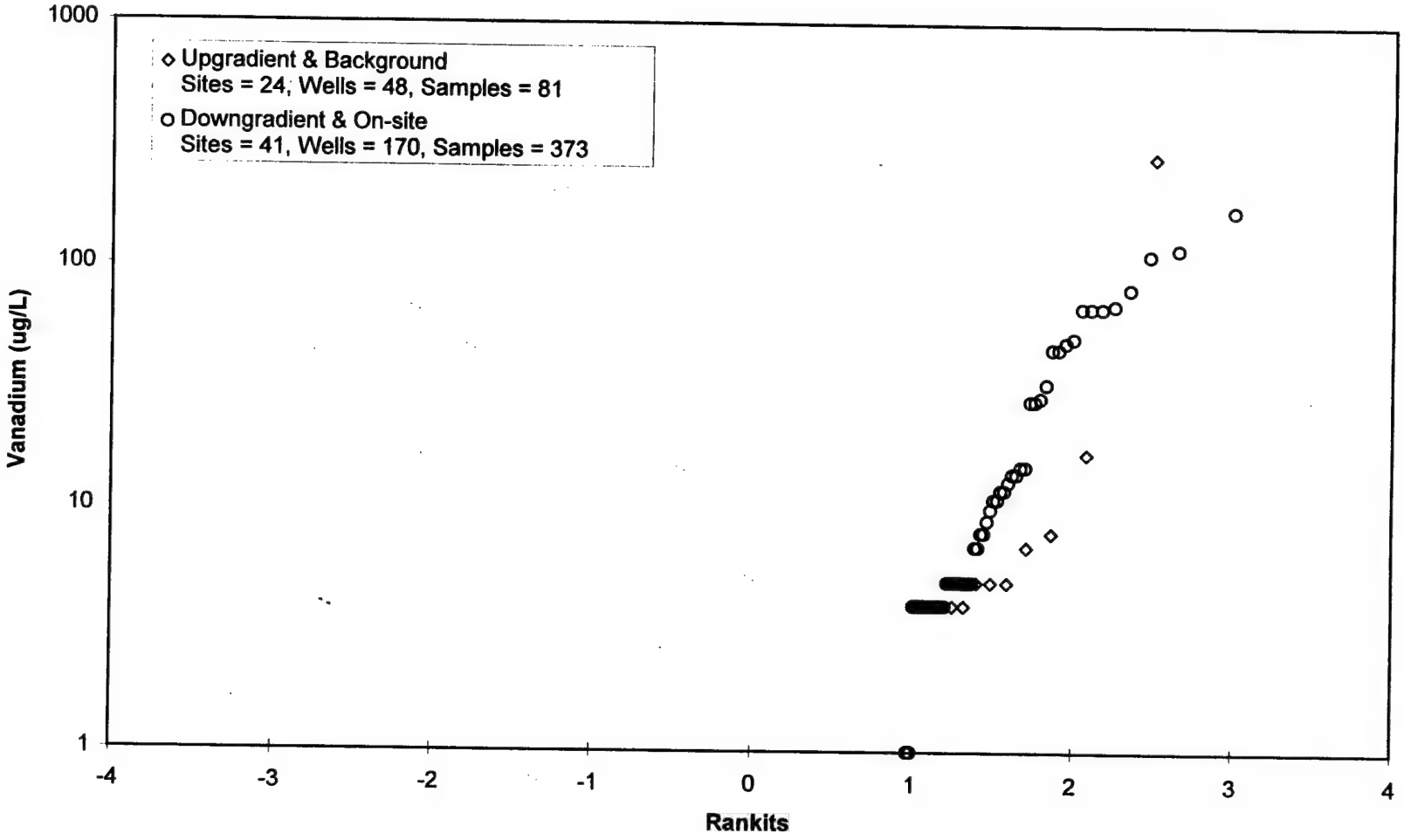

Zinc Rankit Plots for Upgradient/Background & Downgradient/On-site Data Series

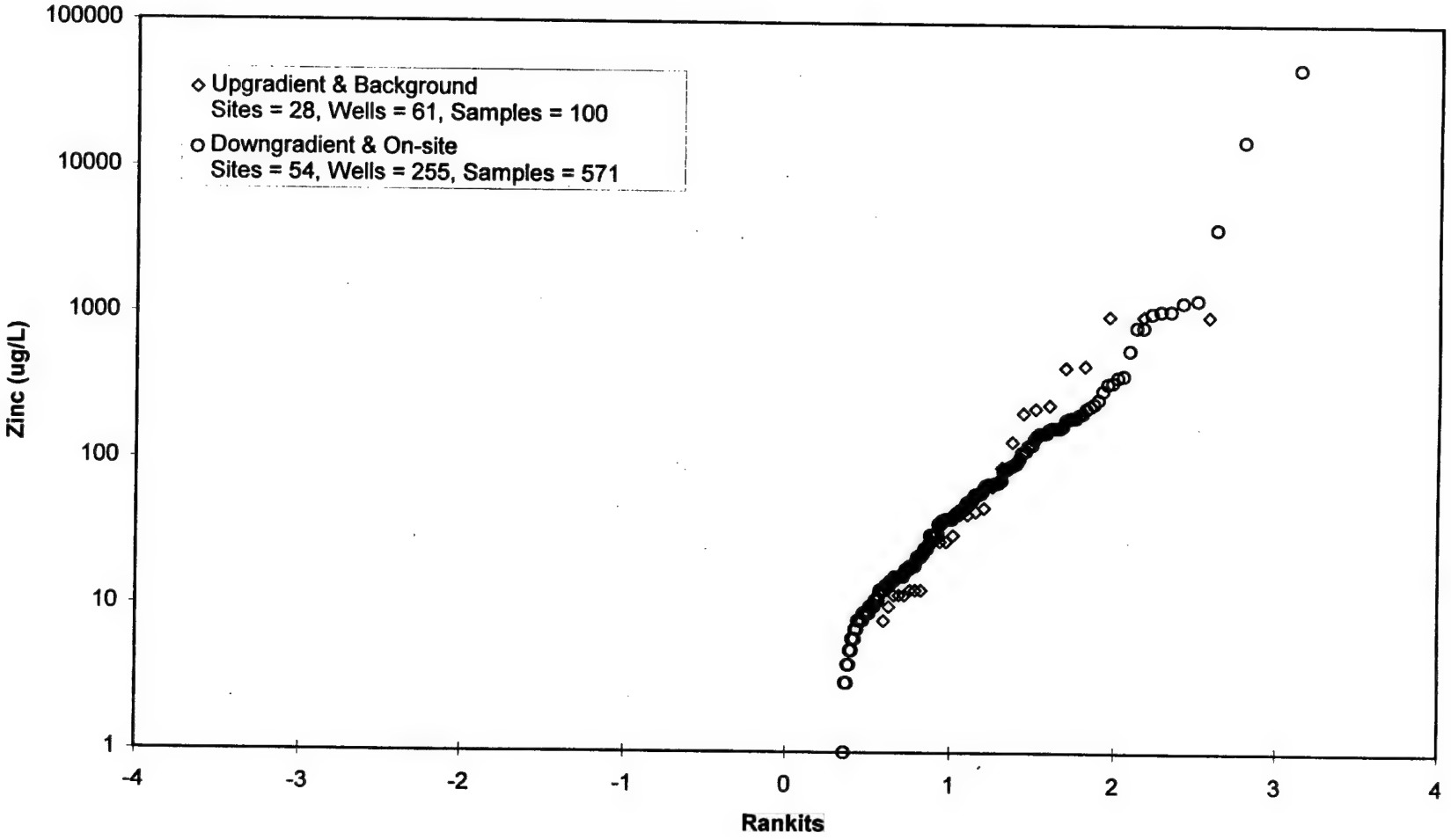

Appendix H: Metal Versus pH Scatter Plots

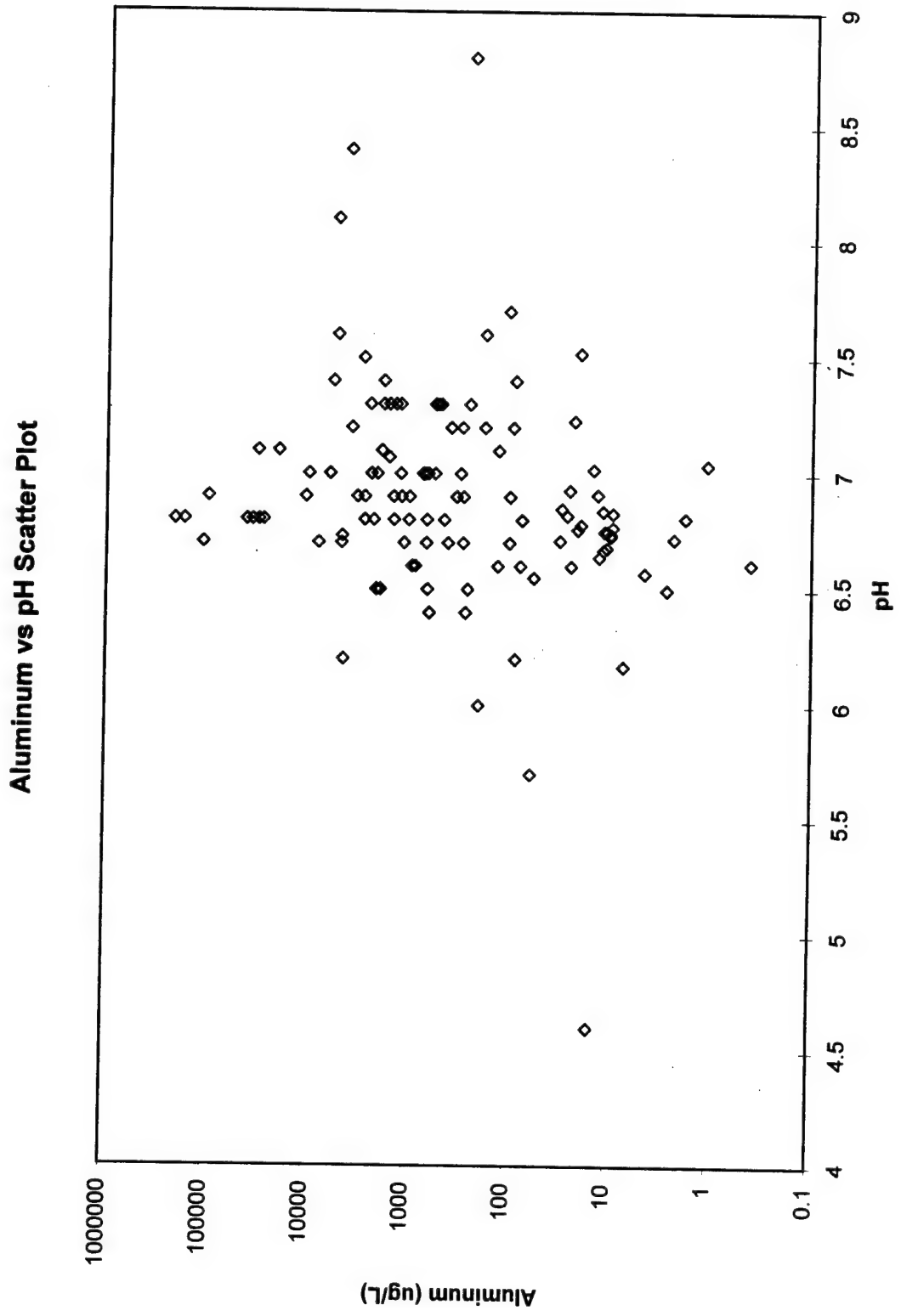

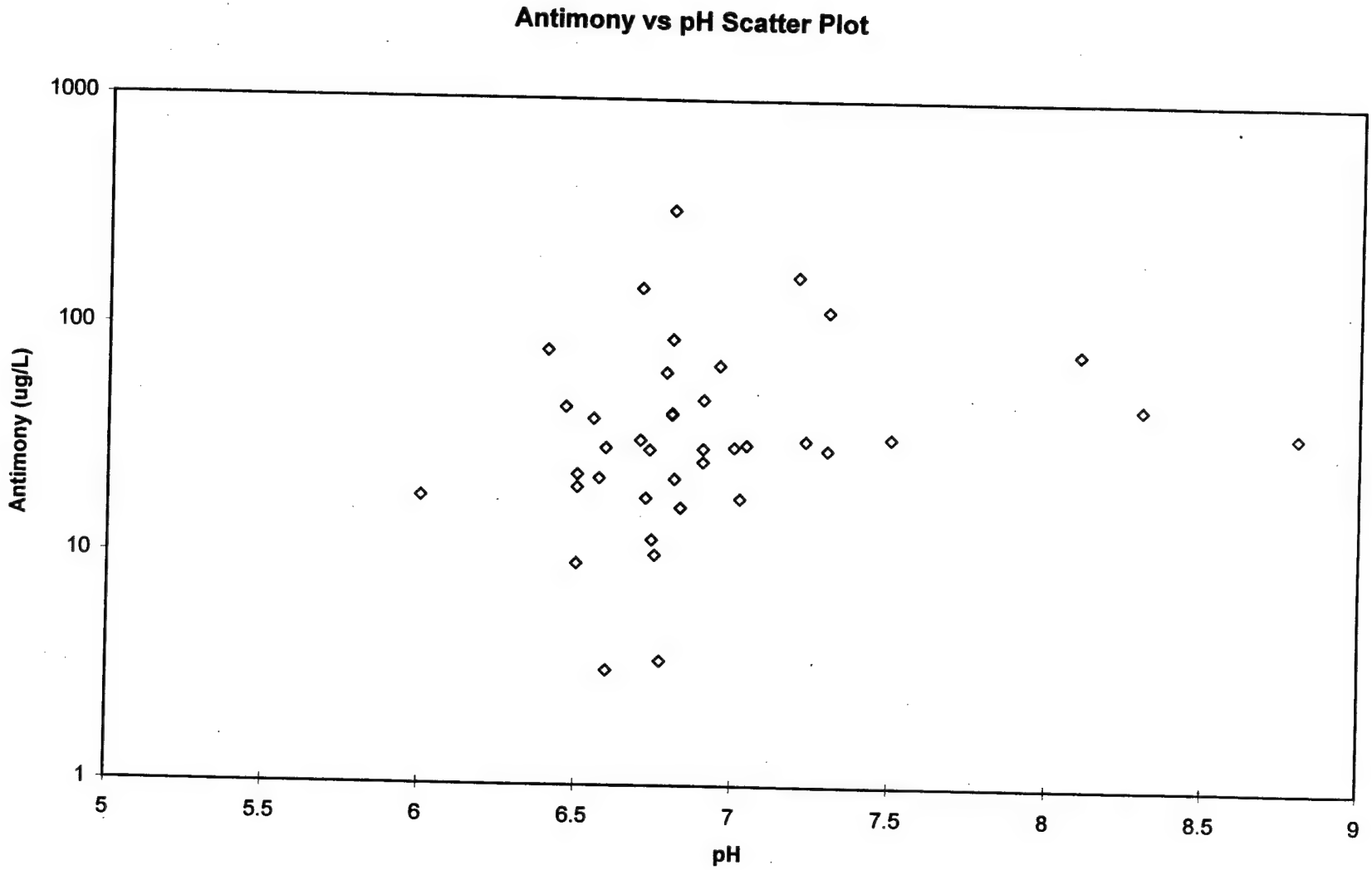
Antimony vs pH Scatter Plot
Antimony (ug/L)
1000
100
10
1
5
5.5
6
6.5
7
7.5
8
8.5
9
pH

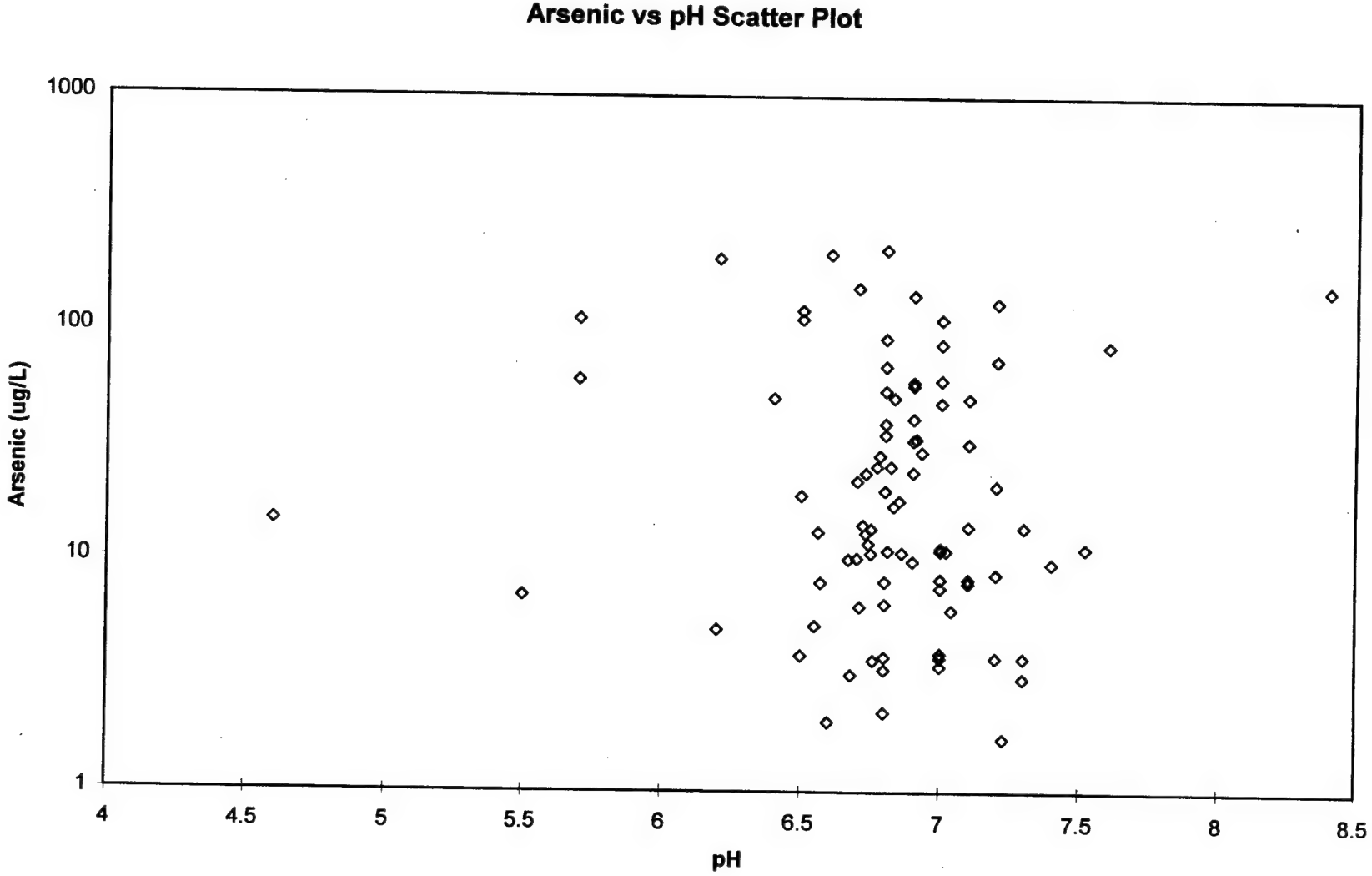
Arsenic vs pH Scatter Plot
1000
100
10
1
Arsenic (ug/L)
4
4.5
5
5.5
6
6.5
7
7.5
8
8.5
pH

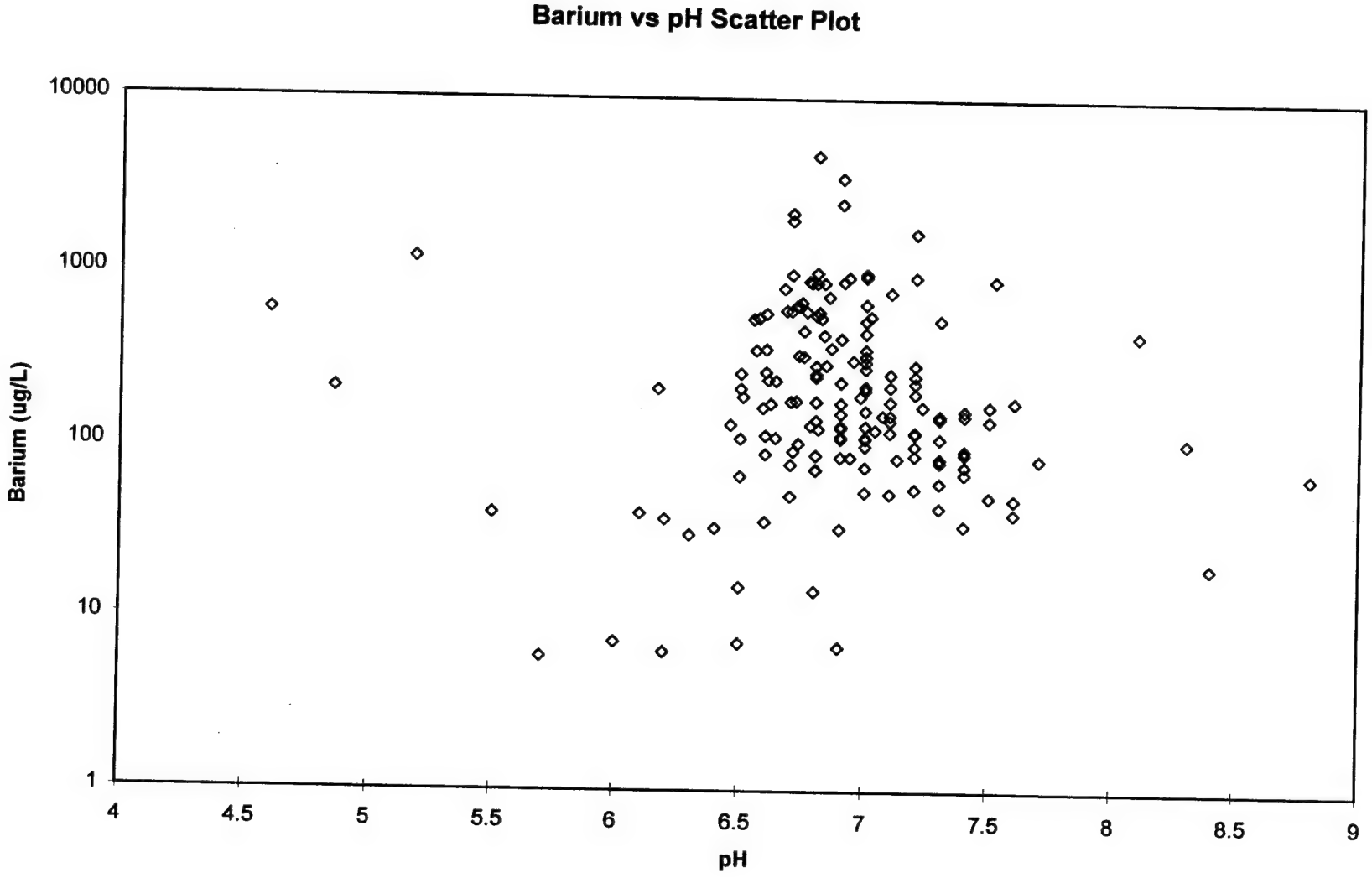
Barium vs pH Scatter Plot
Barium (ug/L)
10000
1000
100
10
1
4
4.5
5
5.5
6
6.5
7
7.5
8
8.5
9
pH

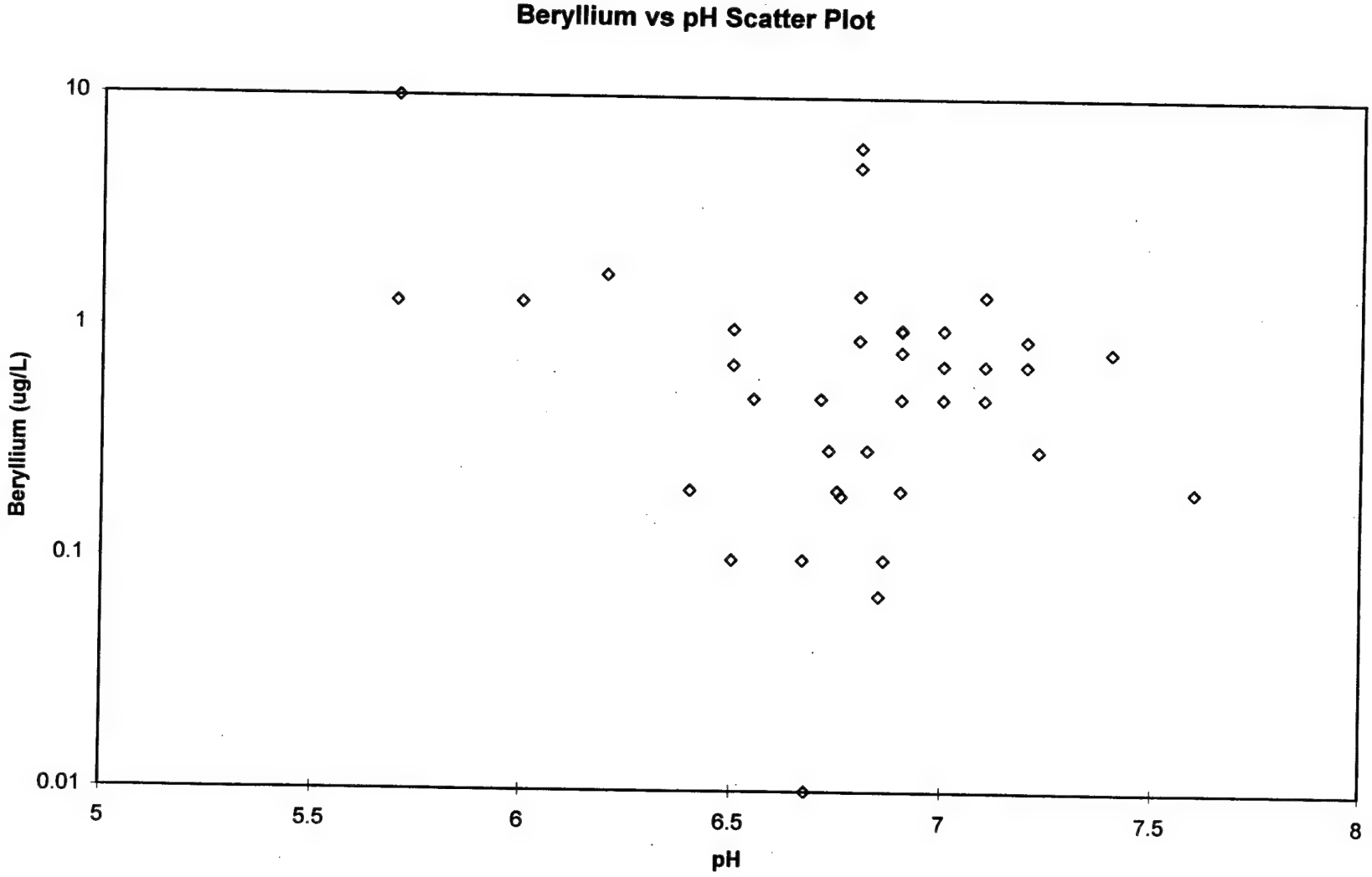
Beryllium vs pH Scatter Plot
Beryllium (ug/L)
10
1
0.1
0.01
5
5.5
6
6.5
7
7.5
8
pH

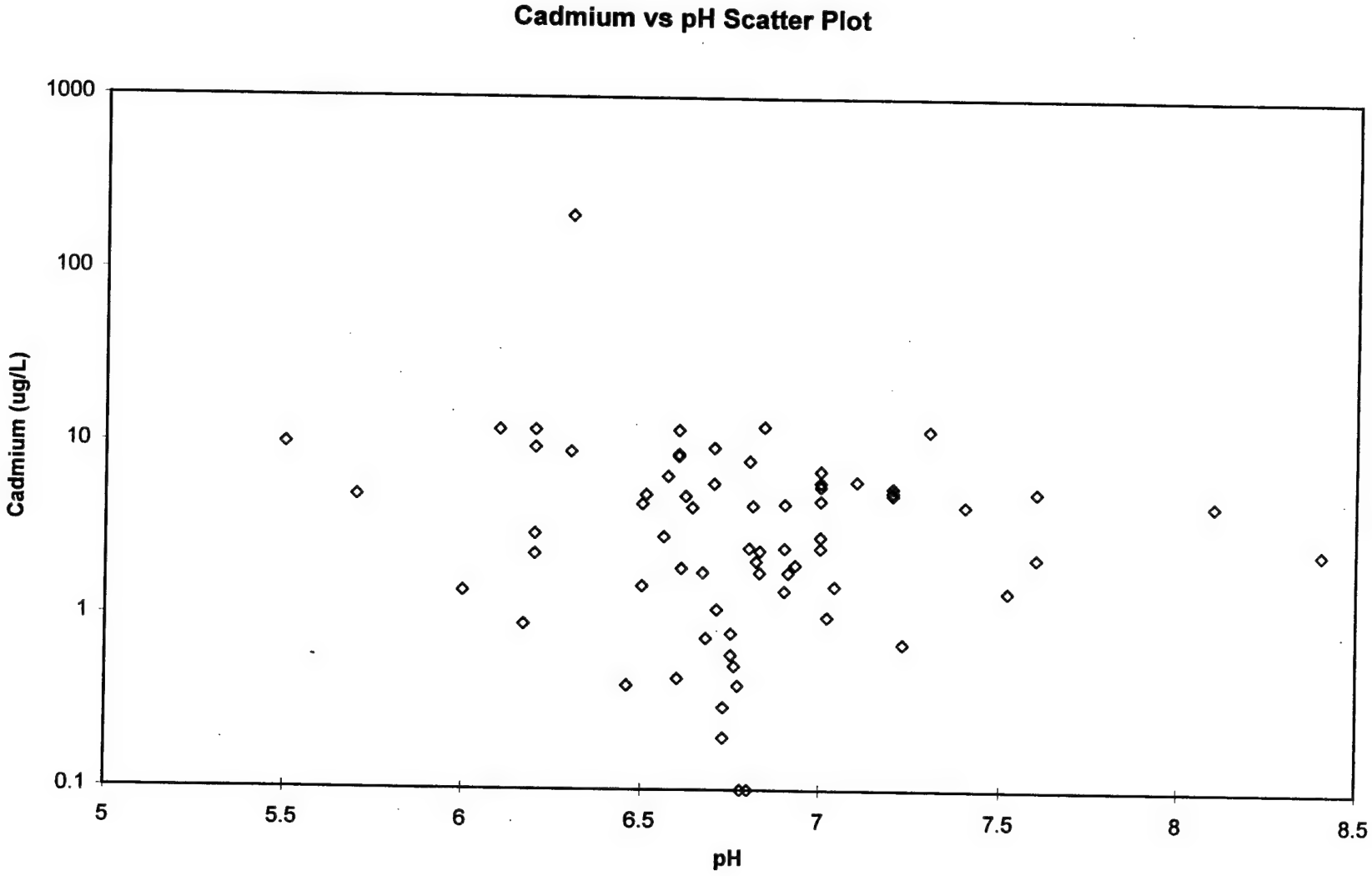
Cadmium vs pH Scatter Plot
1000
100
10
1
0.1
Cadmium (ug/L)
5
5.5
6
6.5
7
7.5
8
8.5
pH

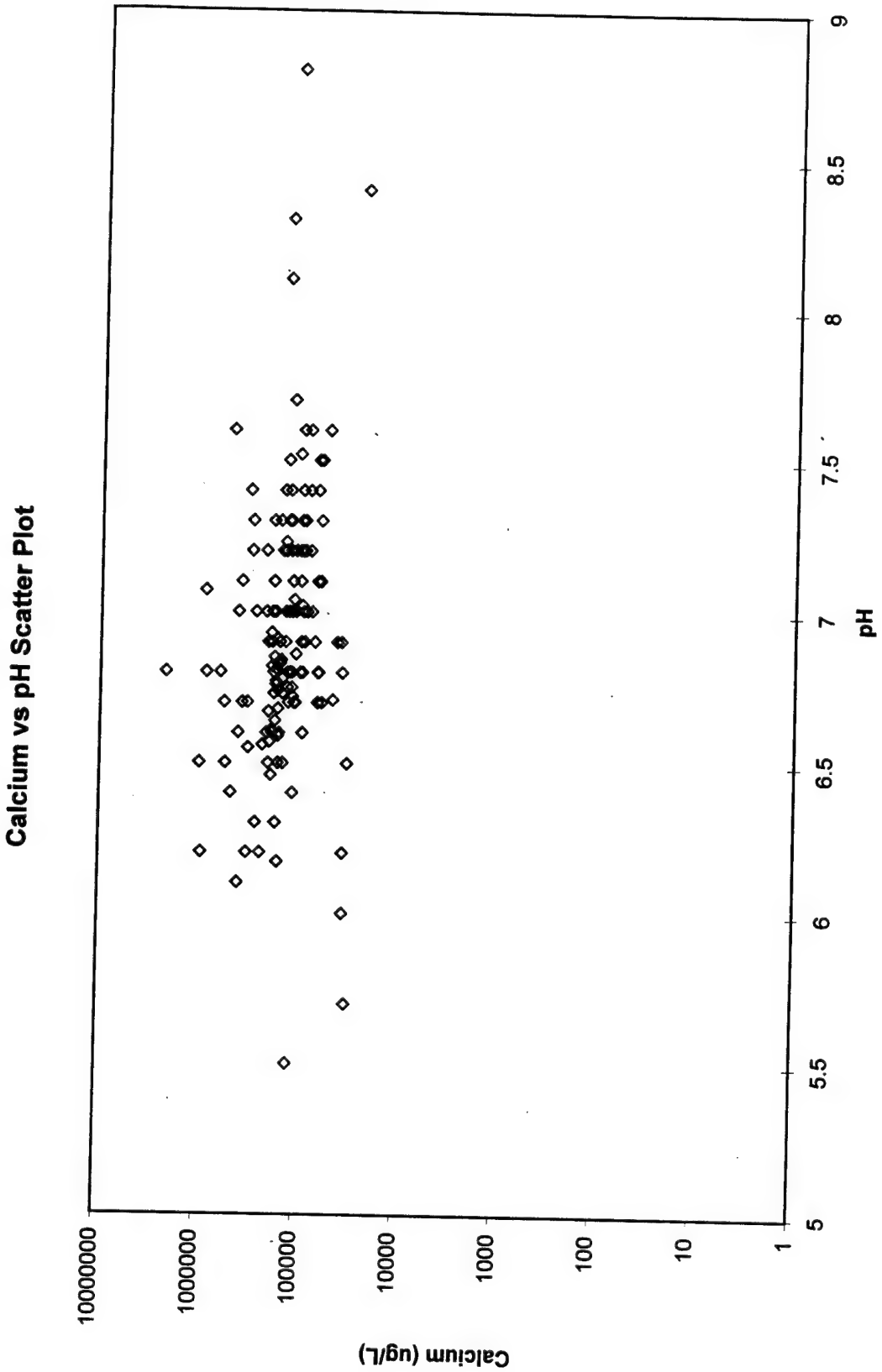
Calcium vs pH Scatter Plot
Calcium (ug/L)
10000000
1000000
100000
10000
1000
100
10
1
pH
5
5.5
6
6.5
7
7.5
8
8.5
9

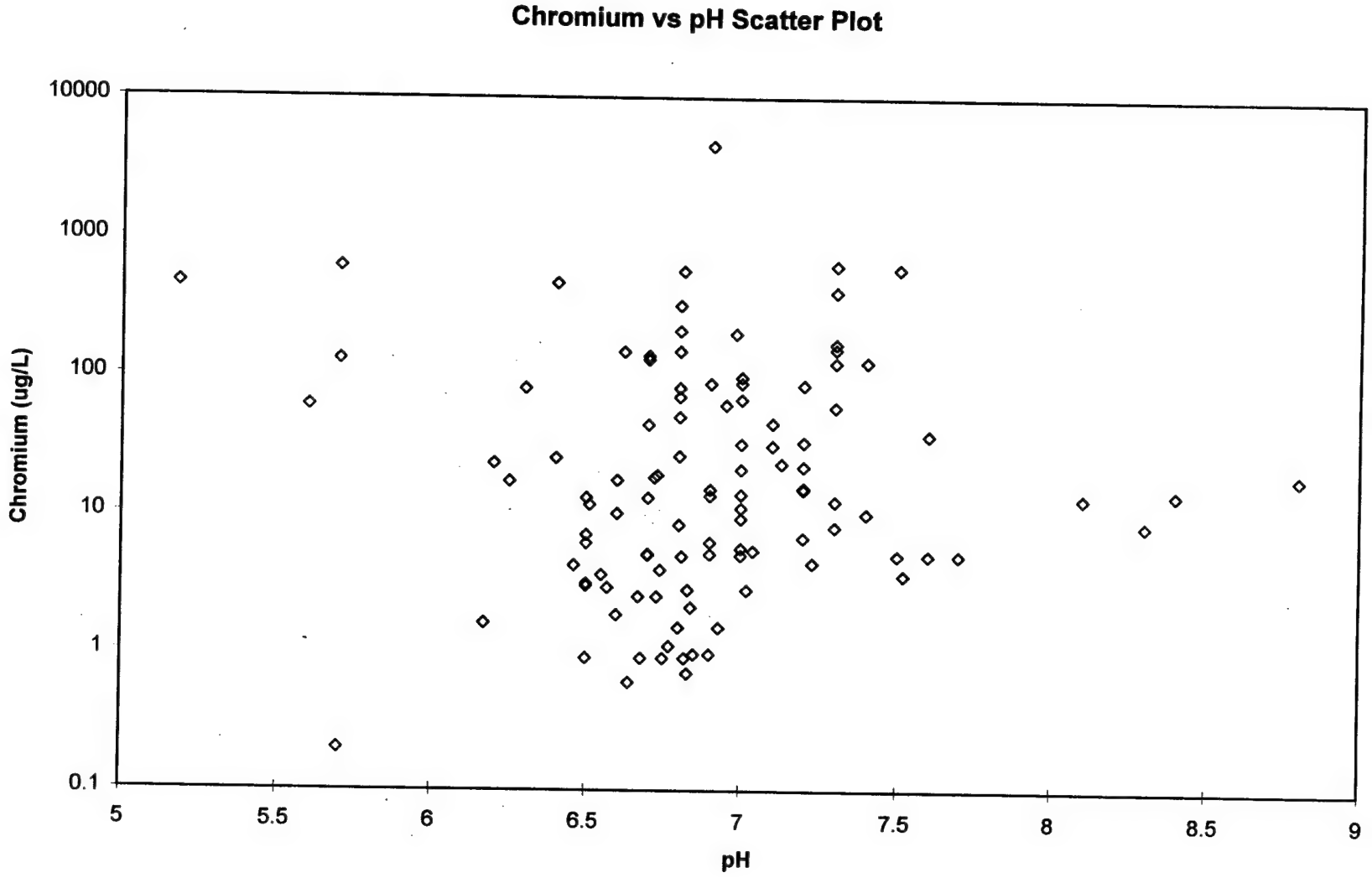
Chromium vs pH Scatter Plot
Chromium (ug/L)
10000
1000
100
10
1
0.1
5
5.5
6
6.5
7
7.5
8
8.5
9
pH

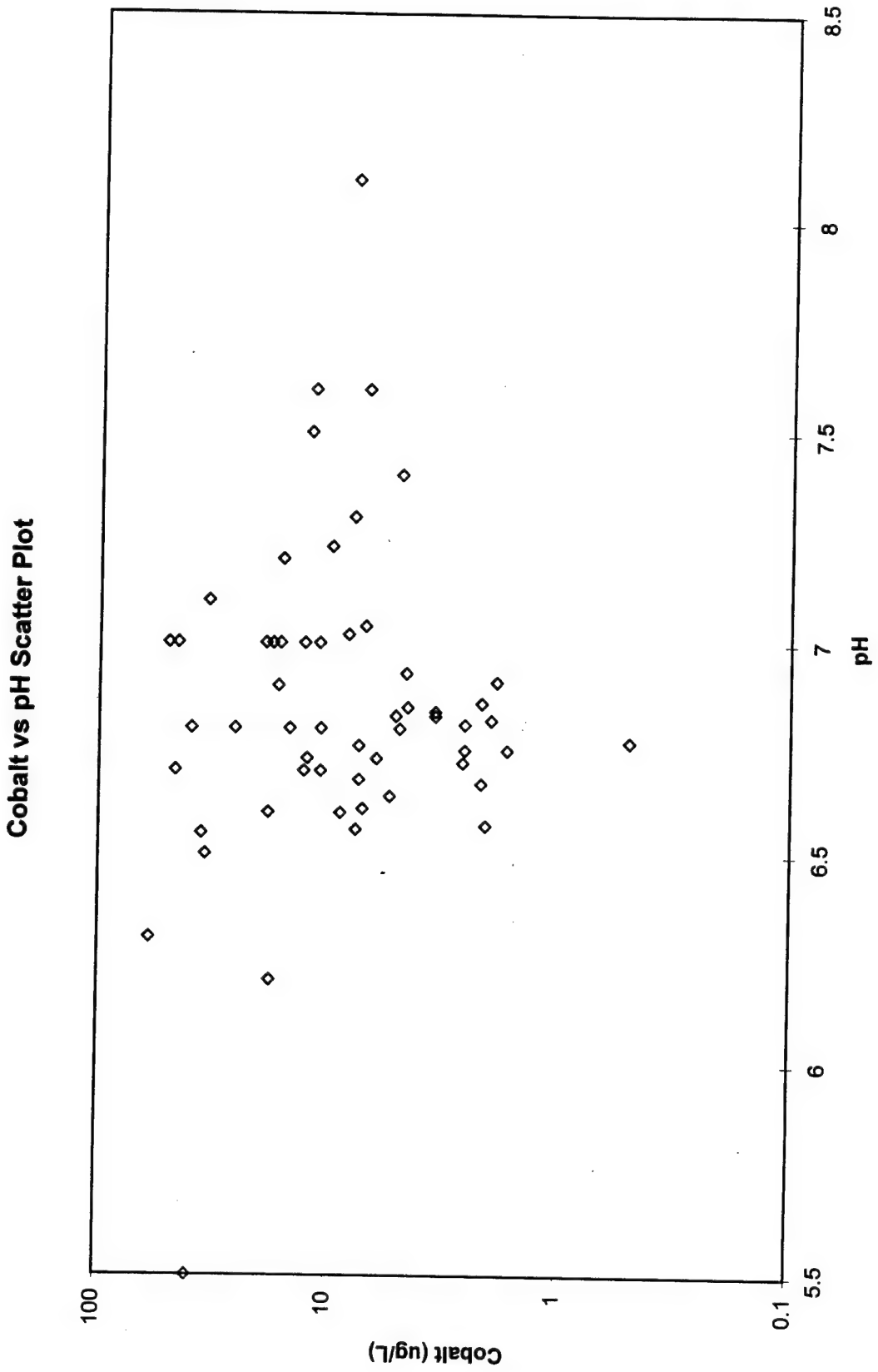
Cobalt vs pH Scatter Plot
Cobalt (ug/L)
100
10
1
0.1
pH
5.5
6
6.5
7
7.5
8
8.5

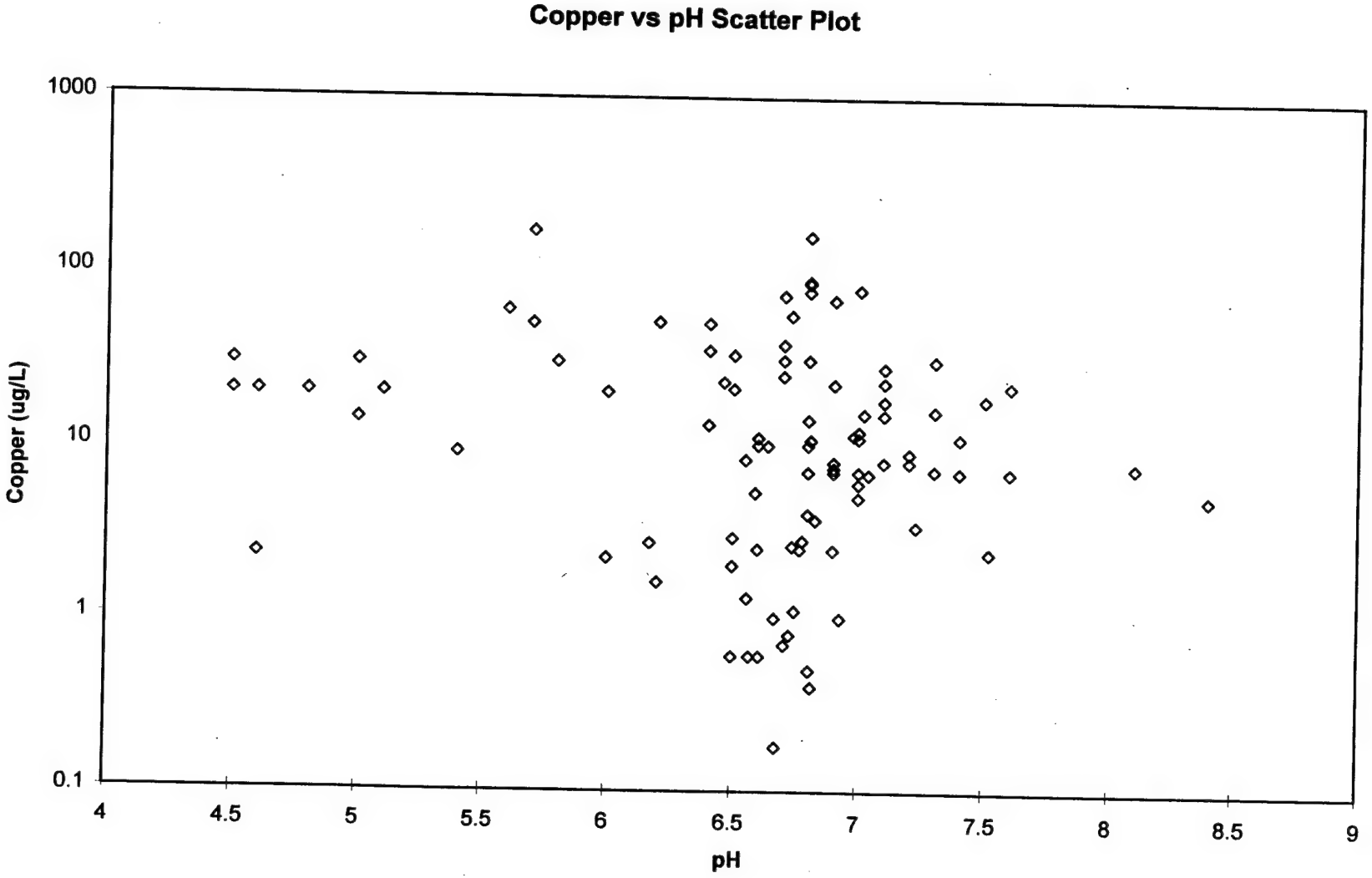
Copper vs pH Scatter Plot
Copper (ug/L)
1000
100
10
1
0.1
4
4.5
5
5.5
6
6.5
7
7.5
8
8.5
9
pH

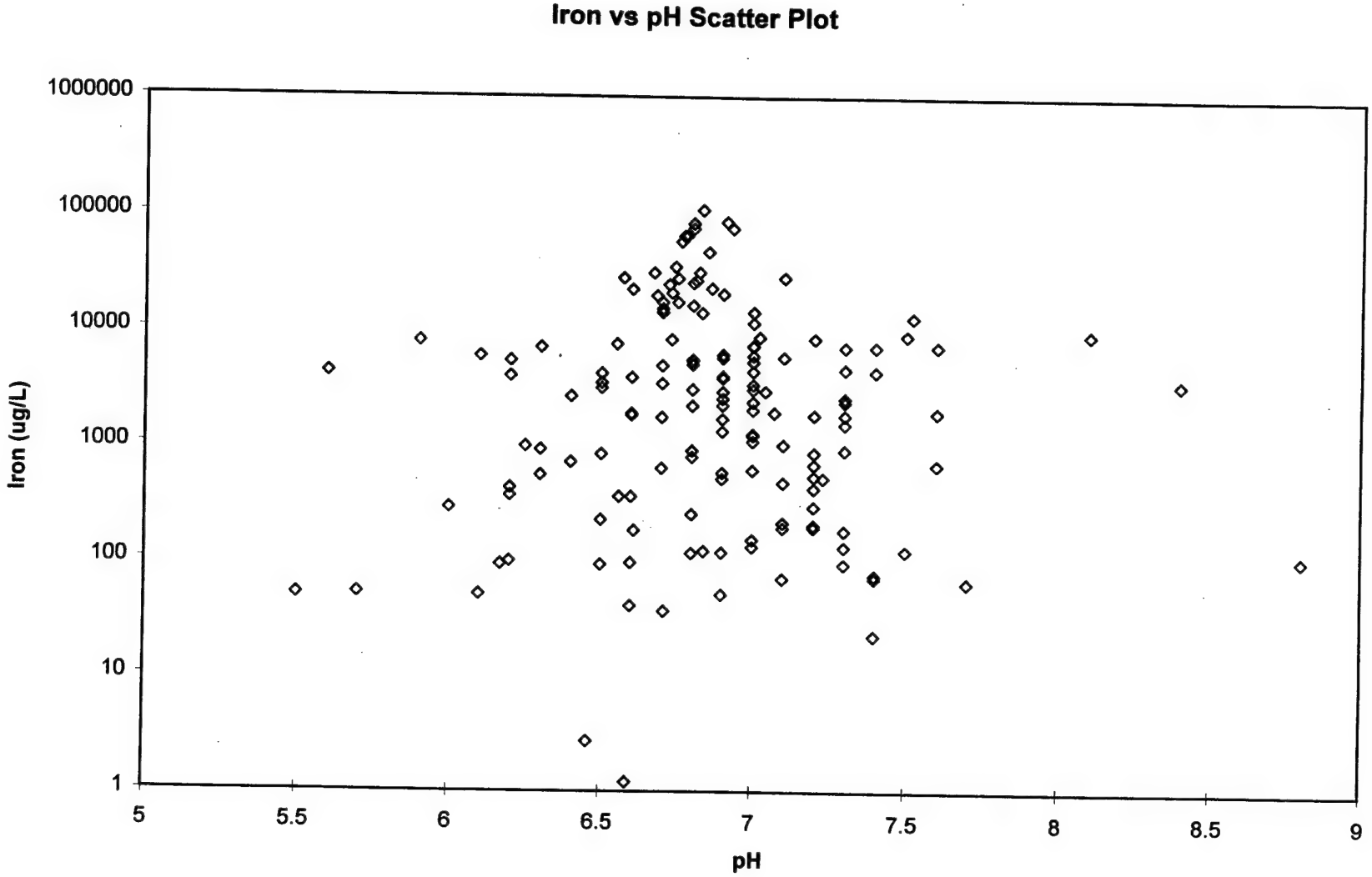
Iron vs pH Scatter Plot
Iron (ug/L)
1000000
100000
10000
1000
100
10
1
5
5.5
6
6.5
7
7.5
8
8.5
9
pH

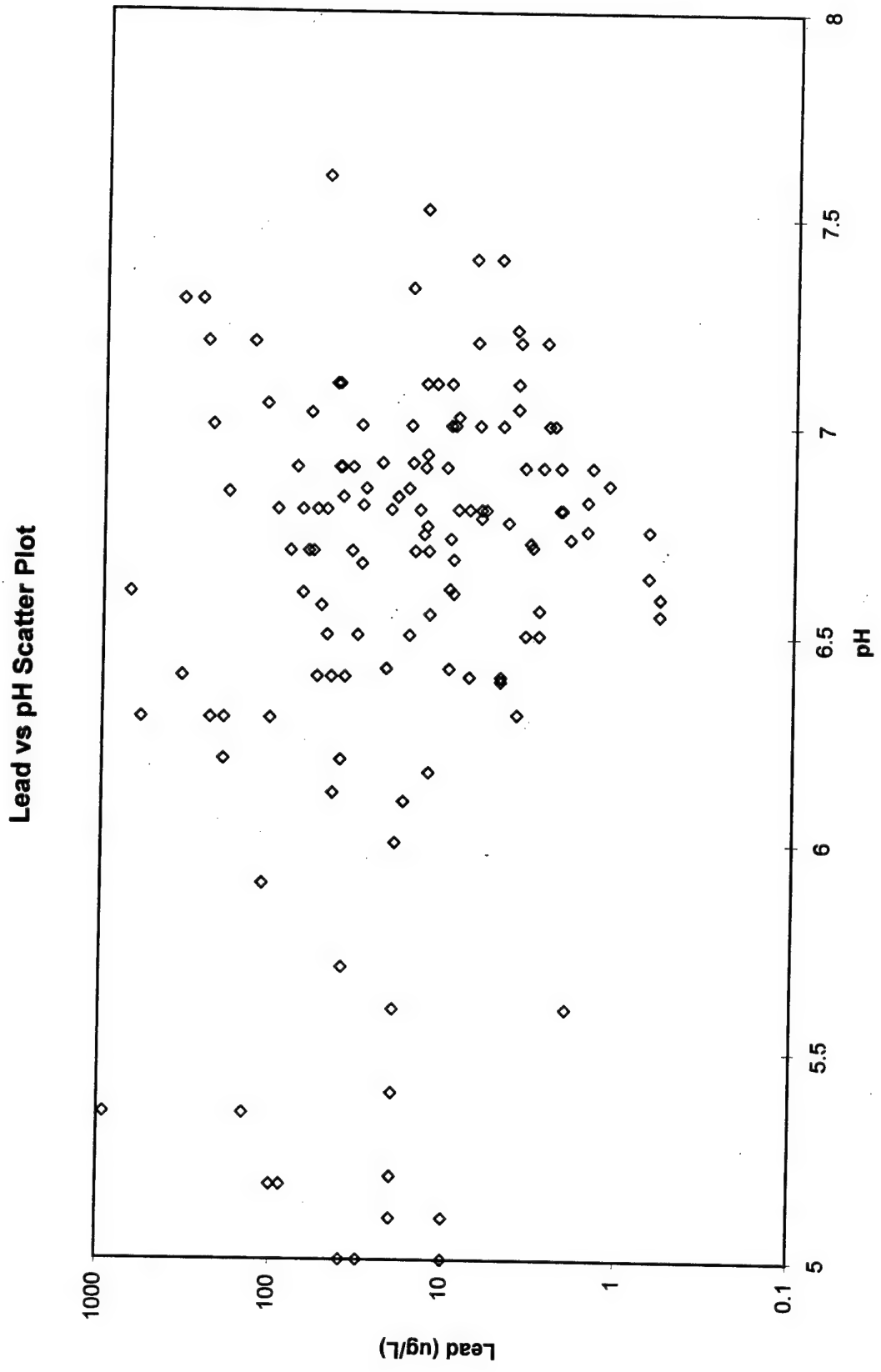
Lead vs pH Scatter Plot
Lead (ug/L)
1000
100
10
1
0.1
pH
5
5.5
6
6.5
7
7.5
8

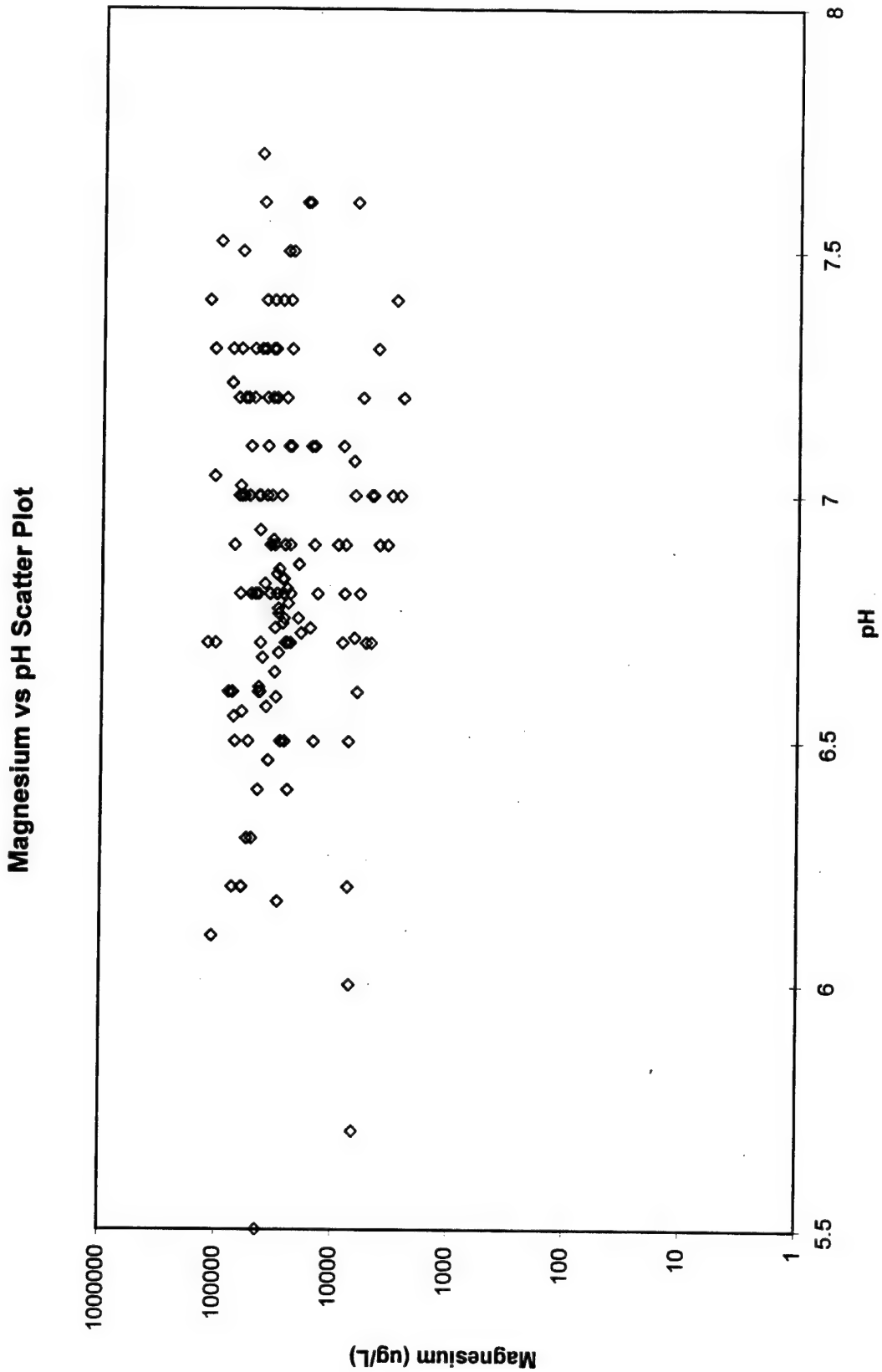
Magnesium vs pH Scatter Plot
Magnesium (ug/L)
1000000
100000
10000
1000
100
10
1
pH
5.5
6
6.5
7
7.5
8

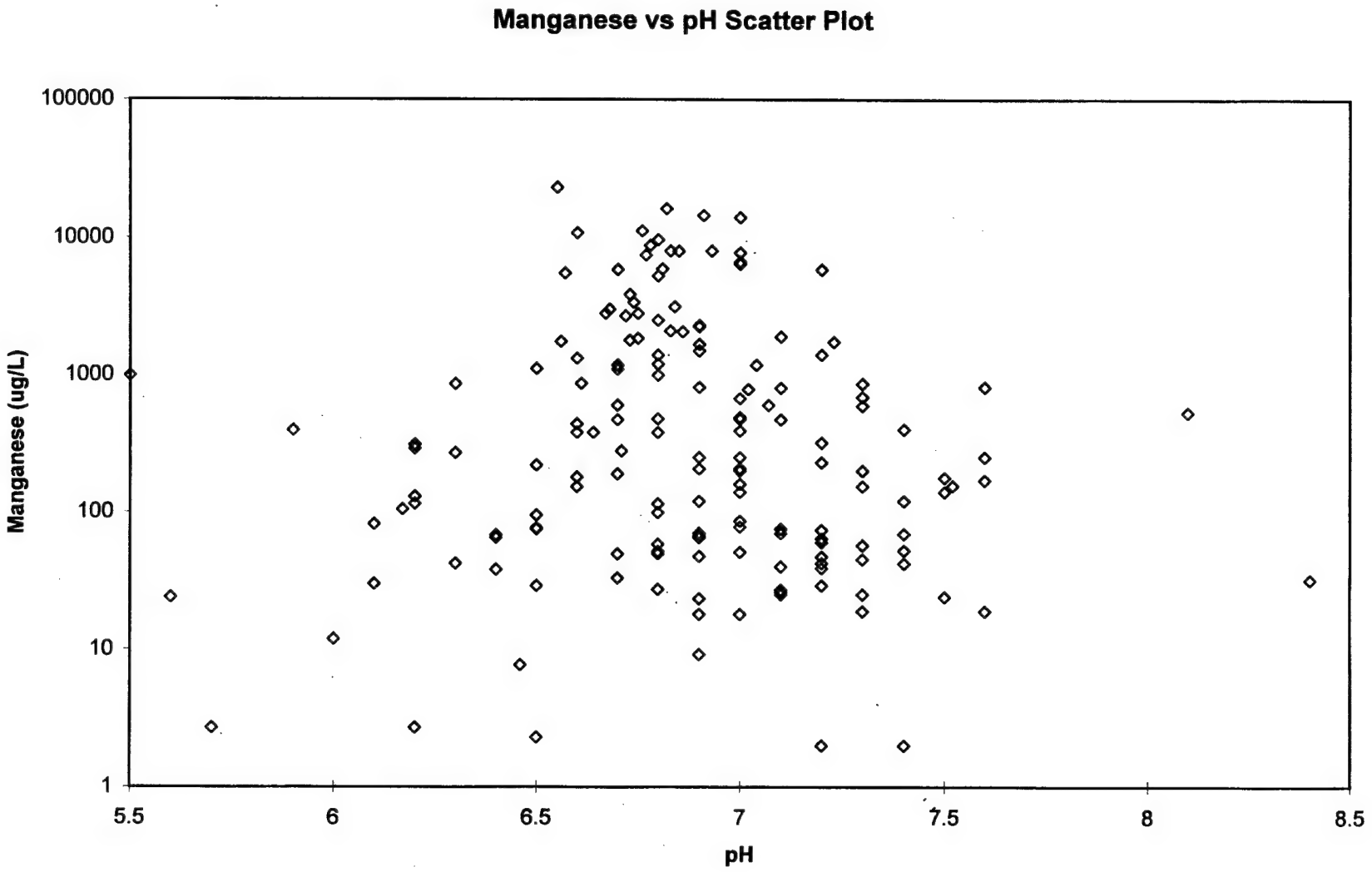
Manganese vs pH Scatter Plot
Manganese (ug/L)
100000
10000
1000
100
10
1
5.5
6
6.5
7
7.5
8
8.5
pH

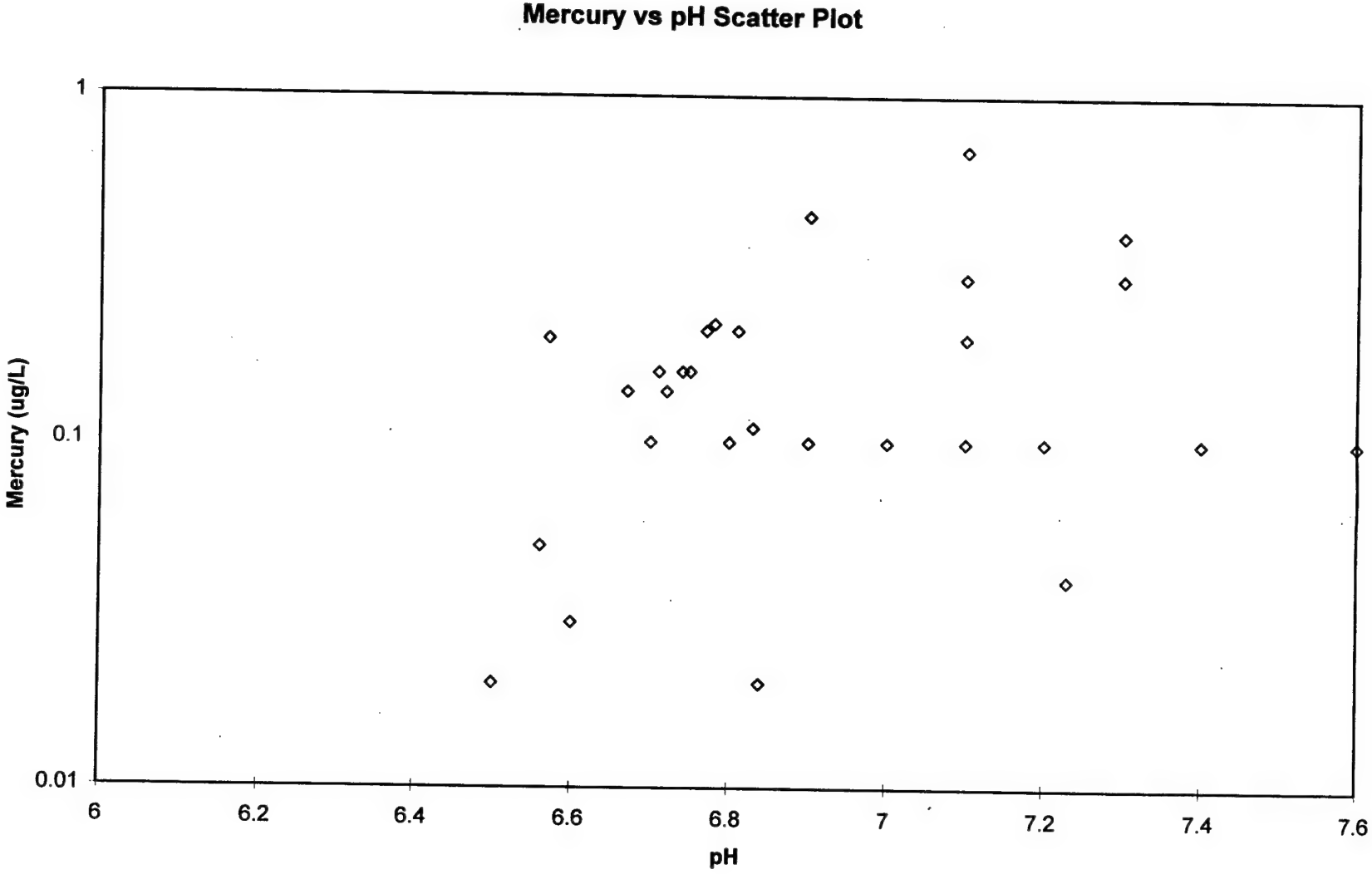
Mercury vs pH Scatter Plot
Mercury (ug/L)
1
0.1
0.01
6
6.2
6.4
6.6
6.8
7
7.2
7.4
7.6
pH

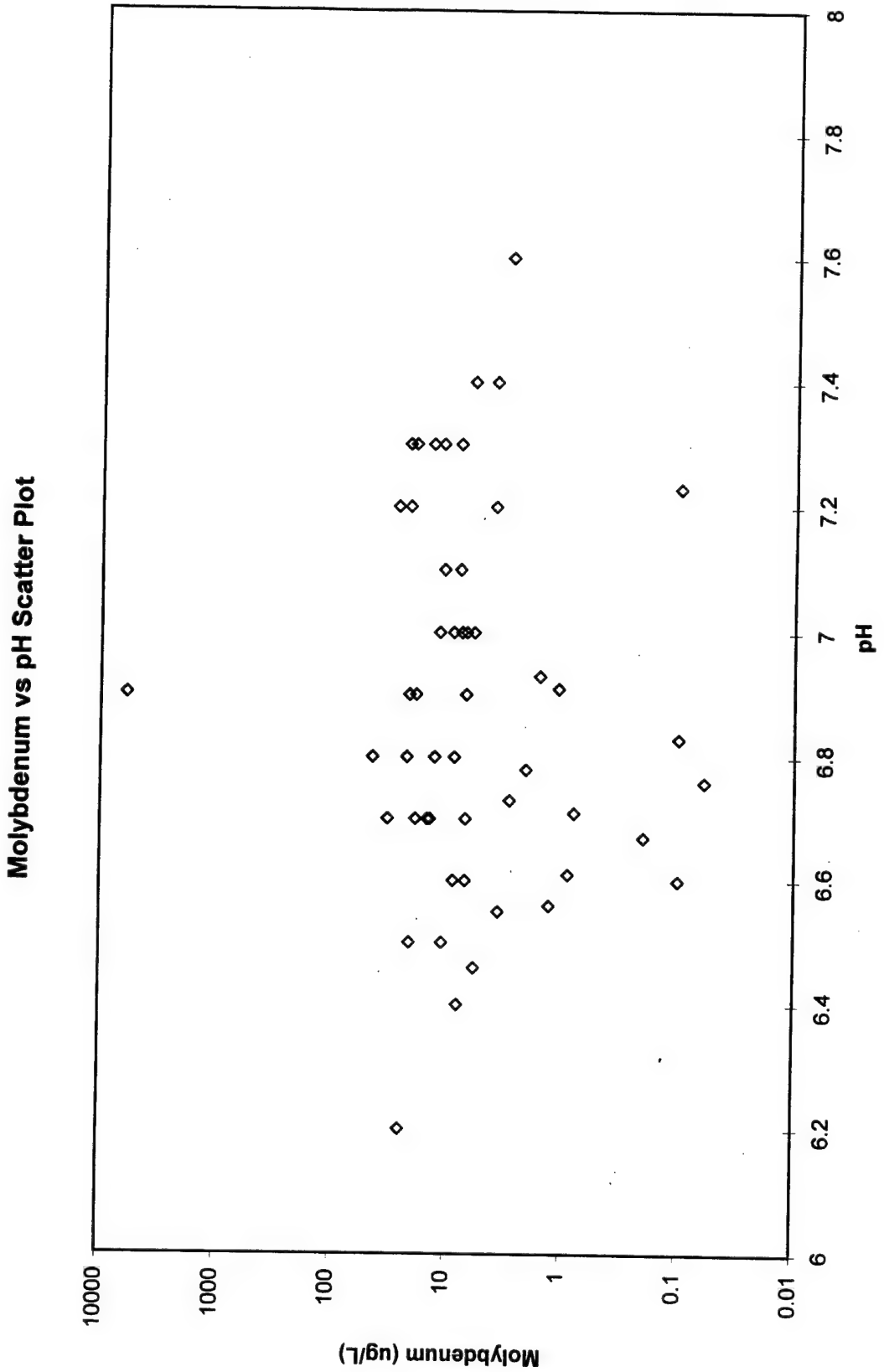
Molybdenum vs pH Scatter Plot
Molybdenum (ug/L)
10000
1000
100
10
1
0.1
0.01
6
6.2
6.4
6.6
6.8
7
7.2
7.4
7.6
7.8
8
pH

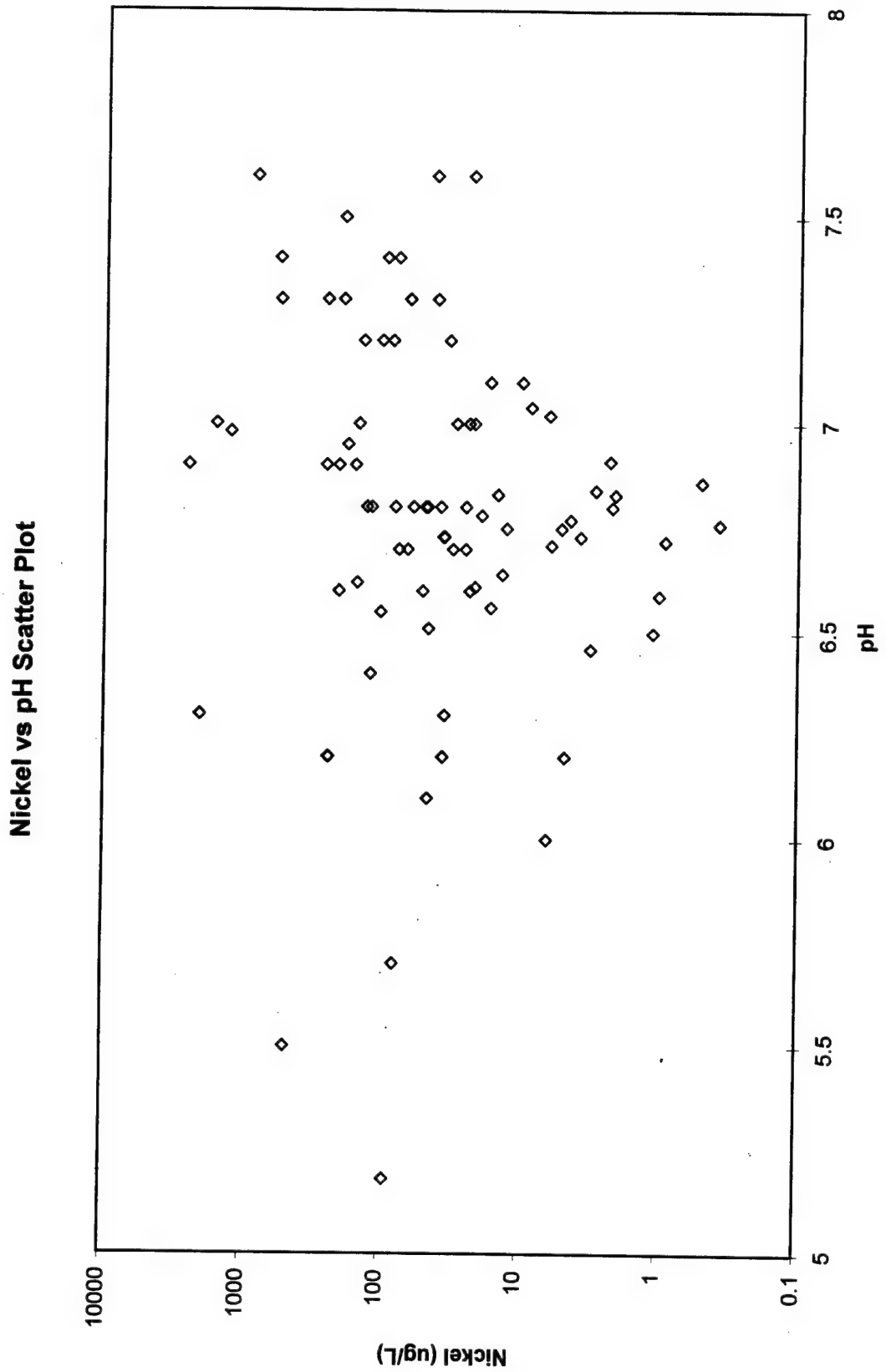
Nickel vs pH Scatter Plot
Nickel (ug/L)
10000
1000
100
10
1
0.1
5
5.5
6
6.5
7
7.5
8
pH

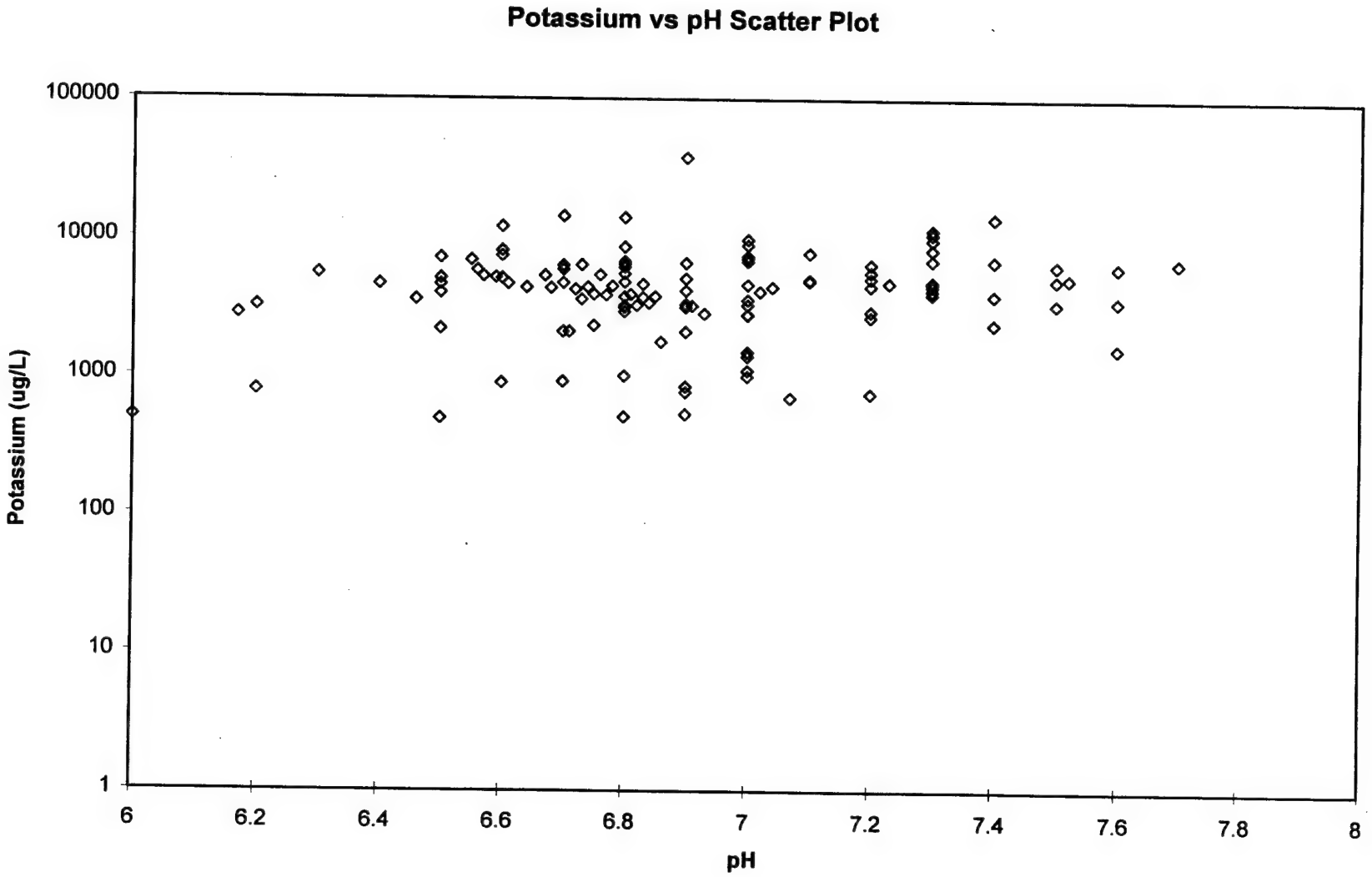
Potassium vs pH Scatter Plot
Potassium (ug/L)
100000
10000
1000
100
10
1
6
6.2
6.4
6.6
6.8
7
7.2
7.4
7.6
7.8
8
pH

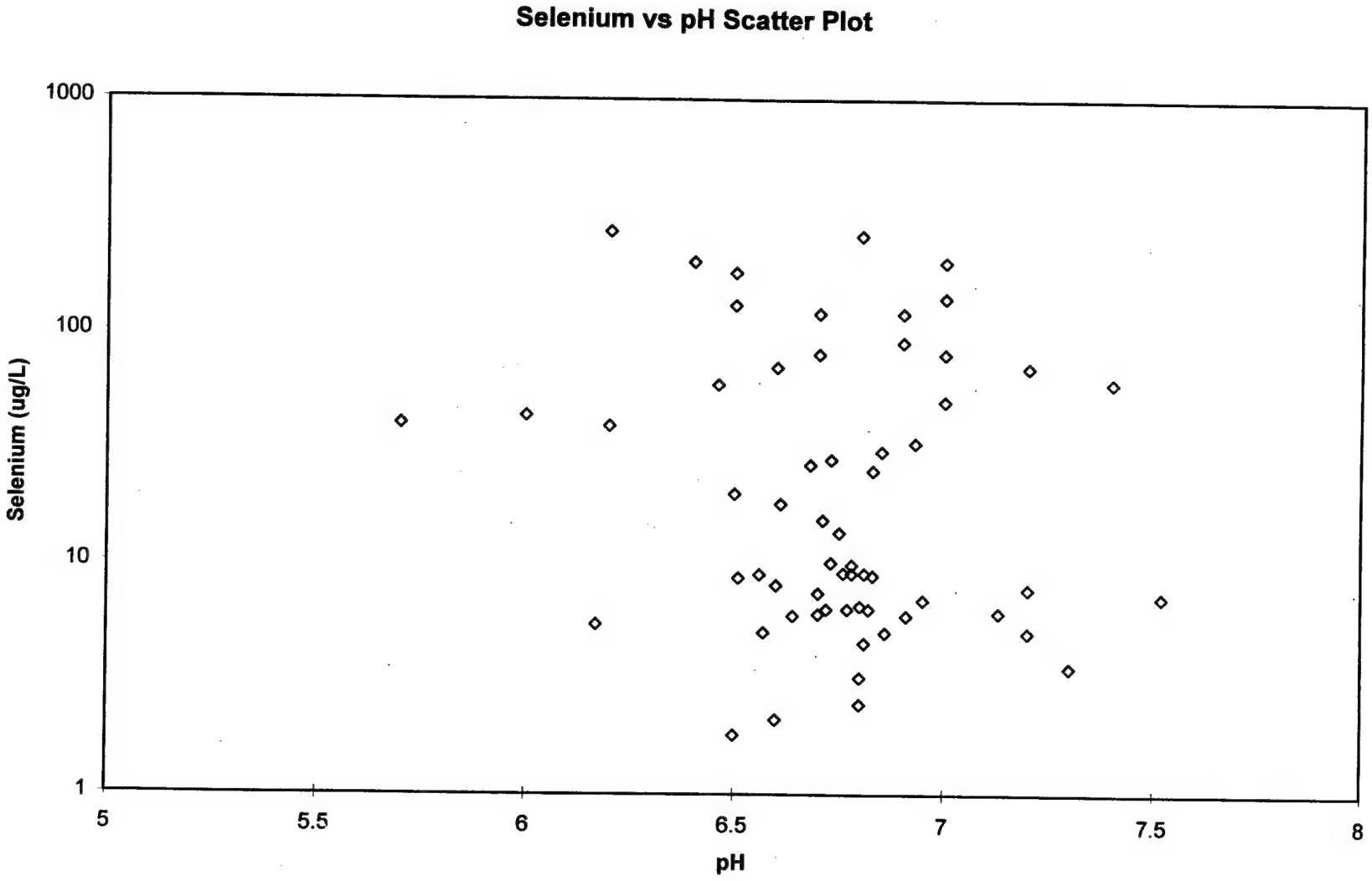
Selenium vs pH Scatter Plot
1000
100
10
1
Selenium (ug/L)
5
5.5
6
6.5
7
7.5
8
pH

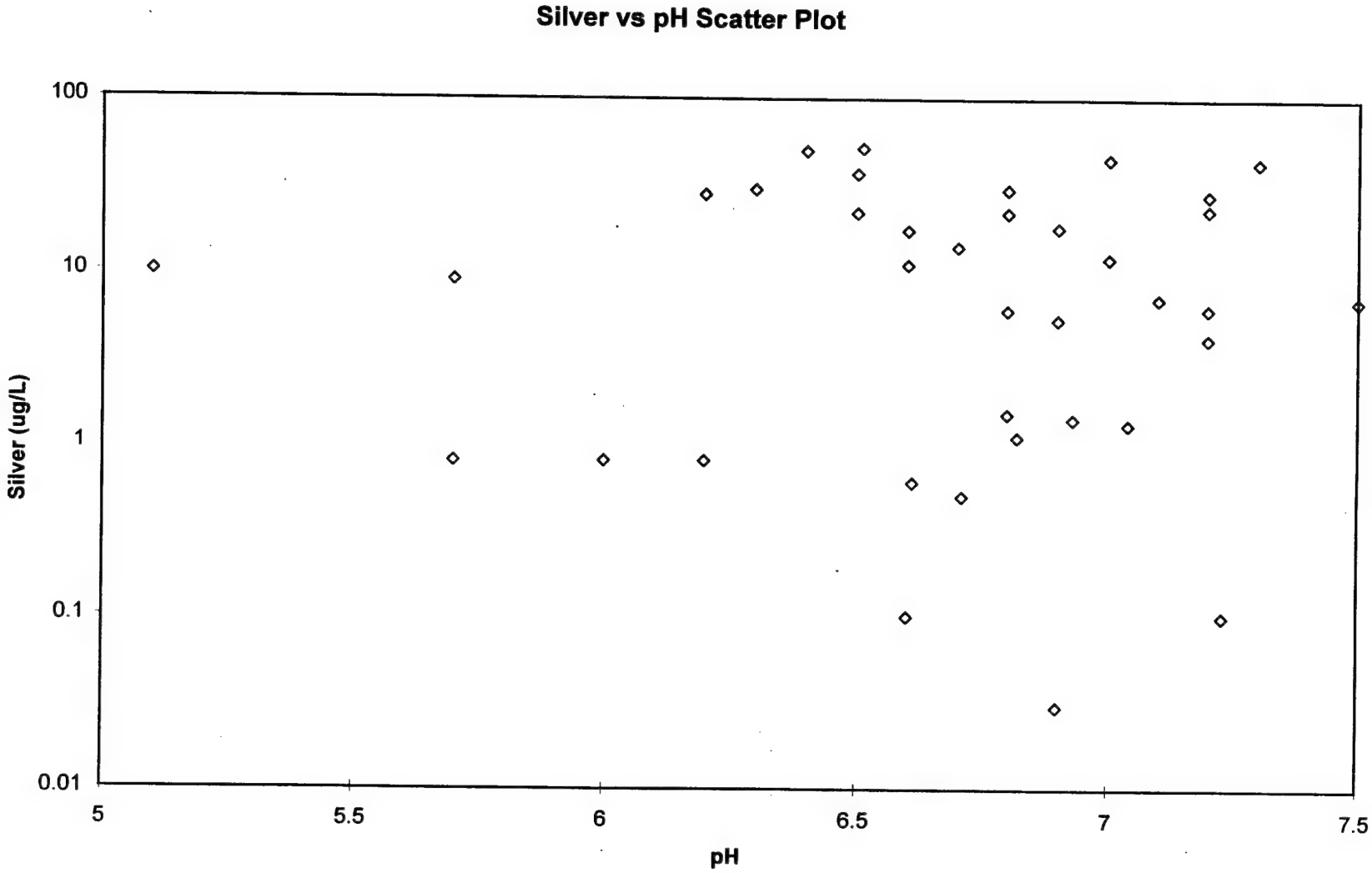
Silver vs pH Scatter Plot
100
10
1
0.1
0.01
Silver (ug/L)
5
5.5
6
6.5
7
7.5
pH

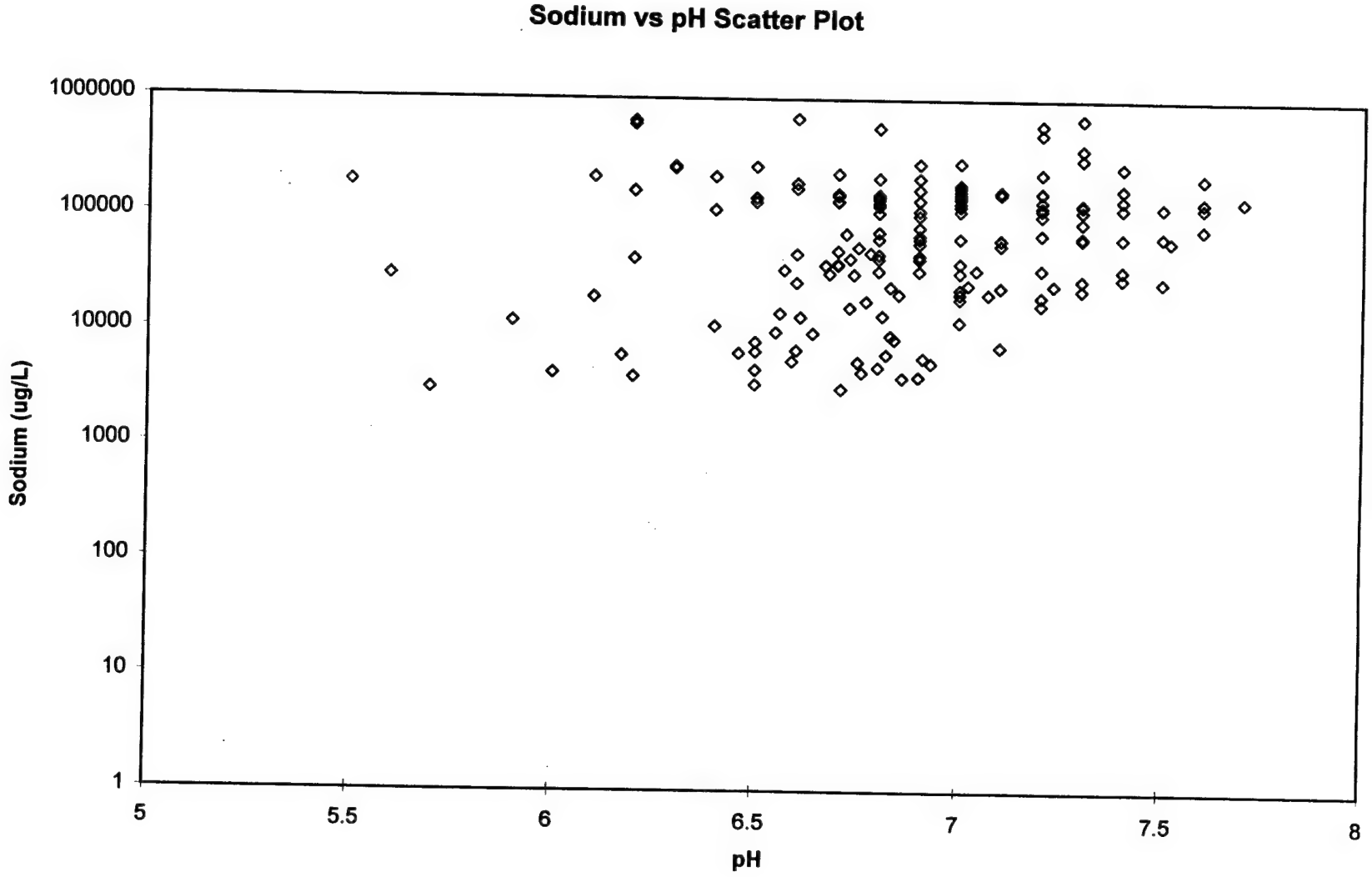
Sodium vs pH Scatter Plot
Sodium (ug/L)
1000000
100000
10000
1000
100
10
1
5
5.5
6
6.5
7
7.5
8
pH

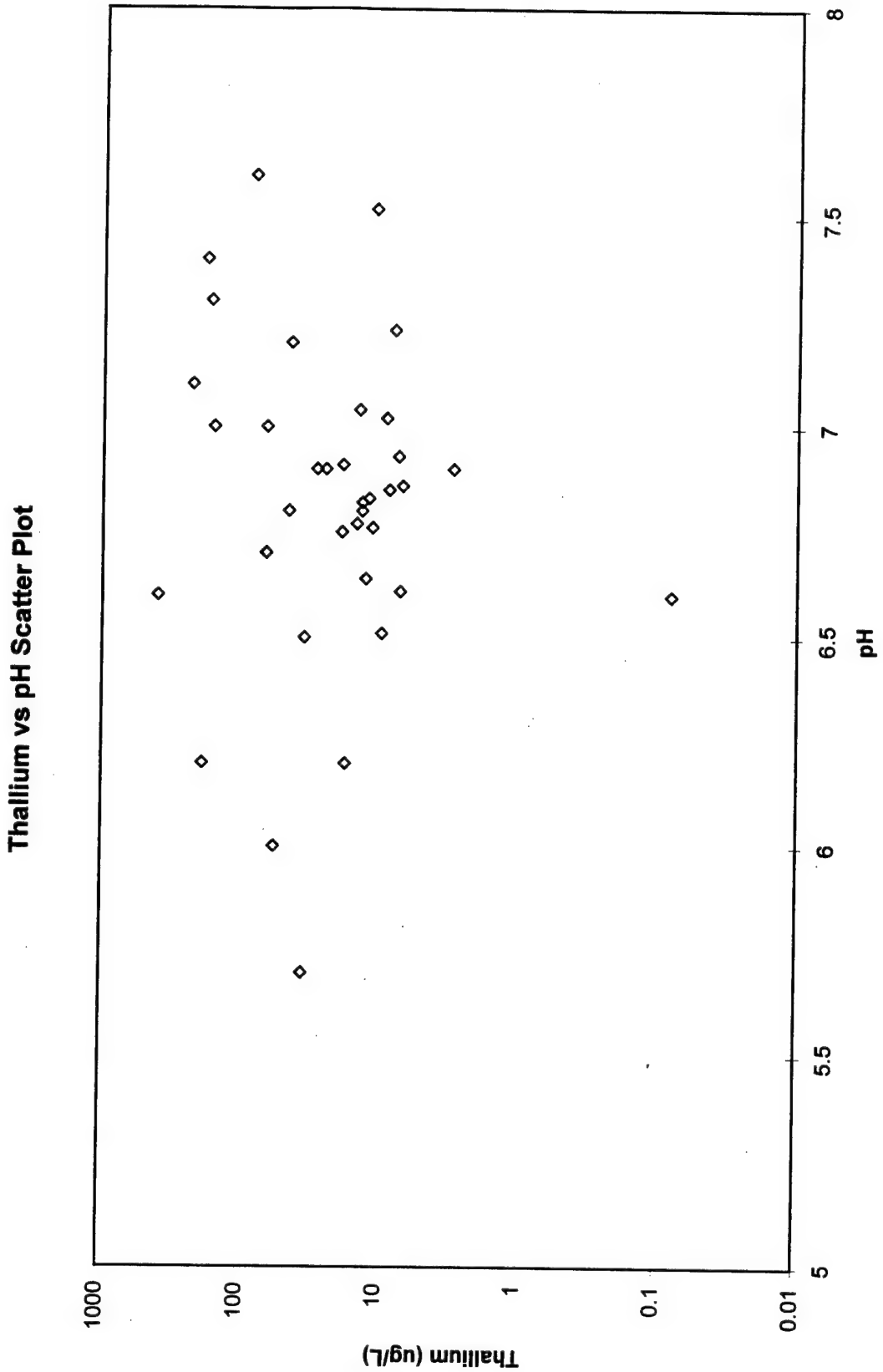
Thallium vs pH Scatter Plot
Thallium (ug/L)
1000
100
10
1
0.1
0.01
5
5.5
6
6.5
7
7.5
8
pH

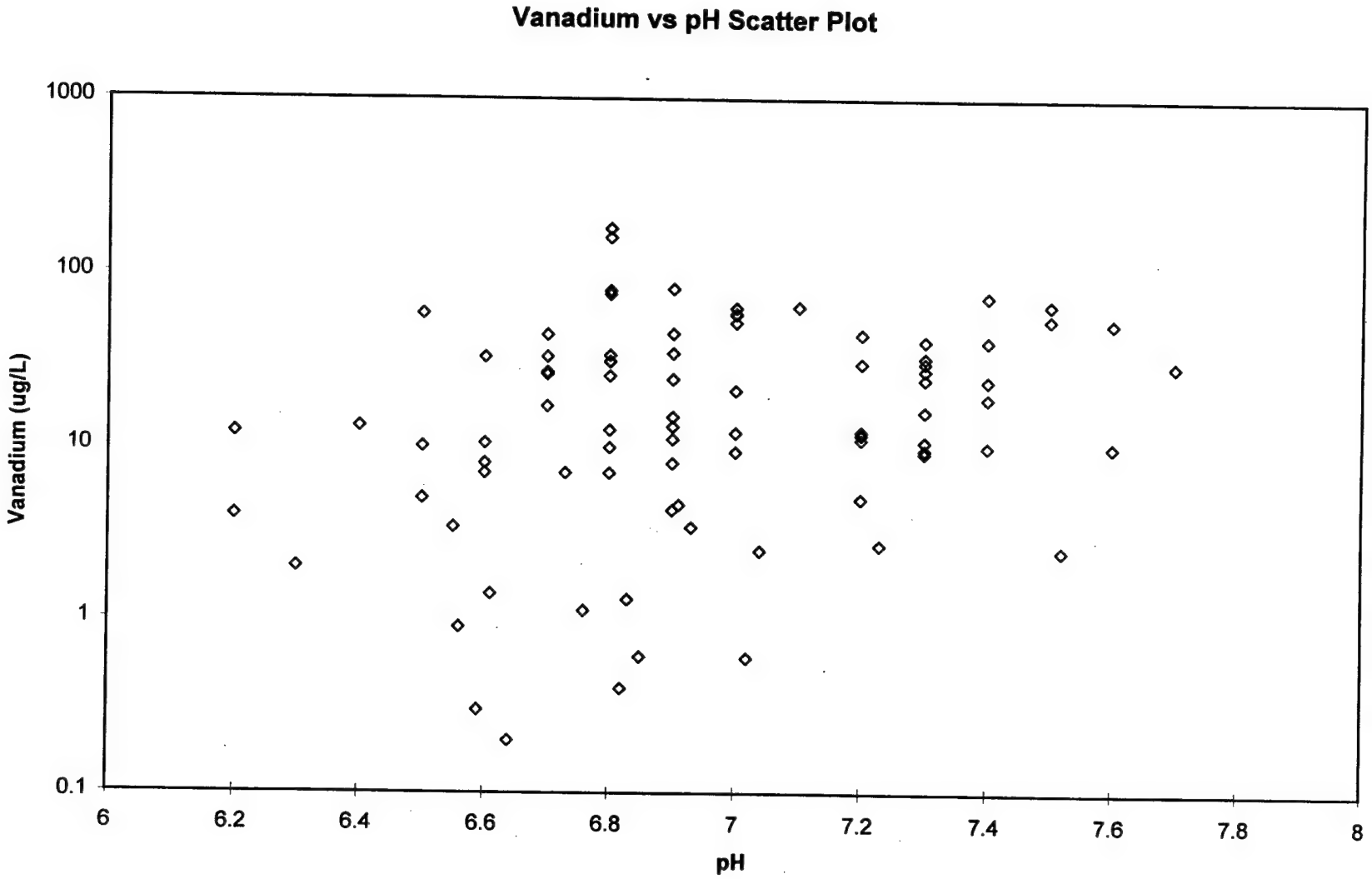
Vanadium vs pH Scatter Plot
Vanadium (ug/L)
1000
100
10
1
0.1
6
6.2
6.4
6.6
6.8
7
7.2
7.4
7.6
7.8
8
pH

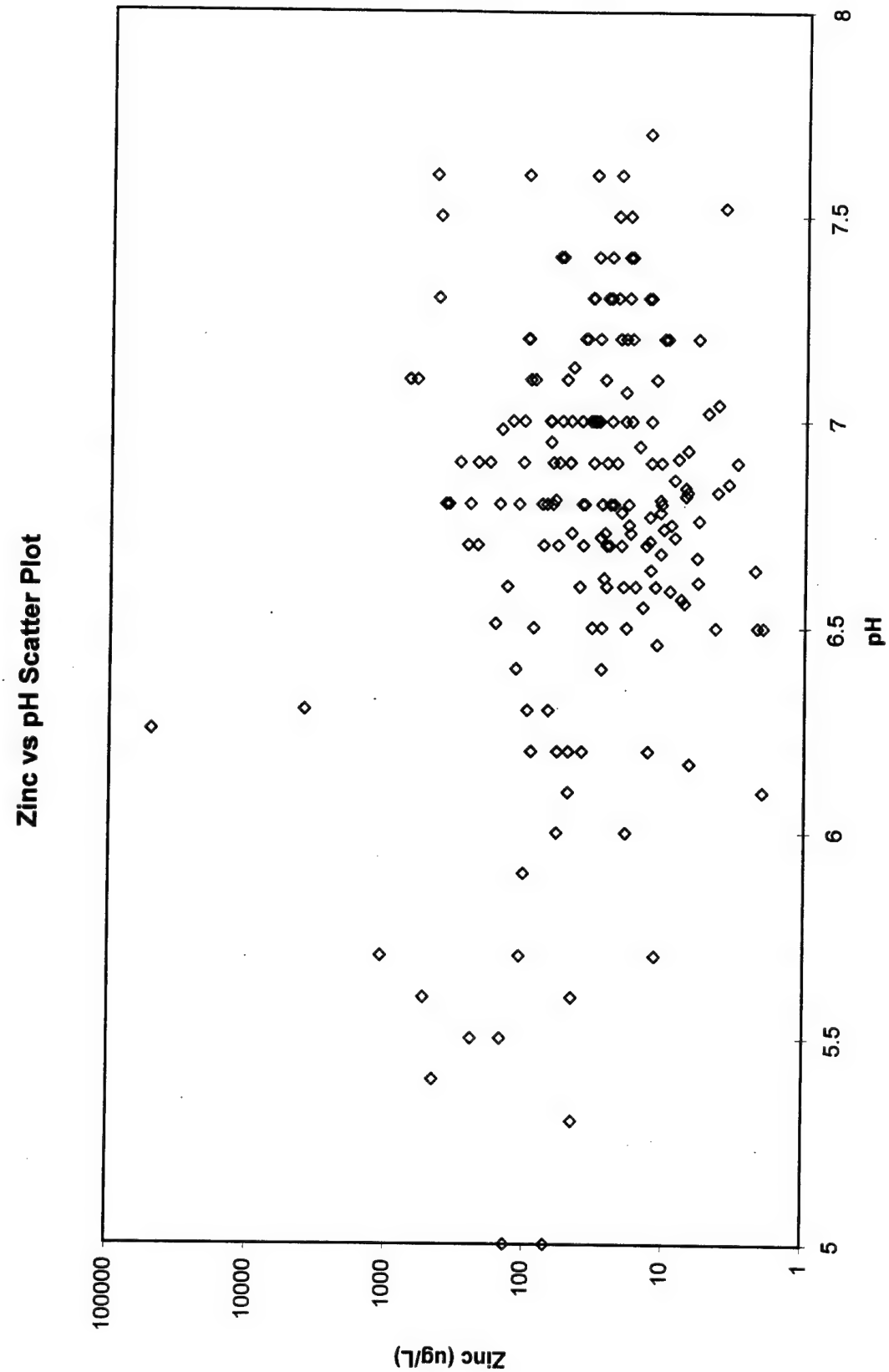
Zinc vs pH Scatter Plot
Zinc (ug/L)
100000
10000
1000
100
10
1
5
5.5
6
6.5
7
7.5
8
pH

Appendix I: Metal Versus Manganese Scatter Plots

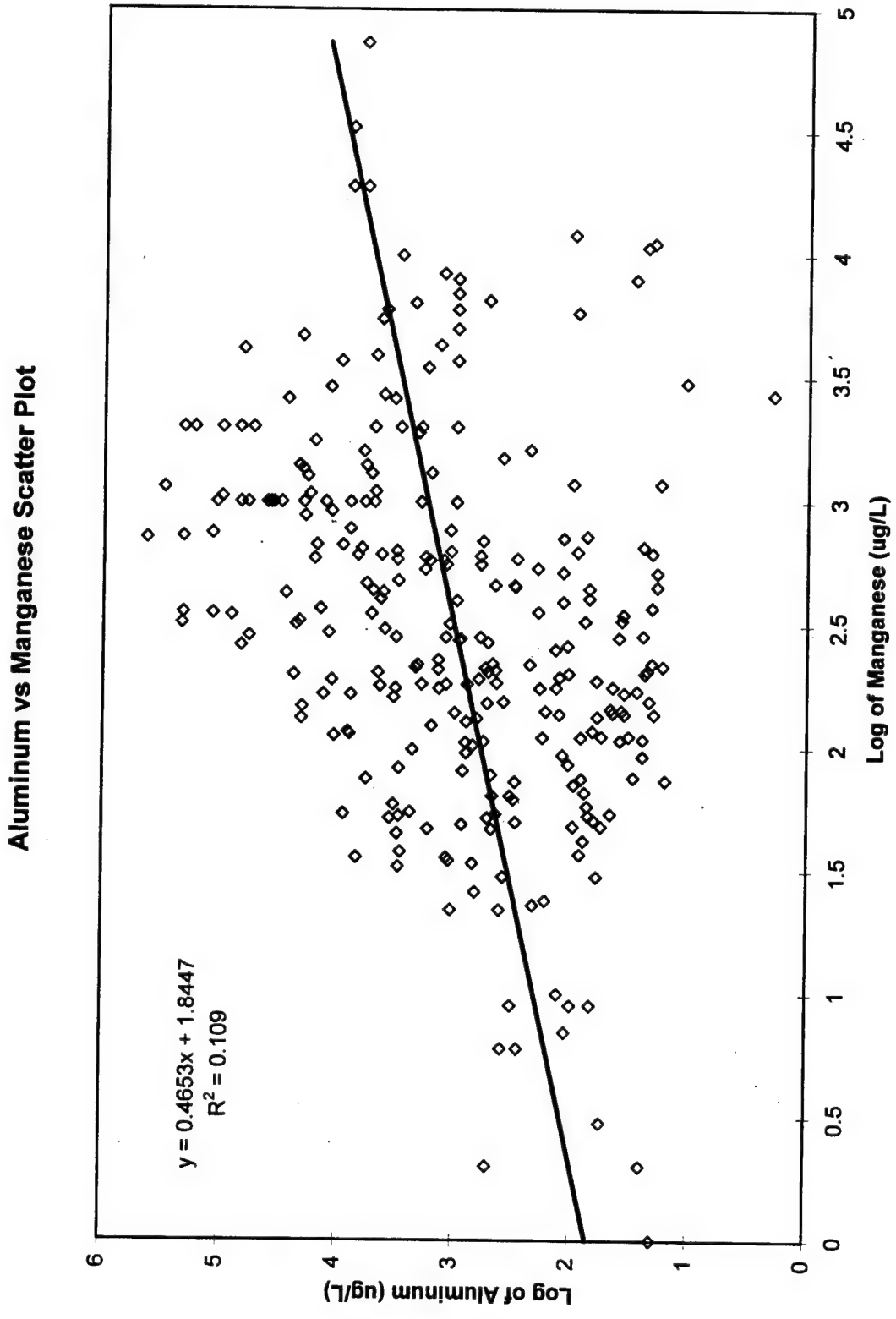

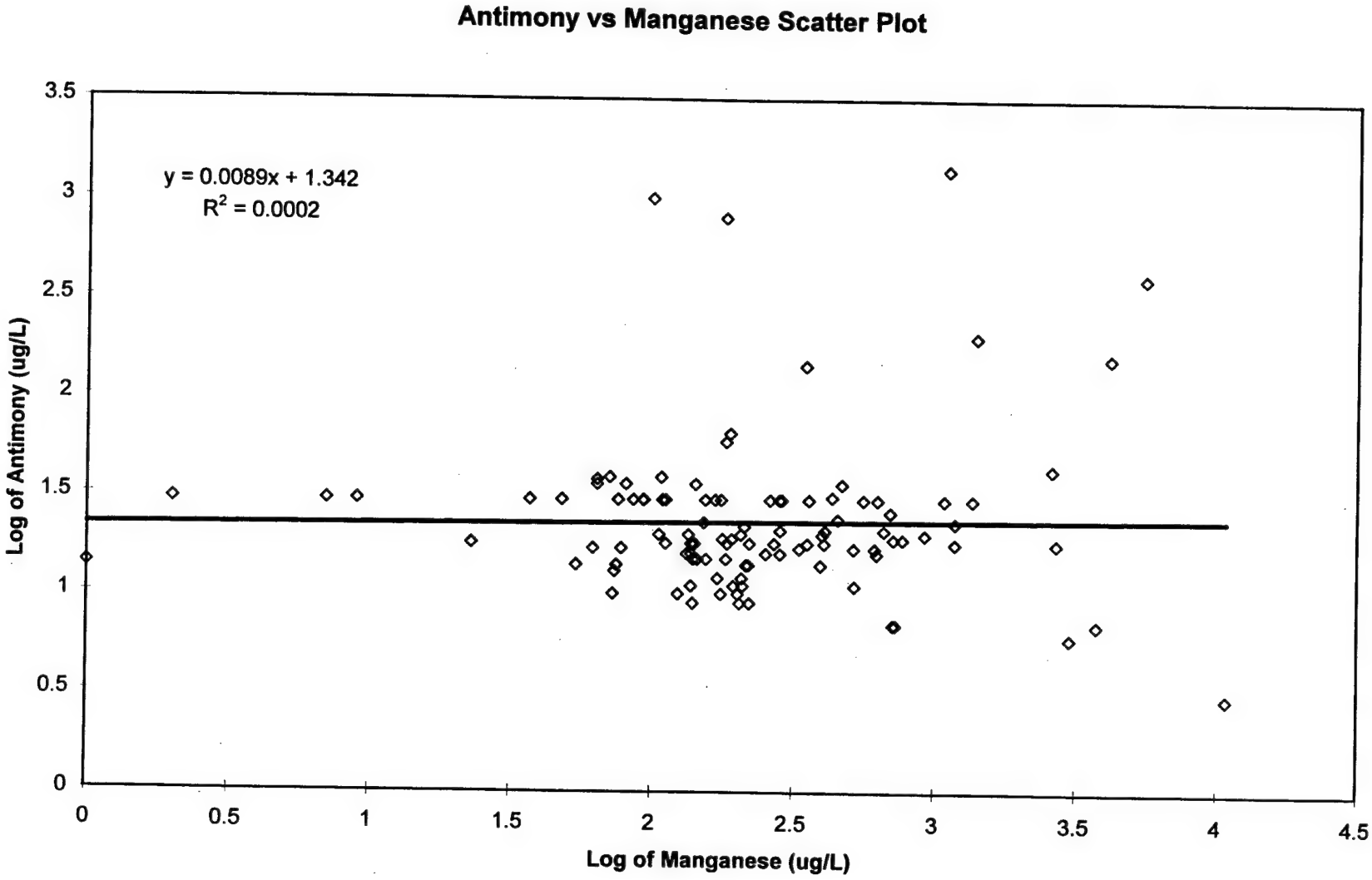
Antimony vs Manganese Scatter Plot
y = 0.0089x + 1.342
R2 = 0.0002
Log of Antimony (ug/L)
Log of Manganese (ug/L)
0
0.5
1
1.5
2
2.5
3
3.5
4
4.5

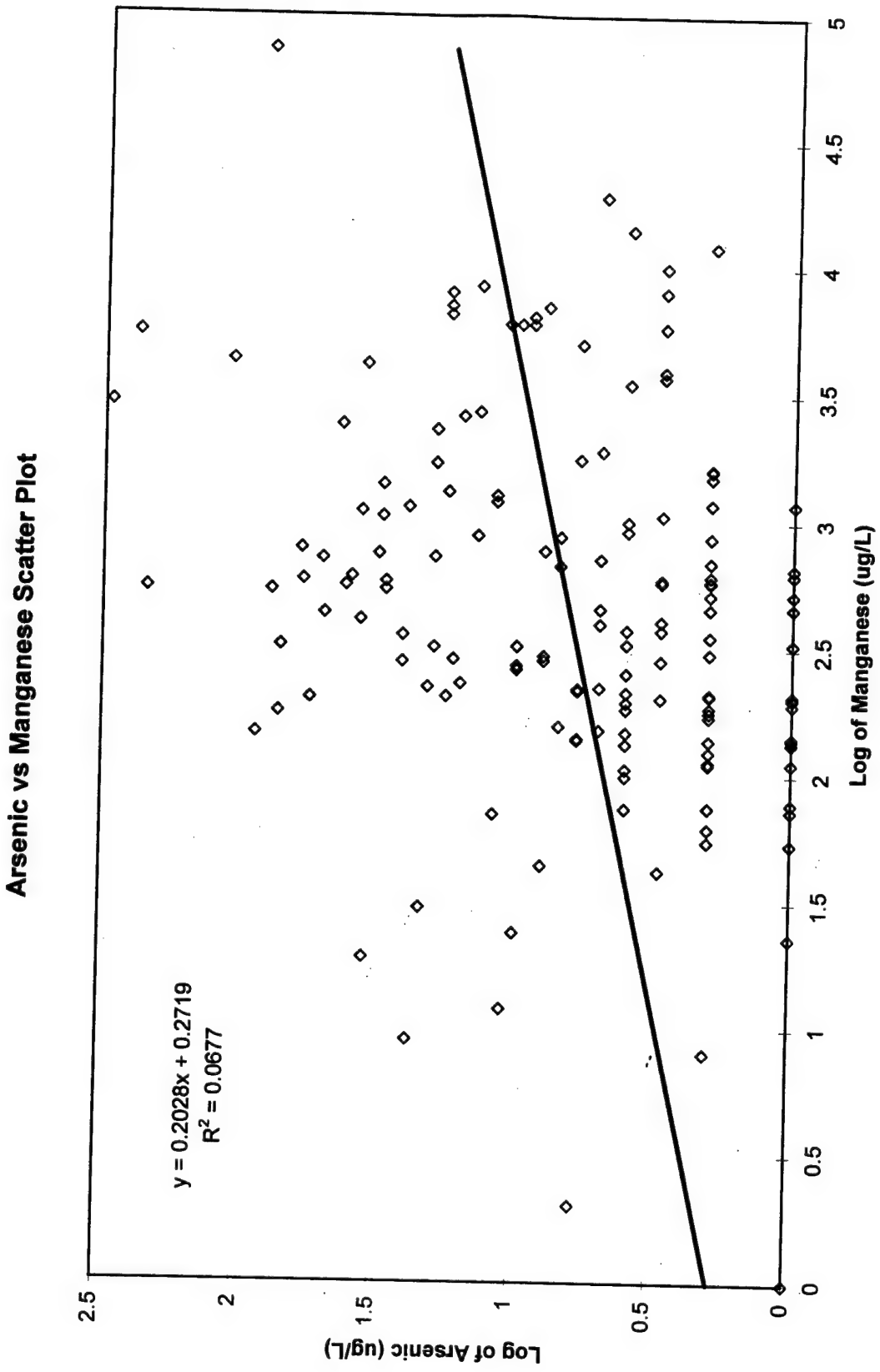
Arsenic vs Manganese Scatter Plot
y = 0.2028x + 0.2719
R2 = 0.0677
Log of Arsenic (ug/L)
Log of Manganese (ug/L)
2.5
2
1.5
1
0.5
0
0
0.5
1
1.5
2
2.5
3
3.5
4
4.5
5

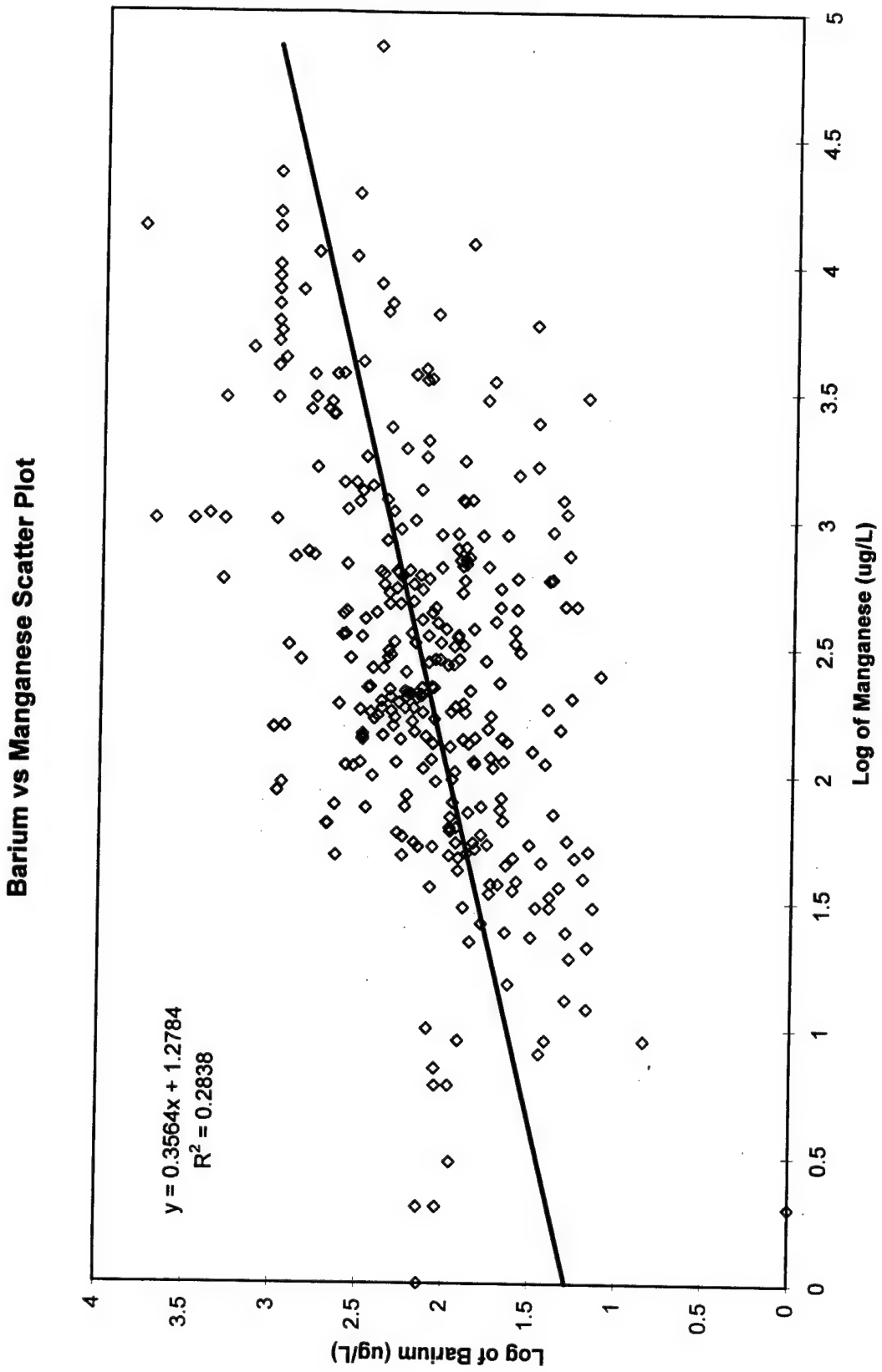
Barium vs Manganese Scatter Plot
y = 0.3564x + 1.2784
R2 = 0.2838
Log of Barium (ug/L)
Log of Manganese (ug/L)
0
0.5
1
1.5
2
2.5
3
3.5
4
4.5
5

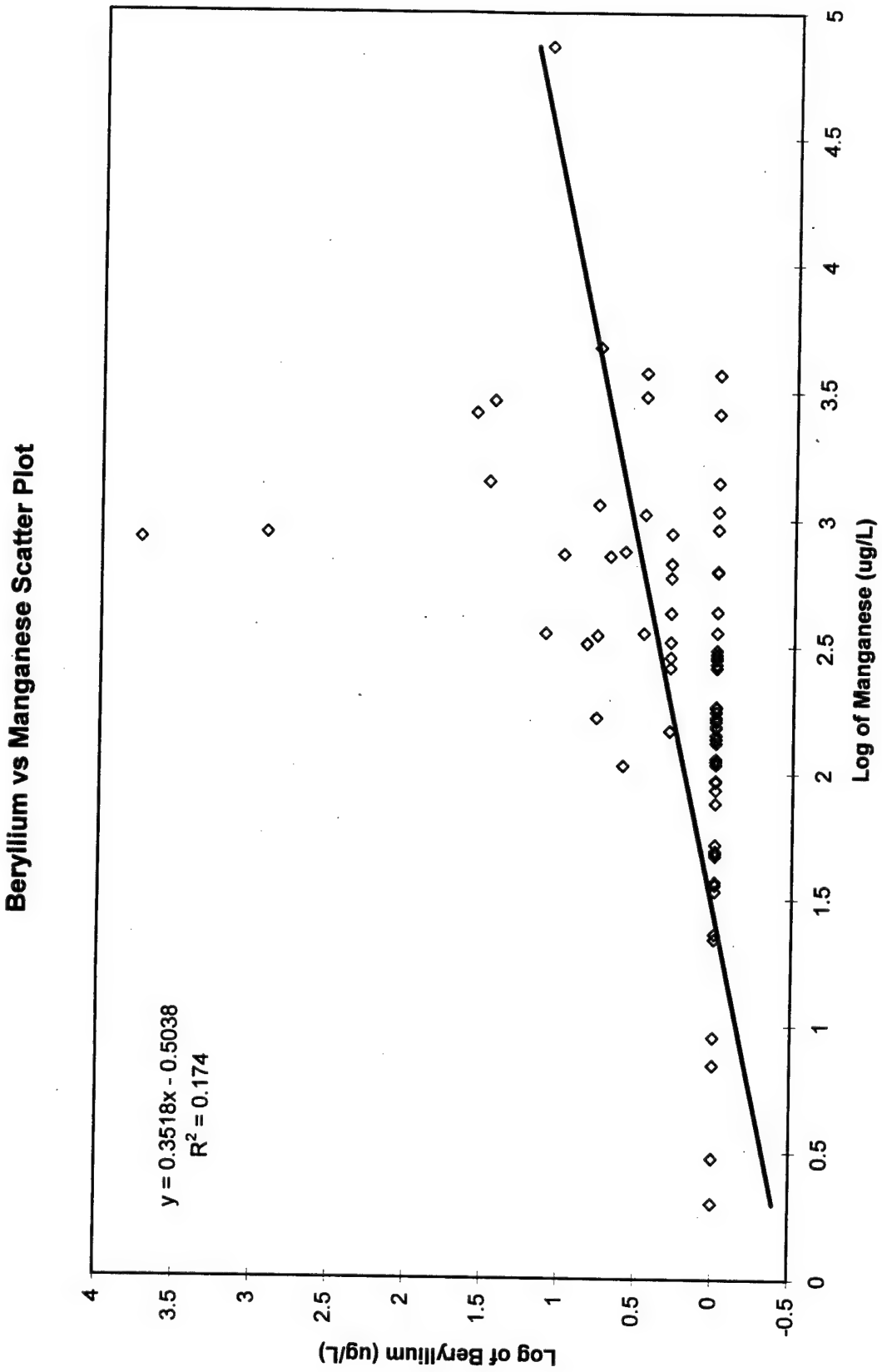
Beryllium vs Manganese Scatter Plot
y = 0.3518x - 0.5038
R2 = 0.174
Log of Beryllium (ug/L)
Log of Manganese (ug/L)
4
3.5
3
2.5
2
1.5
1
0.5
0
-0.5
0
0.5
1
1.5
2
2.5
3
3.5
4
4.5
5

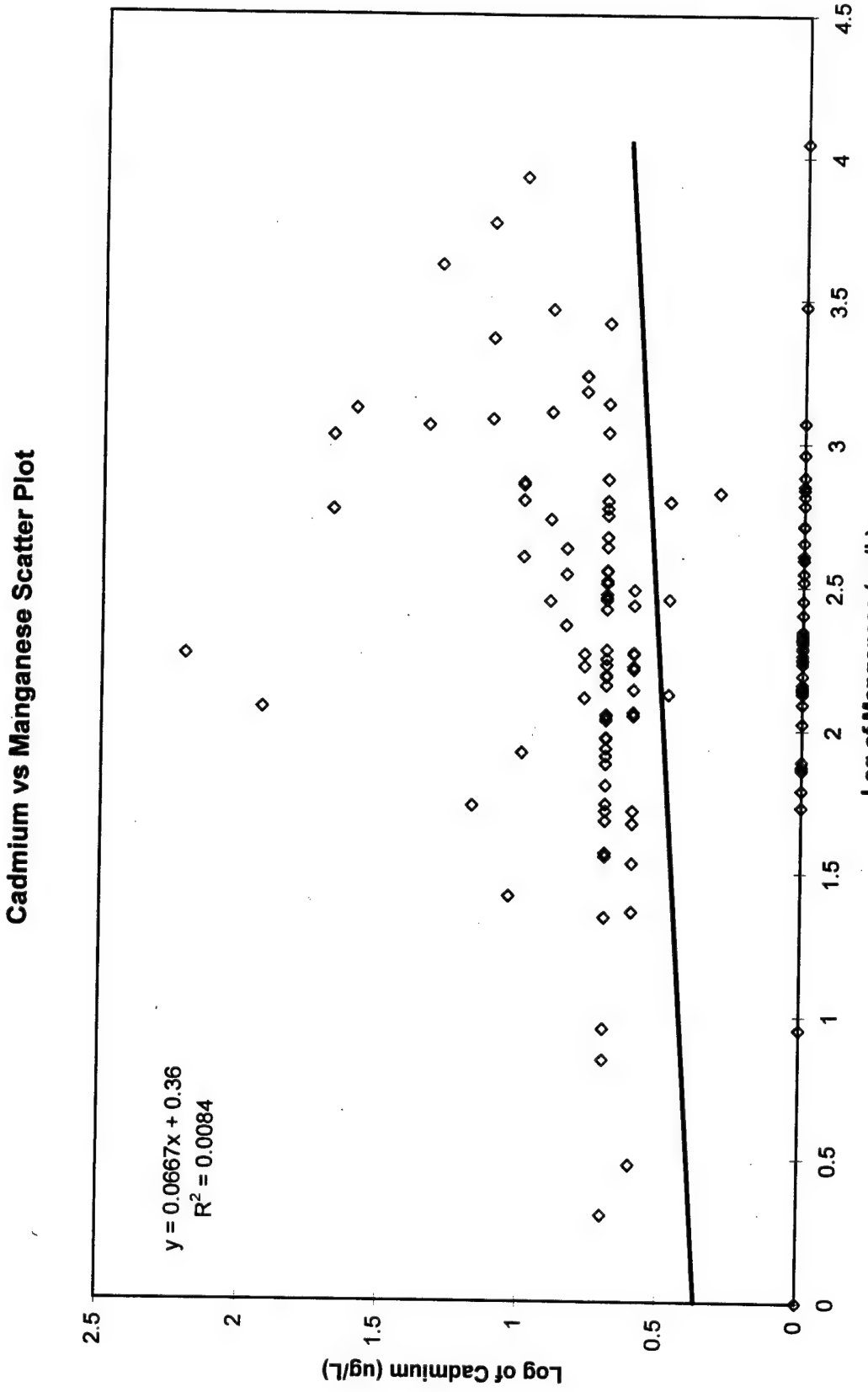
Cadmium vs Manganese Scatter Plot
y = 0.0667x + 0.36
R2 = 0.0084
Log of Cadmium (ug/L)
Log of Manganese (ug/L)
2.5
2
1.5
1
0.5
0
0
0.5
1
1.5
2
2.5
3
3.5
4
4.5

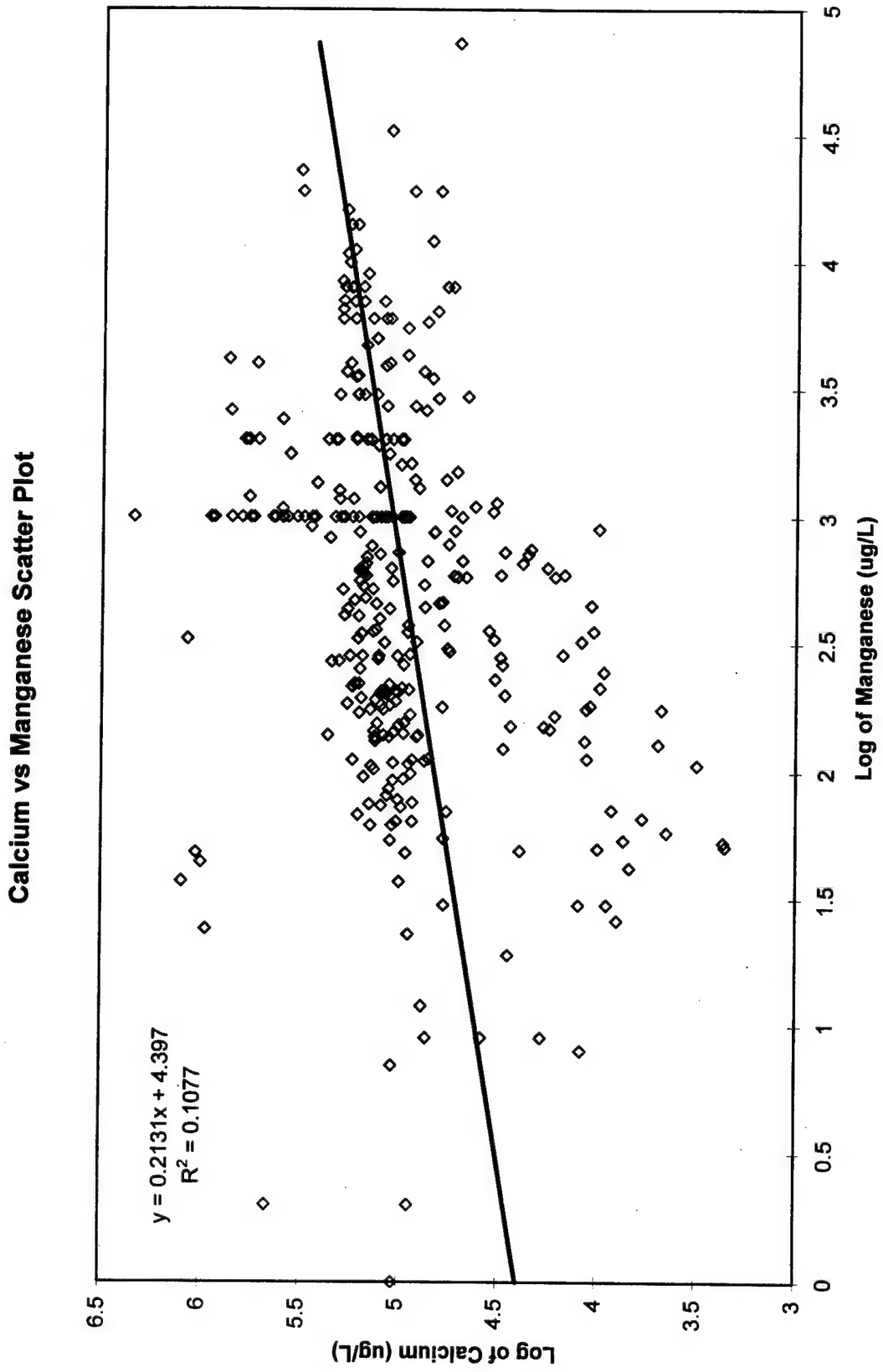
Calcium vs Manganese Scatter Plot
y = 0.2131x + 4.397
R2 = 0.1077
Log of Calcium (ug/L)
Log of Manganese (ug/L)
6.5
6
5.5
5
4.5
4
3.5
3
0
0.5
1
1.5
2
2.5
3
3.5
4
4.5
5

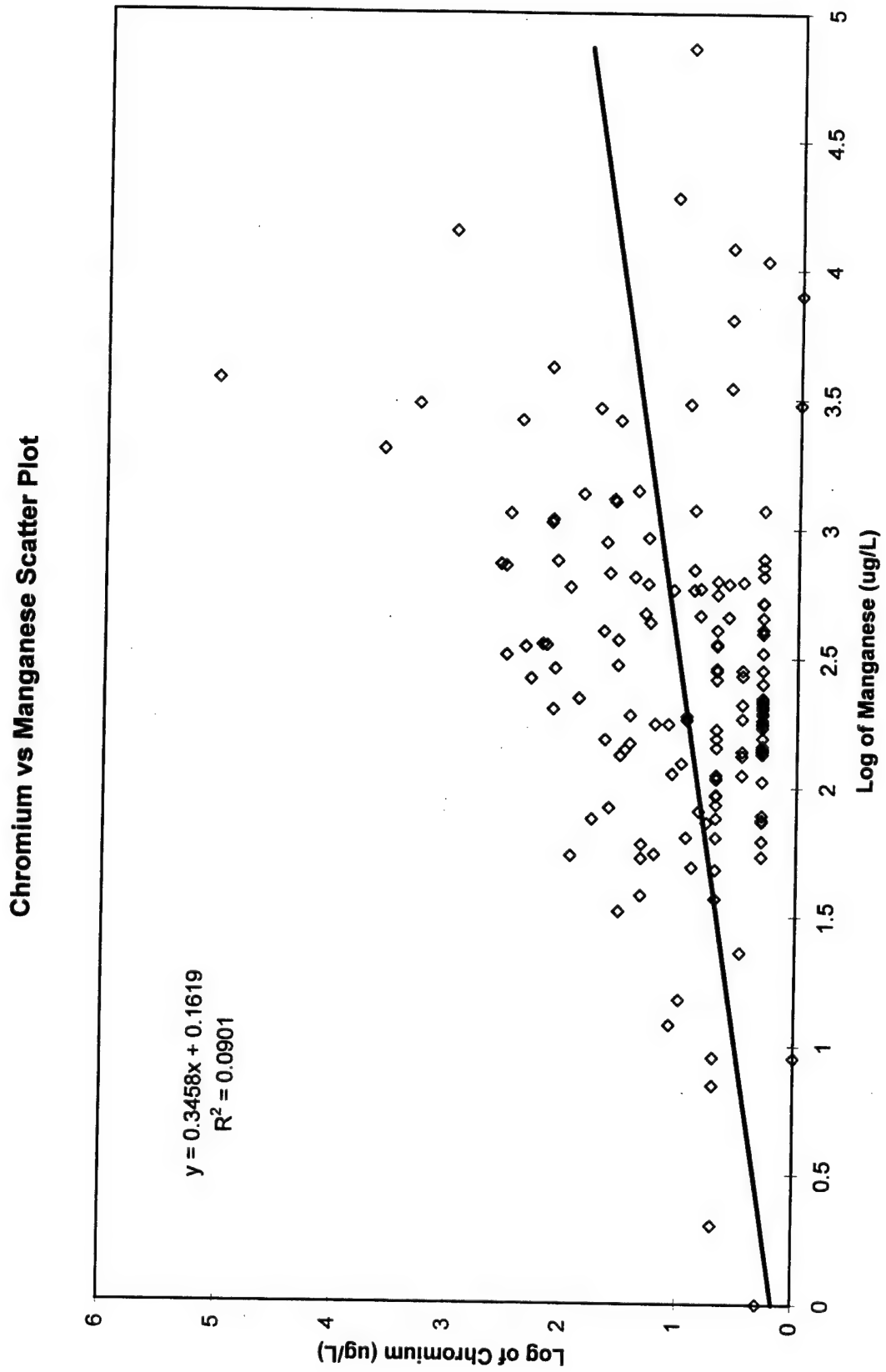
Chromium vs Manganese Scatter Plot
y = 0.3458x + 0.1619
R2 = 0.0901
Log of Chromium (ug/L)
Log of Manganese (ug/L)
0
1
2
3
4
5
6
0
0.5
1
1.5
2
2.5
3
3.5
4
4.5
5

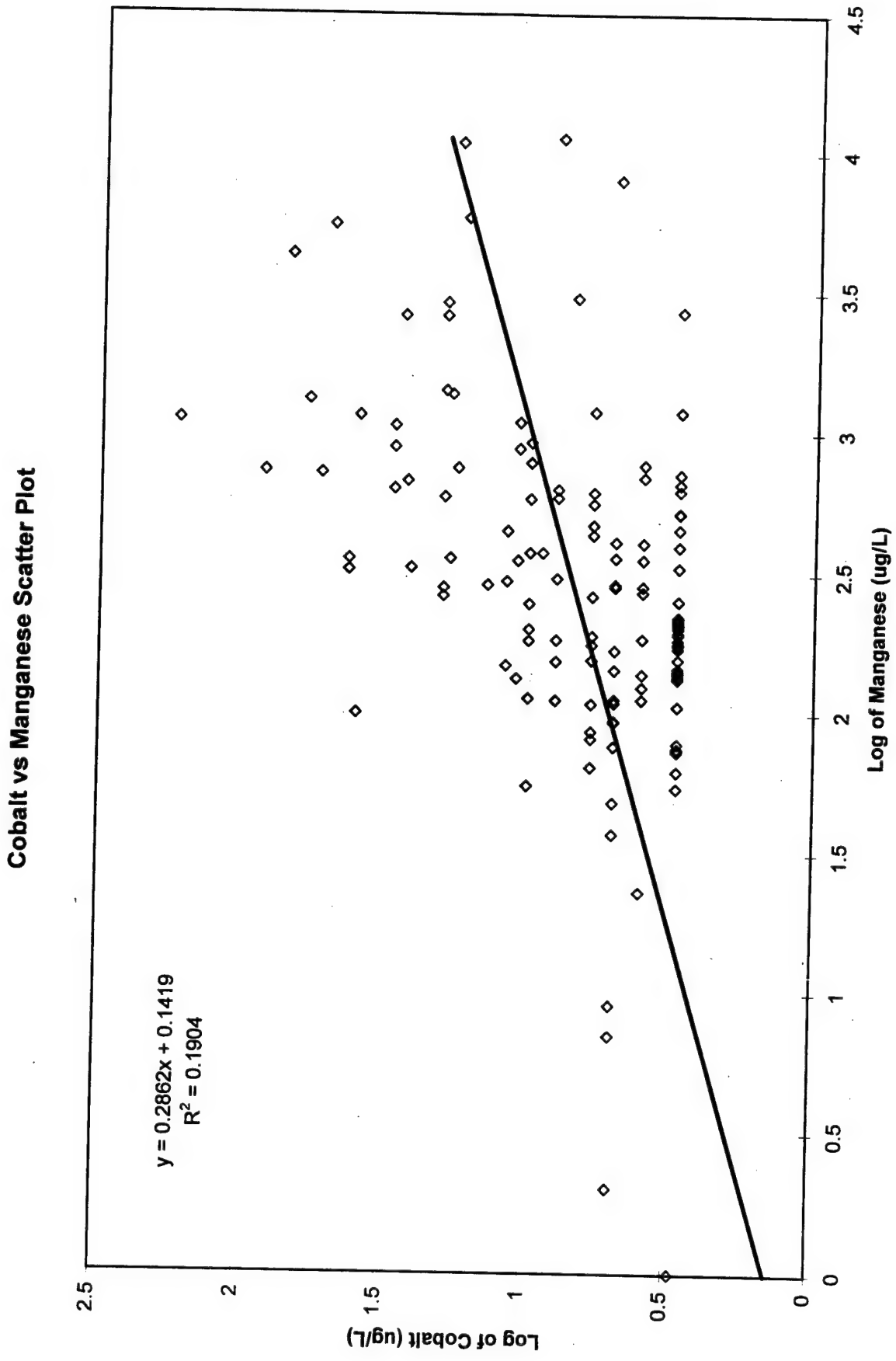
Cobalt vs Manganese Scatter Plot
y = 0.2862x + 0.1419
R² = 0.1904
Log of Cobalt (ug/L)
Log of Manganese (ug/L)
0
0.5
1
1.5
2
2.5
3
3.5
4
4.5

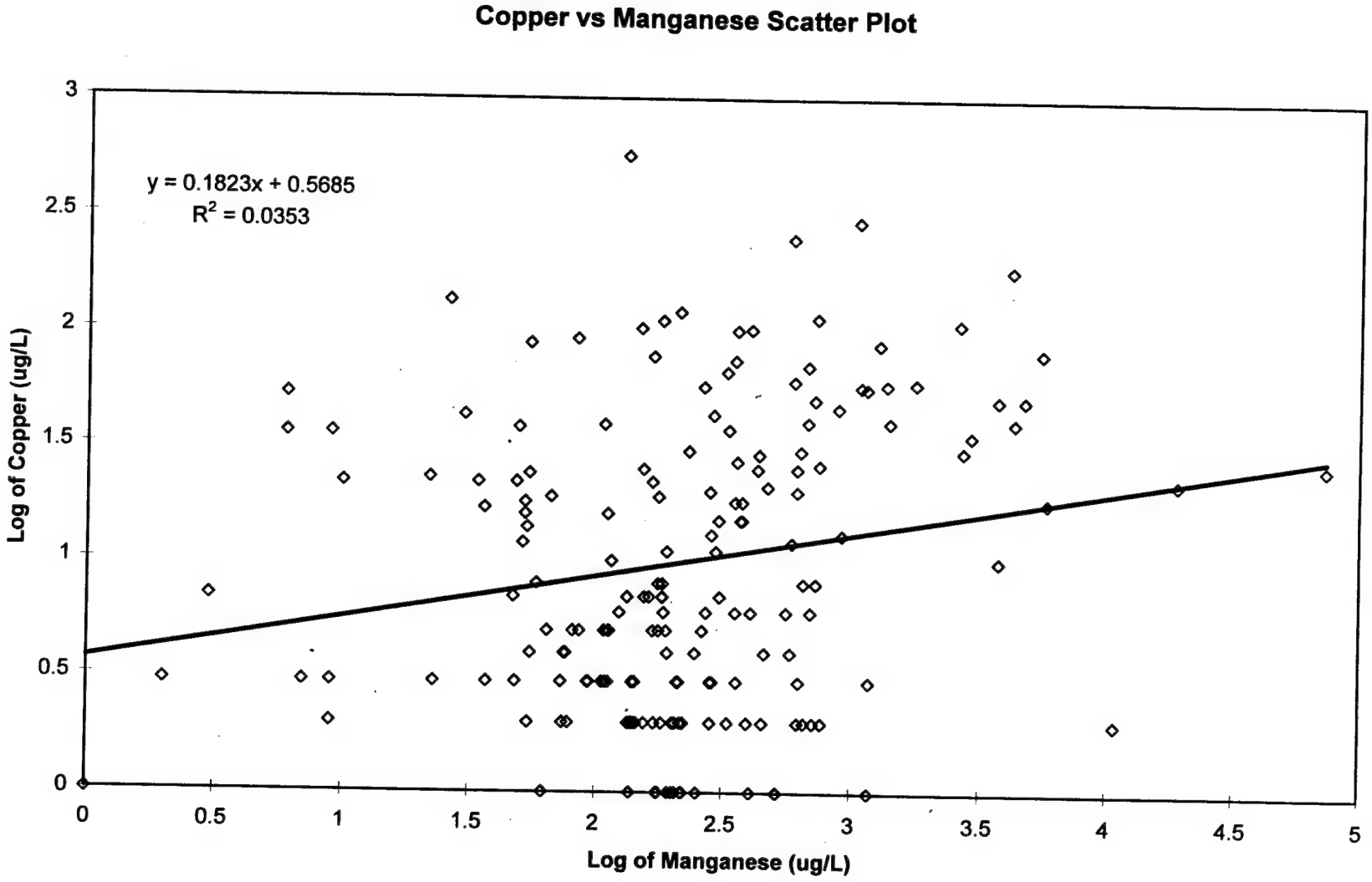
Copper vs Manganese Scatter Plot
y = 0.1823x + 0.5685
R2 = 0.0353
Log of Copper (ug/L)
Log of Manganese (ug/L)
0
0.5
1
1.5
2
2.5
3
3.5
4
4.5
5

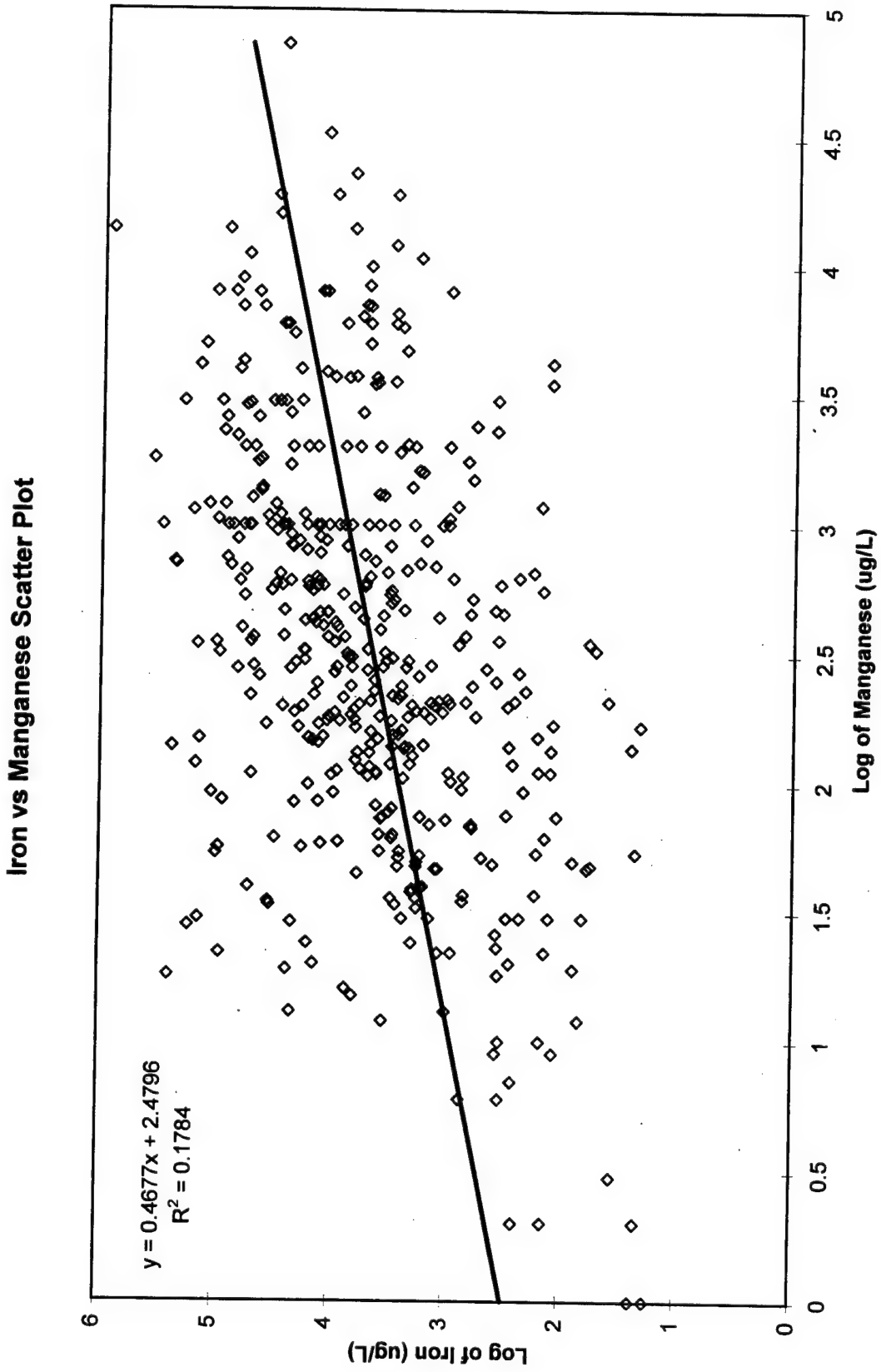
Iron vs Manganese Scatter Plot
y = 0.4677x + 2.4796
R2 = 0.1784
Log of Iron (ug/L)
Log of Manganese (ug/L)
0
1
2
3
4
5
6
0
0.5
1
1.5
2
2.5
3
3.5
4
4.5
5

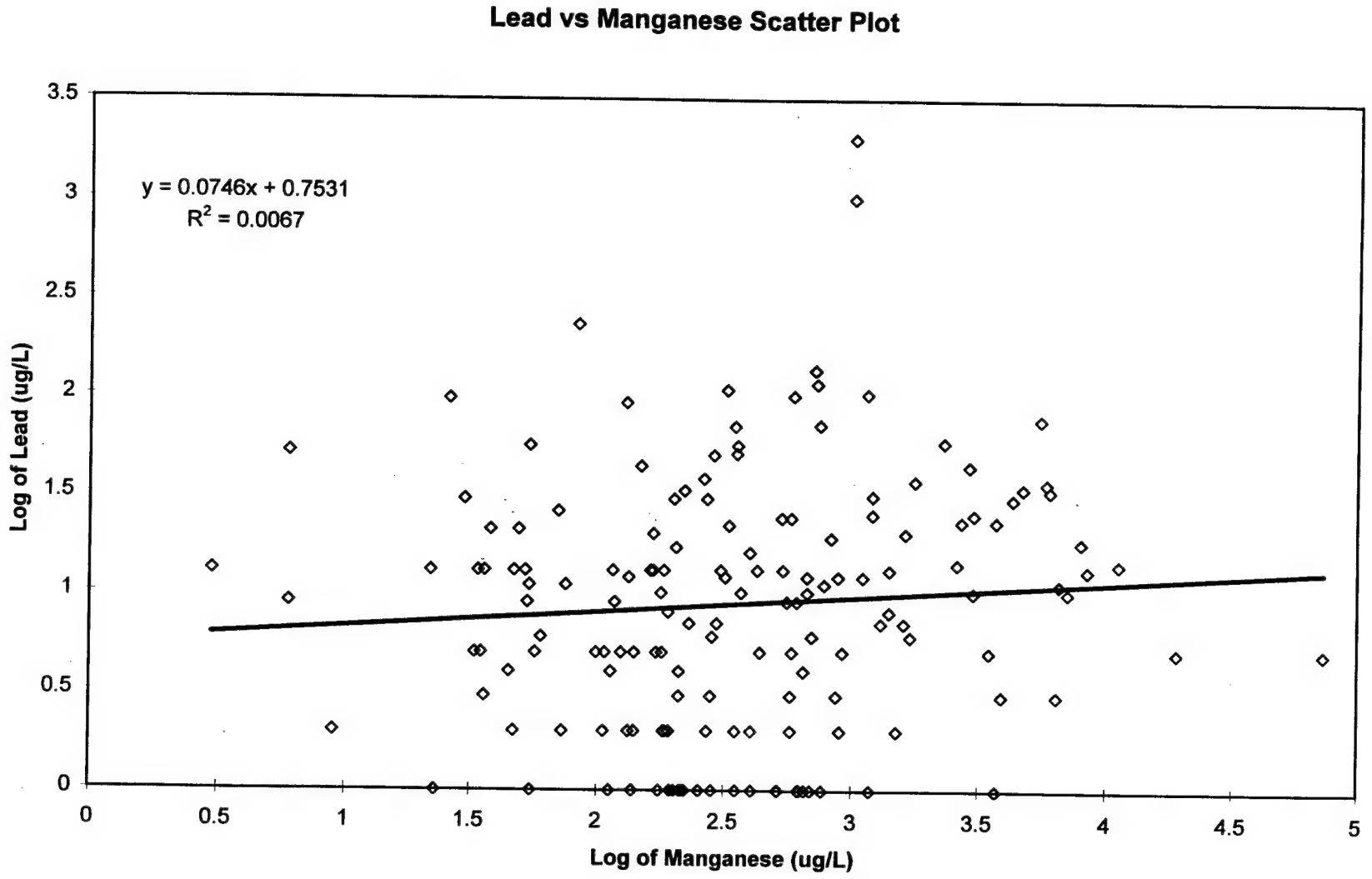
Lead vs Manganese Scatter Plot
y = 0.0746x + 0.7531
R2 = 0.0067
Log of Lead (ug/L)
Log of Manganese (ug/L)
0
0.5
1
1.5
2
2.5
3
3.5
4
4.5
5

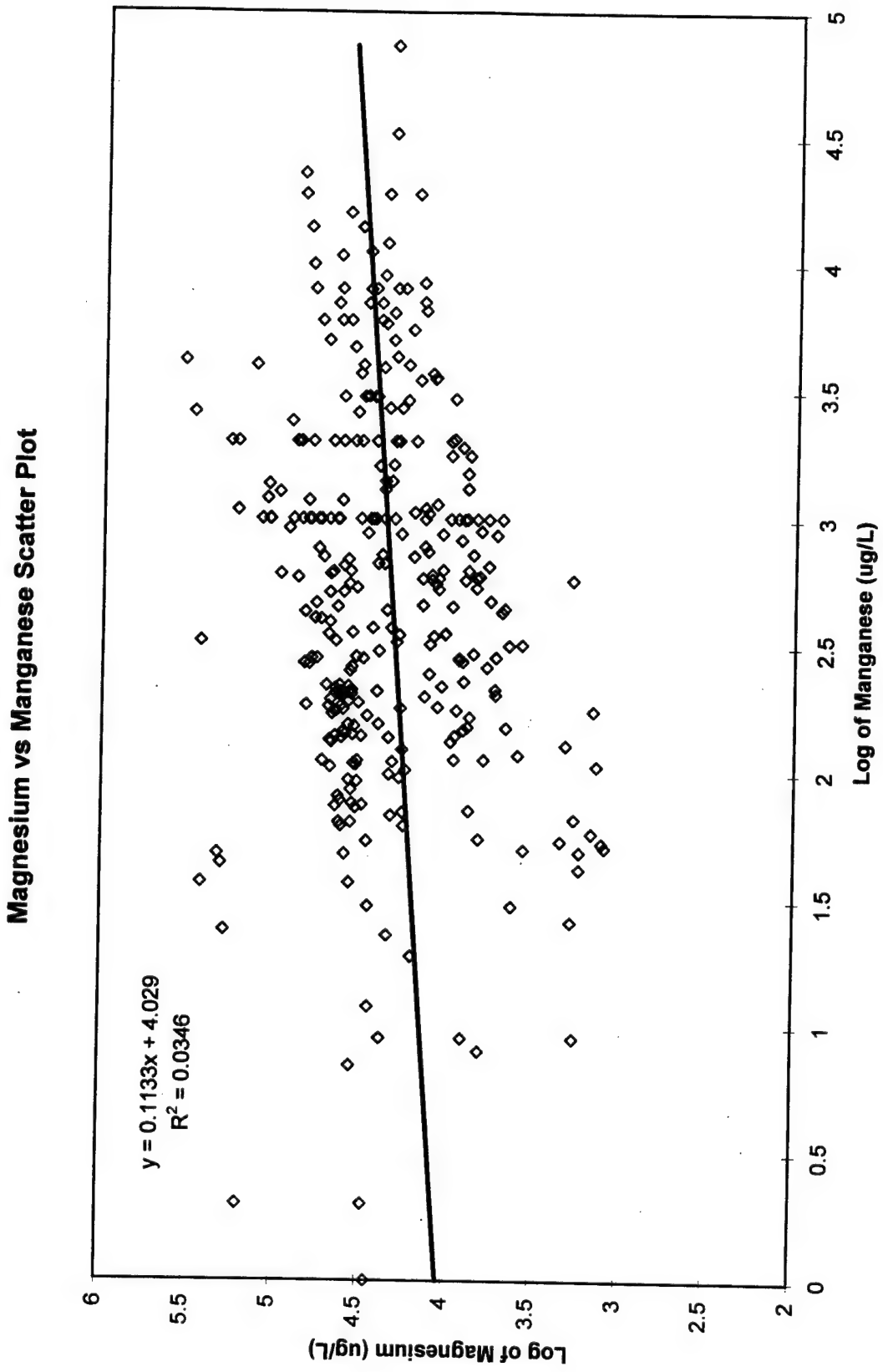
Magnesium vs Manganese Scatter Plot
y = 0.1133x + 4.029
R2 = 0.0346
Log of Magnesium (ug/L)
Log of Manganese (ug/L)
6
5.5
5
4.5
4
3.5
3
2.5
2
0
0.5
1
1.5
2
2.5
3
3.5
4
4.5
5

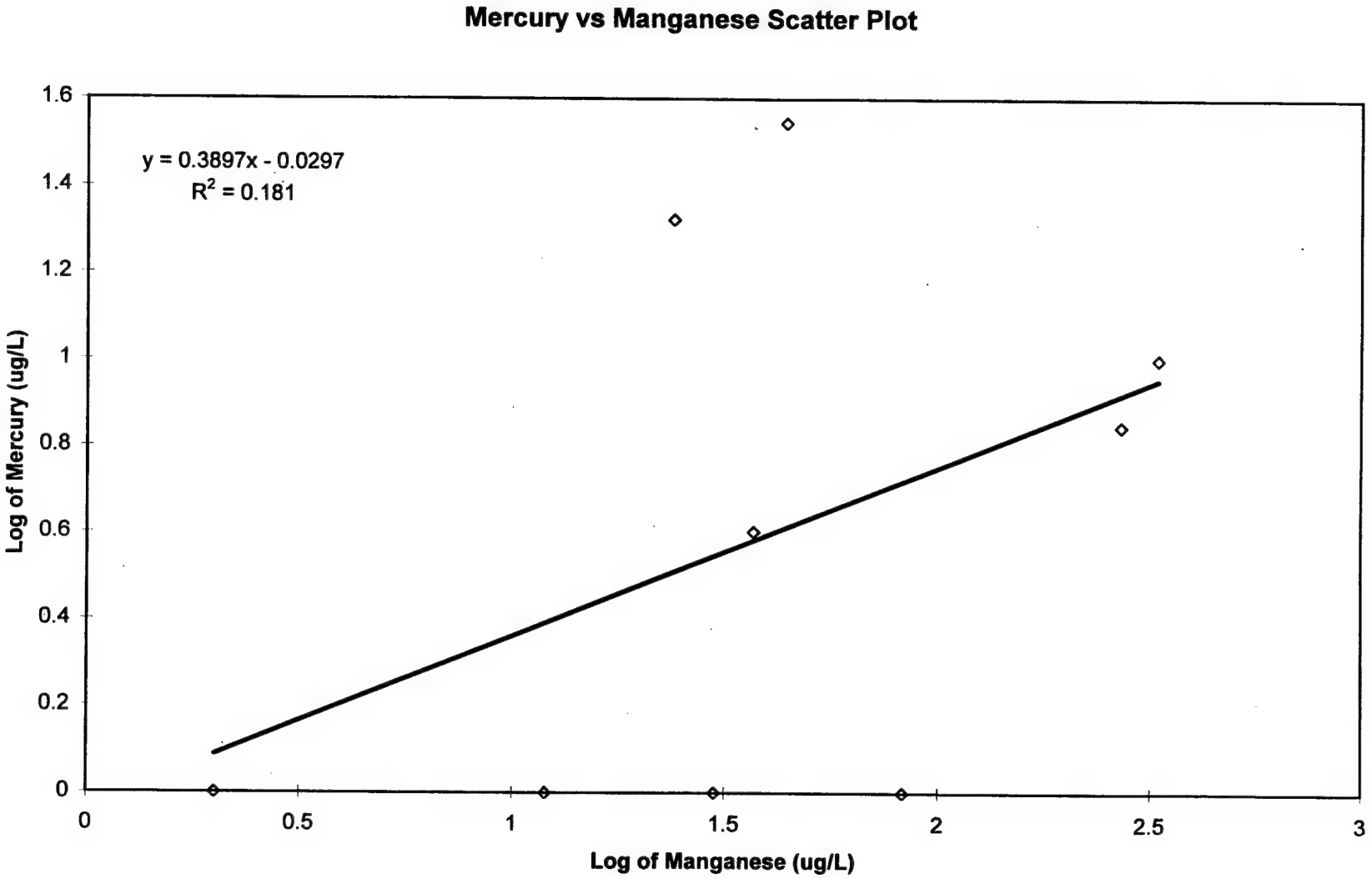
Mercury vs Manganese Scatter Plot
y = 0.3897x - 0.0297
R2 = 0.181
Log of Mercury (ug/L)
Log of Manganese (ug/L)
0
0.2
0.4
0.6
0.8
1
1.2
1.4
1.6
0
0.5
1
1.5
2
2.5
3

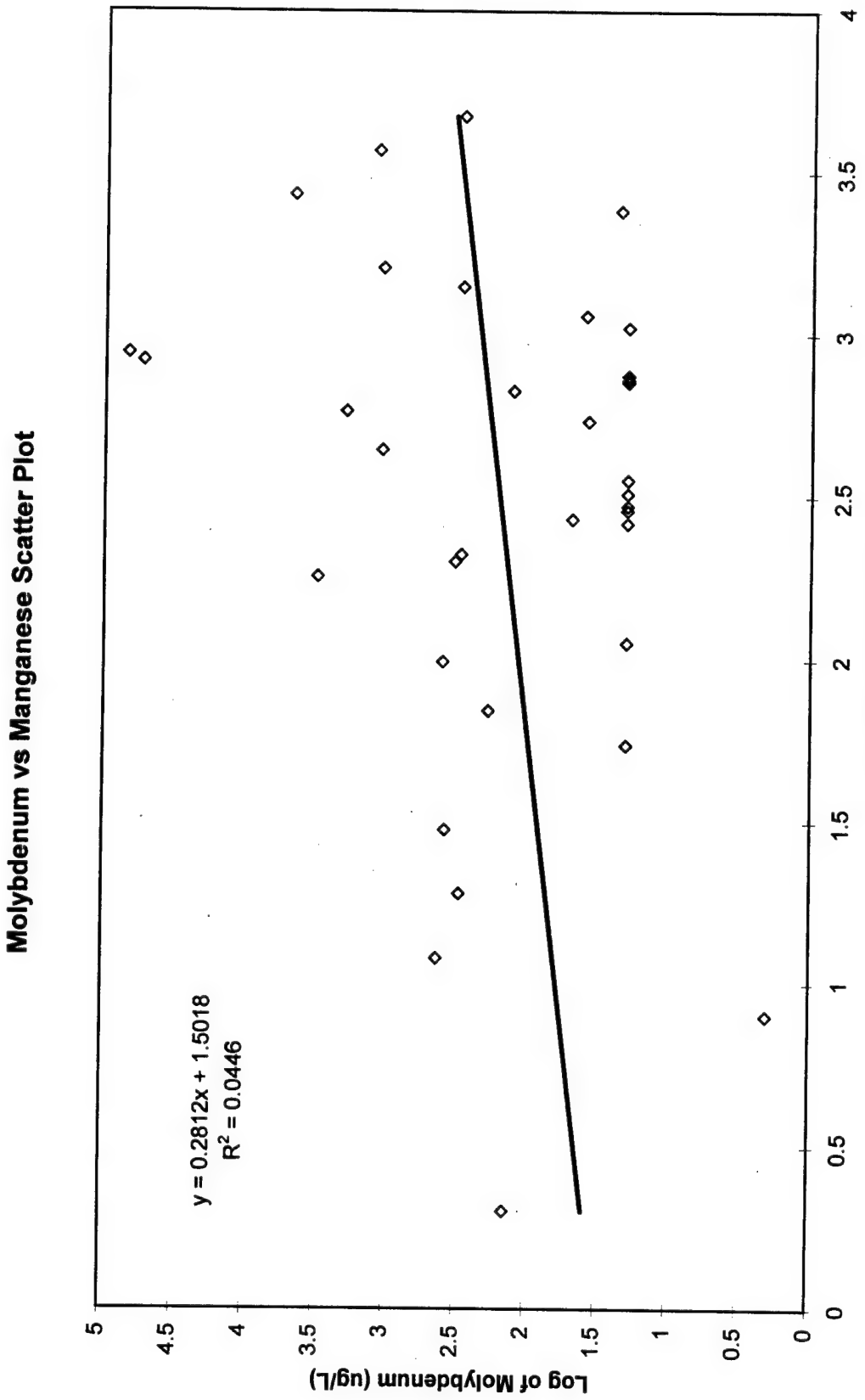
Molybdenum vs Manganese Scatter Plot
y = 0.2812x + 1.5018
R2 = 0.0446
Log of Molybdenum (ug/L)
Log of Manganese (ug/L)
0
0.5
1
1.5
2
2.5
3
3.5
4
4.5
5

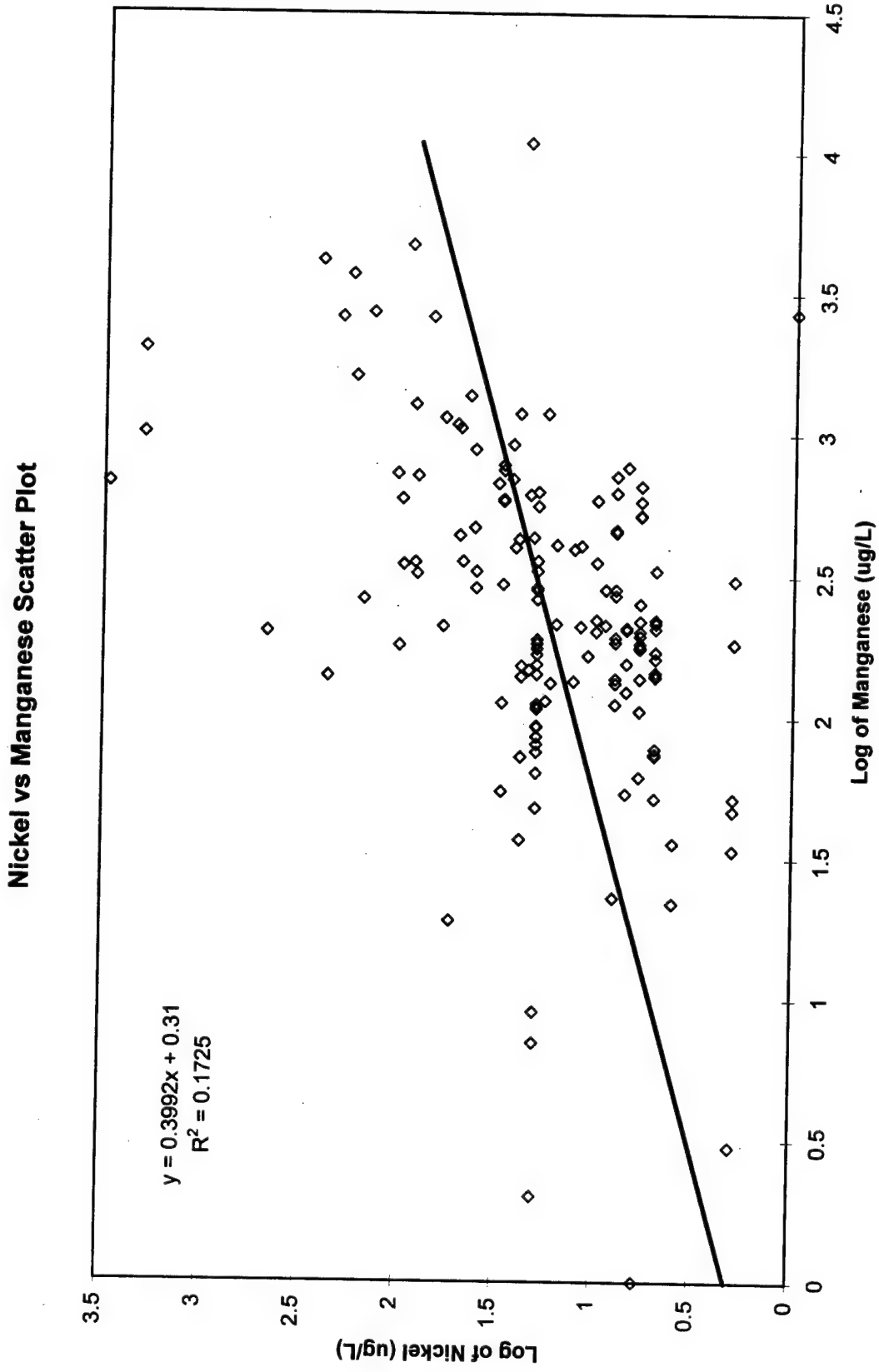
Nickel vs Manganese Scatter Plot
y = 0.3992x + 0.31
R2 = 0.1725
Log of Nickel (ug/L)
Log of Manganese (ug/L)
0
0.5
1
1.5
2
2.5
3
3.5
4
4.5

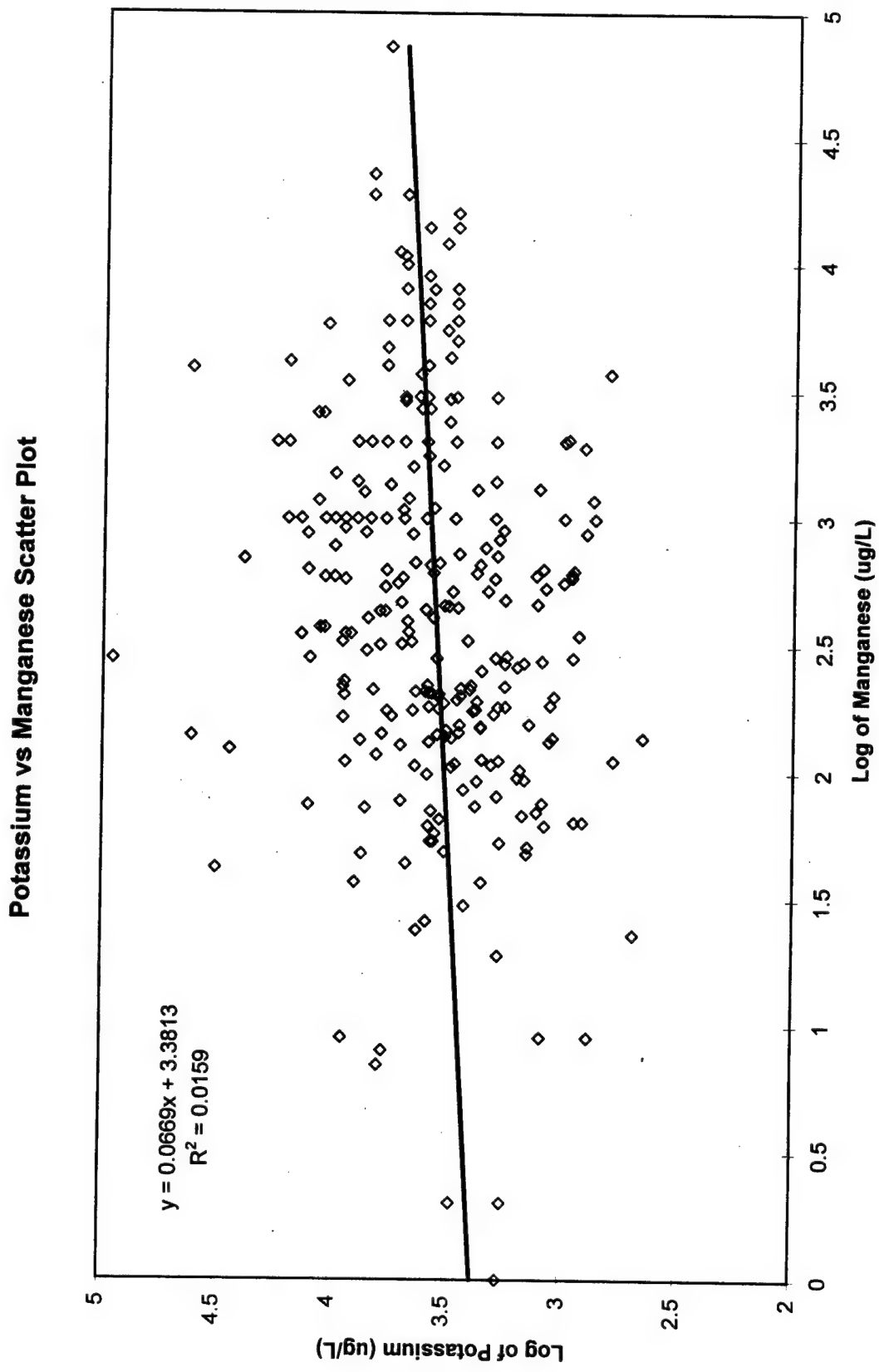
Potassium vs Manganese Scatter Plot
y = 0.0669x + 3.3813
R2 = 0.0159
Log of Potassium (ug/L)
Log of Manganese (ug/L)
5
4.5
4
3.5
3
2.5
2
0
0.5
1
1.5
2
2.5
3
3.5
4
4.5
5

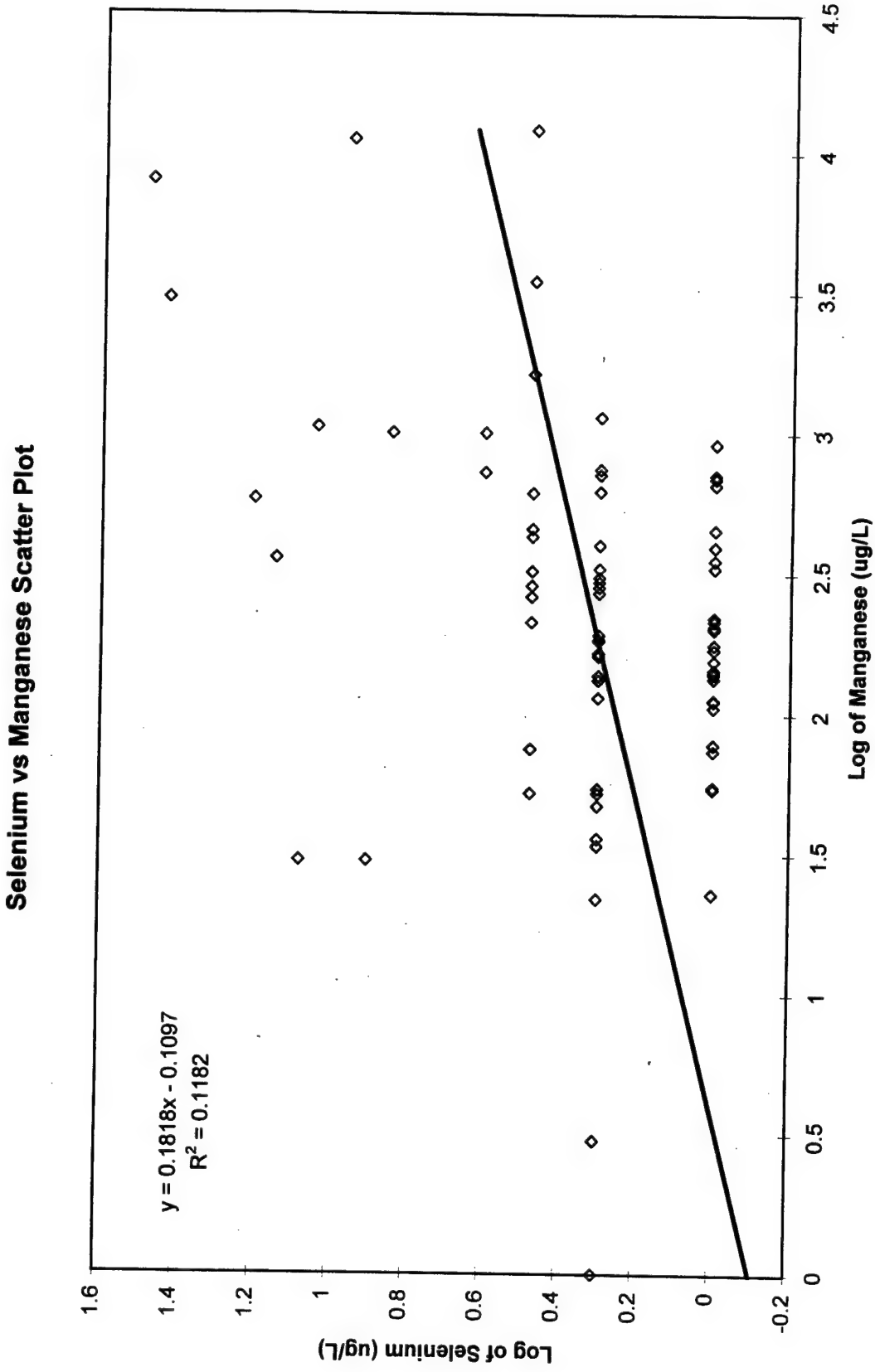
Selenium vs Manganese Scatter Plot
y = 0.1818x - 0.1097
R2 = 0.1182
Log of Selenium (ug/L)
Log of Manganese (ug/L)
1.6
1.4
1.2
1
0.8
0.6
0.4
0.2
0
-0.2
0
0.5
1
1.5
2
2.5
3
3.5
4
4.5

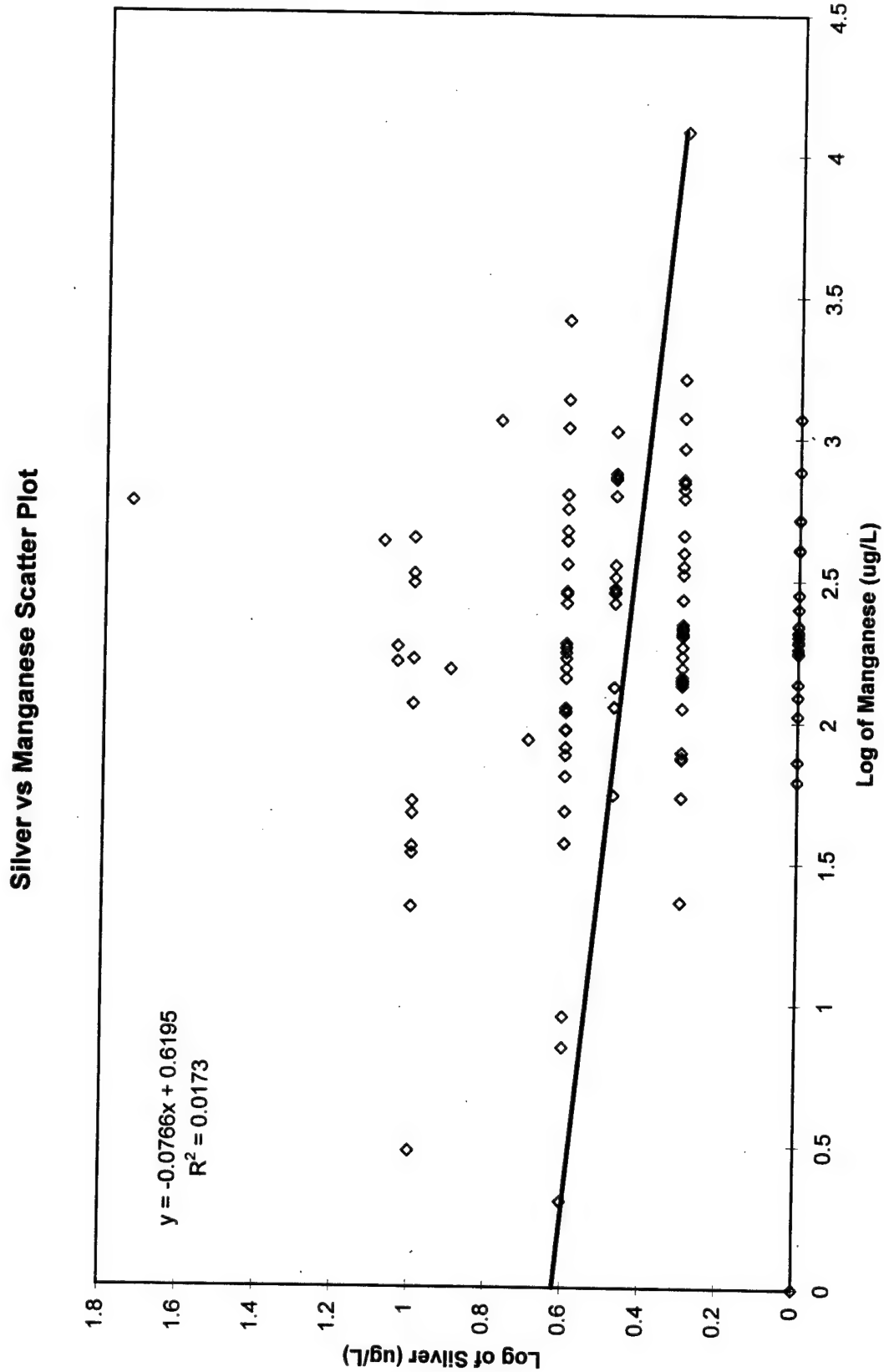
Silver vs Manganese Scatter Plot
y = -0.0766x + 0.6195
R2 = 0.0173
Log of Silver (ug/L)
Log of Manganese (ug/L)
1.8
1.6
1.4
1.2
1
0.8
0.6
0.4
0.2
0
0
0.5
1
1.5
2
2.5
3
3.5
4
4.5

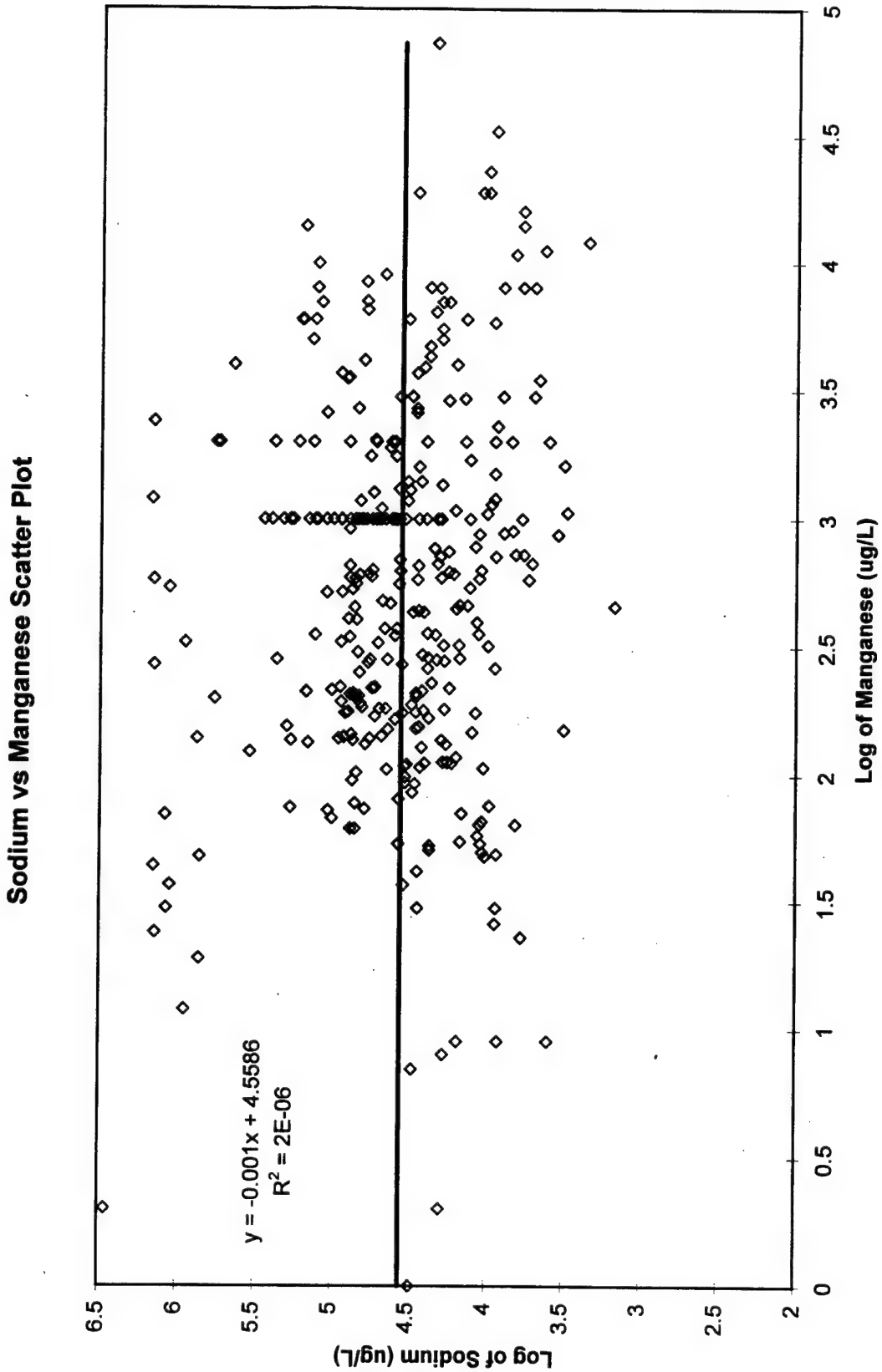
Sodium vs Manganese Scatter Plot
y = -0.001x + 4.5586
R2 = 2E-06
Log of Sodium (ug/L)
Log of Manganese (ug/L)
6.5
6
5.5
5
4.5
4
3.5
3
2.5
2
0
0.5
1
1.5
2
2.5
3
3.5
4
4.5
5

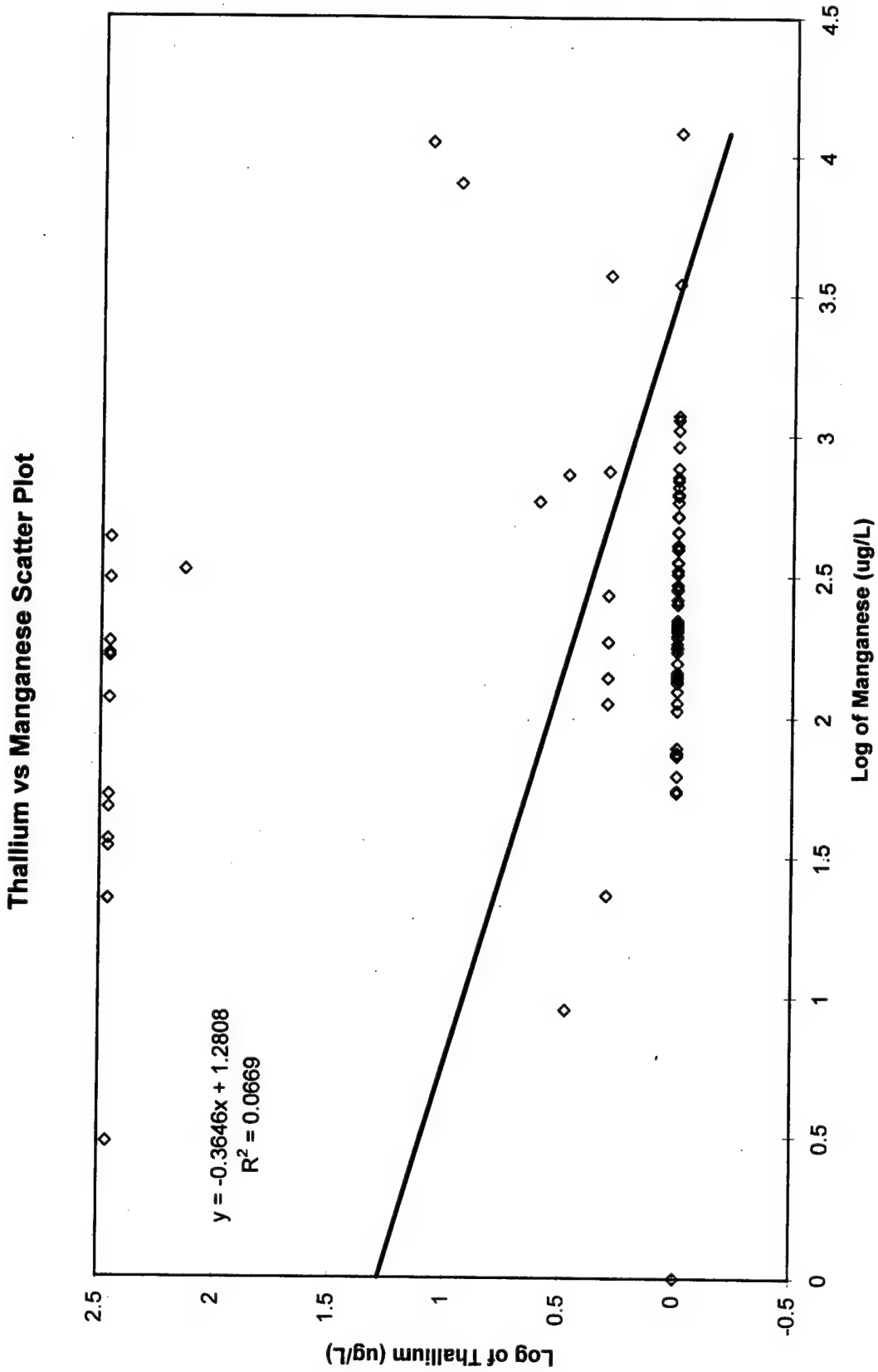
Thallium vs Manganese Scatter Plot
y = -0.3646x + 1.2808
R2 = 0.0669
Log of Thallium (ug/L)
Log of Manganese (ug/L)
2.5
2
1.5
1
0.5
0
-0.5
0
0.5
1
1.5
2
2.5
3
3.5
4
4.5

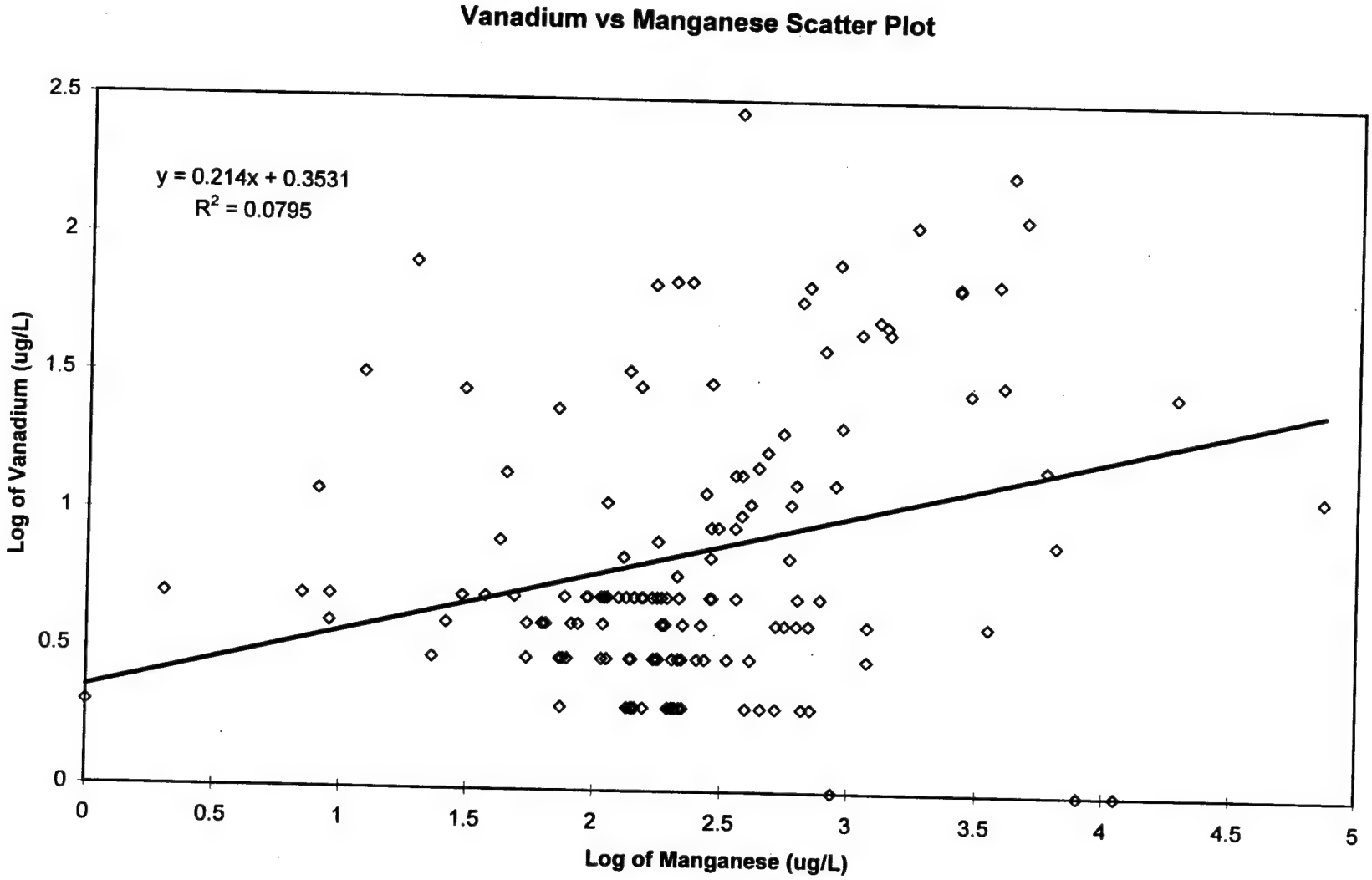
Vanadium vs Manganese Scatter Plot
y = 0.214x + 0.3531
R2 = 0.0795
Log of Vanadium (ug/L)
Log of Manganese (ug/L)
0
0.5
1
1.5
2
2.5
3
3.5
4
4.5
5

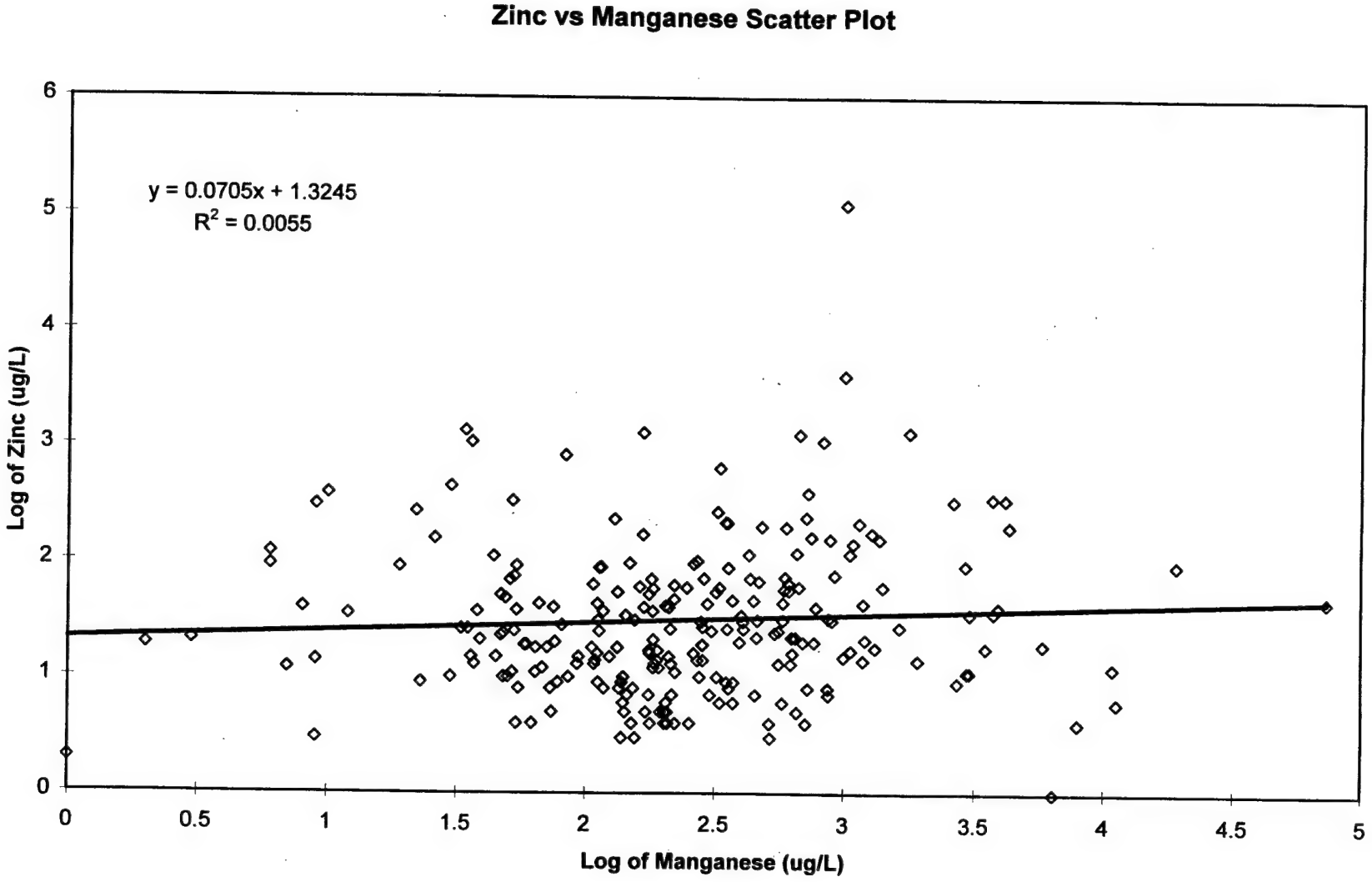
Zinc vs Manganese Scatter Plot
y = 0.0705x + 1.3245
R2 = 0.0055
Log of Zinc (ug/L)
Log of Manganese (ug/L)
0
1
2
3
4
5
6
0
0.5
1
1.5
2
2.5
3
3.5
4
4.5
5

Appendix J: Metal Versus Total Fuel Scatter Plots

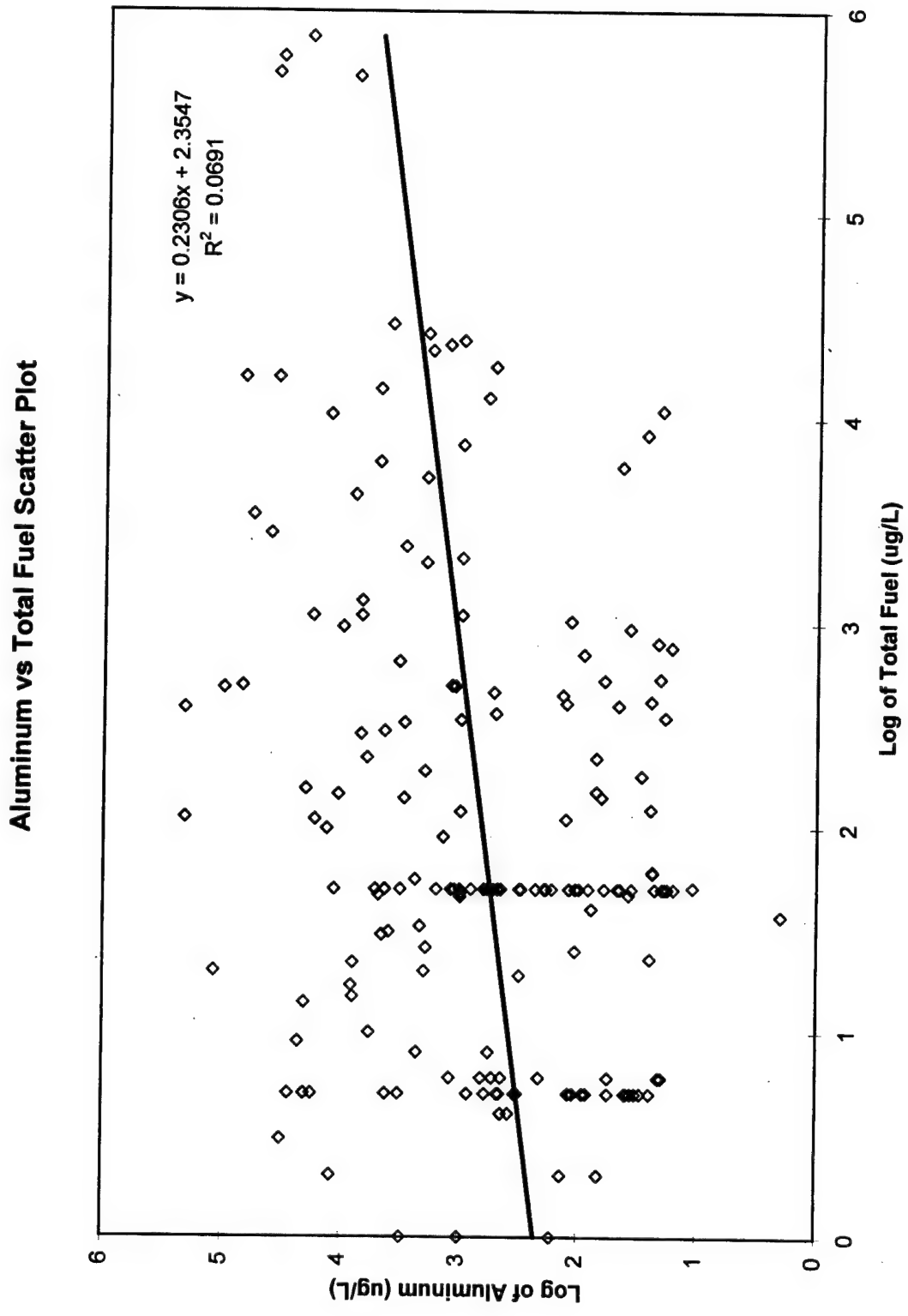

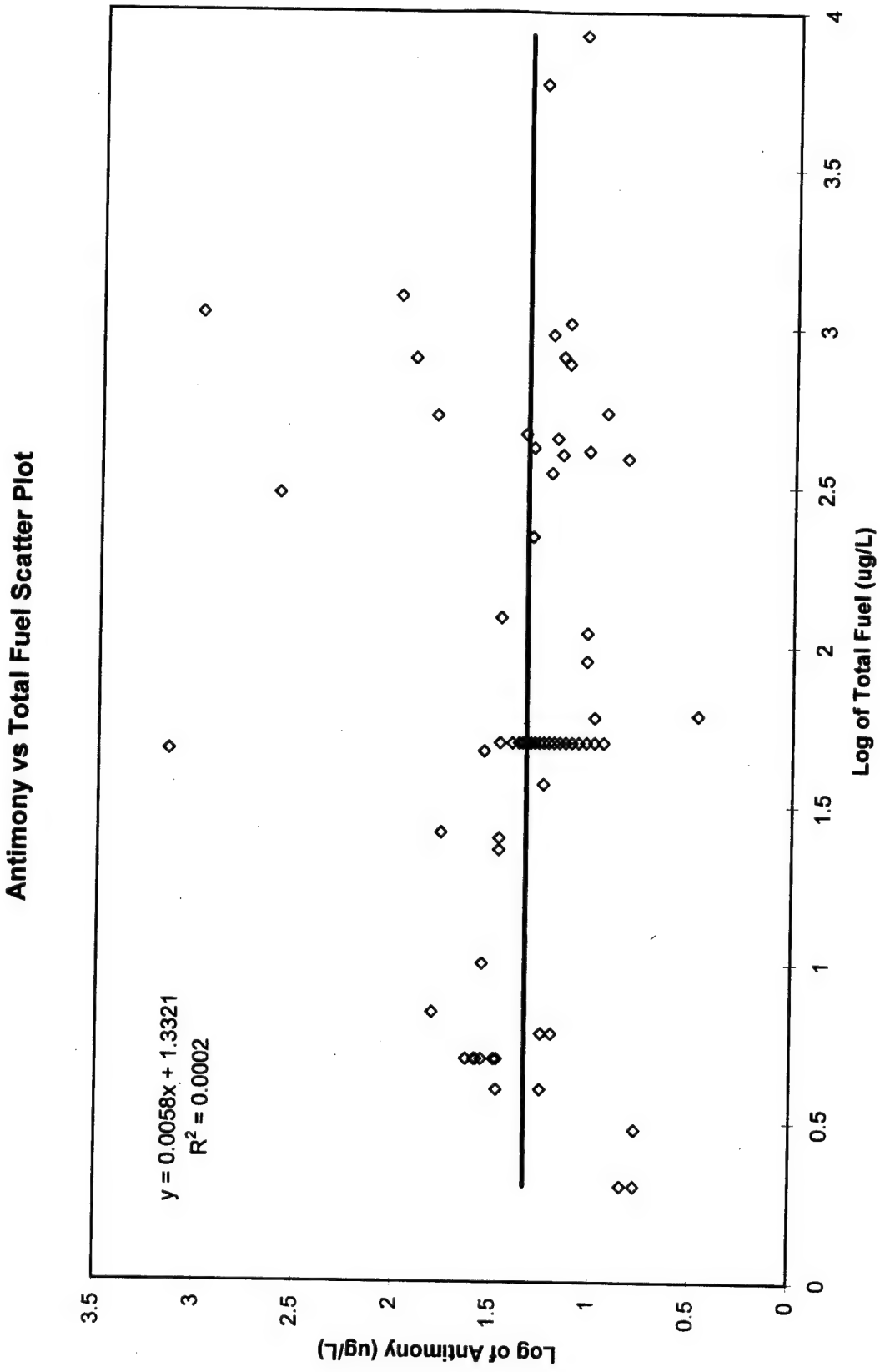
Antimony vs Total Fuel Scatter Plot
y = 0.0058x + 1.3321
R² = 0.0002
Log of Antimony (ug/L)
Log of Total Fuel (ug/L)
0
0.5
1
1.5
2
2.5
3
3.5
4

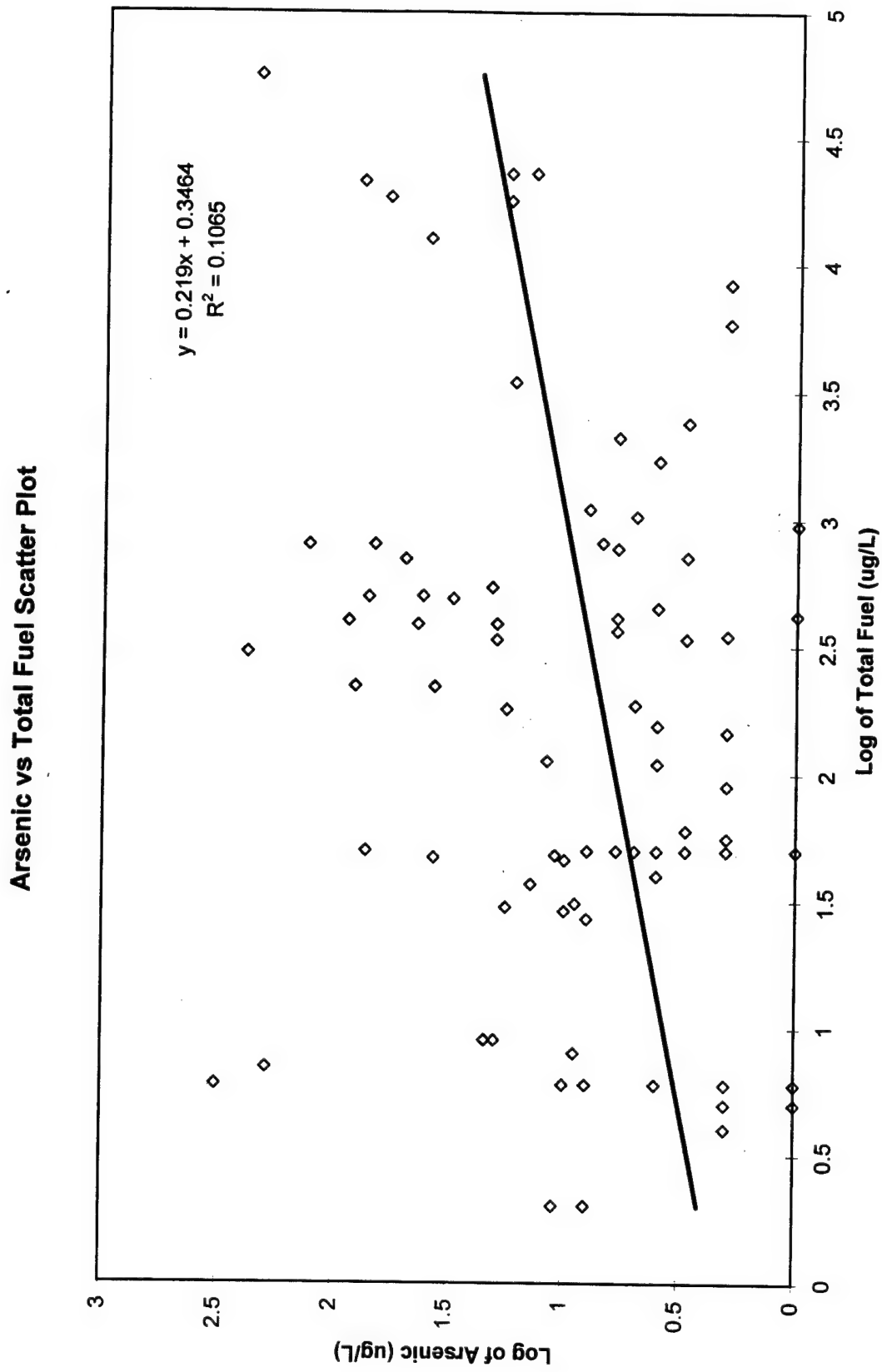
Arsenic vs Total Fuel Scatter Plot
y = 0.219x + 0.3464
R2 = 0.1065
Log of Arsenic (ug/L)
Log of Total Fuel (ug/L)
0
0.5
1
1.5
2
2.5
3
3.5
4
4.5
5

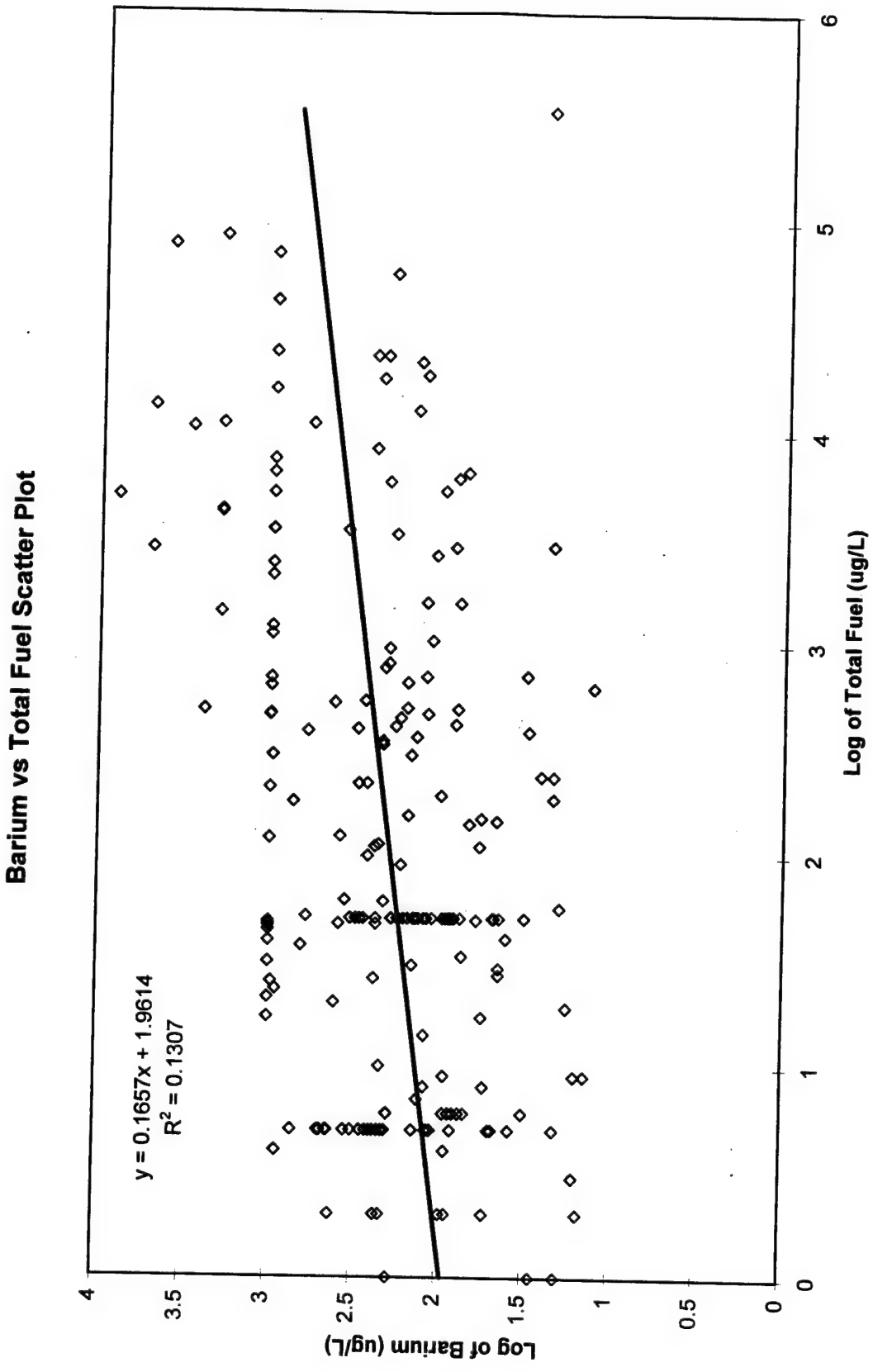
Barium vs Total Fuel Scatter Plot
y = 0.1657x + 1.9614
R2 = 0.1307
Log of Barium (ug/L)
Log of Total Fuel (ug/L)
0
0.5
1
1.5
2
2.5
3
3.5
4
0
1
2
3
4
5
6

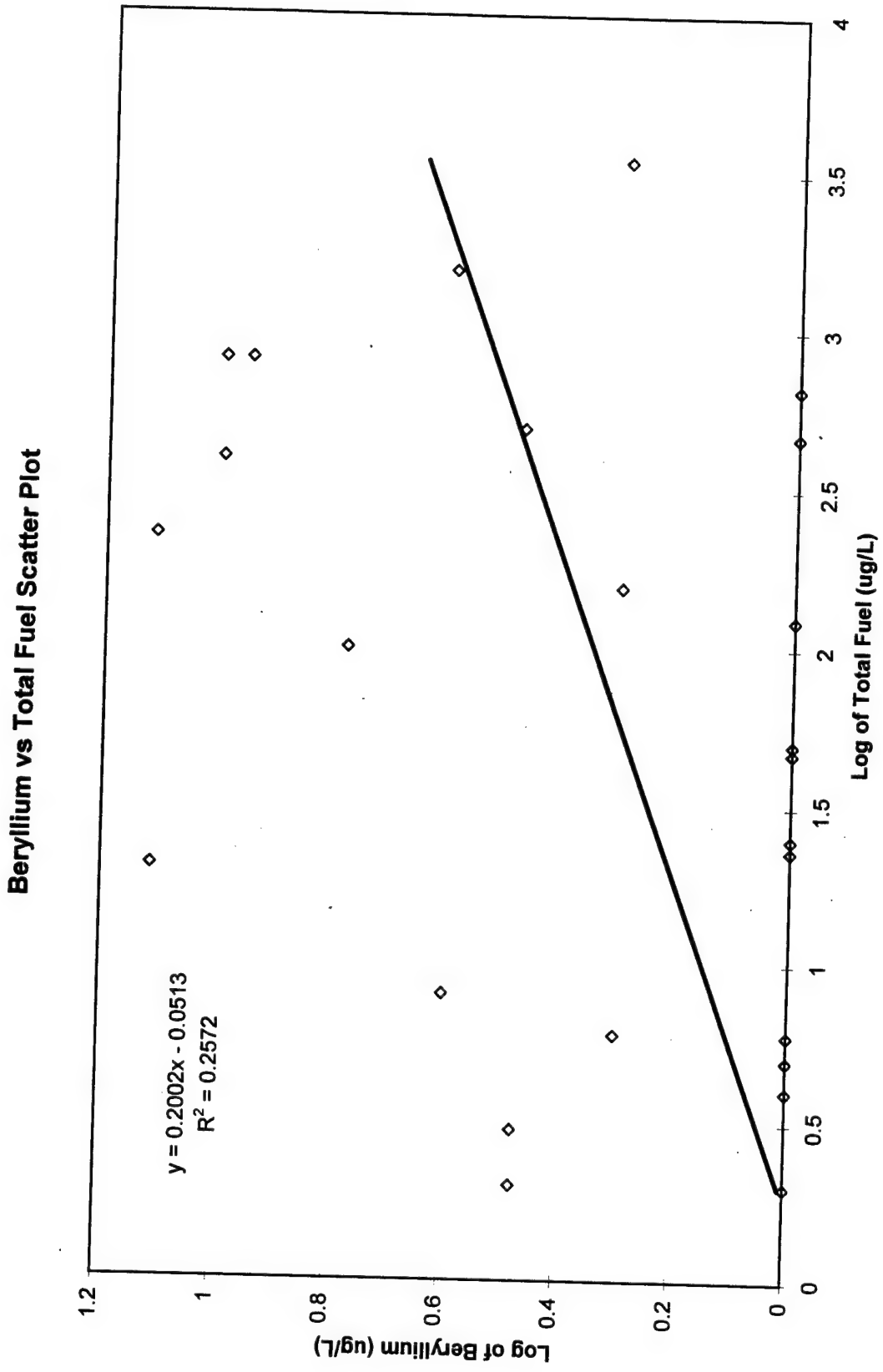
Beryllium vs Total Fuel Scatter Plot
y = 0.2002x - 0.0513
R2 = 0.2572
Log of Beryllium (ug/L)
Log of Total Fuel (ug/L)
1.2
1
0.8
0.6
0.4
0.2
0
0
0.5
1
1.5
2
2.5
3
3.5
4

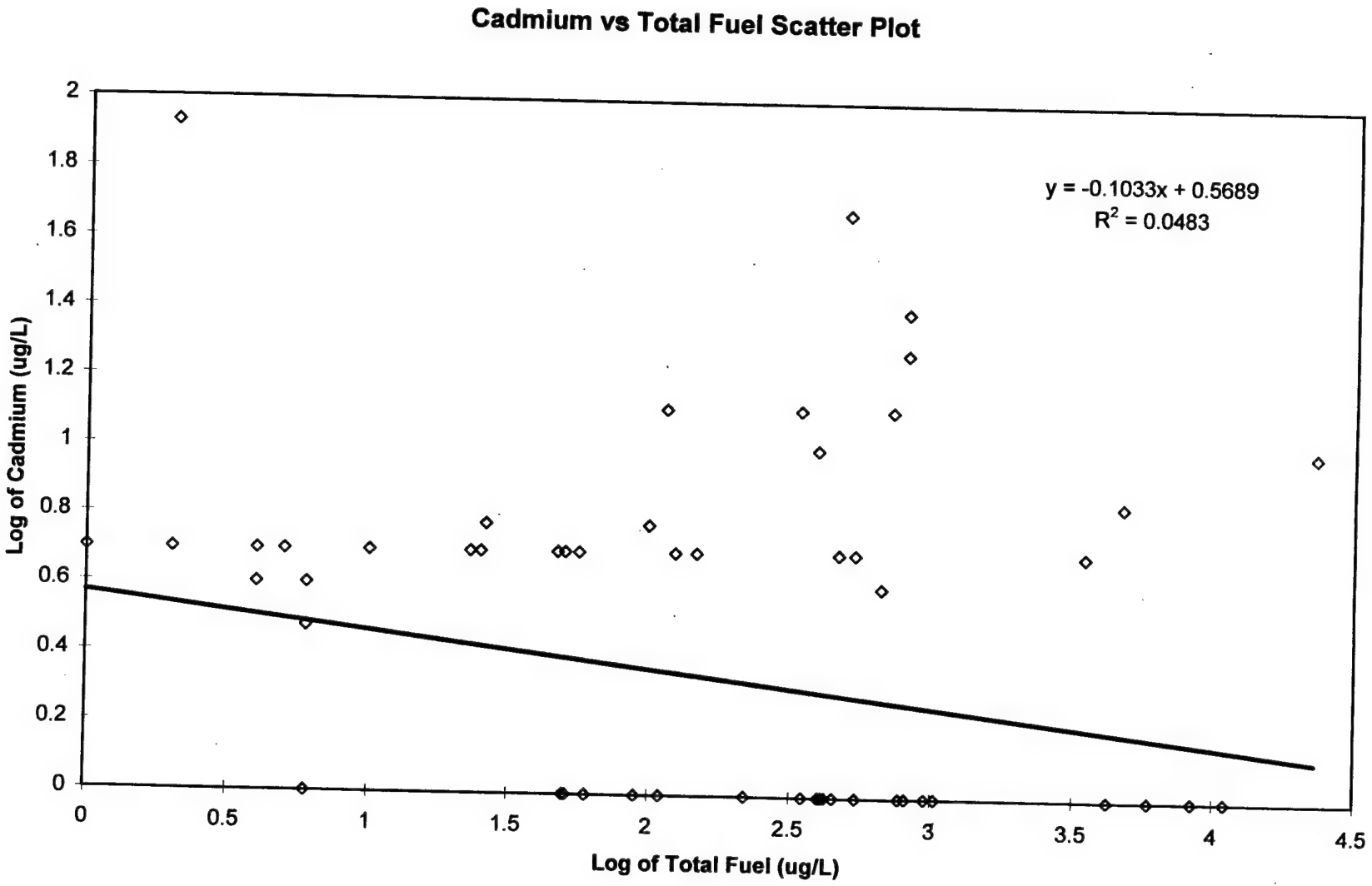
Cadmium vs Total Fuel Scatter Plot
y = -0.1033x + 0.5689
R2 = 0.0483
Log of Cadmium (ug/L)
Log of Total Fuel (ug/L)
0
0.2
0.4
0.6
0.8
1
1.2
1.4
1.6
1.8
2
0
0.5
1
1.5
2
2.5
3
3.5
4
4.5

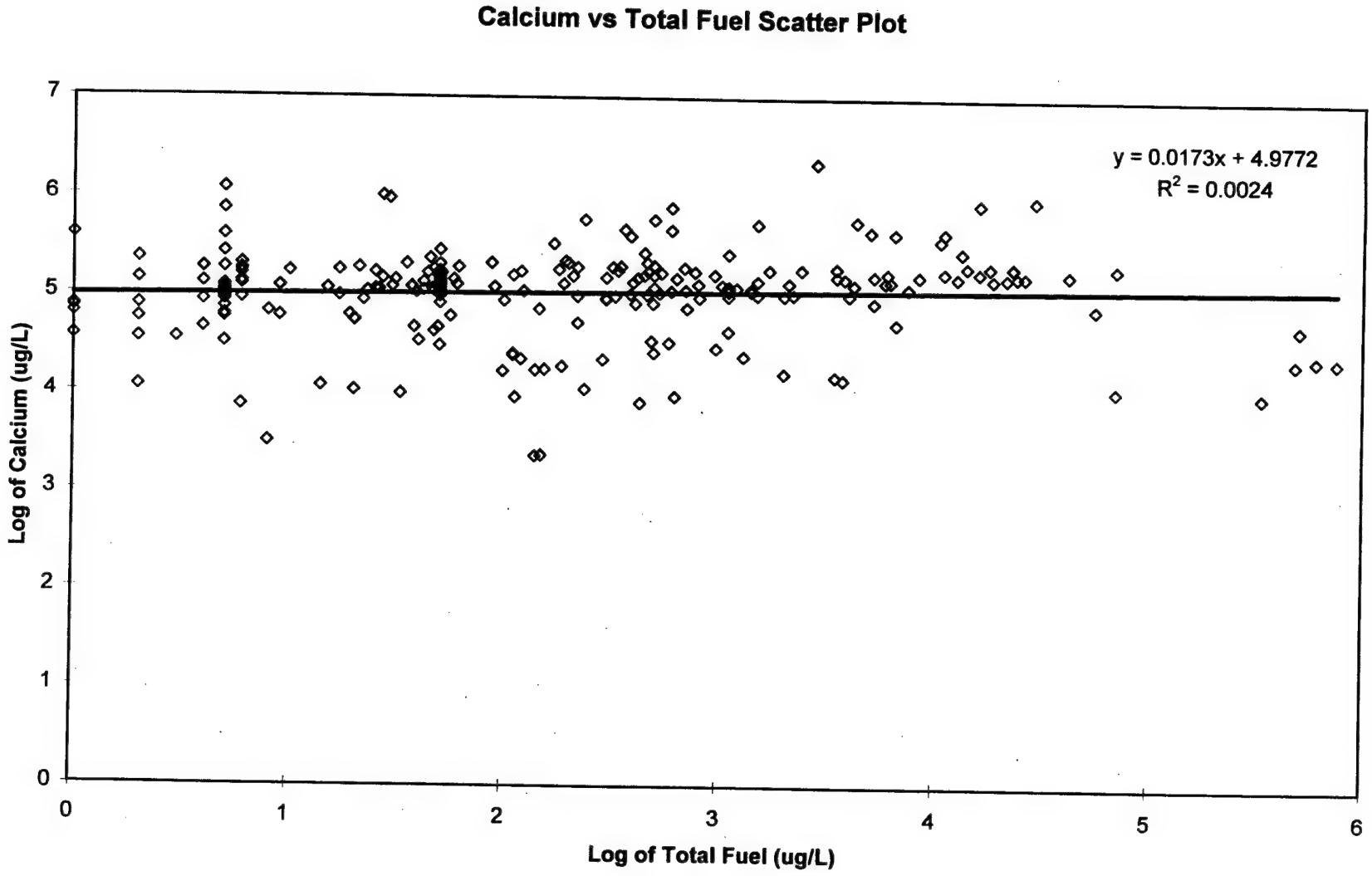
Calcium vs Total Fuel Scatter Plot
y = 0.0173x + 4.9772
R2 = 0.0024
Log of Calcium (ug/L)
Log of Total Fuel (ug/L)
0
1
2
3
4
5
6
7

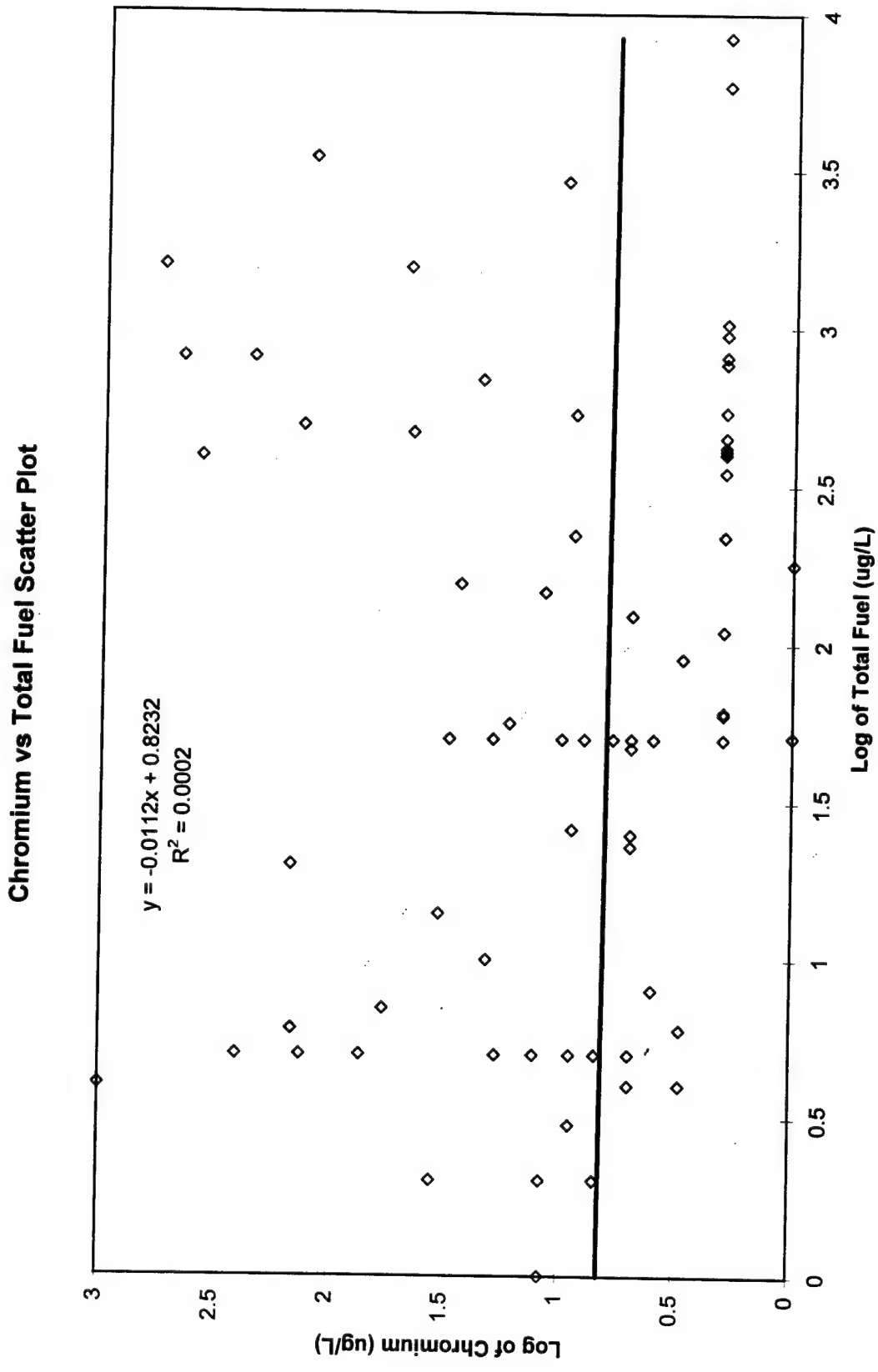
Chromium vs Total Fuel Scatter Plot
y = -0.0112x + 0.8232
R2 = 0.0002
Log of Chromium (ug/L)
Log of Total Fuel (ug/L)
0
0.5
1
1.5
2
2.5
3
3.5
4

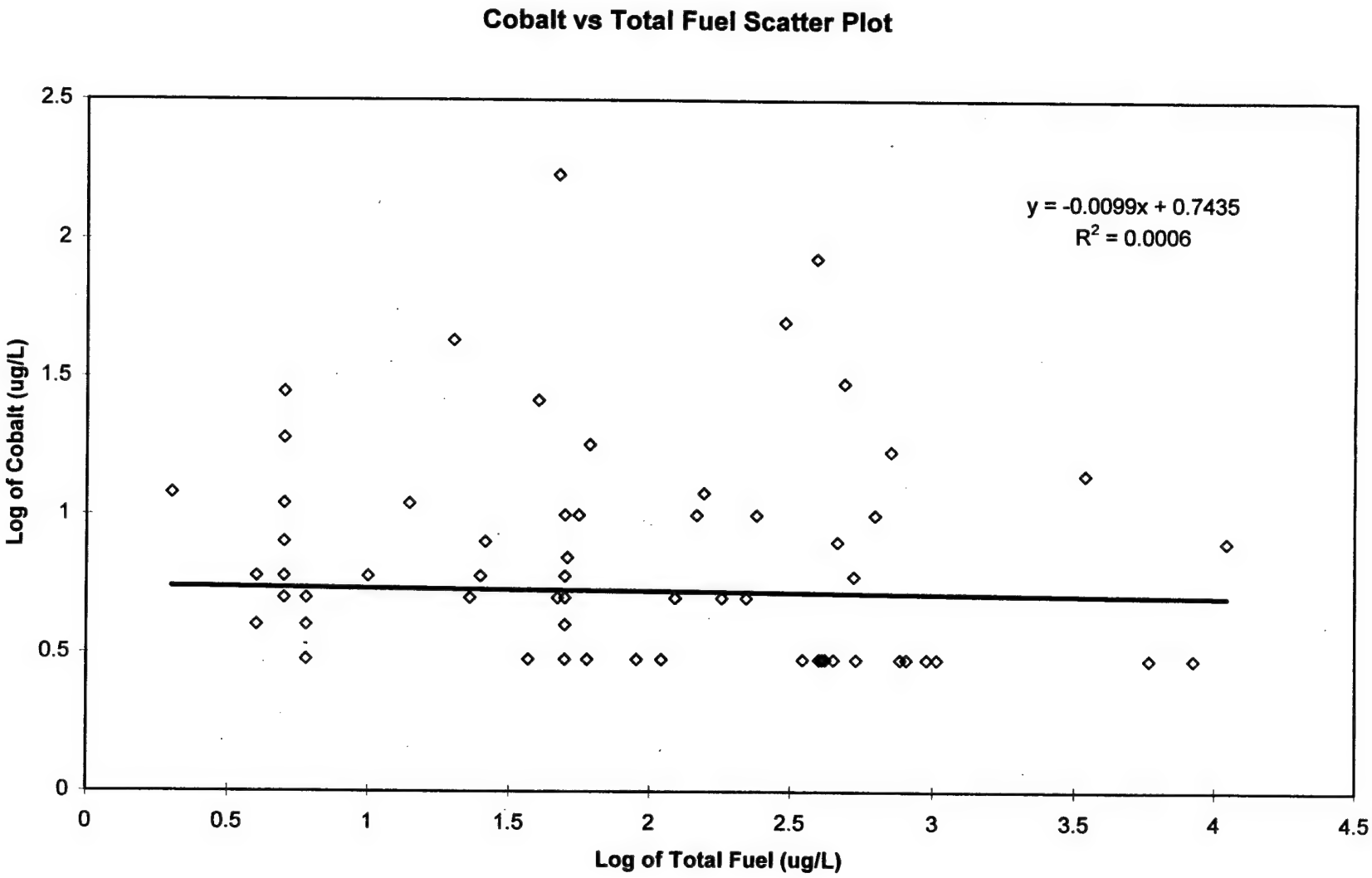
Cobalt vs Total Fuel Scatter Plot
y = -0.0099x + 0.7435
R2 = 0.0006
Log of Cobalt (ug/L)
Log of Total Fuel (ug/L)
2.5
2
1.5
1
0.5
0
0
0.5
1
1.5
2
2.5
3
3.5
4
4.5

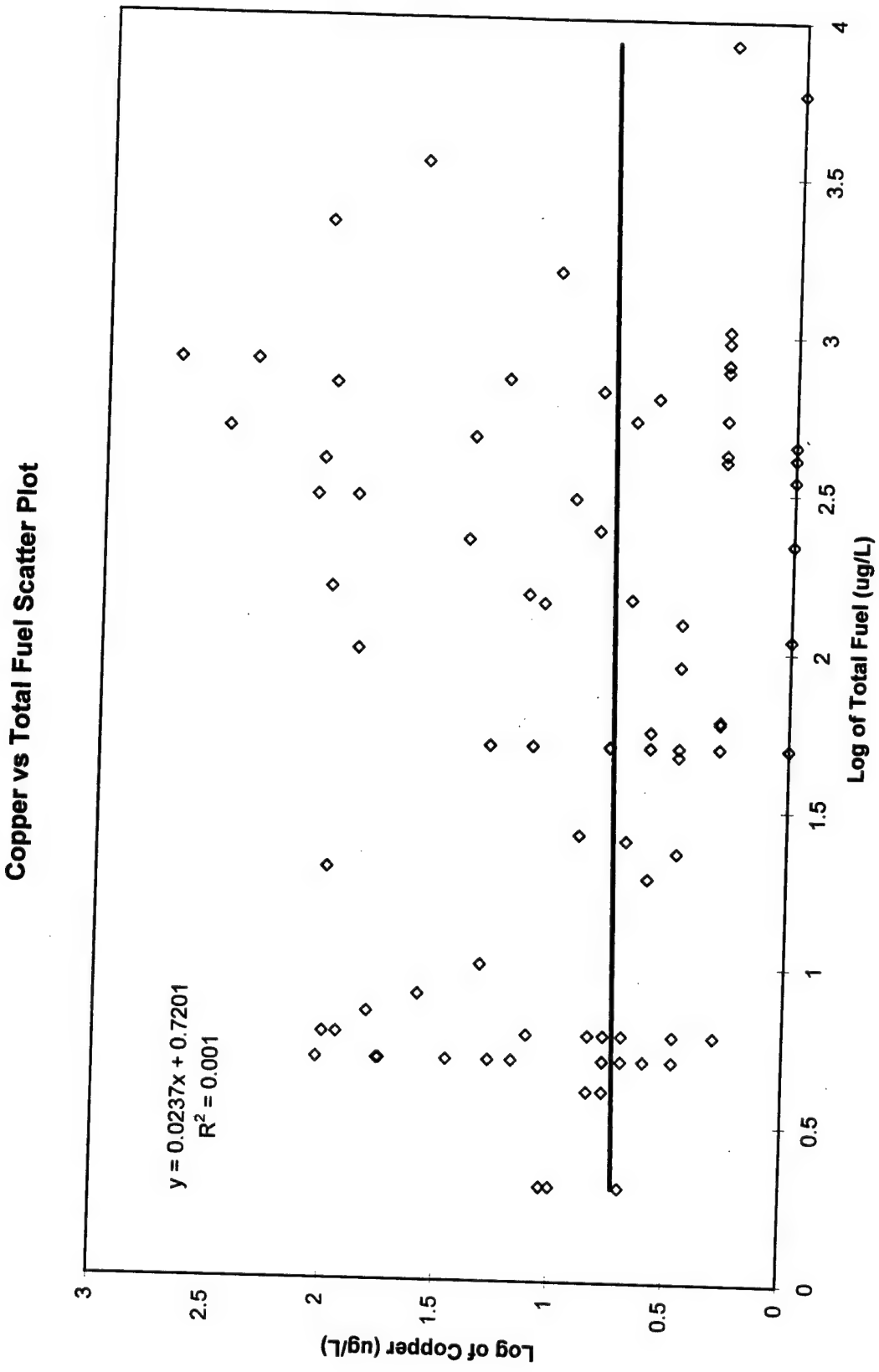
Copper vs Total Fuel Scatter Plot
y = 0.0237x + 0.7201
R2 = 0.001
Log of Copper (ug/L)
Log of Total Fuel (ug/L)
0
0.5
1
1.5
2
2.5
3
3.5
4

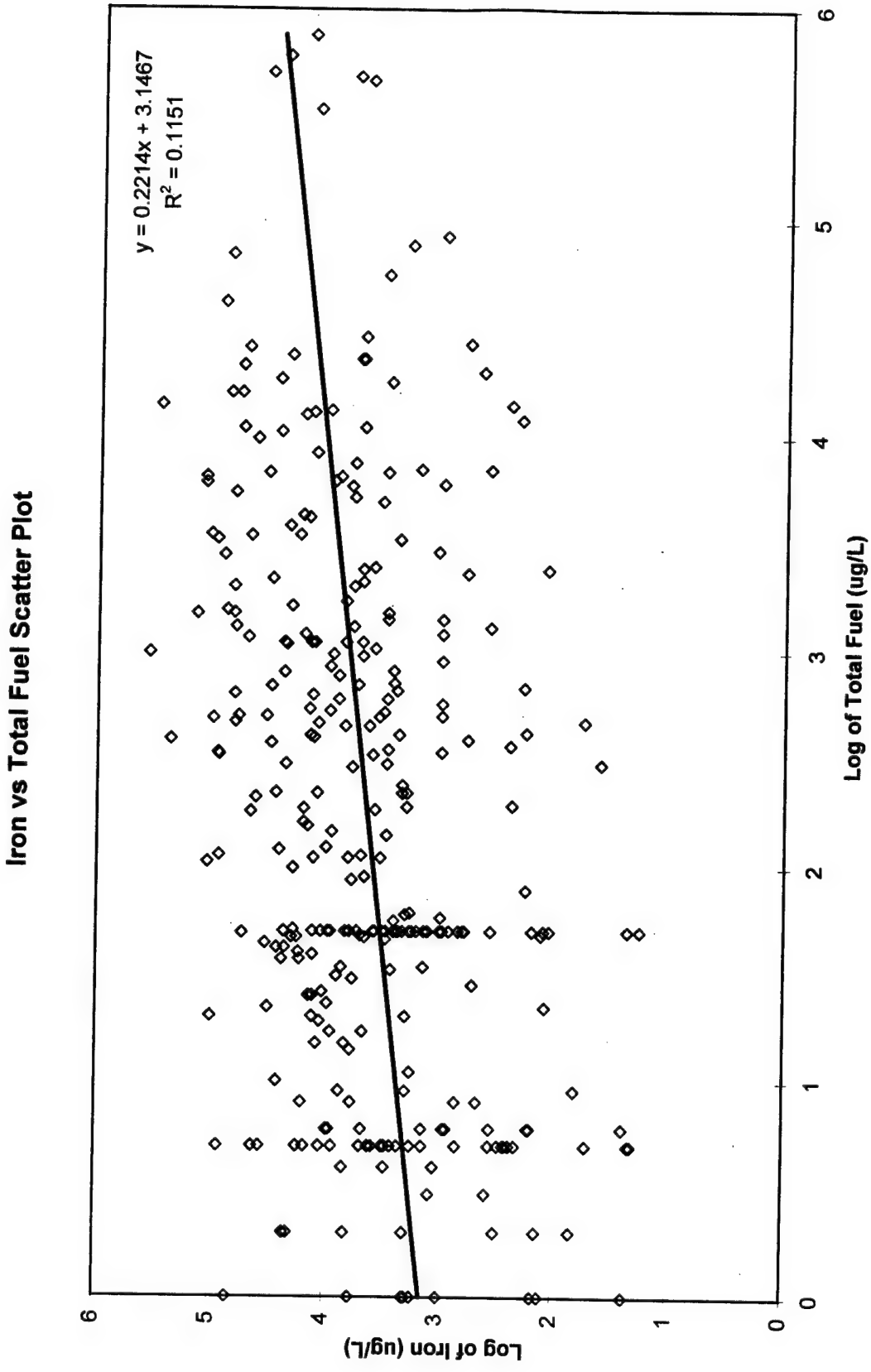
Iron vs Total Fuel Scatter Plot
y = 0.2214x + 3.1467
R2 = 0.1151
Log of Iron (ug/L)
Log of Total Fuel (ug/L)
0
1
2
3
4
5
6

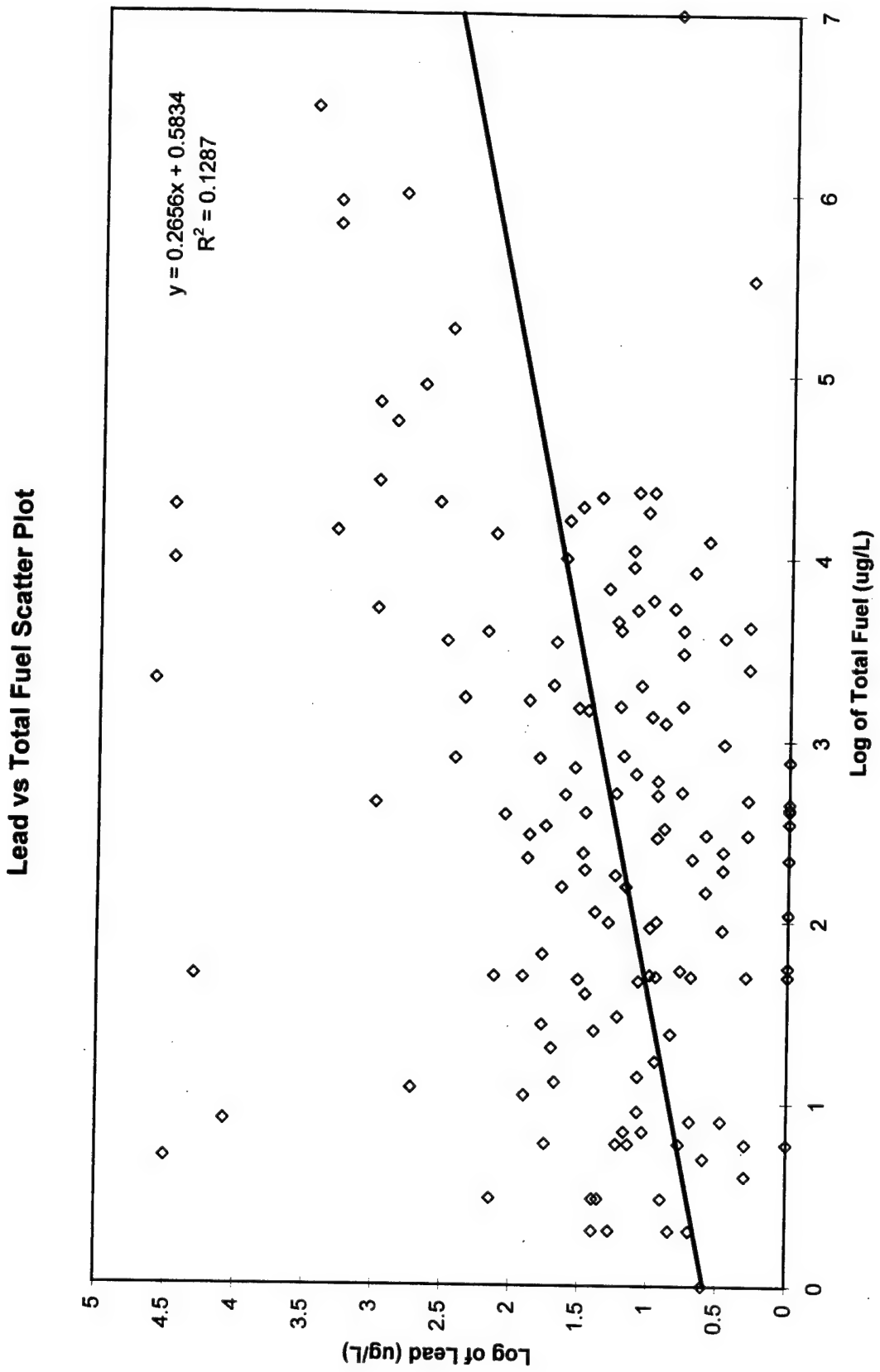
Lead vs Total Fuel Scatter Plot
y = 0.2656x + 0.5834
R2 = 0.1287
Log of Lead (ug/L)
Log of Total Fuel (ug/L)
0
0.5
1
1.5
2
2.5
3
3.5
4
4.5
5
0
1
2
3
4
5
6
7

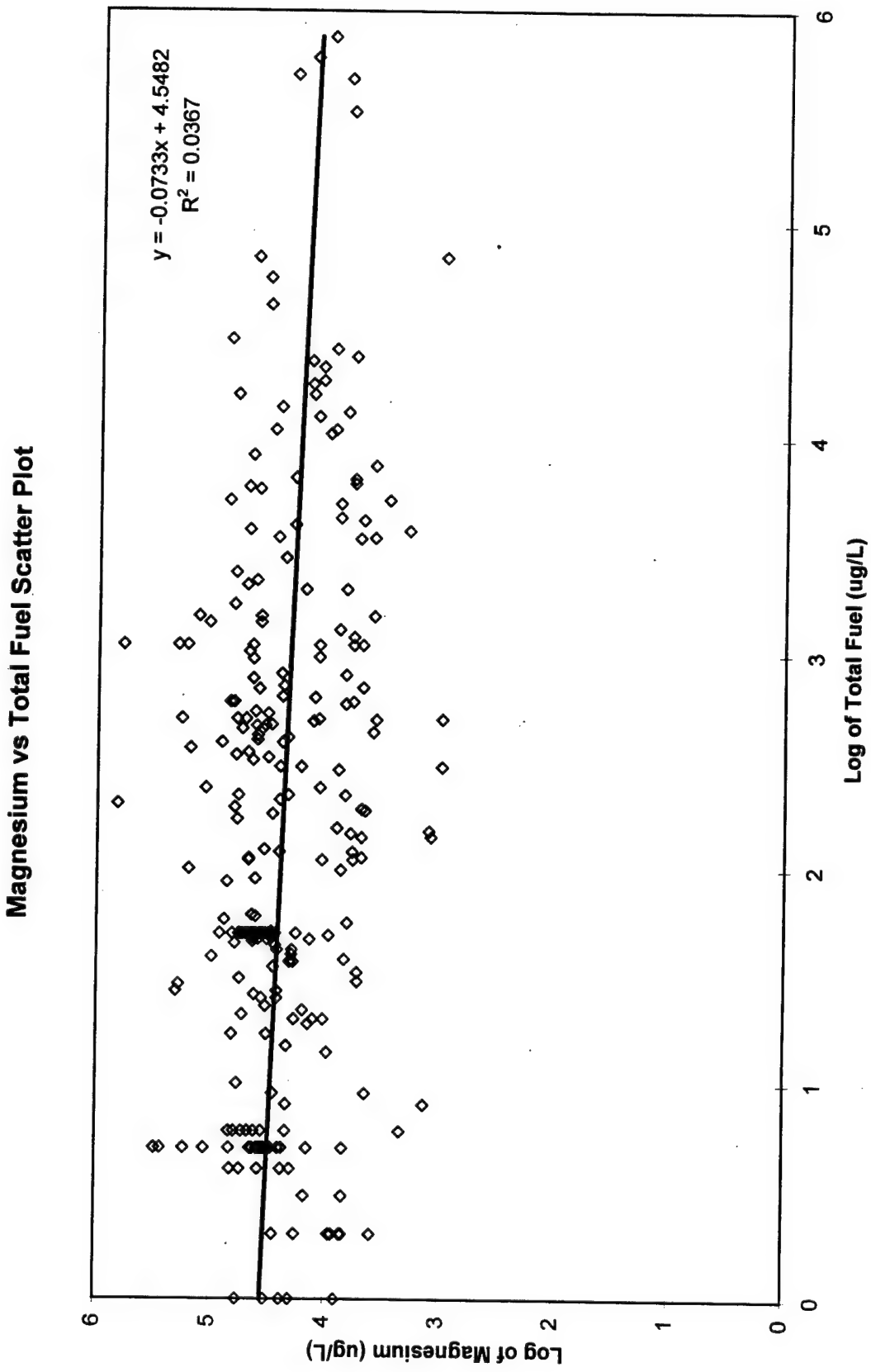
Magnesium vs Total Fuel Scatter Plot
y = -0.0733x + 4.5482
R2 = 0.0367
Log of Magnesium (ug/L)
Log of Total Fuel (ug/L)
0
1
2
3
4
5
6

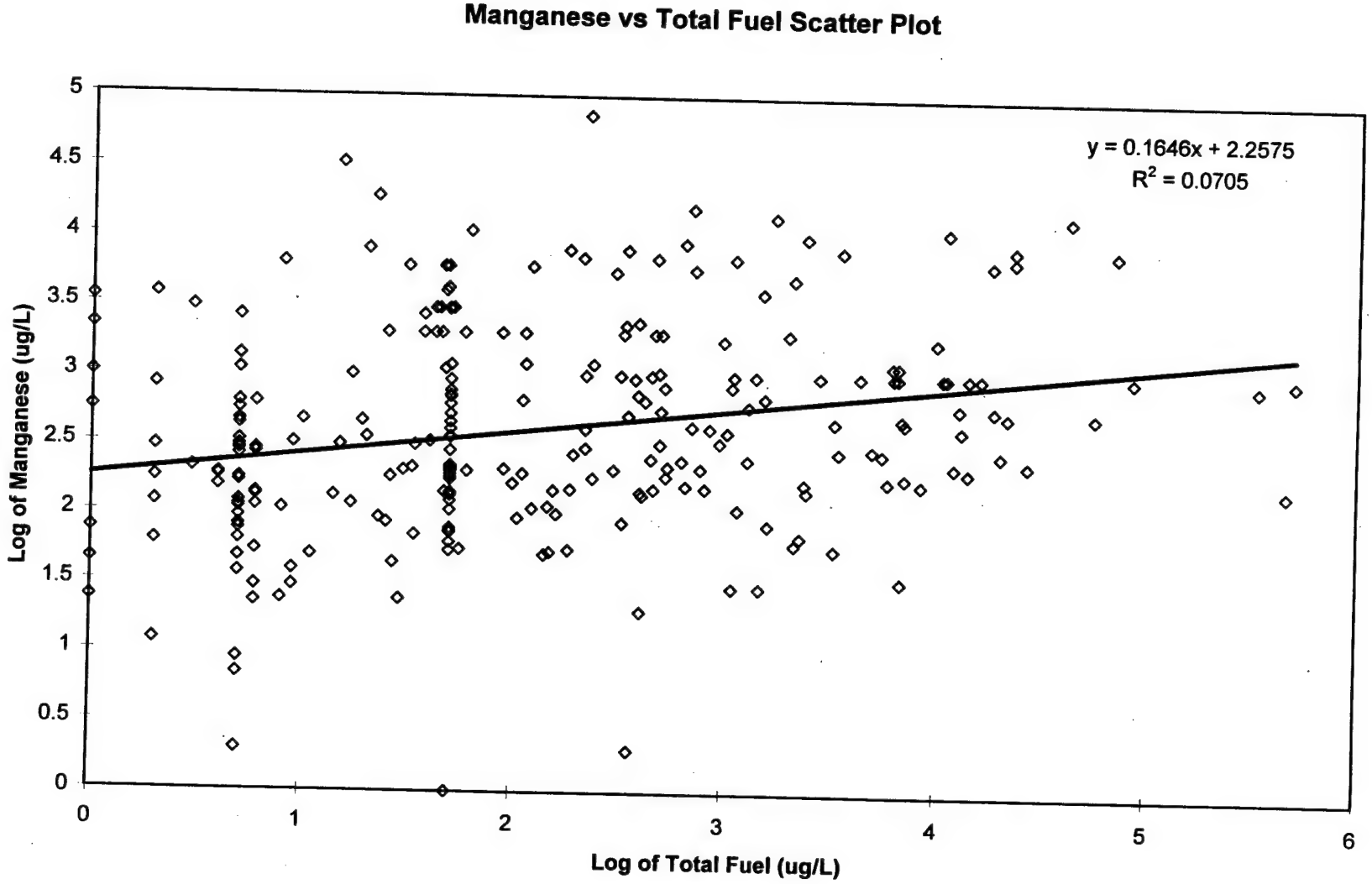
Manganese vs Total Fuel Scatter Plot
y = 0.1646x + 2.2575
R2 = 0.0705
Log of Manganese (ug/L)
Log of Total Fuel (ug/L)
0
0.5
1
1.5
2
2.5
3
3.5
4
4.5
5
0
1
2
3
4
5
6

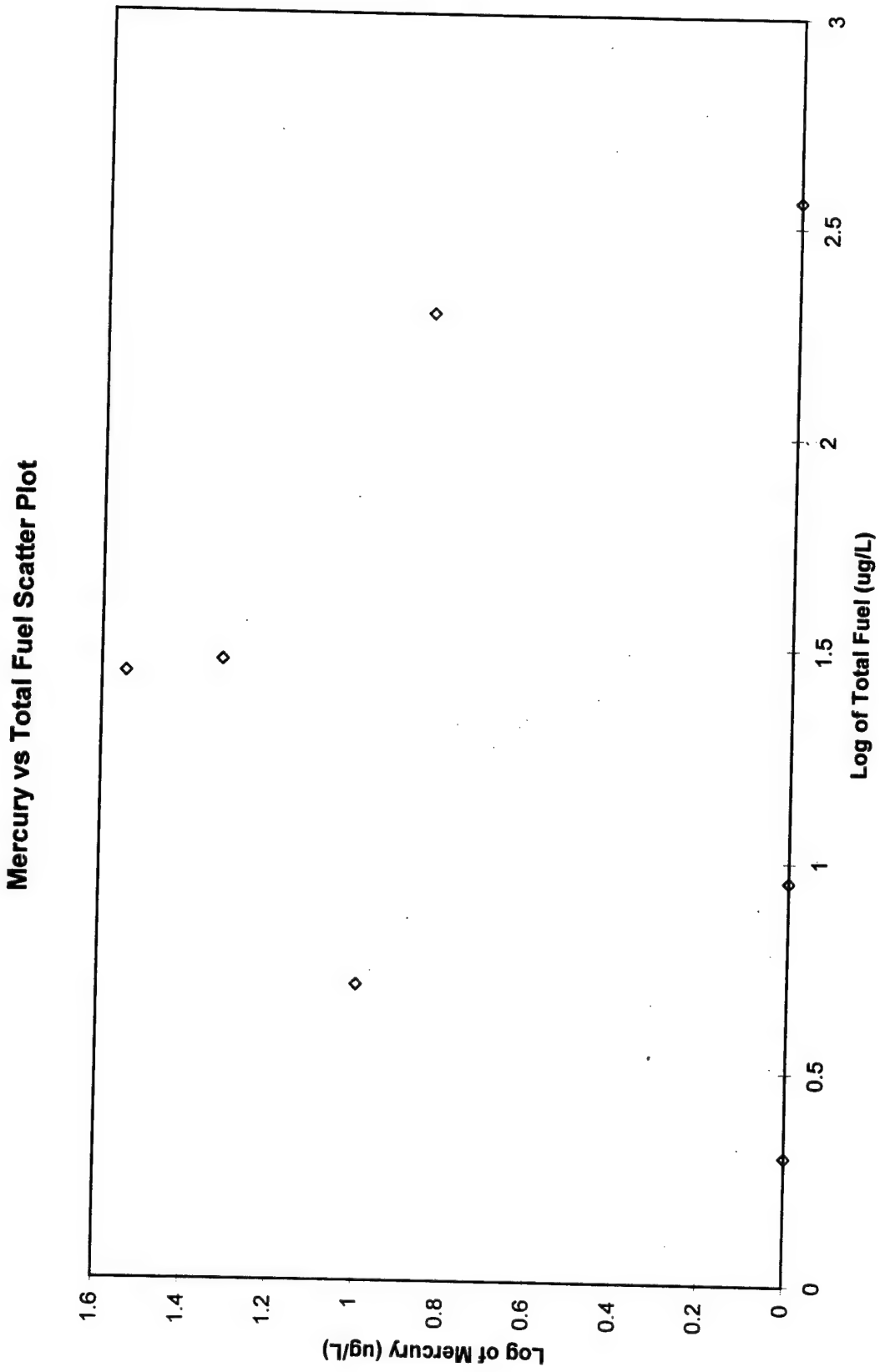
Mercury vs Total Fuel Scatter Plot
Log of Mercury (ug/L)
1.6
1.4
1.2
1
0.8
0.6
0.4
0.2
0
0
0.5
1
1.5
2
2.5
3
Log of Total Fuel (ug/L)

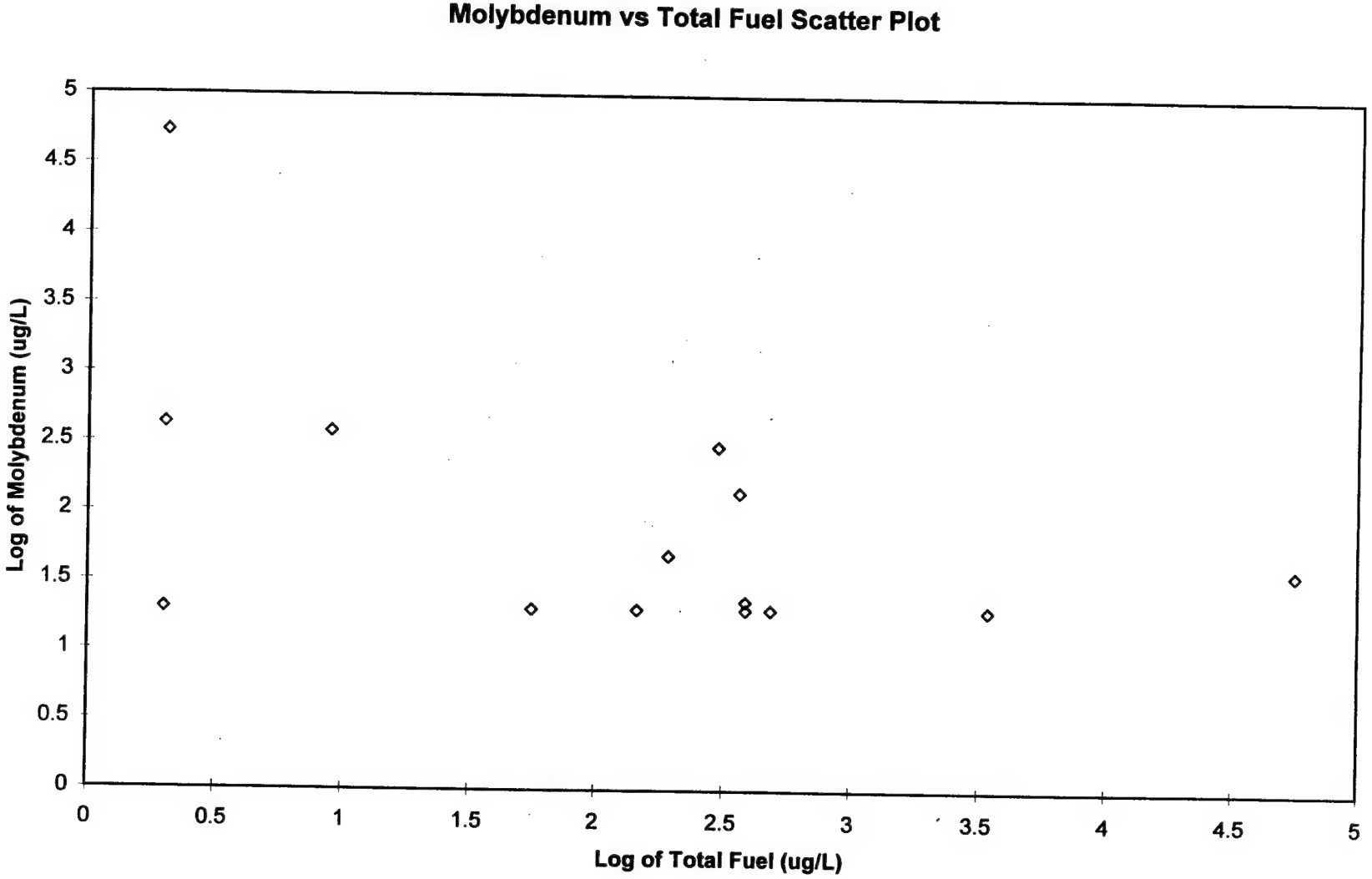
Molybdenum vs Total Fuel Scatter Plot
Log of Molybdenum (ug/L)
Log of Total Fuel (ug/L)
0
0.5
1
1.5
2
2.5
3
3.5
4
4.5
5

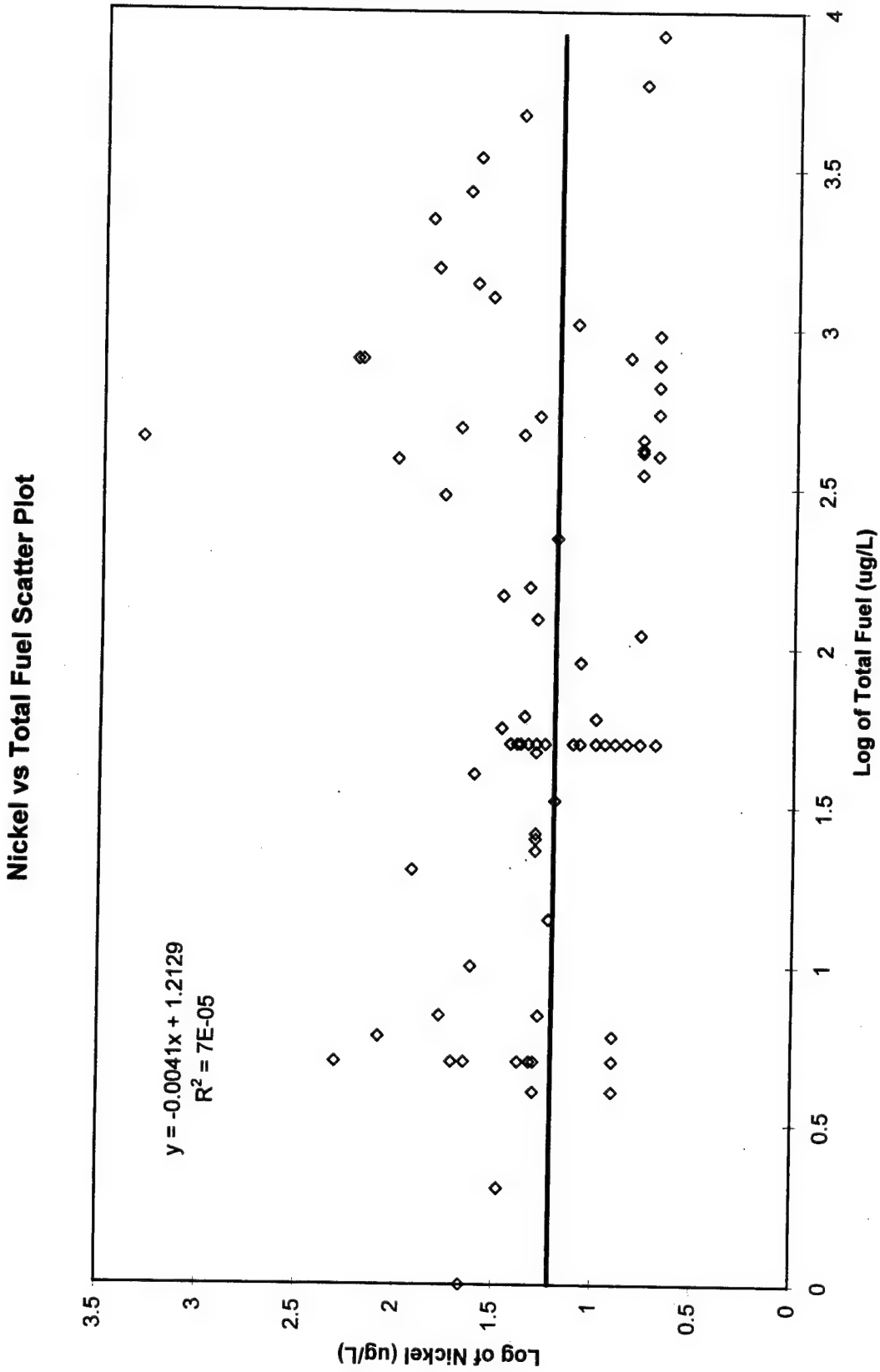
Nickel vs Total Fuel Scatter Plot
y = -0.0041x + 1.2129
R2 = 7E-05
Log of Nickel (ug/L)
Log of Total Fuel (ug/L)
0
0.5
1
1.5
2
2.5
3
3.5
4

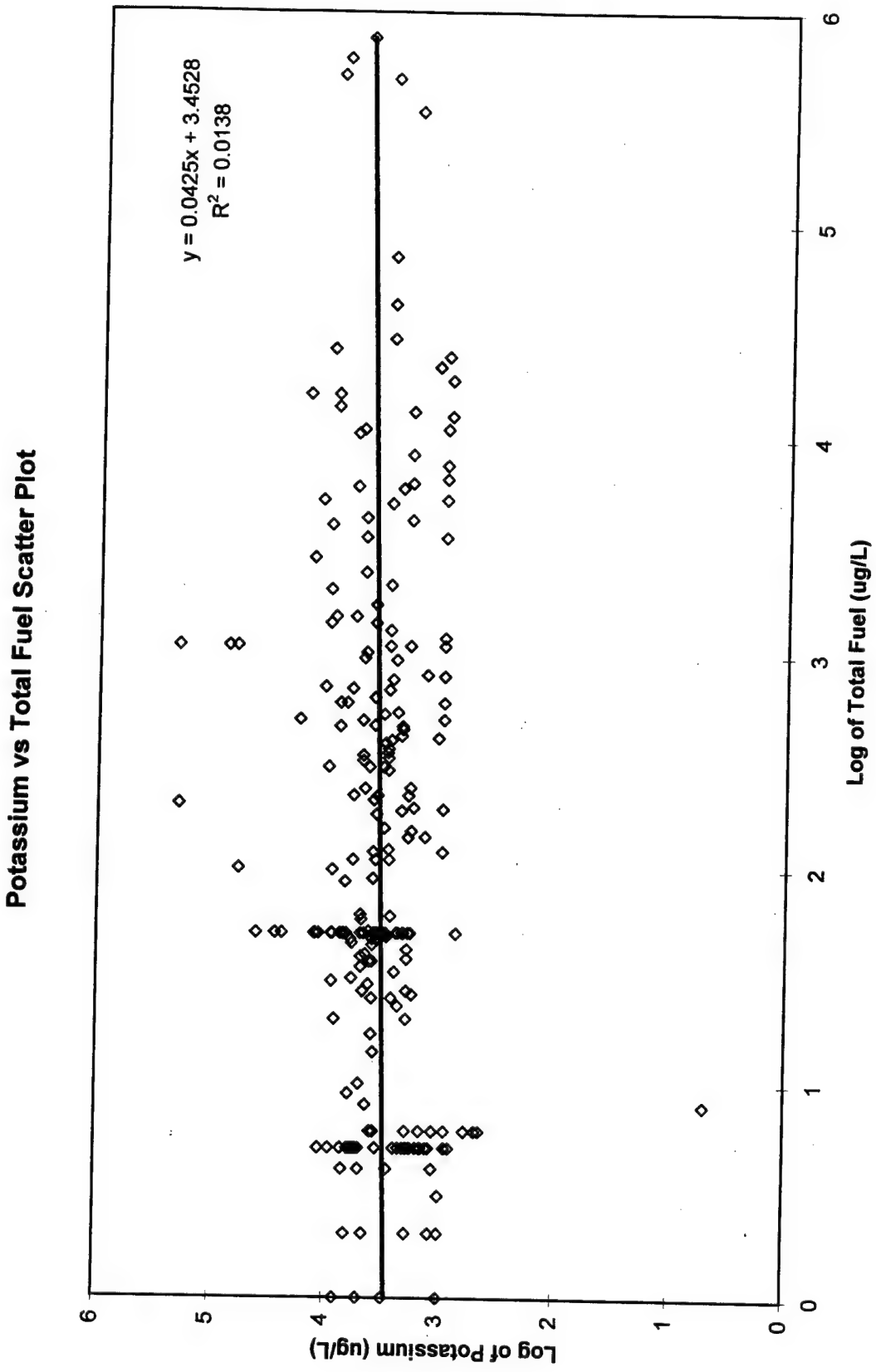
Potassium vs Total Fuel Scatter Plot
y = 0.0425x + 3.4528
R2 = 0.0138
Log of Potassium (ug/L)
Log of Total Fuel (ug/L)
0
1
2
3
4
5
6

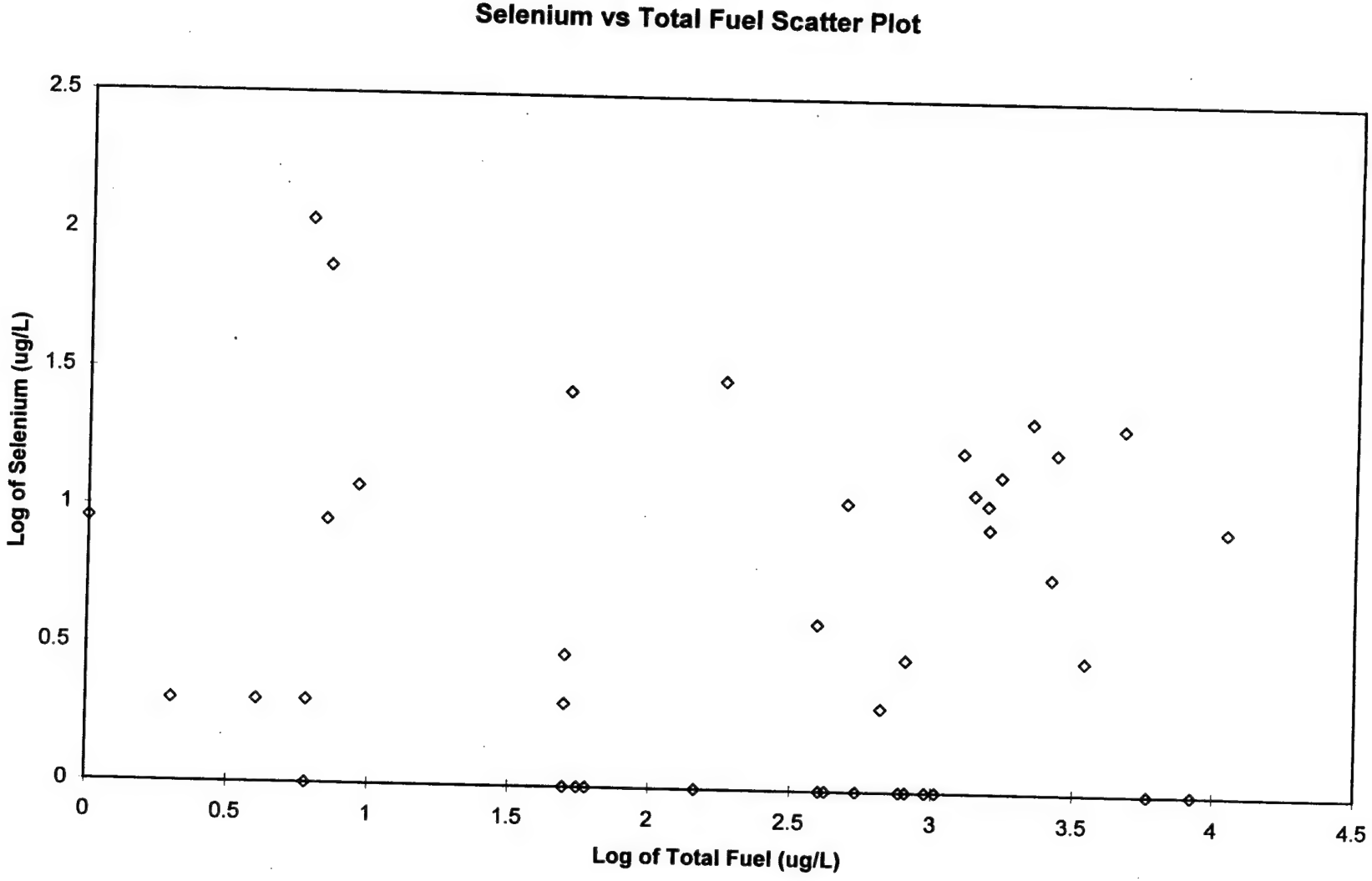
Selenium vs Total Fuel Scatter Plot
Log of Selenium (ug/L)
Log of Total Fuel (ug/L)
2.5
2
1.5
1
0.5
0
0
0.5
1
1.5
2
2.5
3
3.5
4
4.5

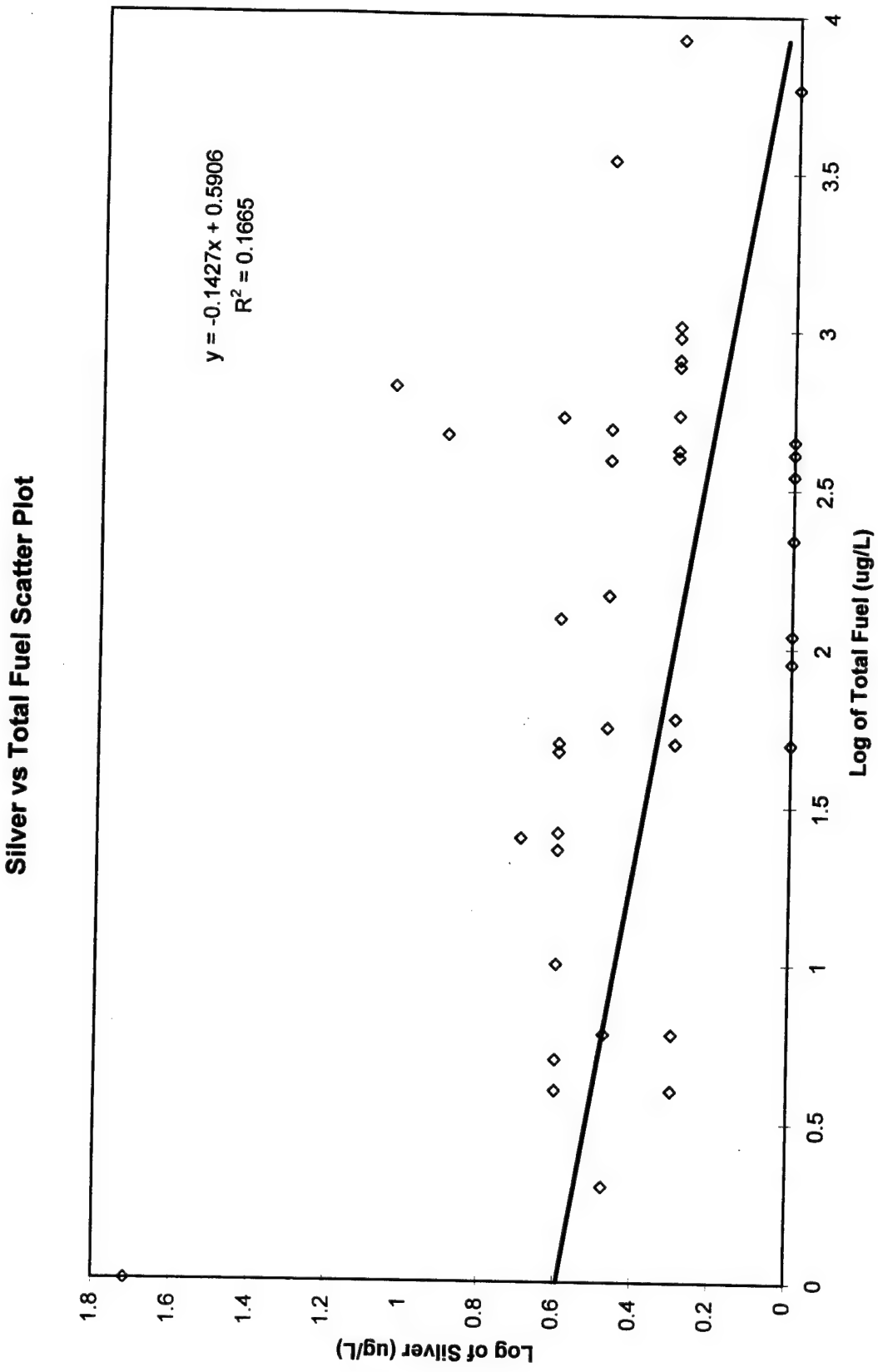
Silver vs Total Fuel Scatter Plot
y = -0.1427x + 0.5906
R2 = 0.1665
Log of Silver (ug/L)
Log of Total Fuel (ug/L)
0
0.2
0.4
0.6
0.8
1
1.2
1.4
1.6
1.8
0
0.5
1
1.5
2
2.5
3
3.5
4

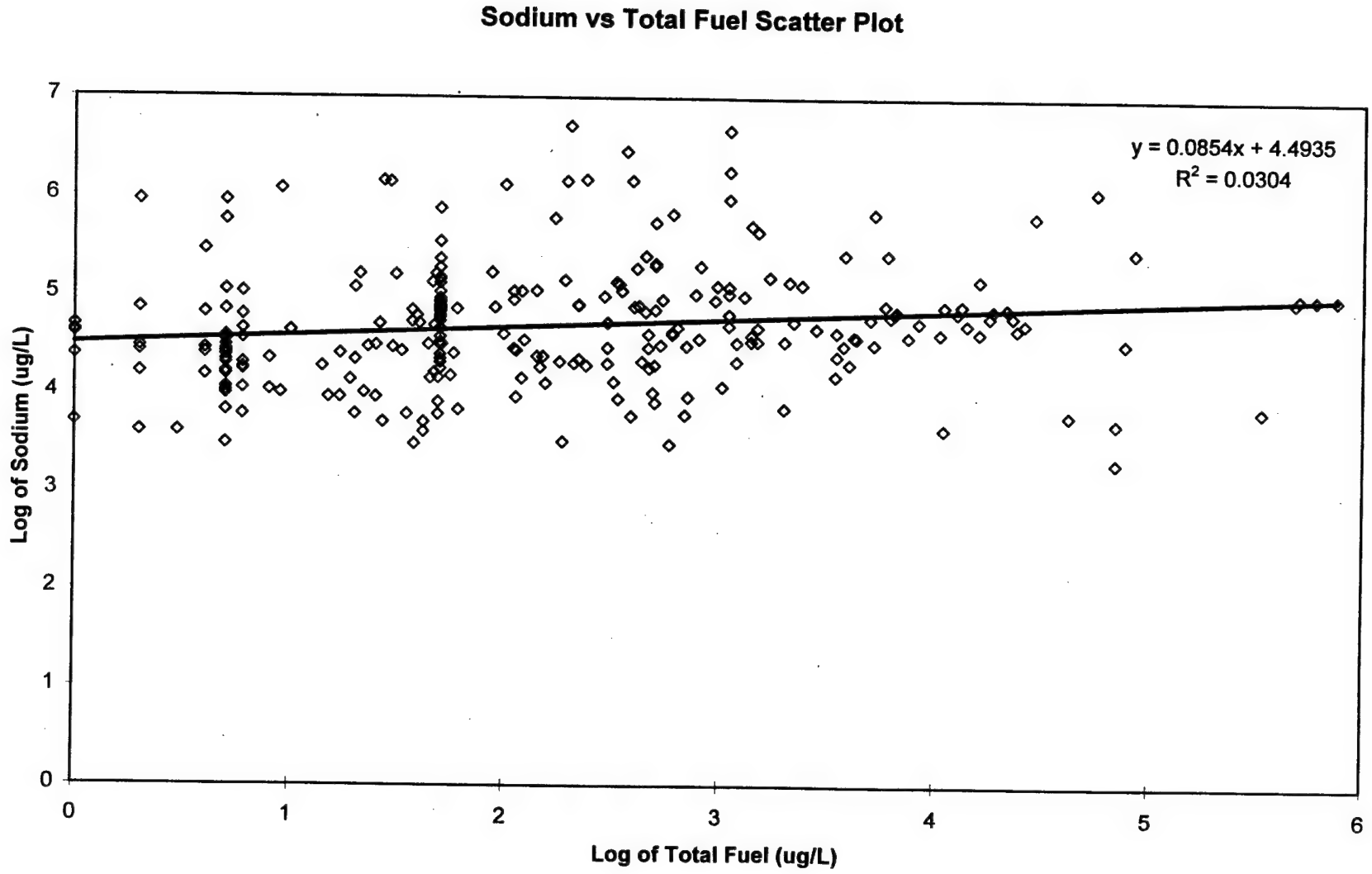
Sodium vs Total Fuel Scatter Plot
y = 0.0854x + 4.4935
R2 = 0.0304
Log of Sodium (ug/L)
Log of Total Fuel (ug/L)
0
1
2
3
4
5
6
7

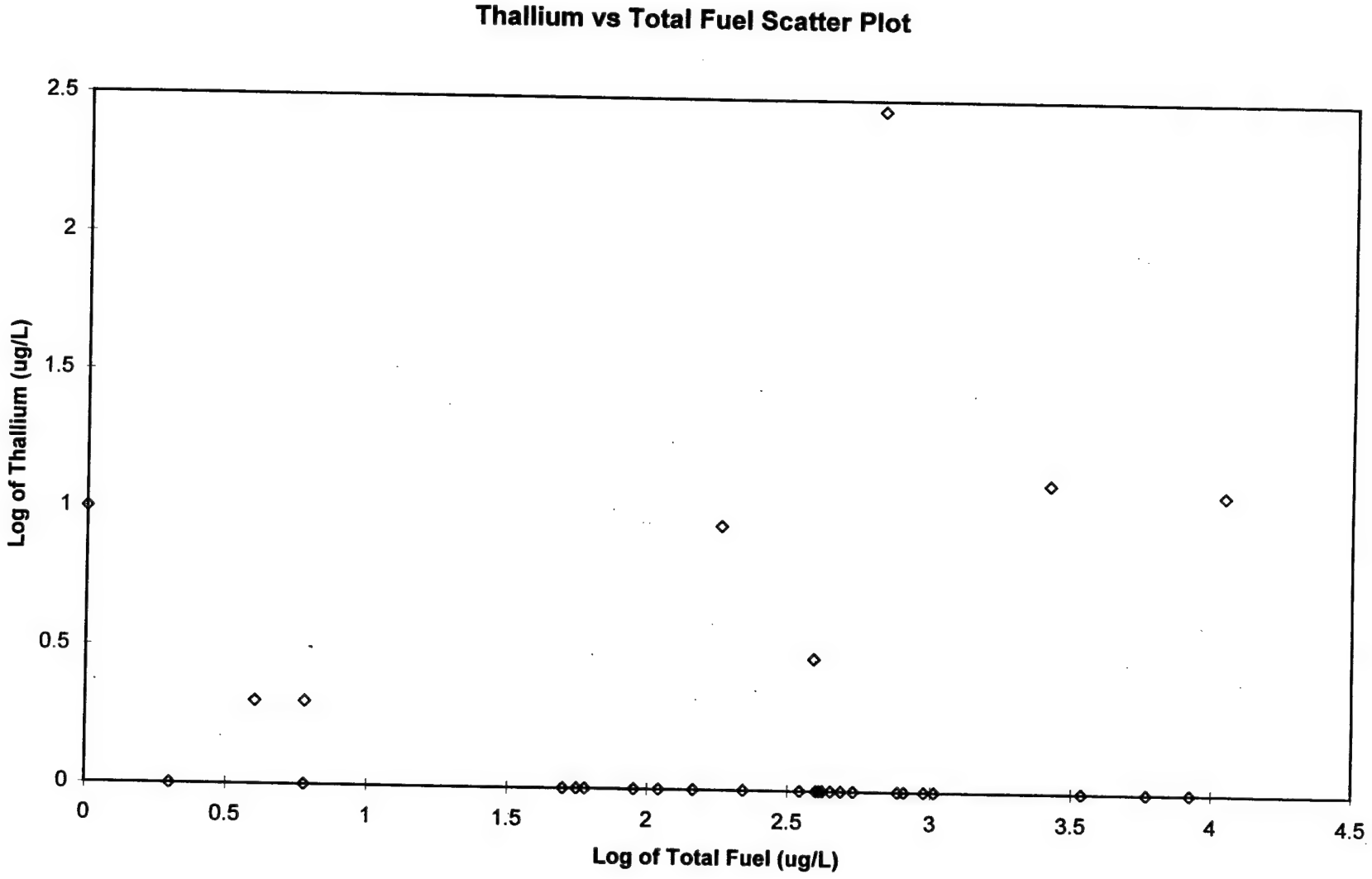
Thallium vs Total Fuel Scatter Plot
Log of Thallium (ug/L)
2.5
2
1.5
1
0.5
0
0
0.5
1
1.5
2
2.5
3
3.5
4
4.5
Log of Total Fuel (ug/L)

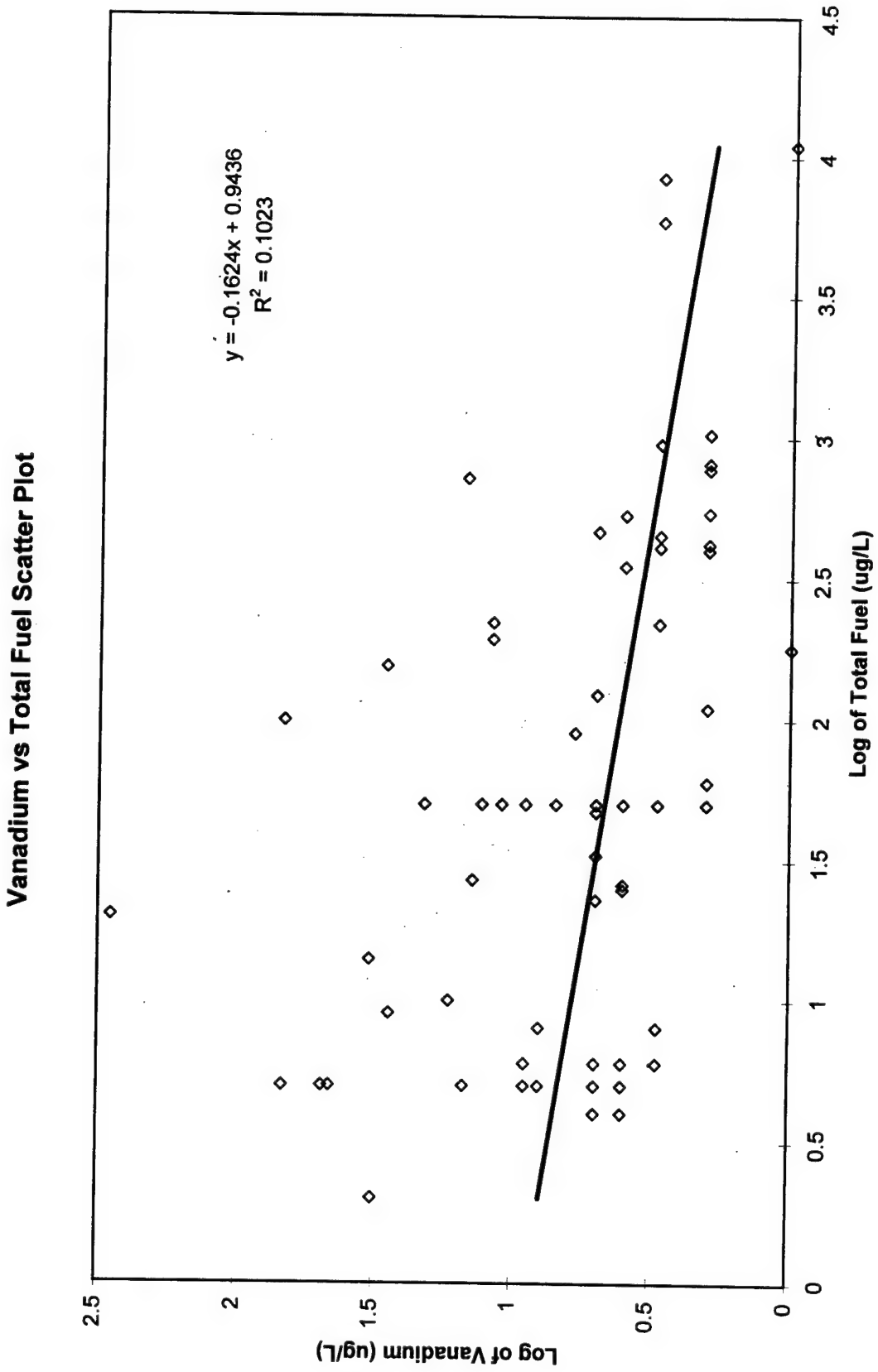
Vanadium vs Total Fuel Scatter Plot
y = -0.1624x + 0.9436
R2 = 0.1023
Log of Vanadium (ug/L)
Log of Total Fuel (ug/L)
0
0.5
1
1.5
2
2.5
3
3.5
4
4.5

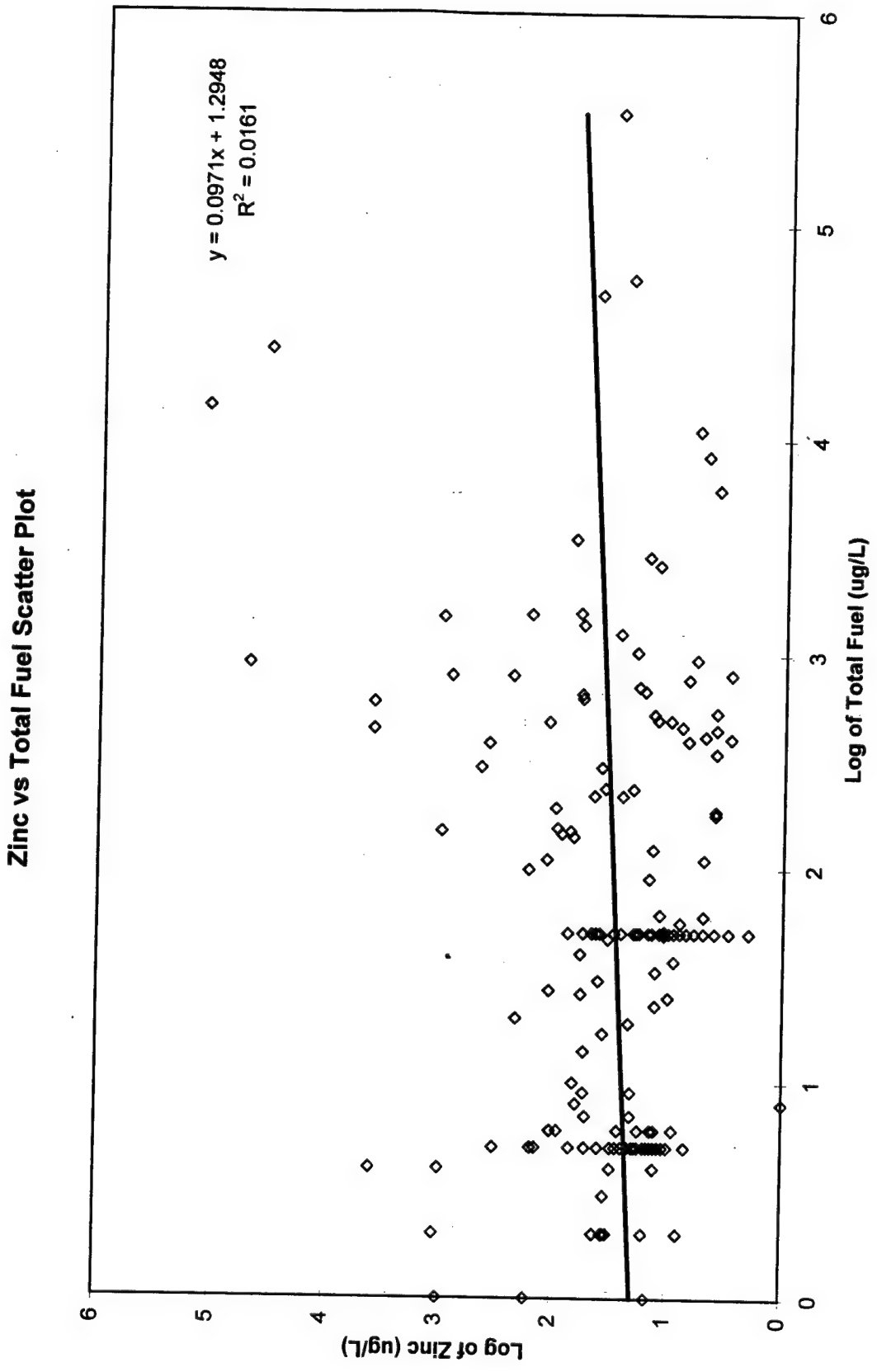
Zinc vs Total Fuel Scatter Plot
y = 0.0971x + 1.2948
R2 = 0.0161
Log of Zinc (ug/L)
Log of Total Fuel (ug/L)
0
1
2
3
4
5
6

References

Alvarez, P. J. and Vogel, T. M. "Substrate Interactions of Benzene, Toluene, and Para-Xylene During Microbial Degradation by Pure Cultures and Mixed Culture Aquifer Slurries," Applied and Environmental Microbiology, 57: 2981-2985 (1991).

Atlas, R. M. "Microbial Degradation of Petroleum Hydrocarbons - An Environmental Perspective," Microbiological Reviews, 45: 180-209 (1981).

Baedecker, M. J. and Back, W. "Hydrogeological Processes and Chemical Reactions at a Landfill," Ground Water, 17: 429-437 (September- October 1979).

Baedecker, M. J., Siegel, D. I., Bennett, P. C., and Cozzarelli, I. M. The Fate and Effects of Crude Oil in a Shallow aquifer:The Distribution of Chemical Species and Geochemical Facies. U.S. Geological Survey Water-Resources Investigations Report, 88-42320: 13-20 (1988).

Baedecker, M. J., Cozzarelli, I. M., Eganhouse, R. P., Siegel, D. I., and Bennett, P. C. "Crude Oil in a Shallow Sand and Gravel Aquifer Biogeochemical Reactions and Mass Balance Modeling in Anoxic Groundwater," Applied Geochemistry, 8: 569-586 (1993).

Barcelona, M. J. and Holm, T. R. "Oxidation-Reduction Capacities of Aquifer Solids," Environmental Science and Technology, 25: 1565-1572 (1991).

Bartha, R. "Biotechnology of Petroleum Pollutant Biodegradation," Microbial Ecology, 12: 155-172 (1986).

Beller, H. R., Reinhard, M., and Grbic-Galic, D. "Metabolic Byproducts of Anaerobic Toluene Degradation by Sulfate-Reducing Enrichment Cultures," Applied and Environmental Microbiology, 58: 3192-9195 (1992a).

Beller, H. R., Grbic-Galic, D., and Reinhard, M. "Microbial Degradation of Toluene Under Sulfate-Reducing Conditions and the Influence of Iron on the Process," Applied and Environmental Microbiology, 58: 786-793 (1992b).

Bennett, P. and Siegel, D. I.. "Increased Solubility of Quartz in Water Due to Complexing by Organic Compounds," Nature, 326: 684-686 (April 1987).

Bennett, P., Melcer, M. E., Siegel, D. I., and Hassett, J. P. "The Dissolution of Quartz in Dilute Aqueous Solutions of Organic Acids at 25°C," Geochimica et Cosmochimica Acta, 52: 1521-1530 (1988).

Bennett, P. "Quartz Dissolution in Organic-Rich Aqueous Systems," Geochimica et Cosmochimica Acta, 55: 1781-1797 (1991).

Bennett, P., Siegel, D. E., Baedecker, M. J., and Hult, M. F. "Crude Oil in a Shallow Sand and Gravel Aquifer - Hydrogeology and Inorganic Geochemistry," Applied Geochemistry, 8: 529-549 (1993).

Bjerg, P. L., Rugge, K., Pedersen, J. K., and Christensen, T. H. "Distribution of Redox-Sensitive Groundwater Quality Parameters Downgradient of a Landfill (Grindsted, Denmark)," Environmental Science and Technology, 29: 1387-1394 (1995).

Bouwer, E. J. "Bioremediation of Subsurface Contaminants," in Environmental Microbiology. Ed. R. Mitchell. New York: Wiley-Liss, 1992.

Cerniglia, C. E. "Microbial Transformation of Aromatic Hydrocarbons," in Petroleum Microbilogy. Ed. R. M. Atlas. New York: Macmillan Publishing Company, 1984.

Champ, D. R., Gullens, J., and Jackson, R. E. "Oxidation-Reduction Sequences in Ground Water Flow Systems," Canadian Journal of Earth Sciences, 16: 12-23 (1979).

Chapelle, F. H., McMahon, P. B., Dubrovsky, N. M., Fujii, R. F., Oaksford, E. T., and Vroblesky, D. A. "Deducing the Distribution of Terminal Electron-Accepting Processes in Hydrologically Diverse Groundwater Systems," Water Resources Research, 31: 359-371 (February 1995).

Chiang, C. Y., Salanitro, J. P., Chai, E. Y., Colthart, J. D., and Klein, C. L. "Aerobic Biodegradation of Benzene, Toluene, and Xylene in a Sandy Aquifer - Data Analysis and Computer Modeling," Ground Water, 27: 823-834 (1989).

Christensen, T. H., Kjeldsen, P., Albrechtsen, H. J., Heron, G., Nielsen, P. H., Bjerg, P. L., and P. E. Holm. "Attenuation of Landfill Leachate Pollutants in Aquifers," Critical Reviews in Environmental Science and Technology, 24: 119-202 (1994a).

Christensen, T. H. Lyngkild, J., Nielsen, P. H., Albrechtsen, H.-J., and Heron, G. "Natural Biological Attenuation: Integrative Transition Zones," in Subsurface Restoration, Ed. H. Ward. Chelsea, MI: Ann Arbor Press, 1994.

Cozzarelli, I. M., Eganhouse, R. P., and Baedecker, M. J. "Transformation of Monoaromatic Hydrocarbons to Organic Acids in Anoxic Groundwater Environment," Environmental Geology and Water Science, 16: 135-141 (1990).

CRC Handbook of Chemistry and Physics. Eds. D. Lide and H. P. R. Frederikse. New York: CRC Press, 1995.

Davis, J. W., Klier, N. J., and Carpenter, A. "Natural Biological Attenuation of Benzene in Groundwater Beneath a Manufacturing Facility," Ground Water, 32: 215-226 (1994).

Edwards, E. A., Wells, L. E., Reinhard, M., and Grbic-Galic, D. "Anaerobic Degradation of Toluene and Xylene by Aquifer Microorganisms Under Sulfate-Reducing Conditions," Applied and Environmental Microbiology, 58: 794-800 (1992).

Edwards, E. A. and Grbic-Galic, D. "Complete Mineralization of Benzene by Aquifer Microorganisms Under Strictly Anaerobic Conditions," Applied and Environmental Microbiology, 58: 2663-2666 (1992).

Eganhouse, R. P., Baedecker, M. J., Cozzarelli, I. M., Aiken, G. R., Thorn, K. A. and Dorsey, T. F. "Crude Oil in Shallow Sand and Gravel Aquifer - II. Organic Geochemistry," Applied Geochemistry, 8: 551-567 (1993).

Erlich, H. L. 'The Geomicrobiology of Silica and Silictes," in Geomicrobiology. Ed. H. L. Erlich. New York: Marcel Dekker, 1981.

Evans, P. J. Mang, D. T. and Young, L. Y. "Degradation of Toluene and M-Xylene and Transformation of O-Xylene by Denitrifying Enrichment Cultures," Applied and Environmental Microbiology, 57: 1139-1145 (1991).

Grbic-Galic, D. and Vogel, T. M. "Transformation of Toluene and Benzene by Mixed Methanogenic Cultures," Applied and Environmental Microbiology, 53: 254-260 (1987).

Grbic-Galic, D. "Methanogenic Transformation of Aromatic Hydrocarbons and Phenols in Groundwater Aquifers," Geomicrobiology Journal, 8: 167-200 (1990).

Hiebert, F. K. and Bennett, P. C. "Microbial Control of Silicate Weathering in Organic-Rich Ground Water," Science, 258: 278-281 (1992).

Hering, J. G. and Morel, F. M. M. "Kinetics of Trace Metal Complexation; Role of Alkaline Earth Metals," Environmental Science and Technology, 22: 1469-1478 (1989).

Heron, G. and Christensen, T. H. "Impact of Sediment-Bound Iron on Redox Buffering in a Landfill Leachate Polluted Aquifer (Vejen, Denmark)," Environmental Science and Technology, 29; 187-192 (1995).

Hinchee, R. E., Downey, D. C., Dupont, R. R., Aggarwal, P. K., Miller, R. N. "Enhancing Biodegradation of Petroleum Hydrocarbons Through Soil Venting," Journal of Hazardous Materials, 27: 315-325 (1991).

Huang, W. H. and Keller, W. K. "Dissolution of Rock-Forming Silicate Minerals in Organic Acids: Simulated First-Stage Weathering of Fresh Mineral Surfaces," The American Mineralogist, 55: 2076-2094 (1970).

Hutchins, S. R., Sewell, G. W., Sewell, D. A., Kovacs, D. A., and Smith, G. A. "Biodegradation of Aromatic Hydrocarbons by Aquifer Microorganisms Under Denitrifying Conditions," Environmental Science and Technology, 25: 68-75 (1991).

Jackson, R. E. and Patterson, R. J. "Interpretation of pH and Eh Trends in a Fluvial-Sand Aquifer System," Water Resources Research, 18: 1255-1268 (August 1982).

Kabata-Pendias, A. and Pendias, H. Trace Elements in Soils and Plants, 2nd Edition. Ann Arbor, MI: CRC Press, 1992.

Lee, M. D. "Biorestoration of Aquifers Contaminated with Organic Compounds," CRC Critical Reviews in Environmental Control, 18: 29-89 (1988).

Leahy, J. G. and Colewell, R. R. "Microbial Degradation of Hydrocarbons in the Environment," Microbiological Reviews, 53: 305-315 (1990).

Levinson, A. A. Introduction to Exploration Geochemistry. Maywood, IL: Applied Publishing Ltd., 1974.

Lindberg, R. D. and Runnells, R. R. "Ground Water Redox Reactions: An Analysis of Equilibrium State Applied to Eh Measurements and Geochemical Modeling," Science, 225: 925-927 (August 1984).

Lovley, D. R. "Organic Matter Mineralization with the Reduction of Ferric Iron: A Review," Geomicrobiology Journal, 5: 375-399 (1987).

Lovley, D. R. and Phillips, E. J. P. "Competivite Mechanisms for Inhibition of Sulfate Reduction and Methane Production in the Zone of Ferric Iron Reduction in Sediments," Applied and Environmental Microbiology, 53: 2636-2641 (November 1987).

Lovley, D. R. and Goodwin, S. "Hydrogen Concentrations as an Indicator of the Predominant Terminal Electron-Accepting Reactions in Aquatic Sediments," Geochimica et Cosmochimica Acta, 52: 2993-3003 (1988).

Lovley, D. R., Baedecker, M. J., Lonergan, D. J., Cozzarelli, I. M., Phillips, E. J. P., and Siegel, D. I. "Oxidation of Aromatic Contaminants Coupled to Microbial Iron Reduction," Nature, 339: 297-299 (1989).

Lovley, D. R., Coates, J. D., Woodward, J. C., and Phillips, E. J. P. "Benzene Oxidation Coupled to Sulfate Reduction," Applied and Environmental Microbiology, 61: 953-958 (1995).

Lyngkilde, J. and Christensen, T. H. "Redox Zones of a Landfill Leachate Pollution Plume," Journal of Contaminant Hydrology, 10: 273 (1992).

Malone, D. R., Kao, C. M., and Border, R. C. "Dissolution and Biorestoration of Nonaqueous Phase Hydrocarbons - Model Development and Laboratory Evaluation," Water Resources Research, 29: 2203-2213 (1993).

McMahon, P. B., Vroblesky, D. A., Bradley, P. M., Chapelle, F. H., and Gullett, C. D. "Evidence for Enhanced Mineral Dissolution in Organic Acid-Rich Shallow Ground Water," Ground Water, 33: 207-216 (March-April 1995).

Morel, F. M. M. and Hering, J. G. Principles and Applications of Aquatic Chemistry. New York: Wiley-Interscience, 1993.

Nordstrom, D. K., Plummer, L. N., Langmuir, D., Busenber, E., May, H. M., Jones, B. F., and Parkhurst, D. L. "Revised Chemical Equilibrium Data for Major Water-Mineral Reactions and Their Limitations," in Chemical Modeling of Aqueous Systems II. Eds. D. C. Melcheor and R. L. Bassett. ACS Ser. 416. Washington D. C.: American Chemical Society, 1990.

Pourbaix, M. Atlas of Electrochemical Equilibria in Aqueous Solutions. Houston, TX: National Association of Corrosion Engineers, 1994.

Revsbech, N. P. and Ward, D. M. "Microelctrode Studies of Interstitial Water Chemistry and Photosynthetic Activity in a Hot Spring Microbial Mat," Applied and Environmental Microbiology, 48: 270-275 (1984).

Rifai, H. S., Bedient, P. B., Wilson, J. T., Miller, K. M., Armstrong, J. M. Biodegradation Modeling at Aviation Fuel Spill Site," Journal of Environmental Engineering, 114: 1007-1029 (1988).

Robertson, W. D. and Blowes, D. W. "Major Ion and Trace Metal Geochemistry of an Acidic Septic-System Plume in Silt," Ground Water, 33: 275-283 (March-April 1995).

Schwertmann, U. and Taylor, R. M. "Iron Oxides," in Minerals in Soil Environments. Madison, WI: Soil Science Society of America, 1977.

Stone, A. T. "Microbial Metabolites and the Reductive Dissolution of Manganese Oxides: Oxalate and Pyruvate," Geochimica et Cosmochimica Acta, 51: 919-925 (1987).

Stumm, W. and Morgan, J. J. Aquatic Chemistry. New York: John Wiley & Sons, 1996.

Tan, K. H. "The Release of Silicon, Aluminum, and Potassium During Decomposition of Soil Minerals by Humic Acid," Soil Science, 129: 5-11 (January 1980).

Vroblesky, D. A. and Chapelle, F. H. "Temporal and Spatial Changes of Terminal Electron-Accepting Processes in a Petroleum Hydrocarbon-Contaminated Aquifer and the Significance for Contaminant Biodegradation," Water Resources Research, 30: 1561-1570 (May 1994).

Wiedemeier, T. H., Wilson, J. T., Kampbell, D. H., Miller, R. N. and Hansen, J. E. Technical Protocol for Implementing Intrinsic Remediation with Long-Term Monitoring for Natural Attenuation of Fuel Contamination Dissolved in Groundwater. Brooks Air Force Base, San Antonio, Texas: Air Force Center for Environmental Excellence, 1995.

Wilson, B. H., Smith, H. B., and Rees, J. F. "Biotransformations of Selected Alkylbenzenes and Halogenated Aliphatic Hydrocarbons in Methanogenic Aquifer Material: A Microcosm Study," Environmental Science and Technology, 20: 1997-1002 (1986).

Vita

1Lt Scott L. Kearney was born on 9 May 71 in Sioux Falls, South Dakota. He graduated from Redfield High School in 1989 and attended South Dakota State University in Brookings, South Dakota. In May 1994, he graduated with a Bachelor of Science degree in Civil Engineering and received a reserve commission into the United States Air Force through ROTC. He married Krystal A. Koob of Volga, South Dakota, on 21 May 94.

1Lt Kearney's first assignment was to the 28th Civil Engineer Squadron at Ellsworth AFB, South Dakota. While there, he held positions as readiness flight chief and environmental compliance manager. In May 1996, he entered the School of Engineering, Air Force Institute of Technology at Wright-Patterson AFB, Ohio. After graduating in December, 1997, with a Master of Science degree in Engineering and Environmental Management, he will report to Offutt AFB, Nebraska.

Permanent Address: 131 W. 6th St.
Redfield, SD 57469

REPORT DOCUMENTATION PAGE

Form Approved OMB No. 0704-0188

1. AGENCY USE ONLY *(Leave blank)*	2. REPORT DATE	3. REPORT TYPE AND DATES COVERED
	December 1997	Master Thesis

4. TITLE AND SUBTITLE
MOBILIZATION OF TRACE ELEMENTS IN AQUIFERS BY BIODEGRADATION OF HYDROCARBON CONTAMINANTS

5. FUNDING NUMBERS

6. AUTHOR(S)
SCOTT L. KEARNEY, 1LT, USAF

7. PERFORMING ORGANIZATION NAME(S) AND ADDRESS(ES)
Air Force Institute of Technology (AFIT)
Wright-Patterson AFB, OH 45433-7765

8. PERFORMING ORGANIZATION REPORT NUMBER
AFIT/GEE/ENV/97D-13

9. SPONSORING/MONITORING AGENCY NAME(S) AND ADDRESS(ES)
OO - ALC/EMR
Hill AFB, UT 84056

10. SPONSORING/MONITORING AGENCY REPORT NUMBER

11. SUPPLEMENTARY NOTES

12a. DISTRIBUTION AVAILABILITY STATEMENT
Approved for public release; distribution unlimited

12b. DISTRIBUTION CODE

13. ABSTRACT *(Maximum 200 words)*

This study had two objectives: (1) to determine the extent of metal mobility within petroleum-contaminated aquifers, (2) to determine if biodegradation of petroleum hydrocarbons can explain metal mobility. The approach reviewed analytical results from 2305 groundwater sampling events, taken from 958 wells, located at 136 sites found at 53 Air Force installations.

The study showed that high levels of metals are present at petroleum hydrocarbon sites where metals would not generally be expected. Of the metals with drinking water maximum contaminant levels (MCLs), mercury and silver were detected the least frequently. Barium and copper were detected at the sites, but fewer than 2.5 percent of the samples exceeded their MCLs. All other metals exceeded their MCLs in at least 2.5 percent of the samples, with antimony and lead exceeding their MCLs in 19 percent and 10 percent of samples, respectively.

Higher concentrations of barium and manganese were most strongly correlated with petroleum hydrocarbon contamination, and relatively strong correlations also existed for aluminum, arsenic, iron, and lead. Major cations such as calcium, magnesium, sodium and potassium were least affected by petroleum hydrocarbons concentrations.

14. SUBJECT TERMS
trace elements, metal mobility, fuel contamination, MCL, metal solubility, redox potential, drinking water standards, biodegradation, complexation, microbes, aquifers, groundwater, petroleum hydrocarbons, remediation

15. NUMBER OF PAGES
216

16. PRICE CODE

17. SECURITY CLASSIFICATION OF REPORT	18. SECURITY CLASSIFICATION OF THIS PAGE	19. SECURITY CLASSIFICATION OF ABSTRACT	20. LIMITATION OF ABSTRACT
Unclassified	Unclassified	Unclassified	UL